Reactivity of a Low Valent Gallium Compound

Aishabibi Kassymbek

Inorganic Chemistry

Submitted in partial fulfillment
of the requirements for the degree of

Doctor of Philosophy

Faculty of Mathematics and Science, Brock University
St. Catharines, Ontario

Abstract

The work described in this thesis is conducted to expand the reactivity of the *β*-diketiminate gallium(I) compound, NacNacGa (**III-1**). The reactivity of **III-1** towards various unsaturated compounds is studied. In particular, reaction between NacNacGa and phenyl isothiocyanate resulted in the oxidative addition of the C=S bond under ambient conditions, leading to the isolation cyclization product NacNacGa(κ^2-S_2CNPh) (**III-4**) and sulfide isocyanide-bridged dimer (NacNacGa)$_2$(μ-S)(μ-CNPh) (**III-5**). Additionally, **III-1** undergoes a [1+4] cycloaddition with a conjugated aldehyde (methacrolein) affording **III-2**, and a [1+2+3] cycloaddition with isocyanate and carbodiimide to give **III-7** and **III-8**, respectively. The oxidative cleavage of P=S bond of triphenylphosphine sulfide at increased temperatures gave the previously reported sulfide bridged gallium dimer **III-4**.

In situ oxidation of NacNacGa **III-1** in the presence of substrates featuring donor sites led to the C-H activation reactions. As such, C-activation of pyridine N-oxide, pyridine, cyclohexanone, DMSO, and Et_3P=O by a transient NacNacGa=O resulting in the corresponding gallium hydroxides (**III-9** to **III-14**) is demonstrated. DFT calculations suggested initial formation of adducts between substrates and NacNacGa=O followed by a C-H bond abstraction from the substrate. Similarly, a transient gallium imide NacNacGa=N$SiMe_3$, generated from the reaction of NacNacGa **III-1** with trimethylsilyl azide, is shown to cleave C-H bonds of pyridine, cyclohexanone, ethyl acetate, DMSO, and Et_3P=O with the formation of gallium amides (**III-15** to **III-19**).

In an attempt to isolate a gallium alkylidene, NacNacGa was treated with trimethylsilyl(diazomethane). Instead, a monomeric gallium nitrilimine (**III-20**) and a

metalated diazomethane (**III-24**) were obtained. The gallium diazomethane **III-24** rearranges to an isonitrile isomer **III-25** over a period of one week. The gallium nitrilimine (**III-20**) undergoes 1,3-addition reaction with phenylsilane and catecholborane forming gallium hydrazonides **III-26** and **III-28**, respectively. The reaction of **III-20** with diborane resulted in the formal nitrene insertion into the B-B bond to produce a gallium diborylamide **III-28**. DFT calculations revealed intermediate gallium alkylidene formation from the reaction of NacNacGa **III-1** with diazomethane that upon reaction with the second equivalent of diazomethane leads to a gallium nitrilimine **III-20**.

All new compounds were characterized by multinuclear NMR spectroscopy and structures of majority of them were elucidated by X-ray diffraction.

Acknowledgements

First, I would like to express my sincere gratitude to Dr. Georgii Nikonov whose advisory and supervision helped throughout my study years. Being part of your team was a very valuable experience that sharpened my skills and broadened my knowledge of chemistry. I am grateful to Dr. Andrey Khalimon who suggested my candidacy to Dr. Georgii Nikonov's research group to follow my path in academia. I would like to thank my committee members Dr. Martin Lemaire and Dr. Heather Gordon for their insightful suggestions during my graduate program.

I would also like to acknowledge Dr. Melanie Pilkington, Dr. Bulat Gabidullin, Dr. Denis Spasyuk, and Dr. Anton Dmitrienko for collecting and solving X-ray diffraction data, Dr. Sergei F. Vyboishchikov and Dr. Dmitry G. Gusev for DFT calculations.

Furthermore, I am grateful to all my colleagues who worked and studied alongside me for all these years: Dr. Iryna Alshakova, Dr. Anton Dmitrienko, Dr. Minh Tho Nguyen, John Lortie, Jan-Willem Lamberink, Josh Clarke, Medet Segizbayev, Dinmukhamed Shakhman, Aliona Baradzenka, Brandon Corbett, Billy Petrushko, Allesandro Fabiano, Sruthi Snenahanand Puthiyaveeti, and Raikhan Zakarina. I also want to express my appreciation to the staff members at Brock University: Jordan Vandenhoff from the glassblowing shop, Alison Moffat and Irene Palumbo from the Science Stores. Also, I would like to acknowledge Razvan Simionescu for his valuable help with NMR experiments.

The last but not least, I would like to extend special thanks to my friends and family who were there and supported me all the way throughout this journey.

Table of Contents

List of Tables

List of Figures

List of Schemes

Abbreviations

°C	degrees Celsius
δ	chemical shift
$\Delta H^{\ddagger}$	activation enthalpy
$\Delta S^{\ddagger}$	activation entropy
Å	Ångström
Dipp	2,6-diisopropylphenyl
atm	atmosphere (1 atm = 1 bar, 760 mm Hg, 101.3 kPa, 14.969 psi)
br	broad (NMR)
CAAC	cyclic alkyl amino carbene
COSY	correlation spectroscopy (NMR)
Cp*	η^5-C_5Me_5
Cy	cyclohexyl
d	doublet (NMR)
dd	doublet of doublets (NMR)
ddd	doublet of doublets of doublets (NMR)
DCM	dichloromethane
DEPT	distortionless enhancement by polarization transfer (NMR)
DFT	density functional theory
Dipp	2,6-diisopropylphenyl
dt	doublet of triplets (NMR)
Et	ethyl
g	gram(s)
h	hour(s)
hept	heptet (NMR)
HOMO	highest occupied molecular orbital
Hz	Hertz
^{i}Pr	isopropyl
J	hyperfine coupling constant (NMR)

k	reaction rate constant
K	Kelvin
LUMO	lowest unoccupied molecular orbital
M	central metal atom in a complex
m	*meta*
m	multiplet (NMR)
Me	methyl
Mes	Mesityl (2,4,6-trimethylphenyl)
MHz	megahertz
mmol	millimole(s)
MO	molecular orbital
Mw	molecular weight
NacNac	*β*-diketiminate
NHC	*N*-heterocyclic carbene
NMR	nuclear magnetic resonance
o	*ortho*
p	*para*
Ph	phenyl
q	quartet (NMR)
RT	room temperature
s	singlet (NMR)
SC-XRD	single crystal X-ray diffraction
t	triplet (NMR)
td	triplet of doublets (NMR)
^{t}Bu	*tert*-butyl
THF	tetrahydrofuran
Tol	tolyl
Tripp	2,4,6-triisopropylphenyl
VT	variable temperature

I. Introduction

The development of new classes of main group compounds that have transition metal-like properties has led to increased interest in the chemistry of main group elements in the last three decades.[1] The previously unknown bond activation reactions on main group element compounds have been demontrated.[1-3] This was followed by several examples of insertion reactions, reversible bond activations, and reductive eliminations which showed a potential application of main group reagents in catalytic reactions[2] that is the field traditionally dominated by transition metal complexes. The idea of main group reagents as alternatives to transition metal catalysts is very attractive because in comparison to transition metals many main group elements (calcium, aluminum, silicon etc.) are non-toxic, inexpensive, and abundant.

Gallium (I) β-diketiminate compound, NacNacGa, was prepared by Power and coworkers in 2000.[4] It is a group 13 carbenoid with filled and empty orbitals available for interaction with small molecules. However, since the first report, there have been a limited number of studies on the reactivity of this compound. Oxidative addition of element-hydrogen single bonds (N–H , P–H, O–H, Sn–H, and H–H) to NacNacGa has been reported by Linti *et al*.[5] Activation of group 13 – 15 halides (Ga-Cl, Sn-Cl, SI-Cl, C-Cl, P-Cl, P-Br, As-Cl)[6, 7], oxide (Bi-O)[8], amides (As-N, Bi-N)[7], and alkyls (Ga-Me, In-Et, Bi-Et)[6, 9, 10] by NacNacGa and reversible insertion of NacNacGa into Sb-Sb and Bi-Bi bonds has also been shown.[11] More recently heterodiatomic compounds containing Ga–E (E = As, Sb, P) double

bonds, gallaarsene,[12] gallastibene,[13] and gallaphosphene[14-17] were prepared and applied in bond activation reactions.

Oxidative addition is an important step in many metal-catalyzed reactions. The goal of this thesis is to investigate further the reactivity of NacNacGa, with the hope of finding new and exciting reactivity patterns. One particular topic that is prevalent in transition metal chemistry and catalysis but is little delineated in the main group chemistry is the preparation and reactivity of heavy (period 3 and below) main group element oxides, imides, and alkylidenes. Their transition metal analogues have been known for many decades and find important applications in the oxidation reactions, imination reactions and olefin metathesis reactions, which has been recognized by several Nobel Prizes (B. Sharpless, R. Grubbs, R. Schrock, Y. Chauvin). In contrast, such reactions are almost untapped in the main group chemistry.

The first part of this thesis focuses on the historical background that will cover reactions of low valent main group compounds with unsaturated molecules and on the overview of group 13 oxides and imides and their reactivity.

In the Results and Discussions chapter of this Thesis, the reactivity of low valent gallium complex, NacNacGa, will be discussed. Particularly, reactions of NacNacGa with unsaturated reagents (Chapter III.1), *in situ* oxidation of the Ga(I) species and the reactivity of intermediate monomeric gallium oxide (Chapter III.2) and imide (Chapter III.3), and the preparation and reactivity study of a gallium nitrilimine (III.4) will be highlighted.

II. Historical

II.1. Reactivity of Main Group Compounds with Unsaturated Molecules

The distinguishing characteristics of transition metals include the availability of several oxidation states and the presence of partially occupied d orbitals. This specific electronic situation makes it possible for coordination and activation of strong single and multiple bonds, which is often the key step in catalytic processes.[18] An easy cleavage of bonds on a metal center is one of the common requirements for faster reactions and benign conditions in catalytic processes, and the fulfillment if this criterion has led to a remarkable success of transition metal catalysis. In contrast, for many years main group compounds have been believed to be unreactive towards small molecules. However, new classes of main group compounds, including reagents containing multiple bonds between heavier main group elements[19] and/or low oxidation states[20, 21] have recently become available (Scheme 1).

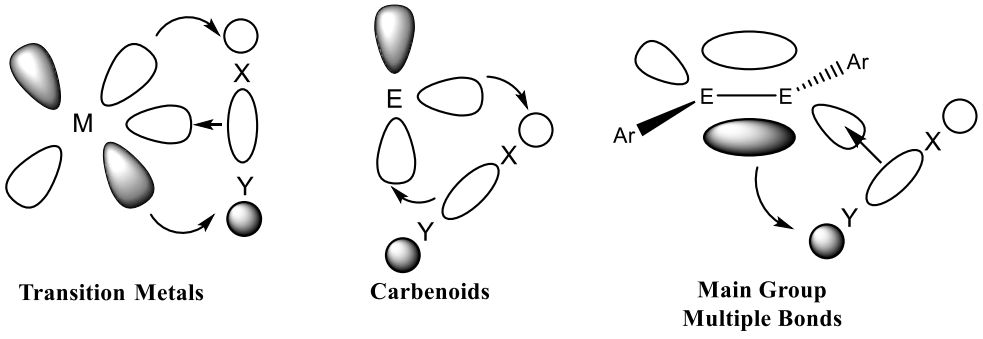

Scheme 1. Interaction of small molecules with transition metals and low oxidation state and multiple-bonded main group compounds.

These reactive compounds possess a lone pair of electrons and an empty orbital localized on the main group element center, which resembles the partially filled d orbitals of transition metals. The unique structures of these reagents provide accessible frontier orbitals amenable to interact with small molecules, as depicted in Scheme 1.

The seminal work of Power and co-workers on the H–H bond cleavage by a digermyne[22] has inspired further studies on strong σ bond activations on main group centers.[2] Even the cleavage of robust C-F bonds on main group element centers has been observed.[23-26] However, the interaction of unsaturated substrates with main group compounds is less studied and needs further development. In this part of the historical review, the progress in investigation of the reactivity of main group compounds towards unsaturated organic compounds will be discussed.

II.1.1. Reactions of Alkenes and Alkynes with Main Group Compounds

Reactions of alkenes and alkynes with transition metals has been studied extensively in the literature and applied in numerous catalytic transformations.[18] Interaction of the C-C double and triple bonds with partially filled d orbitals of transition metals is commonly described by the Dewar−Chatt−Duncanson diagram.[27, 28] Low-valent main group compounds also possess energetically available filled and empty orbitals for the interaction with alkenes and alkynes in a manner similar to transition metals. Therefore, reactivity of main group compounds towards reagents having an unsaturated C-C bond has been a subject of considerable interest with potential application in catalysis. Earlier reports started with cycloaddition of alkenes and alkynes with main group reagents. More recently insertion and reversible addition reactions have been presented.

II.1.1.1. Group 13

Borylenes (RB:) are highly reactive compounds containing a monovalent boron atom possessing an empty orbital and two unshared electrons.[29] Free borylenes have not been isolated and were only investigated by microwave spectroscopic studies[30] and infrared spectroscopy in inert gas matrices.[31, 32] The *in situ* reactivity of free borylenes towards unsaturated hydrocarbons was studied by Timms.[33-35] Transient borylenes XB: (**II-1**, X = F and Cl) generated from the reduction of boron trihalides by solid boron at 2000°C were condensed at -196°C and reacted with acetylene and propene. The reaction of borylenes with acetylene resulted in the formation of 1,4-diboracyclohexa-2,5-diene **II-2** (Scheme 2). The

author proposed formation of an intermediate boracyclopropene from a cyclization of an alkyne with boron carbenoids, borylenes. Boracyclopropene then dimerizes to yield **II-2**.

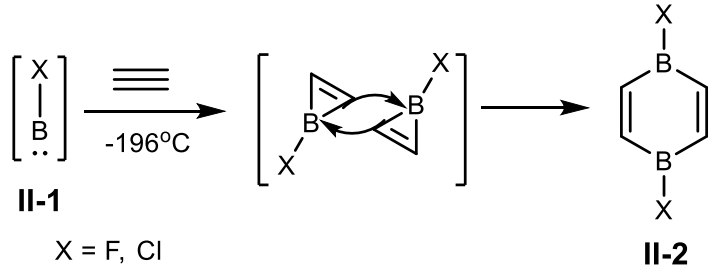

Scheme 2. Reaction of acetylene with borylene **II-1**.

Similarly, 1,4-diboracyclohexane **II-3** was formed from the reaction of BCl with propene believed to be the product of a dimerization of a boracyclopropane intermediate (Scheme 3). In contrast, treatment of BF with propene resulted in 1,2-bis(difluoroboryl)propane **II-4** which is explained by a reaction of residual BF_3 with boracyclopropane.

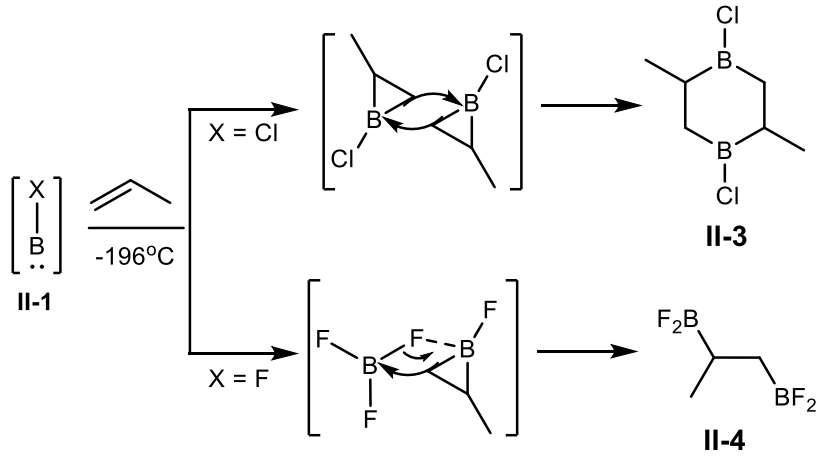

Scheme 3. Reaction of propene with borylene **II-1**.

Borylenes can be stabilized by complexation with transition metals[36, 37] and Lewis bases, such as carbenes.[38, 39] In an attempt to prepare Lewis base-stabilized borylenes, the Robinson group obtained a diborene from the reduction of (NHC)-BBr_3 (NHC – N-heterocyclic carbene) which can be viewed as a dimer of borylene.[40] Phosphine-stabilized diborenes **II-5** and (CAAC)-stabilized (CAAC – cyclic (alkyl)(amino) carbene) diboracumulene **II-7** prepared by Braunschweig *et al*. show reactivity with alkynes (Scheme 4).[41]

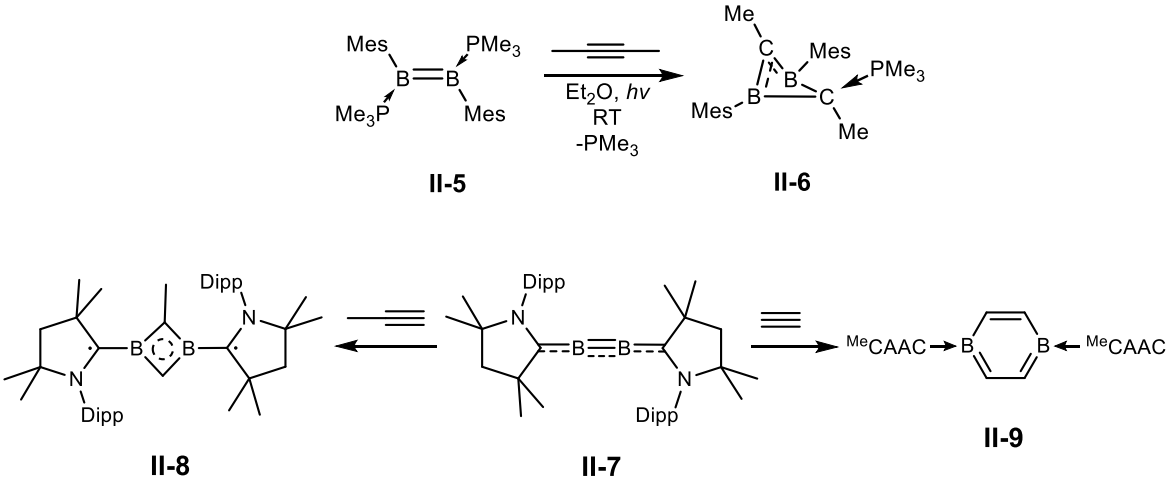

Scheme 4. Reactions of alkynes with diborenes **II-5** and **II-7**.

The reaction of 2-butyne with phosphine-stabilized diborene (**II-5**) under photolytic conditions resulted in phosphine-stabilized 1,3-dihydro-1,3-diborete (**II-6**) having the alternating B-C-B-C motif (Scheme 4).[42] The authors suggested the initial [2+2] cycloaddition between alkyne and diborene forming 1,2-dihydro-1,2-diborete which then rearranges to a more stable 1,3-isomer **II-6**. The CAAC-stabilized diboracumulene **II-7** features a bonding situation intermediate between that of a double and triple B-B bond because of the π-accepting character of the CAAC ligands.[43] Its reaction with propyne leads to a 2π-aromatic diborete biradicaloid **II-8** instead of a 4π-antiaromatic 1,3-

diboracyclobutadiene. Treatment of **II-7** with acetylene resulted in the 6π-aromatic 1,4-diborabenzene product **II-9** having an intact C-C connectivity.

Low-valent aluminum compound **II-10**, which is an aluminum carbenoid, has also been demonstrated to react with alkynes. The first example of aluminacyclopropene **II-11** was produced by Roesky *et al*. from an *in situ* reduction of $NacNacAlI_2$ (NacNac = $[DippNC(Me)CHC(Me)Ndipp]^-$, Dipp = 2,6-$^{i}Pr_2C_6H_3$) in the presence of alkynes.[44] **II-11** can be described as an AlC_2 aromatic heterocycle with delocalized 2π electrons. The isolable low-valent aluminium compound **II-10**,[45] designated below as NacNacAl, was then applied in the reaction with acetylene to form **II-11** as a result of oxidative addition of an alkyne (Scheme 5).[46] Adding a second equivalent of an alkyne to **II-11** led to the insertion of the C-H bond of alkyne into the Al-C bond to form an alkenylalkynylaluminum compound **II-12**. Roesky and Cui later extended the reactivity of Al(I) **II-10** to other alkynes and showed that they react in the same manner (Scheme 5).[47] The Al-η^2C_2 bond dissociation energies of **II-11** were calculated to be 82.6 – 155 kJ mol^{-1}, pointing to a weak Al-η^2C_2 bond and its reactivity to the second equivalent of alkyne.

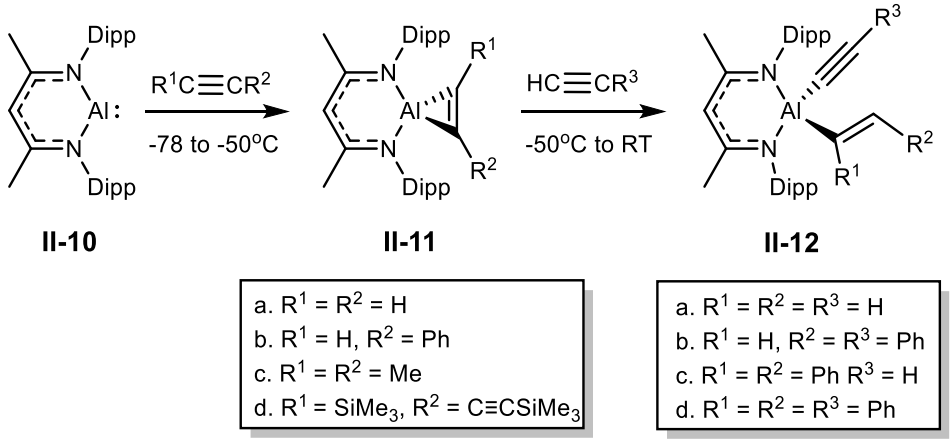

Scheme 5. Reaction of Al(I) **II-10** with alkynes.

A comprehensive study of the reactivity of NacNacAl **II-10** towards various olefins was performed by the Crimmin group. Treatment of the compound **II-10** with norbornene resulted in addition of C=C bond to Al(I) with the formation of aluminacyclopropane **II-13** (Scheme 6).[25] The product of the reaction was then heated above 60°C, which led to the elimination of the alkene as monitored by VT NMR spectroscopy (VT – variable temperature). This is a rare example of a reversible redox process on a low-valent main group center.

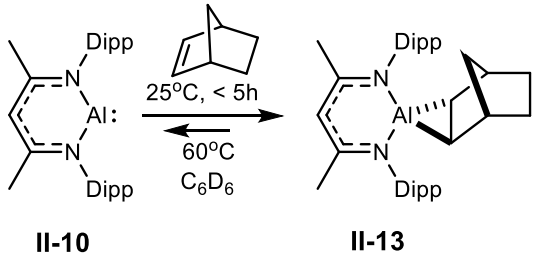

Scheme 6. Reaction of Al(I) **II-13** with norbornene.

The scope of the reversible addition of the C=C bond to the Al center was expanded to a series of terminal and internal alkenes (Scheme 7).[48] Treatment of **II-10** with ethylene, propylene, hex-1-ene, 3,3-dimethyl-1-butene, allylbenzene and 4-allylanisole resulted in [1+2] cycloaddition with the formation of corresponding metallocyclopropanes (**II-14 a-f**).

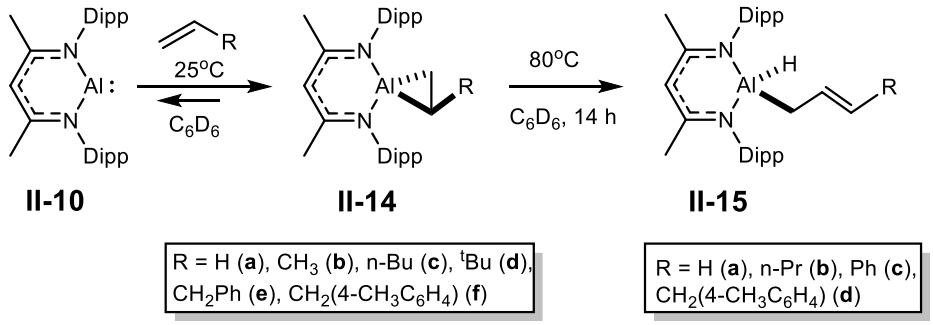

Scheme 7. Reversible alkene binding to **II-10**.

All the reactions were reversible under mild conditions (25 – 80°C), with higher temperatures favoring reactants, and the position of equilibrium depended on the nature of the olefin (Table 1). A van't Hoff analysis showed binding of norbornene and hex-1-ene to the compound **II-10** to be exergonic, with $\Delta G°_{298\ K}$ = -7.9 and -4.3 kcal mol^{-1}, respectively. Heating aluminacyclopropane for a prolonged amount of time led to allylic C-H activation forming aluminum hydride complexes **II-15 a-d**.

Alkene	II-10 : II-14
norbornene	<1 : >99
ethylene	<1 : >99
propylene	14 : 86
1-hexene	18 : 82
3,3-dimethyl-1-butene	10:90
allylbenzene	2 :98

Table 1. Equilibrium data for alkene binding to **II-10**.

The Al(I) compound **II-10** undergoes a [1+4] cycloaddition reaction with 1,3-cyclohexadiene to form a [2.2.1] metallobicycle **II-16** (Scheme 8).[49] In contrast to the formation of aluminacyclopropanes (**II-14**), the process described in Scheme 7, this reaction is not reversible. A solution of **II-16** in deuterated benzene was treated with 1 atm of CO, which led to insertion of CO into the Al-C bond resulting in an aluminum-based [2,2,2] metallobicycle **II-17**. A reverse reaction with the release of CO occurs upon heating the compound **II-17** at 100°C.

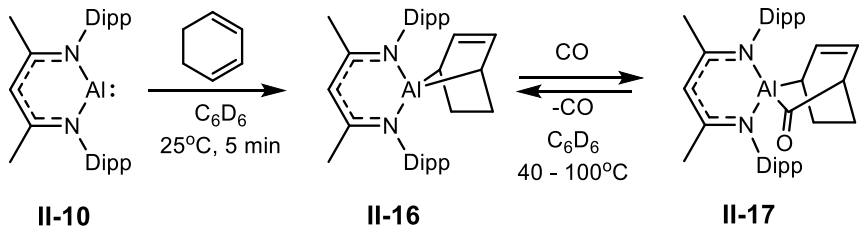

Scheme 8. Reaction of **II-10** with cyclohexadiene and reversible CO insertion to **II-16**.

Nitrogen-based dianionic ligands were applied to stabilize anionic low-valent group 13 compounds. Anionic low-valent gallium compounds have been known for over 20 years and their coordination chemistry is well-established (Scheme 9).[20, 50-52]

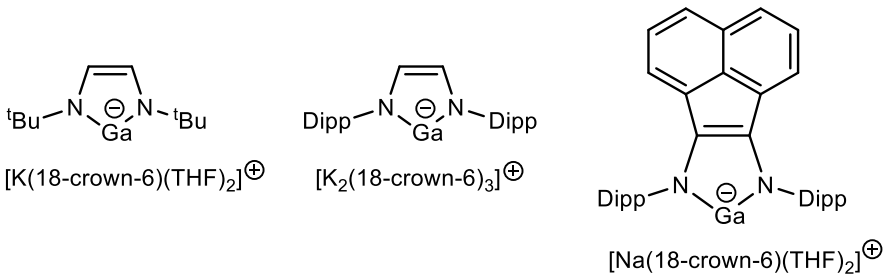

Scheme 9. Anionic gallium(I) compounds.

In contrast, the first example of an anionic aluminum (I) complex (**II-18**) was prepared in 2018 by Aldridge and co-workers.[53, 54] Potassium aluminyl **II-18** $[K(Al(NON)]_2$ (NON=4,5-bis(2,6-diisopropylanilido)-2,7-di-tert-butyl-9,9-dimethyl xanthene), features a nucleophilic aluminum center and is highly reactive. For example, it was applied in activation of dihydrogen and the C-H bond cleavage of benzene.[53] **II-18** also showed a [1+2] cycloaddition reaction with ethylene yielding compound **II-19** (Scheme 10).[54, 55]

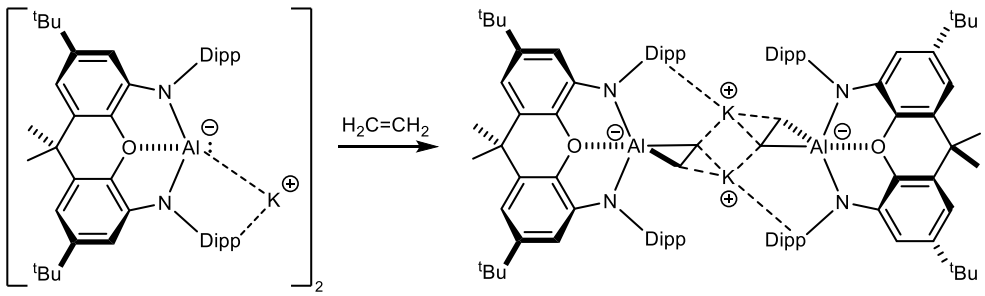

II-18 **II-19**

Scheme 10. Reaction of aluminyl anion **II-18** with ethylene.

Dialkylaluminum anion **II-20** prepared by Yamashita *et al*.[56] undergoes [1+2] cycloaddition with diphenylacetylene and E/Z stilbene, as demonstrated in Scheme 11.[57] Reacting (E)- and (Z)-stilbenes with the Al(I) compound **II-20** resulted in the *trans*-cycloaddition product **II-21** exclusively. DFT calculations suggested involvement of a carbanionic transition state for the addition of (Z)-stilbene, which explains the *trans* configuration of the product. Cyclization of diphenylacetylene and stilbene happens in a concerted fashion with the formation of three-membered cyclic products **II-21** and **II-22**, respectively.

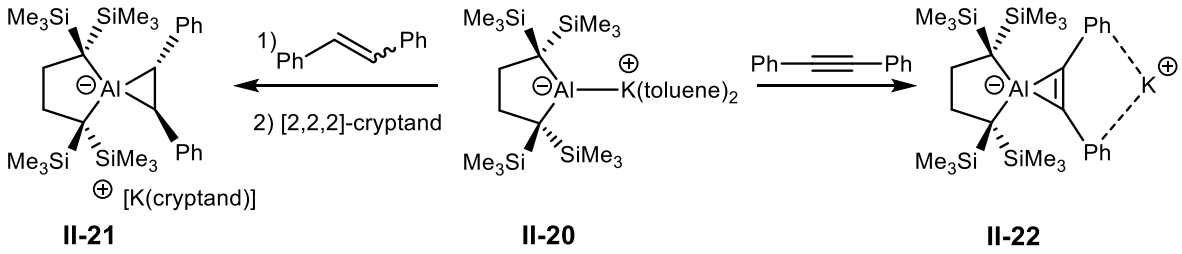

Scheme 11. Reaction of dialkylaluminum anion **II-20** with alkene and alkyne.

Dimetalanes with a single bond between the main group elements are another interesting example of subvalent main group compounds. Fedushkin *et al*. reported activation of alkynes by the Al(II) compound (dpp-bian)Al–Al(dpp-bian) (**II-23**, dpp-bian = 1,2-[(2,6-dipp)NC]$_2$C$_{12}$H$_6$) supported by a redox-active diamide ligand (Scheme 12).[58] Acetylene and phenylacetylene undergo cycloaddition across the Al-N-C moiety giving the adduct **II-24**, which has new C-C and Al-C bonds. Heating the adducts with terminal alkyne, phenylacetylene, resulted in the formation of an aluminum compound with two bridging alken-1,2-diyl moieties and a radical-anionic bis(amido) ligand **II-25**. Dialane **II-23** was reacted with an internal alkyne, methylphenylacetylene, as well. However, the reaction

required excess of alkyne to produce the double cycloaddition product **II-24c**. Heating **II-24c** at 60°C led to elimination of one molecule of alkyne and isolation of a monoadduct of dialane with the internal alkyne, **II-26**.

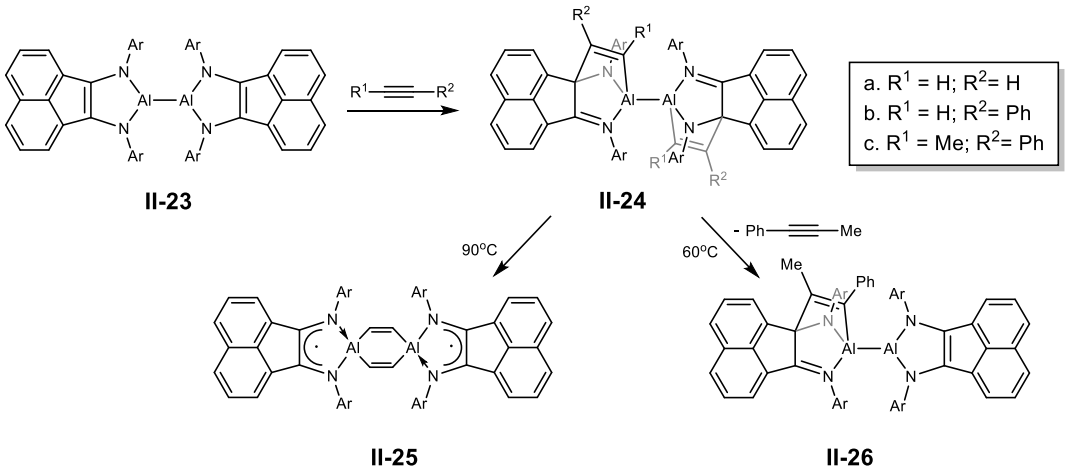

Scheme 12. Reaction of dialane **II-23** with alkynes.

Reactivity of dialumane compound **II-27**, supported by an α-diimine ligand, towards various alkenes was studied by Yang *et al*. (Scheme 13).[59] Treatment of the Al(II) compound **II-27** with (E)- and (Z)-stilbene and styrene resulted in insertion of C=C into the Al-Al bond with the formation of Al(III) products **II-28** and **II-29**, respectively**.** Furthermore, reactions of **II-27** with various conjugated dienes, 2,3-dimethyl-1,3-butadiene and 2-methyl-1,3-butadiene, in the presence of sodium metal led to cycloaddition products **II-30**, **II-31**, and **II-32**: [1+4] cycloaddition was seen in toluene, whereas [2+4] double cycloaddition was observed in dimethoxyethane. To study the mechanism of reaction, DFT calculations were performed. The proposed mechanism involves initial reduction of dialumane to dialumene with an Al-Al double bond. It was also suggested that the dialumene exists in equilibrium with an Al(I) carbenoid monomer. Al(I) monomeric species can undergo [1+4] cycloaddition with butadienes yielding aluminacyclopentenes **II-30** and **II-31**. For the [2+4] cyclization,

the first step involves dialumene cycloaddition with one molecule of diene to give a biradicaloid. This biradicaloid then undergoes barrierless cyclization with a second molecules of butadiene with the formation of **II-32**.

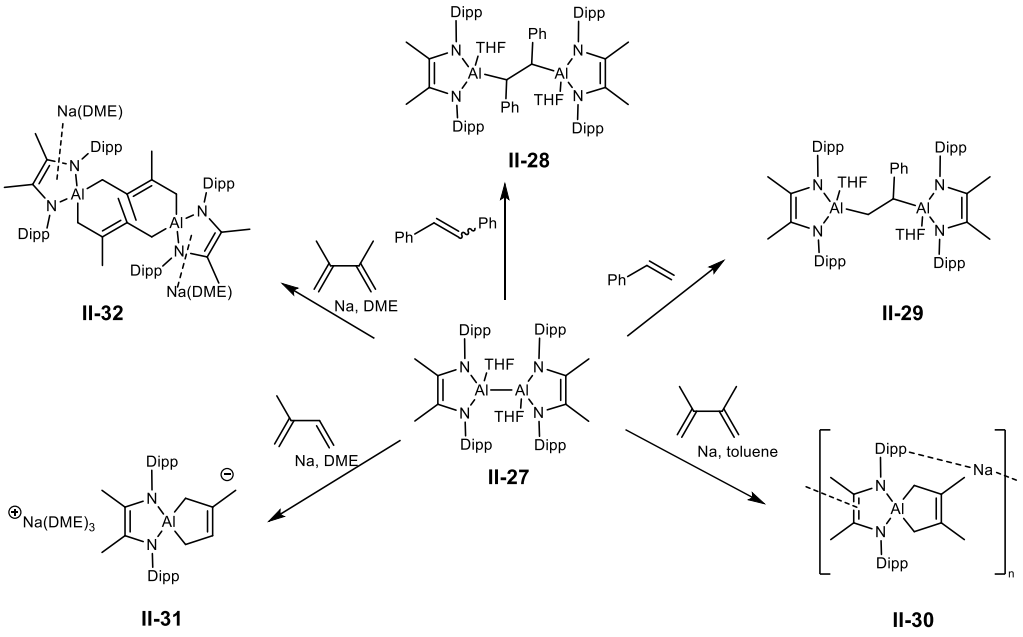

Scheme 13. Reaction of dialane **II-27** with alkenes.

Dialumane **II-27** was also reacted with alkynes (Scheme 14).[60] Treatment of **II-27** with one equivalent of diphenylacetylene led to the insertion of the C-C triple bond into the Al-Al bond, producing **II-33**. In contrast, a reaction of **II-27** with an excess of a terminal alkyne resulted in cycloaddition of the alkyne across the Al-N-C fragment forming **II-34**. Using only one equivalent of phenylacetylene did not produce an insertion product; instead, it resulted exclusively in cyclization. From this, the authors concluded that cycloaddition is more favorable than insertion and the use of diphenylacetylene leads to insertion due to steric reasons.

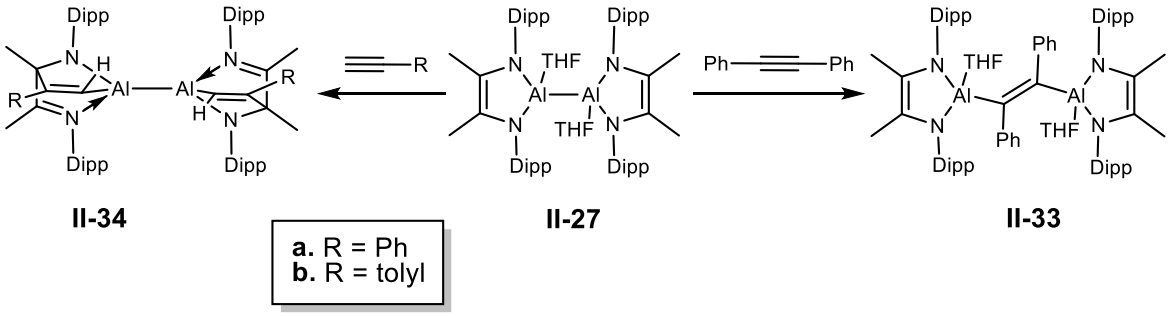

Scheme 14. Reaction of **II-27** with alkynes.

Synthesis of Al–Al double-bonded compounds (RAl=AlR) has been a challenging task and attempts to isolate them have led to masked dialumenes formed as a result of a [2+4] cycloaddition between the Al=Al bond and benzene or toluene.[61, 62] In 2017, the Inoue group isolated the first stable Al–Al double-bonded species (**II-35**, Scheme 15) stabilized by strong σ-donating tertbutyl(methyl)silyl groups and NHC ligands.[63] An X-ray structure of the compound **II-35** showed a *trans*-planar geometry with a short Al-Al bond of 2.3943(16) Å. DFT calculations also supported the double bond character of the Al–Al bond in **II-35.** Compound **II-35** undergoes a [2+2] cycloaddition reaction with ethylene producing **II-36** (Scheme 15). Reaction of **II-35** with phenylacetylene resulted in a [2+2] cycloaddition and C-H insertion to produce **II-37** and **II-38**. A derivative of dialumene with aryl groups instead of silyl groups was prepared more recently[64] and it was found to be more reactive than **II-35**. The aryl derivative of **II-35** was shown to react with an internal alkyne, diphenylacetylene, which was explained by a better steric accessibility of dialumene and by its higher electrophilicity.

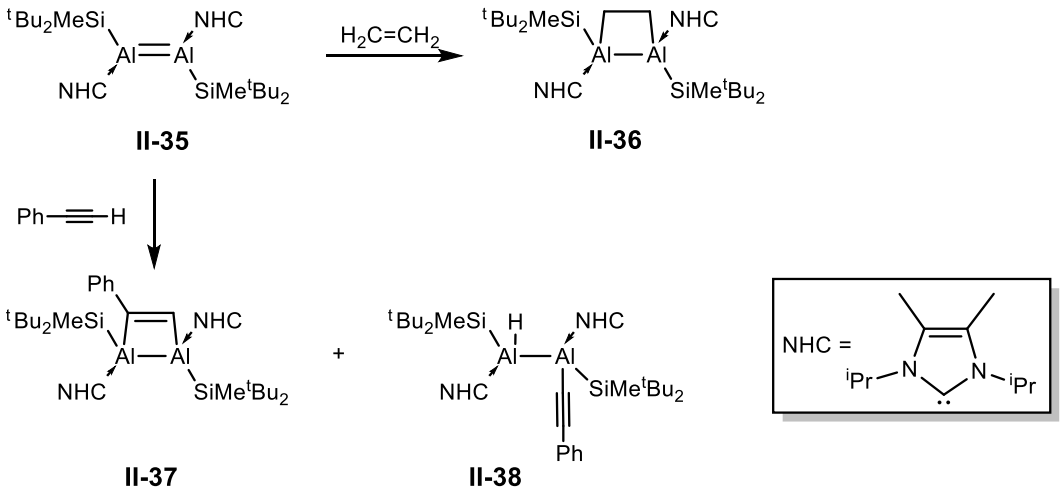

Scheme 15. Reaction of **II-35** with alkene and alkyne.

Power *et al*. prepared a series of Ga(I) compounds with bulky terphenyl ligands which, depending on the size of the terphenyl groups, exist either as monomers (ArGa) or dimers (ArGa=GaAr) in the solid state, and digallenes (ArGa=GaAr) that dissociate into monomers in solution.[65] Treatment of the Ga(I) compound ArGa (**II-39**, Ar = 2,6-(2,4,6-$^{i}Pr_3$-C_6H_2)$_2$-C_6H_3) with 2,3-dimethyl-1,3-butadiene led to the cycloaddition product **II-40** with a 10-membered Ga_2C_8 ring (Scheme 16). The Ga---Ga separation of 5.736 Å points to the absence of a Ga-Ga interaction suggested by the comparison to the doubled value of the covalent radius of gallium (2 × 1.22 Å = 2.44 Å).[66]

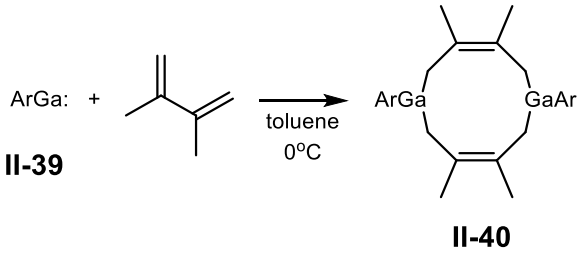

Scheme 16. Reaction of Ga(I) **II-39** with diene.

Digallene ArGa=GaAr (**II-41**, Ar = 2,6-Dipp$_2$-C$_6$H$_3$) reacts with two equivalents of phenylacetylene to form 1,4-digallatacyclohexadiene (**II-42**) (Scheme 17).[67] Two-electron reduction of **II-42** with potassium metal afforded 1,4-digallatabenzene (**II-43)**. Analysis of **II-43** with NMR spectroscopy and DFT calculations suggested that 1,4-digallatabenzene is a 6π aromatic system and its X-ray diffraction study revealed a planar Ga_2C_4 ring with K^+ ions above and below the plane.

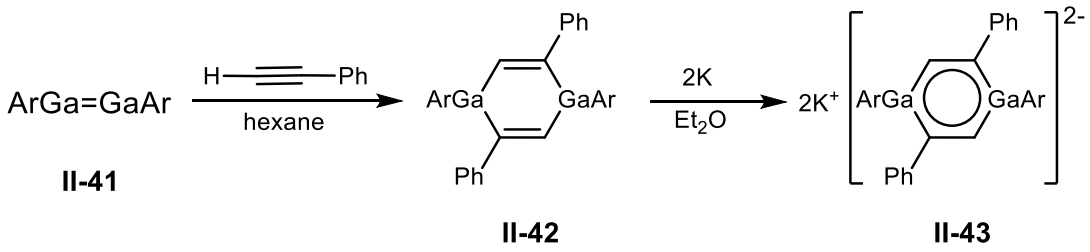

II-41 **II-42** **II-43**

Scheme 17. Reaction of digallene **II-41** with phenylacetylene.

Digallene ArGa=GaAr **II-41** was also reacted with a series of terminal olefins: ethylene, propene, 1-hexene and styrene (Scheme 18).[68] X-ray characterization of the products of these reactions (**II-44 a-d**) revealed 1,4-digallacyclohexane structures. In contrast, internal olefins did not show any reactivity with **II-41**. Even though digallenes are known to dissociate into monomers in solution, DFT calculations predict that it is the intact ArGa=GaAr dimer that undergoes stepwise [2+2+2] cycloadditions with olefins.[69]

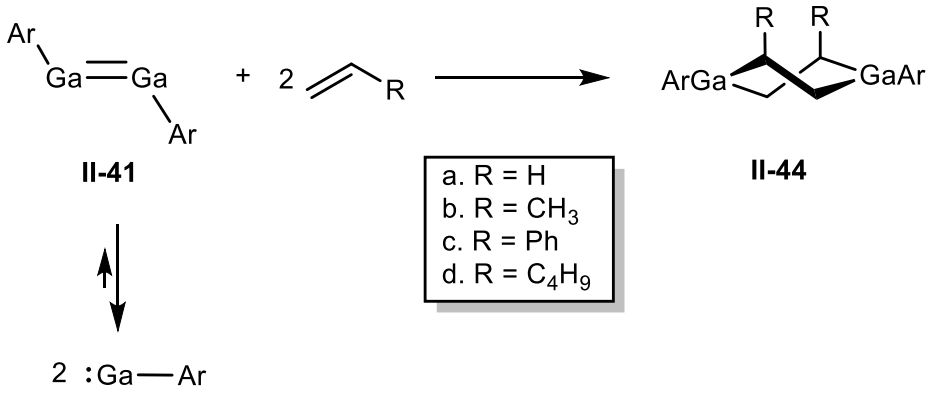

Scheme 18. Reaction of **II-41** with terminal alkenes.

A gallium compound supported by a redox-active chelating diamide ligand (dpp-bian)Ga–Ga(dpp-bian)[70] (**II-45**) undergoes reversible cycloaddition reaction with alkynes (Scheme 19).[71, 72] The cycloaddition of acetylene, phenylacetylene, and alkylbutynoate across the Ga-N-C fragment of the gallium complex with the formation of compounds **II-46 a-d** was reported by the Fedushkin group. Elimination of alkyne with the formation of the starting digallane **II-45** was observed at elevated temperatures. Thermodynamic parameters for alkyne elimination were determined to be $\Delta G°$=2.4 kJ mol^{-1}, $\Delta H°$=46.0 kJ mol^{-1}, $\Delta S°$=146.0 $JK^{-1}mol^{-1}$.

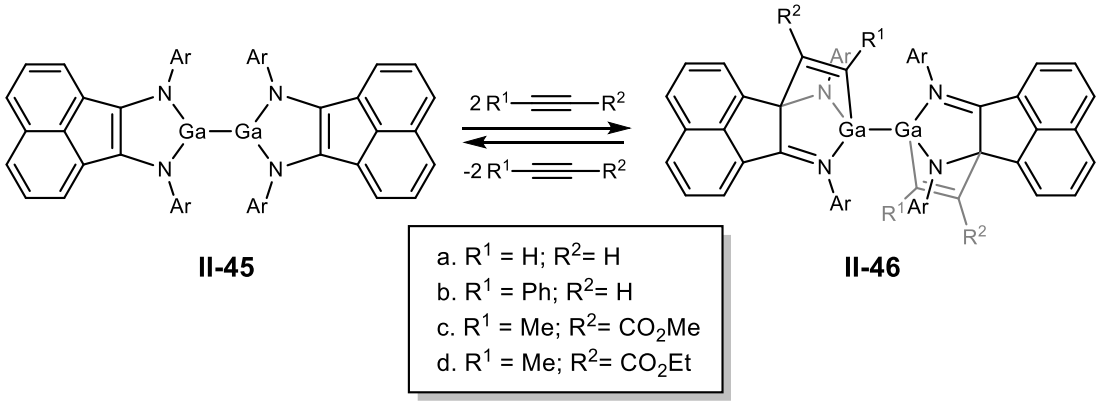

Scheme 19. Reactions of **II-45** with alkynes.

Reversible addition of alkynes to digallane **II-45** was utilized in catalytic hydroamination of phenylacetylene with anilines and hydroarylation with aminoanthracene (Scheme 20).[72] Hydroamination was proposed to go via a nucleophilic attack of aniline on the cycloaddition product **II-46** followed by a proton transfer. The elimination of the α-aminoalkene regenerates the catalyst. The α-aminoalkene then tautomerizes to a more stable imine product. Hydroarylation of phenylacetylene with aminoanthracene was explained by an increase in nucleophilicity of the ortho-carbon in the extended π-system.

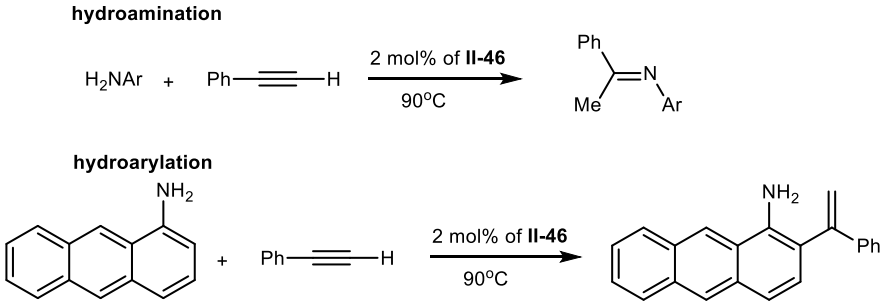

Scheme 20. Hydroamination and hydroarylation of phenylacetylene catalyzed by **II-46**.

II.1.1.2. Group 14

Carbenes (R_2C:) are compounds containing a two-valent carbon with an empty orbital and two unshared electrons. Depending on substituents, carbenes exist in either triplet or singlet ground states. *In situ* generated carbenes undergo [1+2] cycloaddition reactions with alkenes forming cyclopropanes.[73] Isolable carbenes, such as N-heterocyclic carbenes, generally do not react with alkenes. However, electrophilic diamido carbenes have been shown to react with alkenes and alkynes forming, cyclopropanes and cyclopropenes.[74]

Heavier group 14 analogues of carbenes, such as silylenes, have singlet ground states and generally react with alkenes and alkynes in a concerted manner, forming silacyclopropanes (siliranes) and silacyclopropenes (silirenes).[75] Earlier reports on reactions of silylenes with alkenes and alkynes involved silylenes generated *in situ* by thermolysis or photolysis.[75] Kira *et al*. reported a reaction of an isolable dialkylsilylene **II-47**[76] with alkenes and alkynes (Scheme 21).[77] The expected siliranes **II-48 a-b** and silirenes **II-49 a-b** were obtained as a result of a [1+2] cycloaddition between the silylene and the C-C unsaturated bond.

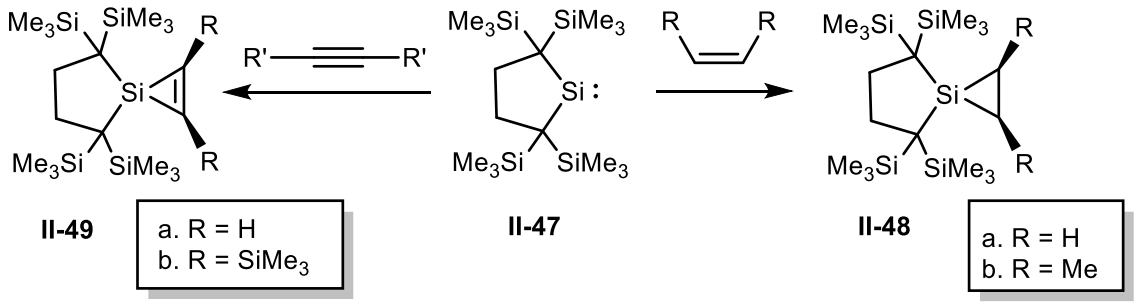

Scheme 21. Reactions of silylene **II-47** with alkenes and alkynes.

More recently there have been remarkable reports on reversible alkene binding to Group 14 compounds. Bacareido and Kato described the synthesis of phosphonium silaylides **II-50**, heavier analogues of the Wittig reagent.[78] Treatment of the compound **II-50** with ethylene at room temperature resulted in the formation of a pentacoordinate silirane **II-51** (Scheme 22).[79] Ethylene pressure directly affects the reaction. Decrease in the pressure of ethylene gas led to regeneration of the starting compound **II-51**. Solutions of adducts **II-51a** and **II-51b** are stable at low temperatures (< -20°C). A van't Hoff analysis of the addition of ethylene to **II-51a** showed a small value of $\Delta G = -0.717 \pm 0.452$ kJ mol^{-1} at 20°C, which is in agreement with the reversibility of the reaction. The stability of silacyclopropane depends on the nucleophilicity of the phosphine group. Thus, when R = Ph the adduct is stable and the reverse reaction is not observed even at elevated temperatures.

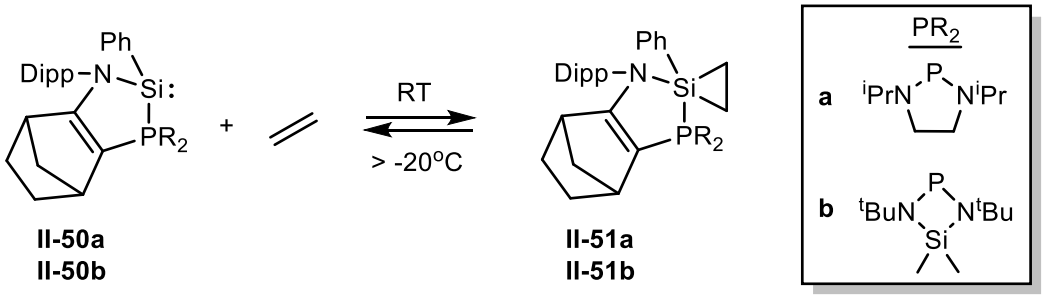

Scheme 22. Reversible reaction of silylene **II-50** with ethylene.

The reversible reaction of a two-coordinate dithiolato silylene **II-52** with ethylene was demonstrated by Power *et al*. (Scheme 23).[80] The reaction was monitored by NMR spectroscopy which showed signals for the silirane **II-53** together with free silylene **II-52** and ethylene, indicative of a dissociation equilibrium. A van't Hoff analysis of the addition reaction was performed by VT NMR spectroscopy and showed $\Delta G = -24.9(\pm 2.5)$ kJ mol^{-1}

at 300 K, which indicates the ethylene binding to **II-52** is more favorable than to the silylene phosphine adduct **II-50**.

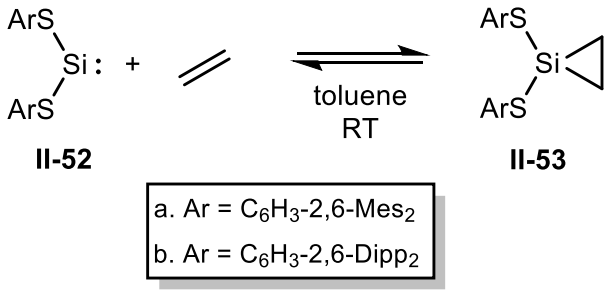

Scheme 23. Reversible reaction of silylene **II-52** with ethylene.

The first example of migratory insertion of an alkene into the Si-Si bond was reported by Rieger *et al*. (Scheme 24).[81] Treatment of acyclic silylsilylene **II-54** with ethylene at room temperature affords the silirane product **II-55**. Heating compound **II-55** in the atmosphere of ethylene at 60°C led to the unique insertion of ethylene into the Si-Si bond of silirane, forming compound **II-56**.

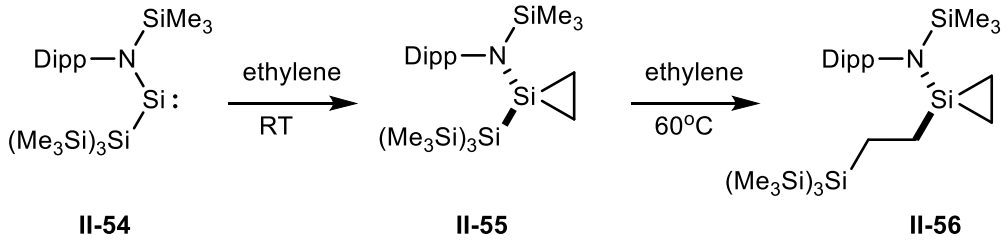

Scheme 24. Reaction of silyl silylene **II-54** with ethylene.

Deuterated ethylene was employed to elucidate the mechanism of the insertion. Monitoring NMR spectra of the reaction progress revealed intramolecular insertion of coordinated ethylene from silirane **II-55** into the Si-Si bond, followed by coordination of a second

molecule of ethylene. Compound **II-54** was also reacted with 2,3-dimethyl-1,3-butadiene to give a [1+4] cycloaddition product silacyclopent-3-ene.

Chlorosilylene **II-57** LSiCl (L = $PhC(NtBu)_2$) was reacted with diphenylacetylene to produce the disilacyclobutene **II-59** (Scheme 25).[82] The proposed mechanism involves an initial oxidative addition of alkyne to chlorosilylene **II-57** with the formation of an intermediate three-membered cyclic species **II-58**. A second equivalent of silylene inserts into the C-Si bond of silirene **II-58** to afford the disilacyclobutene **II-59** with a new Si-Si bond.

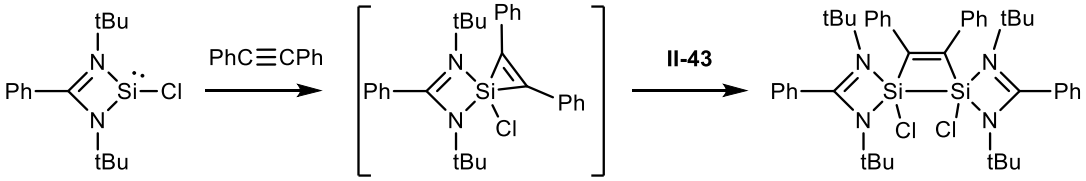

II-57 **II-58** **II-59**

Scheme 25. Reaction of chlorosilylene **II-57** with diphenylacetylene.

The temperature-dependent reaction of the zwitterionic silylene[83] **II-60** with terminal alkynes was studied by Driess *et al*. (Scheme 26).[84] The reaction resulted in the C-H insertion (products **II-61a** and **II-61b**) at room temperature and [1+2] cycloaddition (products **II-62a** and **II-62b**) at -78°C. The preference for the C-H insertion is explained by the 1,4-dipolar nature of the silylene **II-60**. Reacting **II-60** with an internal alkyne, diphenylacetylene, resulted exclusively in the [1+2] cyclization with the formation of a silirene **II-63.** The treatment of the insertion product **II-61** with the starting silylene **II-60** led to a double insertion product **II-64**. Attempts to generate the insertion product **II-61** by heating the silirene **II-62** failed, which ruled out the intermediacy of a silacyclopropane in the C-H

insertion. The silylene **II-60** also undergoes a [1+4] cycloaddition with 2,3-dimethylbuta-1,3-diene to form a silacyclopentene as discussed in a later report.[85]

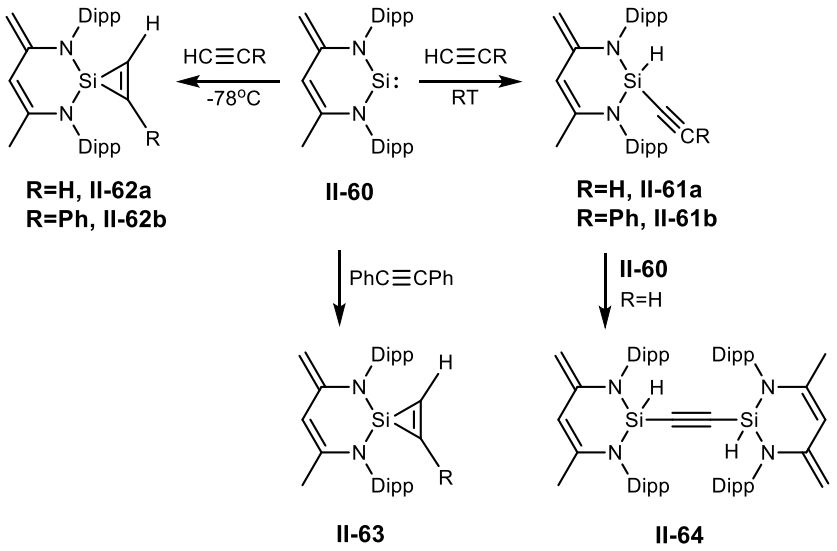

Scheme 26. Reactions of silylene **II-60** with alkynes.

Sekiguchi *et al*. prepared the first example of a Si-Si triple-bonded compound, the disilyne RSi≡SiR (R=Si^{i}Pr[CH(SiMe$_3$)$_2$]$_2$) (**II-65**) in 2004.[86] The reactivity of disilyne **II-65** with alkenes and alkynes was then studied (Scheme 27).[87]

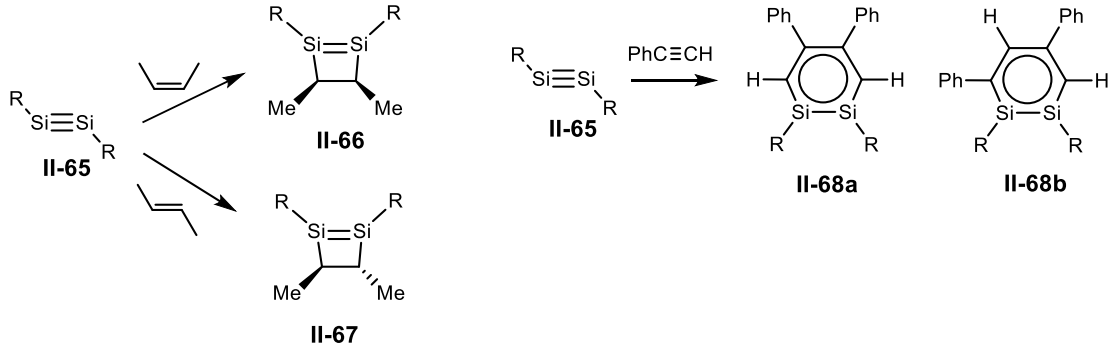

Scheme 27. Reactions of disilyne **II-65** with *cis/trans*-butadiene and phenylacetylene.

Addition of *cis*-2-butene to **II-65** results in *cis*-3,4-dimethyl-1,2-disilacyclobutene **II-66** whereas *trans*-2-butene led to *trans*-3,4-dimethyl-1,2-disilacyclobutene **II-67**. Theoretical calculations on the reaction mechanism revealed a [1+2] cycloaddition, forming the silirane, to be the first step, then an intramolecular insertion of silylene into the Si-C bond results in silacyclobutene products. A reaction of **II-65** with phenylacetylene resulted in 1,2-disilabenzene derivatives **II-68a** and **II-68b**, which are formed via a 1,2-disilacyclobutadiene-like intermediate.

The Tokitoh group reported a reaction of disilyne, supported by bulky aryl groups ArSi≡SiAr **II-69**, with ethylene that results in product **II-70** (Scheme 28).[88] The reaction is proposed to proceed via a silacyclobutene that dissociates into a bis-silylene, which then undergoes a [1+2] cycloaddition with excess of the alkene.

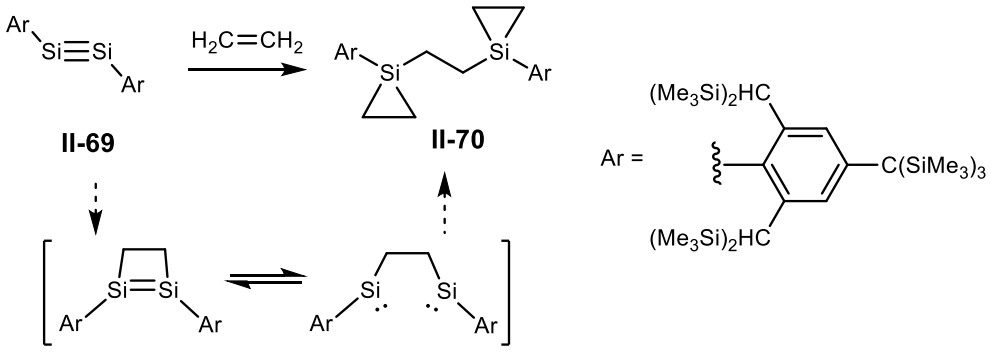

Scheme 28. Reaction of disilyne **II-69** with ethylene.

The Ando group studied the reactivity of germylene with ethylene. Treatment of the germylene R_2Ge: **II-71** (R = $(Me_3Si)_2CH$) with ethylene resulted in the 1,2-digermacyclobutane **II-73** (Scheme 29).[89] Monitoring the reaction via NMR spectroscopy showed the formation of an intermediate which was assigned to be the germirane **II-72**

formed from cycloaddition between the germylene and ethylene. A second equivalent of germylene then inserts into the Ge-C bond of germirane to form **II-73**.

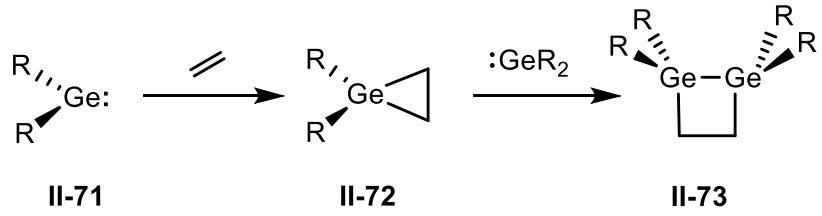

Scheme 29. Reaction of germylene **II-71** with ethylene.

A germanium analogue of alkyne, ArGe≡GeAr (**II-74**) was also reacted with ethylene (Scheme 30).[90] The initial product of the reaction was 1,2-digermacyclobutene **II-75**. The formation of 1,2-digermacyclobutene **II-75** can be explained by a [1+2] cycloaddition between ethylene and digermyne, forming a germylene germirane intermediate followed by insertion of the germylene into the Ge-C bond. **II-74** further reacts reversibly with an excess of ethylene in benzene generating the bis(germiranyl)ethane (**II-76**).

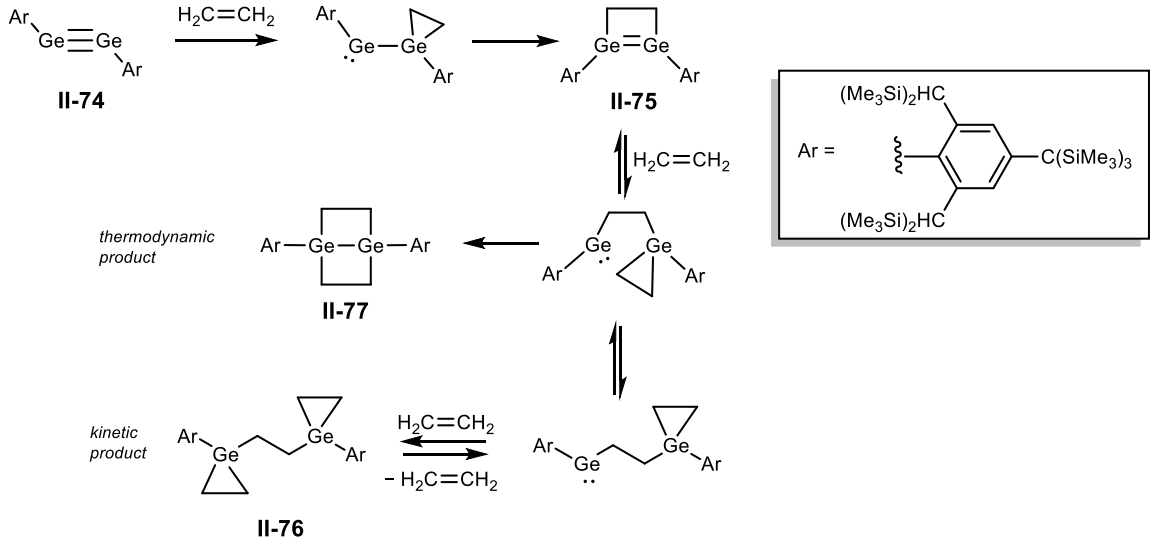

Scheme 30. Reaction of digermyne **II-74** with ethylene.

Compound **II-76** reconverts into **II-75** when exposed to an inert atmosphere. Exposing **II-75** to 1 atm of ethylene in THF resulted in the 1,4-digermabicyclo[2.2.0]hexane (**II-77**). From these results and theoretical investigations, the authors assigned **II-76** as a kinetic product and **II-77** as a thermodynamic product of the reaction. In a more recent report, **II-74** was shown to undergo a reversible [2+2] cycloaddition with 1-hexene and styrene.[91]

Diarylgermylenes **II-78a** and **II-78b** were demonstrated to react reversibly with ethylene (Scheme 31).[92] Propylene also reacts reversibly with a germylene having more sterically encumbered aryl groups, forming the product **II-79c**. Heating a solution of compound **II-79b** in hexane at 60°C led to the digermene **II-80**. The mechanism was proposed to proceed by the homolytic cleavage of the Ge-Ar bond, H abstraction from the ·GeAr radical, and ethylene insertion into the Ge-H bond.[93]

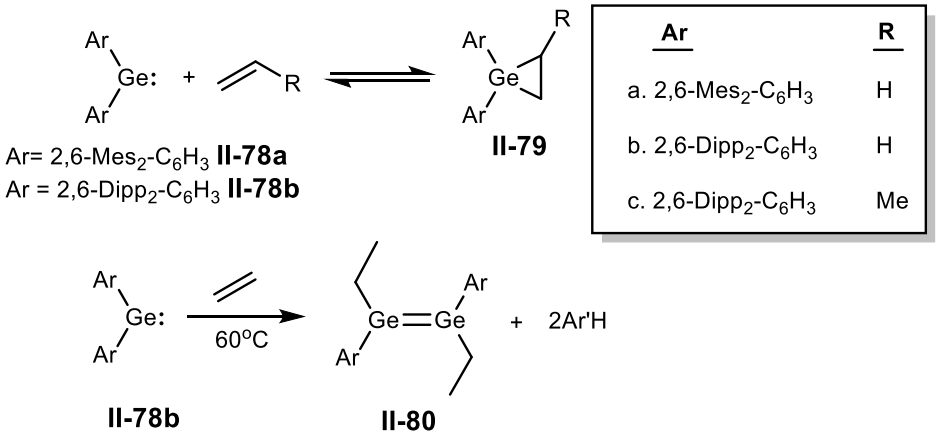

Scheme 31. Reactions of diarylgermylene **II-78** with alkenes.

There were fewer examples reported in the literature of reversible addition of alkynes, as compared to that of alkenes, to Group 14 compounds. Power *et al*. demonstrated a reversible reaction of unstrained alkynes with diarylgermylene **II-81** (Scheme 32).[94] 3-

hexyne, diphenylacetylene, trimethylsilylacetylene, and phenylacetylene react with **II-81** with the formation of the corresponding germirene **II-82** products. Thermodynamic parameters of alkyne binding were measured by VT NMR spectroscopy and showed small negative values of Gibbs free energies of association consistent with a reversible reaction. As was expected, bulkier alkynes showed more reversibility due to steric reasons.

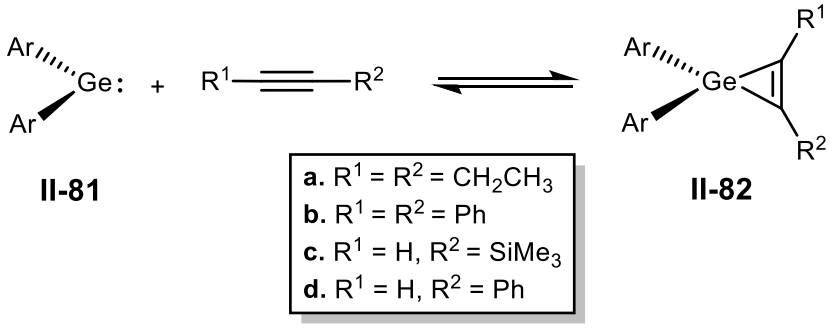

Scheme 32. Reactions of diarylgermylene **II-81** with alkynes.

Power and co-workers discovered the first example of a reversible addition of ethylene to a main group center in 2009 (Scheme 33).[95] A reaction of ethylene with distannynes **II-83a** and **II-83b** resulted in a cycloaddition to afford the distannocyclobutanes **II-84a** and **II-84b**. Concentration of solutions of adducts **II-84a** and **II-84b** under reduced pressure led to a retro-cycloaddition with the formation of ethylene and the starting distannynes.

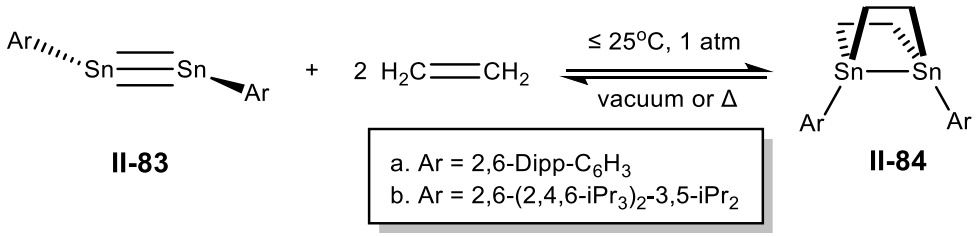

Scheme 33. Reversible addition of ethylene to distannyne **II-83**.

Despite the normal Sn-C bond lengths (2.19(2)Å in the crystal structure of compound **II-84a**) dissociation of ethylene points to weak Sn-C bonds. A van't Hoff analysis of VT ^{1}H NMR spectra allowed the determination of the enthalpy of association, ΔH_{assn} = –48(4) kJ mol^{-1} (**II-84a**) and –27(3) kJ mol^{-1} (**II-84b**), at 298.16 K, which confirms the presence of weak Sn-C bonds in distannocyclobutanes. The strained geometry of distannocyclobutanes featuring bond angles far from tetrahedral and the presence of bulky aromatic substituents *cis* to each other was proposed to be two of the reasons for this instability.

Ethylene insertion into the Sn-C bond was reported more recently.[96] In contrast to silylenes and germylenes that form siliranes and germiranes, diarylstannylenes **II-85** react with ethylene at 60°C to give the olefin insertion products **II-86** (Scheme 34). There was no reactivity between **II-85** and propene, 2-butene or styrene, most probably due to steric hindrance. A stannylene with smaller aromatic groups Ar_2Sn: (Ar = 2,6-$Mes_2C_6H_3$) also showed no reactivity towards ethylene, which is explained by the larger HOMO-LUMO gap as was deduced from UV-Vis absorption studies.

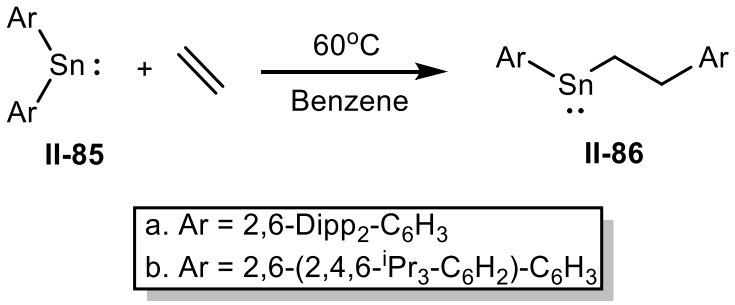

Scheme 34. Insertion of ethylene into the Sn-C bond of stannylenes **II-85**.

Calculations revealed simultaneous formation of the Sn-C and the C(*ipso*)-C bonds to ethylene, which results in the insertion product. A stannacyclopropane intermediate was

calculated to be unstable (ΔH = -3.6 kcal mol^{-1}, ΔG = +9.0 kcal mol^{-1}) and does not lead to the insertion.

Dialkylstannylene **II-87** reversibly binds to the cyclic alkyne 3,3,6,6-tetramethyl-1-thiacyclohept-4-yne to form stannacyclopropene **II-88** (Scheme 35).[97] The strained structure of the alkyne makes the reaction favorable. A rapid equilibrium was observed between the compounds **II-87** and **II-88** above -16°C, with higher temperatures favoring the reactants.

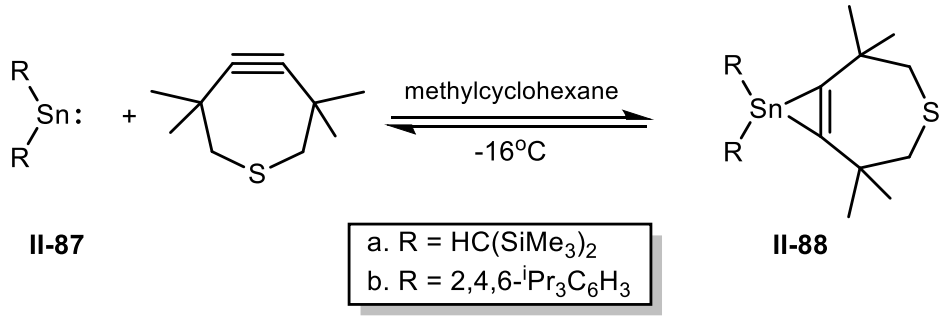

Scheme 35. Reversible addition of alkyne to **II-87**.

II.1.1.3. Group 15

Phosphinidenes (RP) are low oxidation state phosphorus compounds. They can exist either in singlet (two lone pairs and one empty p orbital) or triplet (one lone pair and two singly occupied p orbitals) ground states, with the triplet ground state being around 20–28 kcal/mol lower in energy.[98, 99] Triplet phosphinidenes have a limited synthetic value due to instability and the lack of selectivity.[100]

Singlet $^1\Delta$ Triplet $^3\Sigma$

One way to stabilize phosphinidenes is through complexation with transition metal complexes, and depending on ligands on the transition metals, the phosphorus center can be either nucleophilic or electrophilic.[101-103] For metal-free phosphinidenes, π-donor substituents, such as $-NR_2$ or $-PR_2$, should be utilized for the singlet ground state to be favoured.[104]

Phospha-Wittig reagents ($RP{=}PR'_3$), first reported by Mathey *et al.*,[105] can be considered as phosphine-stabilized phosphinidenes and when reacted with carbonyl compounds, result in the formation of phosphaalkenes.[106] The phospha-Wittig reagent **II-89** prepared by Fritz *et al*. is unstable and decomposes forming the cyclic oligomer $[P(P^tBu_2)]_n$, suggesting formation of an intermediate phosphinidene (Scheme 36).[107] The decomposition reaction of **II-89** in the presence of 2,3-dimethyl-1,3-butadiene and cyclohexene resulted in

[1+2] cycloaddition products of phosphinidene with an alkene, forming the phosphiranes **II-90** and **II-91**, respectively.

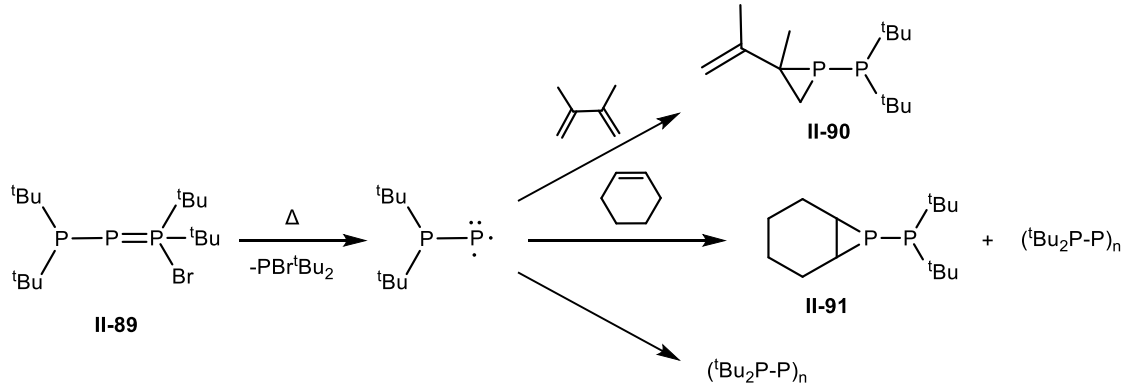

Scheme 36. Reaction of phospha-Wittig reagent **II-89** with alkenes.

Phosphinidenes can also be stabilized by NCN pincer ligands, as reported more recently.[108, 109] The only example of an isolable stable monosubstituted singlet phosphinidene was prepared by Bertrand and co-workers in 2016. The singlet phosphinidene **II-93** was supported by a strong π-donor phosphino ligand having bulky aromatic substituents (Scheme 37).[110] The synthetic procedure involved a reaction of chlorodiazaphospholidine with NaPCO to form the phosphaketene **II-92**, which upon UV irradiation yielded the phosphino-phosphinidene **II-93**. Spectroscopic and computational data, such as a Wiberg bond index of 2.34, indicate P-P multiple bond character with the terminal phosphorus having a negative charge. The HOMO and HOMO-1 are found to be the P-P π orbitals. Despite this, compound **II-93** forms adducts with carbenes and phosphines, pointing to the electrophilicity of the (phosphino)phosphinidene.[111] Phosphinidene **II-93** was reacted with maleic anhydride resulting in the formation of phosphirane **II-94** as a result of cycloaddition of the C=C bond to phosphinidene.

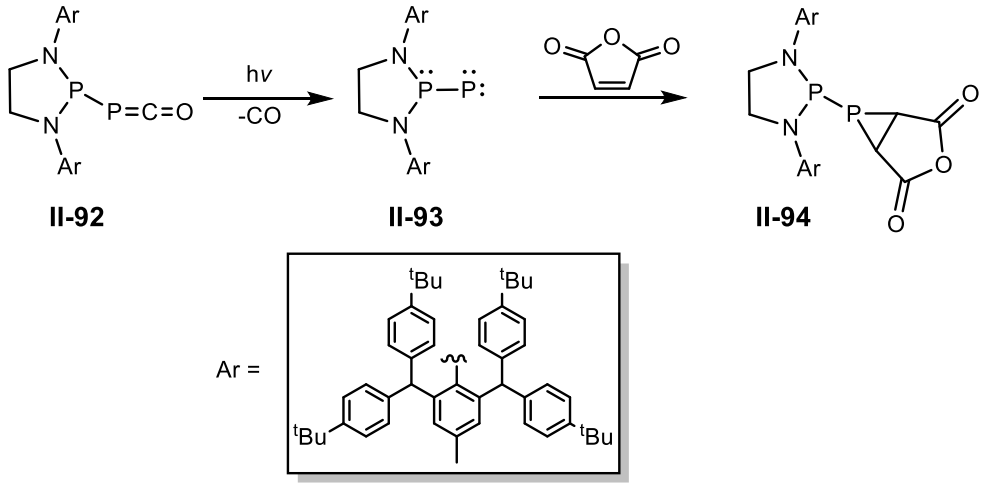

II-92 **II-93** **II-94**

Scheme 37. Synthesis of phosphinidene **II-93** and its reaction with an alkene.

Phosphinidene-transfer agents were developed by several groups (Scheme 38). Weber *et al*. reported transfer of phosphinidene from the phosphaalkene **II-95** to diphenylketene.[112] **II-95** generates intermediate phosphinidene [PR] which forms an adduct with a ketene, RP-O-C=CPh_2. 1,3-dipolar cycloaddition between phosphinidene and a second equivalent of a ketene results in five-membered heterocyclic products. The Driess group reported the zwitterionic phosphasilene **II-96** which transfers the parent phosphinidene (PH) to an NHC carbene at room temperature.[113] The reaction is apparently driven by the formation of a stable silylene and a stronger P=C double bond.

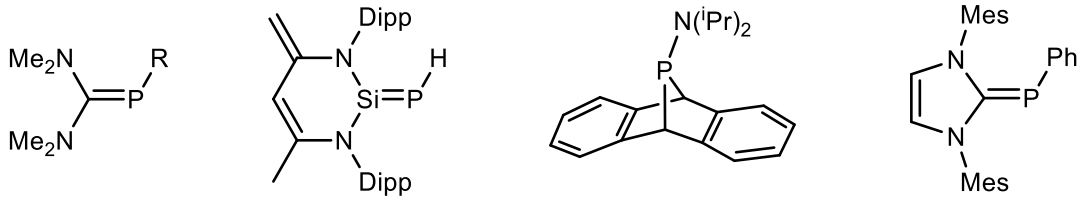

II-95 **II-96** **II-97** **II-98**

Scheme 38. Phosphinidene-transfer agents.

Cummins *et al.* prepared the dibenzo-7-phosphanorbornadiene **II-97**.[114] Heating **II-97** in the presence of an alkene or an alkyne results in the extrusion of transient aminophosphinidene [PN(^{i}Pr)$_2$] and its cycloaddition with the C-C unsaturated bond, forming a phosphirane or a phosphirene. Grützmacher and co-workers developed a Lewis acid ($ZnCl_2$) that promotes phosphinidene transfer from an NHC-phosphinidene adduct **II-98** to phenanthrene-9,10-quinone, diphenylketene, and *trans*-chalcone as will be described in Chapter II.1.2.3.[115]

In conclusion, low valent and multiple bonded main group compounds were introduced and their reactivity towards unsaturated compounds were covered in this chapter. Particularly, cycloaddition reactions between C-C unsaturated bonds and main group reagents resembling the reactivity of transition metal complexes were discussed. More recent developments in reversible addition reactions have opened potential avenue towards catalytic application of main group reagents.

II.1.2. Reactions of Carbon-Heteroatom Unsaturated Bonds with Main Group Compounds

Reactions of heterocumulenes such as carbon dioxide and carbon oxysulfide with low valent main group species were the earliest reports on multiple bond activations on main group centers.[116, 117] Cleavage of a X=Y bond is a four-electron process and most low valent main group compounds have only two electrons available for the oxidative addition reactions. CO_2, CS_2, COS, RNCO, and RNCS are the best reagents of choice to test the possibility of multiple bond activation on main group centers because, upon the cleavage of the carbon-heteroatom double bond (C=O or C=S), what remains is a stable a molecule: CO, CS, and RNC, respectively.[2]

II.1.2.1 Group 13

Diborene **II-99** undergoes a [2+2] cycloaddition with CO_2 forming a dibora-β-lactone **II-100** (Scheme 39). The compound **II-100** converts into diboracarbonyl compound **II-101** under CO_2 atmosphere in four days. A reaction of diboryne **II-7** with CO_2 led to the formation of compound **II-102**. DFT calculations were performed to study the mechanism of this reaction. The authors proposed an initial [1+2] cycloaddition between CO_2 and one of the boron centers, forming intermediate epoxide and increasing the double bond character in the second B-C^{CAAC} bond. A second molecule of CO_2 adds to the B-C^{CAAC} bond, forming a four-membered ring and a new C-C bond. Oxygen transfer from the epoxide to the second boron leads to ring expansion and the B-C^{CAAC} bond cleavage, forming the product **II-102**.

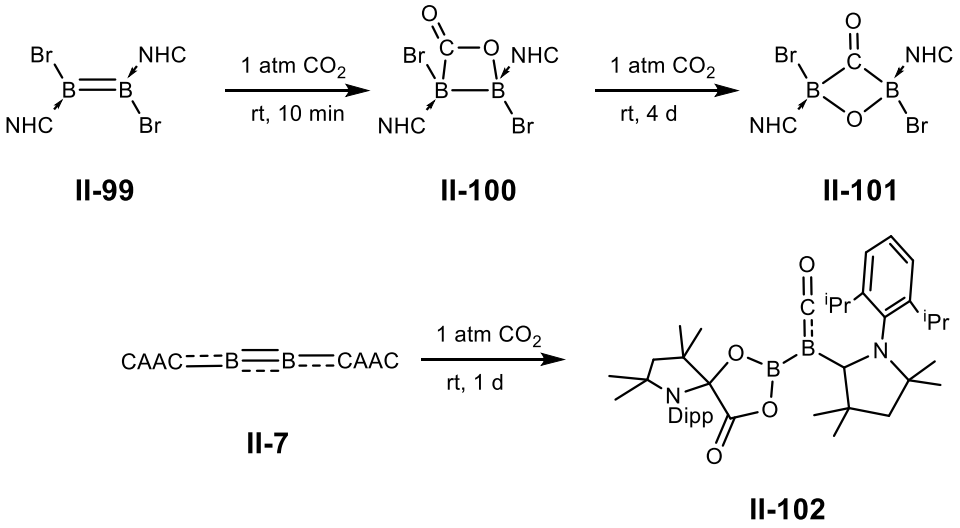

Scheme 39. Reaction of diborenes with carbon dioxide.

In situ reduction of NacNacAlI$_2$ (**II-103**) in the presence of benzophenone resulting in the formation of an aluminum pinacolate (**II-104**), was reported by Roesky and co-workers. (Scheme 40).[44] The reaction is proposed to proceed via a radical pathway. Ph_2CO is known to form the ketyl radical $K^+(OCPh)^{\bullet -}$ in the presence of potassium metal. The ketyl radical reacts with NacNacAlI$^{\bullet -}$ to form NacNacAl(Oph)$^{\bullet -}$ which then reacts with a second ketyl radical, yielding the aluminum pinacolate **II-104**.

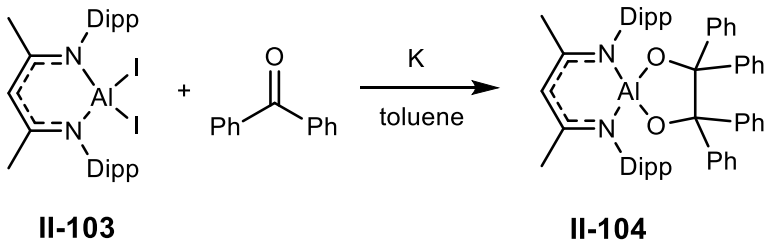

Scheme 40. In situ reduction of Al(III) compound **II-103** in the presence of Ph_2CO.

The alkyne adduct NacNacAl[η^2-$C_2(SiMe_3)_2$] (**II-105**) was also prepared by an *in situ* reduction of the Al(III) compound **II-103** in the presence of $(Me_3Si)C{\equiv}C(SiMe_3)$. The aluminacyclopropene **II-105**, containing a strained three-membered ring, reacts with benzonitrile, carbon dioxide, and benzophenone (Scheme 41). Aluminum five-membered heterocyclic compounds **II-106, II-107,** and **II-108** were obtained as a result of insertion of the C≡N and C=O bonds into the Al-C bond of **II-105**.

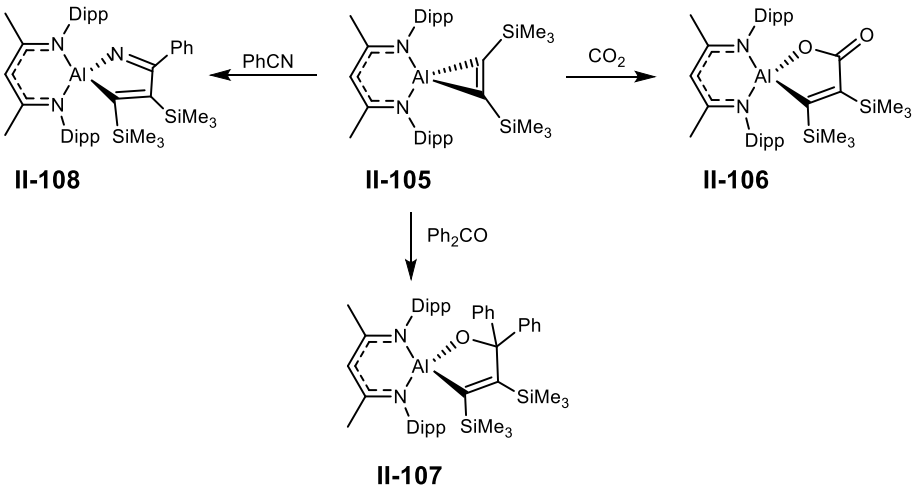

Scheme 41. Reactions of **II-105** with PhCN, Ph_2CO, and CO_2.

The Nikonov group demonstrated that a reaction of NacNacAl (**II-10**) with one equivalent of benzophenone leads to a [1+4] cycloaddition forming the η^2(C,O) adduct **II-109** with a dearomatized phenyl ring (Scheme 42).[118] Adding a second equivalent of benzophenone resulted in the aluminum pinacolate **II-104**. The adduct **II-109** is also reactive towards a variety of unsaturated substrates. As such, the compound **II-109** undergoes coupling reactions with aldimine, quinoline, benzonitrile, and trimethylsilylnitrene (produced from trimethylsilyl azide), producing derivatives **II-110**, **II-111**, **II-112**, and **II-113**, respectively. Interestingly, unlike the case of aluminacyclopropene **II-105**, in these

reactions C=O, C=N, C≡N unsaturated bonds and nitrene do not insert into the Al-C bond of **II-109**, but the former carbonyl carbon forms new C-C or C-N bonds. Reaction of **II-109** with thiourea led to an unusual C-N cleavage producing **II-114** rather than a cyclization through the C=S bond.

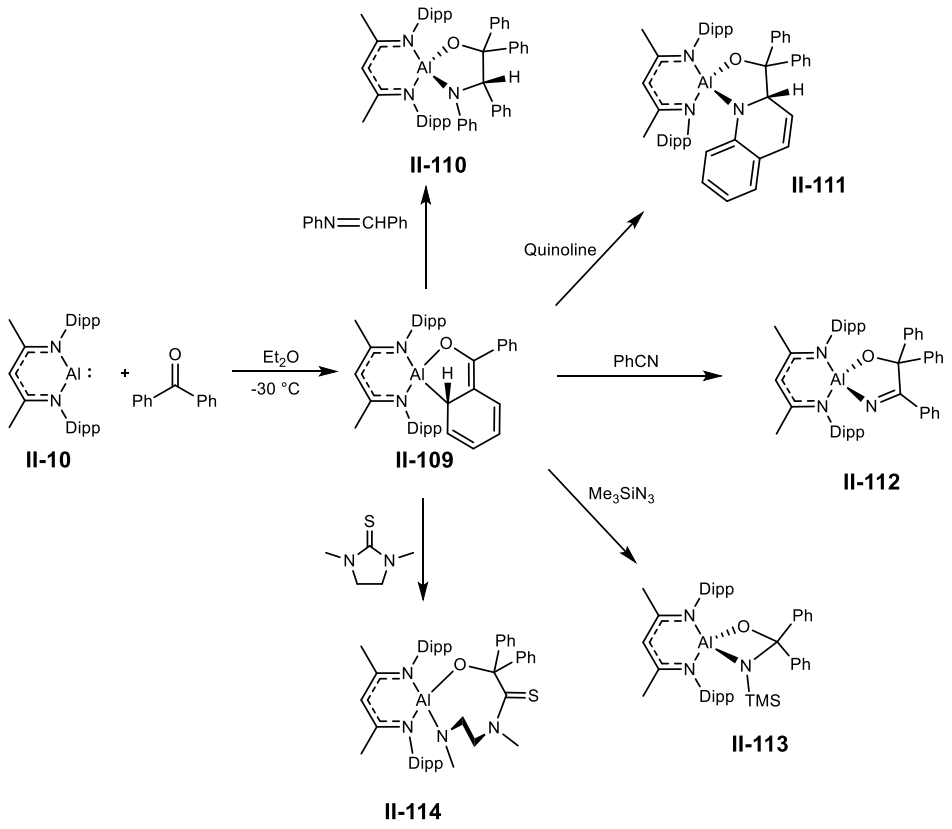

Scheme 42. Synthesis of **II-109** and its reactions with aldimine, quinoline, PhCN, trimethylsilyl azide, and thiourea.

Selective cross-coupling reactions between pyridine and benzophenone, fenchone, isophorone, p-tolyl benzoate, N,N-dimethylbenzamide, and (1-phenylethylidene)aniline) on the Al(I) center (**II-10**) were reported by the same group.[119] Noteworthy, the compound **II-10** reacts separately with both ketones and pyridines,[119] but adding it to a mixture of the carbonyl and heterocyclic compounds leads to a chemoselective cross-coupling of the two

substrates. The resulting coupling products (**II-115** to **II-119**) are illustrated in Scheme 43. With a smaller ketone, (1*R*)-(+)-camphor, Al(I) does an enolization reaction forming an aluminum hydrido enolate while pyridine stayed intact. Reacting a mixture of p-tolyl benzoate and pyridine with **II-10** led to the ester bond cleavage and an ortho-C-H bond abstraction in pyridine, forming compound **II-120** (Scheme 40). Treating the Al(I) **II-10** compound with (R)-(-)-fenchone resulted in a C-H activation of an isopropyl group of the NacNac ligand with the formation of **II-121**, which suggests a charge transfer from the Al(I) center to the ketone.

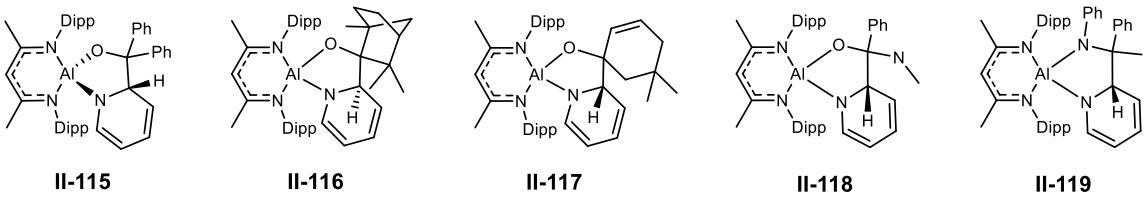

Scheme 43. Coupling products of pyridine and carbonyl derivatives on an Al center.

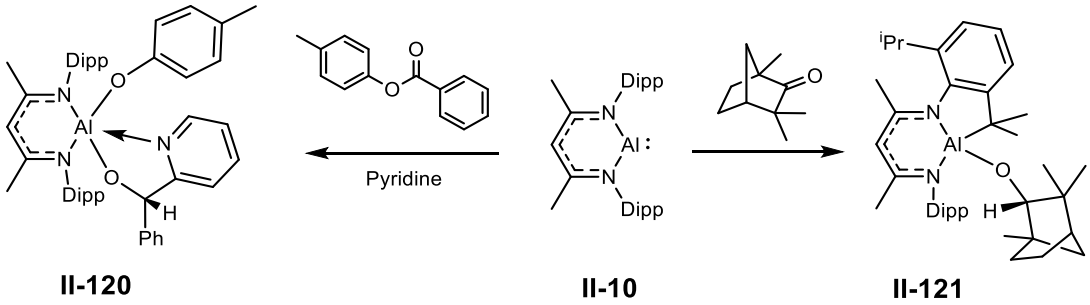

Scheme 44. Reactions of **II-10** with a mixture of ester and pyridine and with (R)-(-)-fenchone.

A reaction of NacNacAl (**II-10**) with the cyclic urea 1,3-dimethyl-2-imidazolidinone afforded an Al(III) hydride adduct of urea **II-122** (Scheme 45).[120] DFT calculations on the mechanism of the reaction, starting with the adduct NacNacAl(O=SIMe), revealed a

bimolecular hydrogen atom transfer pathway where the Al(I) center deprotonates the weakly acidic methyl group of the ligand backbone, resulting in the compound **II-122**. A reaction of a cyclic guanidine with **II-10** resulted in unprecedented cleavage of the C=N bond, forming an aluminum amide compound **II-123** (Scheme 45) .[121] DFT calculations suggested oxidative addition of the C=N bond forming a transient aluminum imide which deprotonates a methyl group of the ligand backbone via a bimolecular mechanism, leading to the amido carbene product **III-123**.

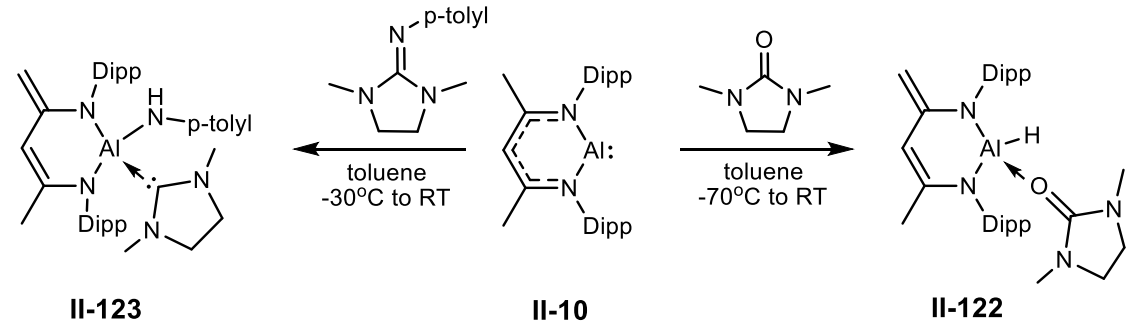

Scheme 45. Reactions of **II-10** with cyclic urea and guanidine.

Oxidative addition of the C=S bond of thiourea to the Al(I) compound **II-10** resulted in the formation of a carbene-stabilized terminal aluminum sulfide **II-124** (Scheme 46),[122] the first example of a neutral monomeric aluminum sulfide.

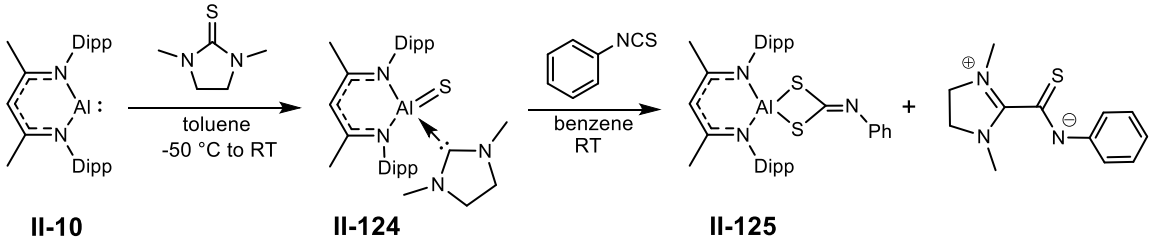

Scheme 46. Reactions of **II-10** with thiourea.

The authors suggested Al–S multiple bonding character based on an X-ray diffraction study (e.g. a short Al-S bond of 2.104(1) Å) and DFT calculations. A [2+2] cycloaddition between the compound **II-124** and phenylisothiocyanate, yielding **II-125**, further supported this conclusion.

The reactivity of aluminyl anion **II-18** $[K(NON)Al]_2$ towards C=O-containing compounds was reported by the Aldridge group (Scheme 47).[123] Treatment of **II-18** with two equivalents of carbon dioxide and phenyl isocyanate resulted in the aluminum carbonate **II-126** and carbamate **II-127**, respectively. The authors suggested that the reactions proceed through a highly reactive aluminum oxide intermediate $[K(NON)AlO]_n$ that is generated via oxidative addition of the C=O bond.

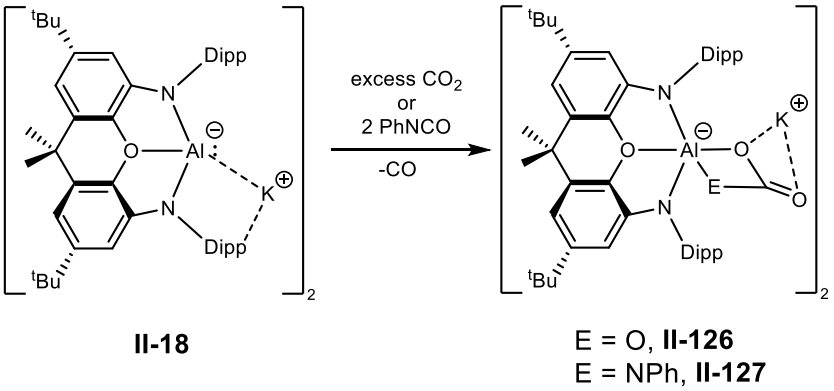

Scheme 47. Reactions of **II-18** with CO_2 and PhNCO.

Coles and co-workers also showed a reaction of the related aluminyl anion $K_2[Al(^{Ar}NON)]_2$ **II-128** ($^{Ar}NON = [O(SiMe_2Ndipp)_2]^{2-}$) with carbon dioxide, resulting in the aluminum carbonate **II-129** and the release of CO gas (Scheme 48).[124]

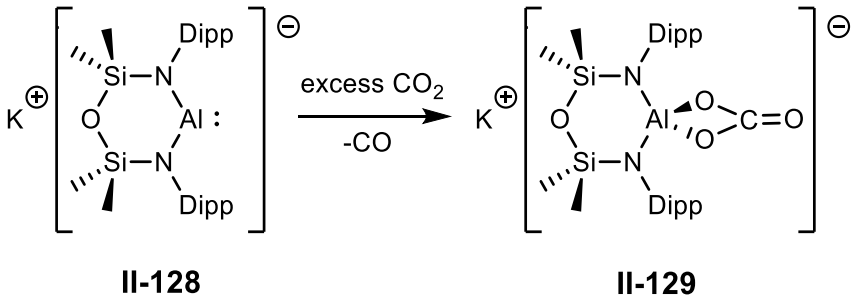

II-128 **II-129**

Scheme 48. Reactions of **II-128** with CO_2.

Monomeric aluminum oxide was suggested to be an intermediate formed from the cleavage of the C=O bond of carbon dioxide. Aluminum oxide then undergoes a [2+2] cyclization with a second equivalent of CO_2 resulting in **II-129**.

A reaction of dialumane **II-23** with carbon dioxide was reported by Fedushkin *et al.* (Scheme 49).[125] Treatment of **II-23** with CO_2 at 0°C in toluene resulted in cycloaddition across the Al-N-C moiety, leading to the product **II-130**. The reaction is reversible, and CO_2 is released at elevated temperatures.

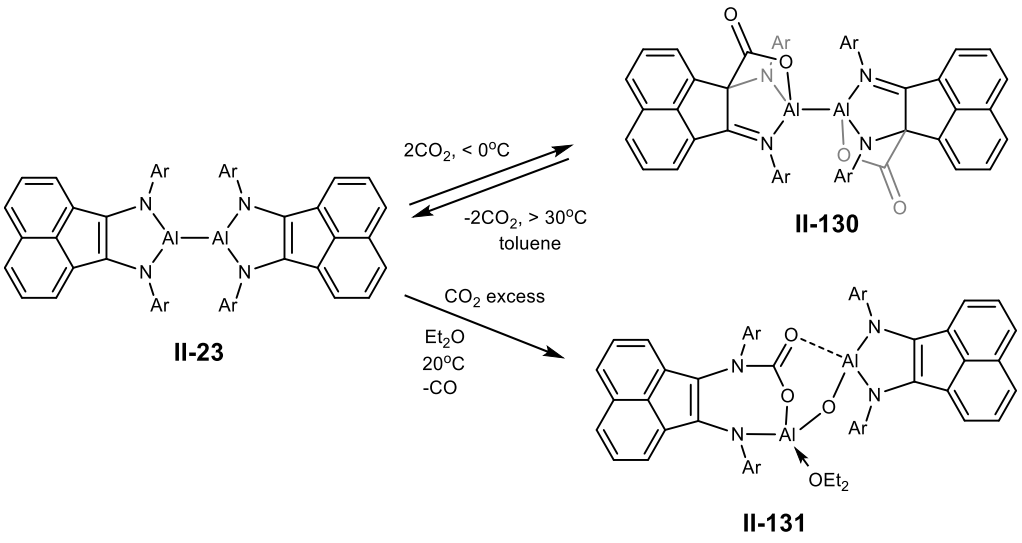

II-23 **II-130** **II-131**

Scheme 49. Reactions of **II-23** with CO_2.

Carrying out the reaction in diethyl ether resulted in the formation of an oxo-bridged carbamato derivative **II-131** as a result of CO_2 insertion into Al-N bond and C=O bond cleavage. According to DFT calculation, Et_2O coordination to the aluminum center induces the formation of product **II-131**.

Treatment of dialumene **II-35** with carbon dioxide resulted in a [2+2] cycloaddition with the formation of **II-132** (Scheme 50).[126] Heating **II-132** at 50°C led to the bridging carbonyl oxo dialuminum **II-133**. DFT calculations predicted **II-133** formation via isomerization of **II-132** that is similar to the boron analogue **II-100**. Heating **II-132** in the presence of CO_2 resulted in a carbonate-bridged dialuminum compound **II-134** with CO gas evolution.

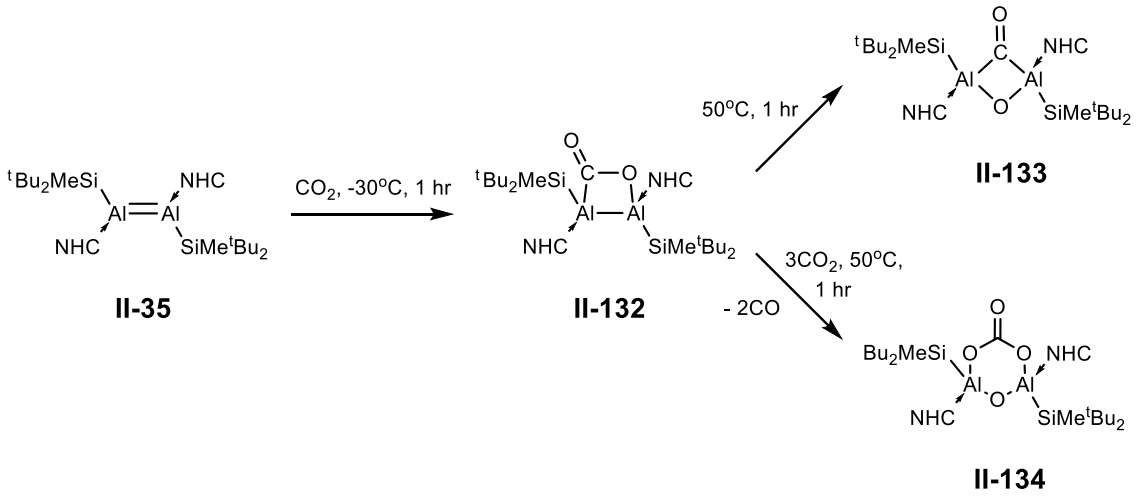

Scheme 50. Reactions of **II-35** with CO_2

Dialumene **II-35** was found to be active in catalytic hydroboration of carbon dioxide (Scheme 51).[64] Mechanistic studies of the catalytic process ruled out an aluminum hydride route and revealed the carbonate **II-134** to be the active species in the reduction of CO_2. The proposed catalytic cycle involves coordination of HBpin to the carbonate followed by the

rate determining hydride transfer. After that, coordination of CO_2 to the opposite plane of the Al-Al bond releases the formic acid derivative and regenerates compound **II-134** in a concerted step.

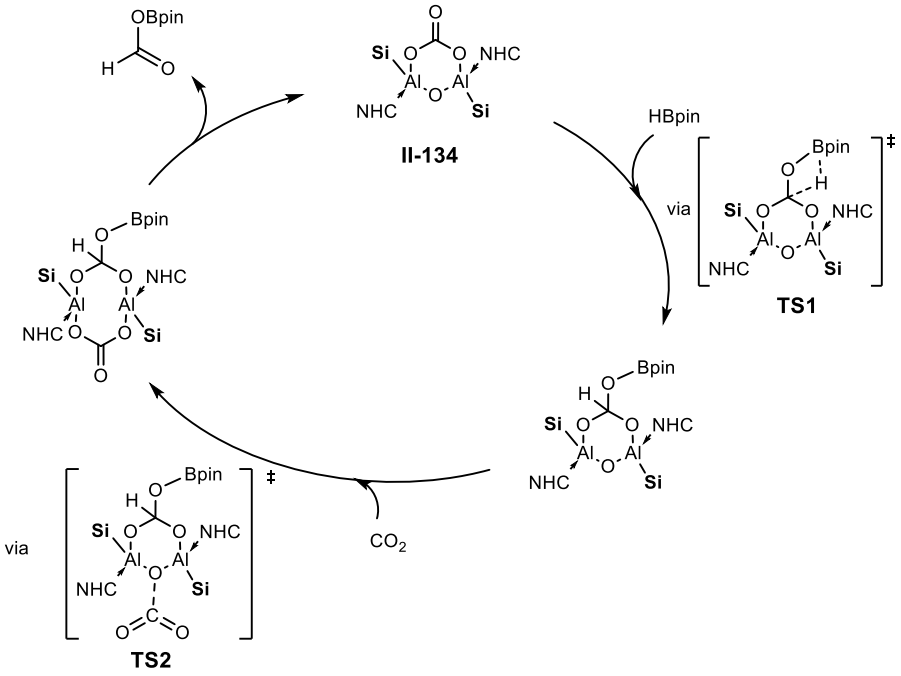

Scheme 51. Proposed catalytic cycle for **II-35**-catalyzed hydroboration of CO_2.

Fedushkin *et al.* reported the reactivity of digallanes, supported by non-innocent α-diimine ligands (dpp-dad)Ga – Ga(dpp-dad)[127] **II-135** (dpp-dad = $[(2,6\text{-dipp})NC(CH_3)]_2$) and (dpp-bian)Ga–Ga(dpp-bian) **II-45**, towards isothiocyanates (Scheme 52).[128] Reacting the compounds **II-135** and **II-45** with two equivalents of PhNCS resulted in a [2+4] cycloaddition across the GaN_2C_2 ring, leading to **II-136** and **II-139**, respectively. The process is reversible at elevated temperatures in the case of **II-139**, which according to the authors could be related to the extended π-system of the ligand. Treatment of **II-135** with three equivalents of PhNCS resulted in the C=S bond cleavage with the formation of a

sulfide-bridged dimer (**II-137**). Reaction of PhNCS with **II-45** at 120°C also led to the C=S bond cleavage producing a bridging Ga sulfide with a radical-anionic bis(amido) ligand **II-140**. The C=S bond activation was also observed when the reaction was performed in the presence of Na metal. Thus, a reaction of **II-135** with PhNCS in the presence of Na metal leads to a sulfide-bridged digallium with four-membered Ga_2S_2 core (**II-138**), whereas **II-41** produces a radical anionic gallium sulfide dimer (**II-141**).

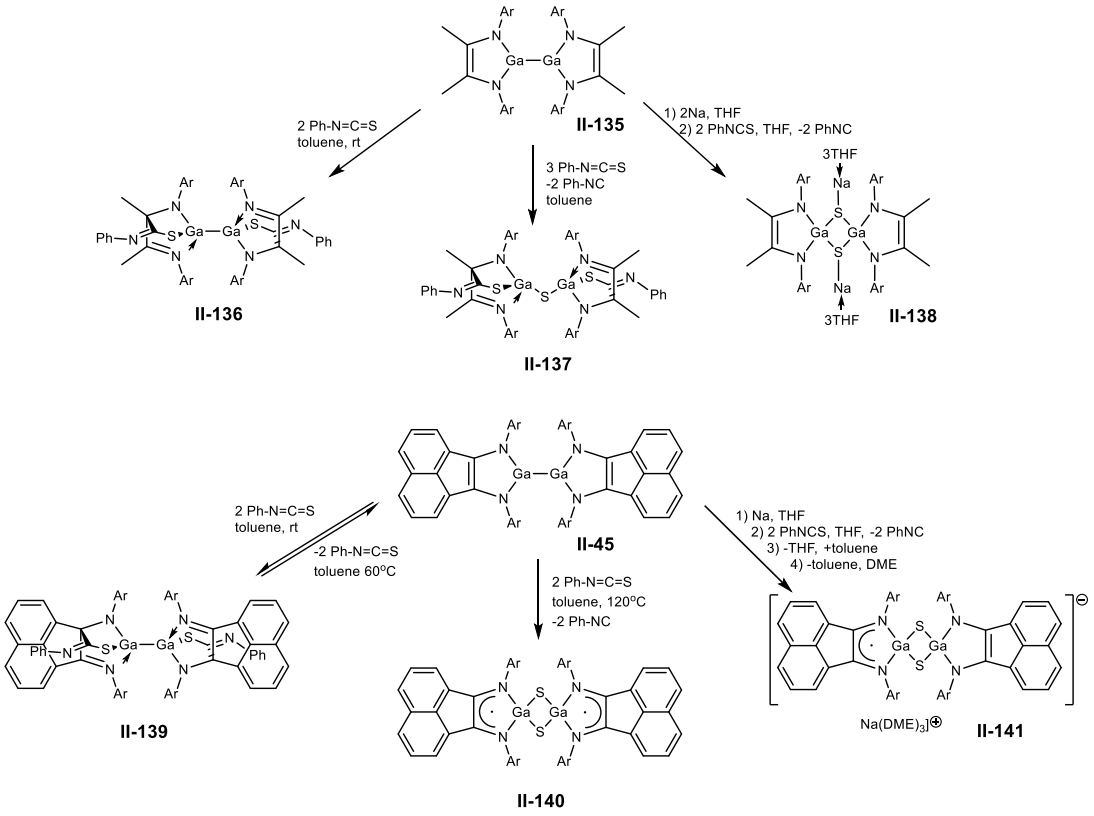

Scheme 52. Reactions of **II-45** and **II-135** with PhNCS.

Reductive coupling of carbodiimides by anionic Ga(I) compounds **II-142**, **II-143**, and **II-144** was demonstrated by same group (Scheme 53).[129] Two molecules of diisopropyl carbodiimide and cyclohexyl carbodiimide undergo cyclization on the Ga center, forming products **II-146 a-e**. The mechanism of the reaction was probed by DFT calculations and

predicted the initial formation of a gallium carbodiimide [1+2] cycloadduct followed by insertion of a second equivalent of carbodiimide into the Ga-C bond. Compound **II-145** supposedly forms from the C=N bond cleavage and then cyclization with a second equivalent of carbodiimide. Carbodiimide with a bulky aromatic group leads to a product of insertion of the C=N bond into the Ga-Na bond **II-147**.

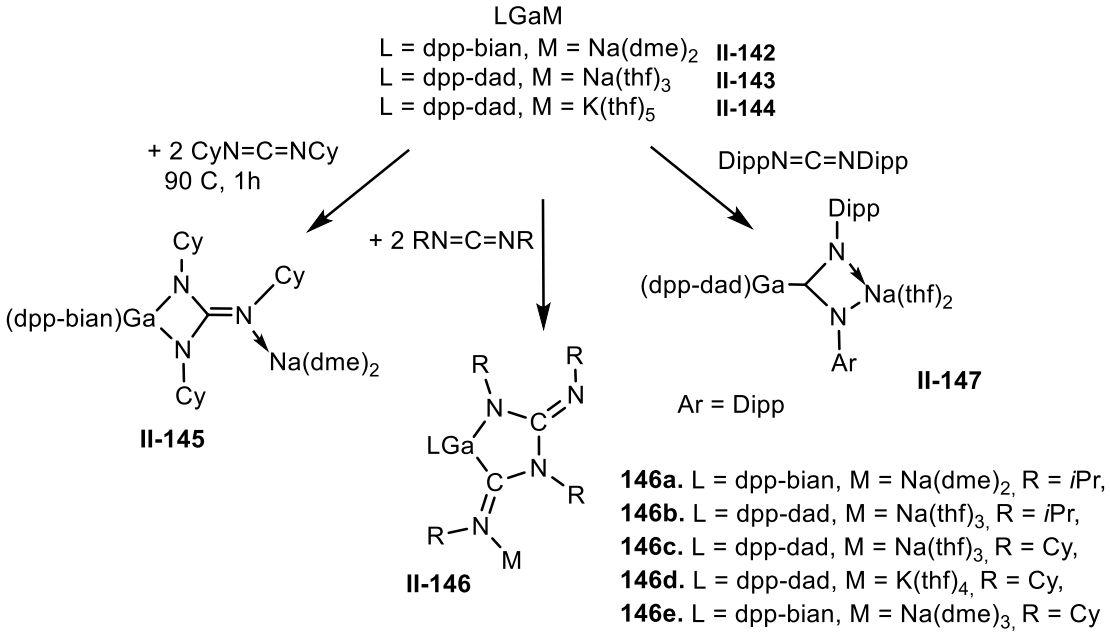

Scheme 53. Reactions of **II-142, II-143**, and **II-144** with carbodiimides.

Gallylene **II-142** was also reacted with heterocumulenes containing a C=O bond (Scheme 54). Carbon dioxide activation by the gallylene **II-142** yields the dimeric product **II-148**.[130] The reaction of **II-142** with isocyanates resulted in cycloaddition products **II-149** and **II-150**. The authors proposed a formal cycloaddition of two molecules of cyclohexyl isocyanate with the gallium oxide leading to the product **II-149**. Similarly, one equivalent of phenyl isocyanate was proposed to undergo a [2+2] cycloaddition with an intermediate gallium oxide forming **II-150**. However, DFT calculations showed that the gallium oxide

formation with the release of carbon monoxide is a high energy process and the reactions were suggested to proceed via a [$GaCO_2$] adduct instead.

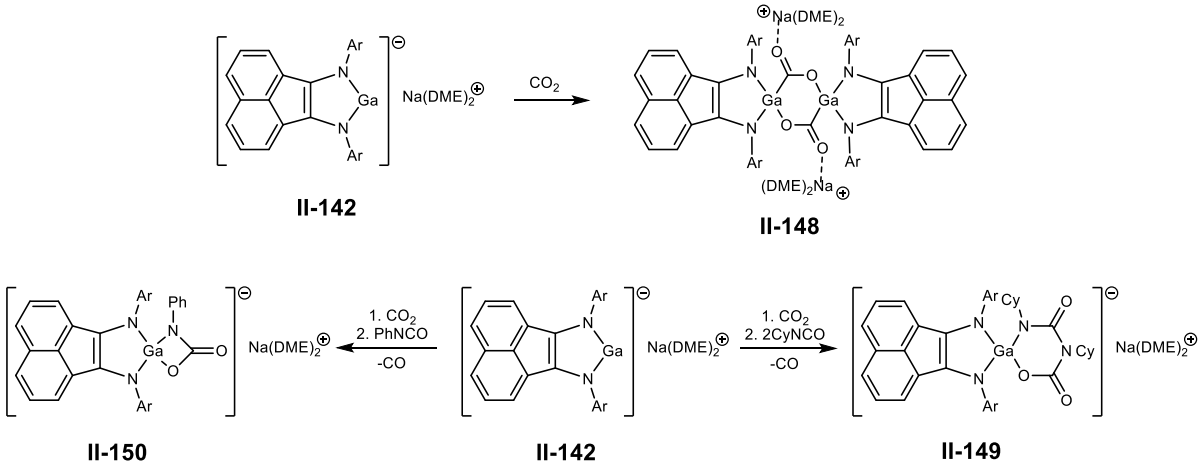

Scheme 54. Reactions of **II-142** with carbon dioxide and isocyanates.

II.1.2.2. Group 14

Jutzi *et al*. described the C=S bond cleavage of carbon oxysulfide and isothiocyanates by the decamethylsilicocene Cp^*_2Si[131] **II-151** (Scheme 55). [100] A reaction of COS with **II-151** resulted in the formation of a sulfide-bridged silicon dimer, $[Cp^*_2Si(\mu\text{-}S)]_2$ **II-152**.[116, 117] The mechanism of the reaction is proposed to go via a [1+2] cyclization of the C=S bond with silylene followed by CO elimination to generate a silathione intermediate, which then undergoes dimerization forming **II-152**. Treatment of **II-151** with RNCS (R=Me, Ph) led to a [2+2] cycloaddition product of silathione with isothiocyanate **II-153. II-153** reacts with the silylene **II-151** further at 100°C to afford **II-154** as a result of Cp^*_2Si insertion into the C-S bond of **II-153**.

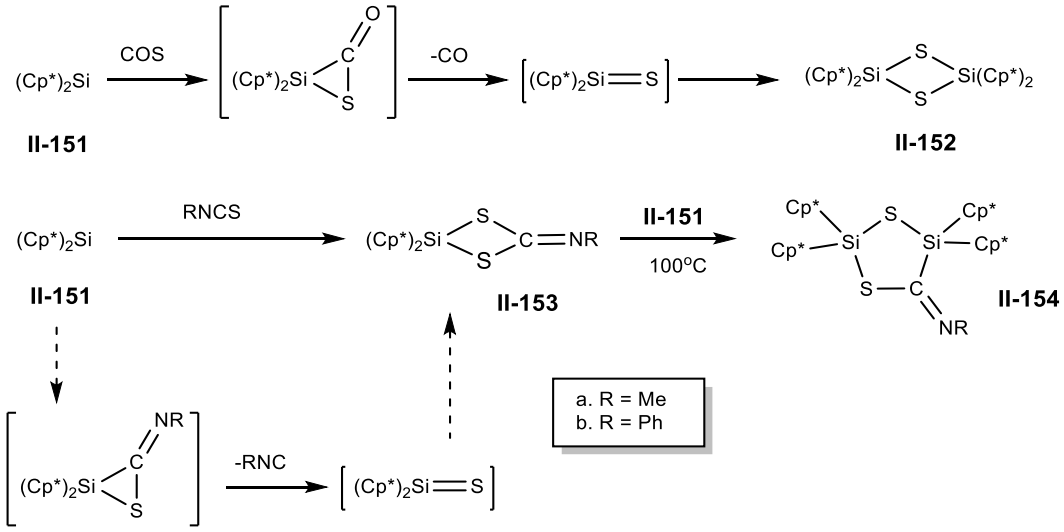

Scheme 55. Reaction of **II-151** with COS and RNCS.

Two products were isolated from the reaction of silylene **II-151** with CO_2 depending on the solvent used (Scheme 56).[117] In toluene, a spiro compound **II-156** was isolated, whereas in pyridine the eight-membered heterocycle **II-157** was obtained. The mechanism

of reaction was proposed to follow [1+2] cycloaddition of CO_2 with silylene, followed by CO evolution forming a silanone intermediate, which then undergoes cycloaddition with a second equivalent of CO_2, to form intermediate **II-155**. After cycloaddition, product **II-156** is obtained via a [2+2] cyclization of silanone with **II-155** in toluene. The product **II-157** is formed from a ring opening and dimerization of **II-155** in pyridine.

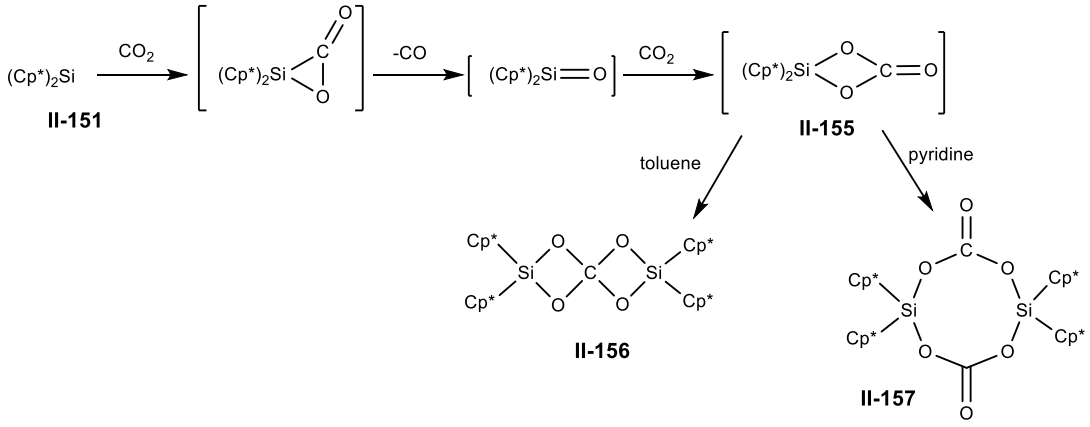

Scheme 56. Reaction of **II-151** with CO_2.

Sterically hindered disilene (Z)-R(Mes)Si=Si(Mes)R (R = 2,4,6-tris[bis(trimethylsilyl)-methyllphenyl, Mes = mesityl)[132] (**II-158**) reacts with carbon disulfide in a similar manner (Scheme 57).[133]

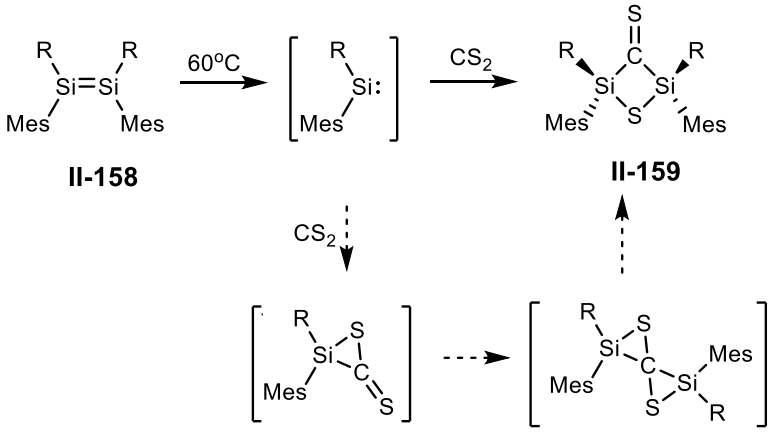

Scheme 57. C=S bond cleavage of CS_2 by **II-158**.

It was proposed that upon heating at 60ºC the disilene dissociates to form a silylene. The silylene reacts with CS_2 to furnish a cyclic intermediate which reacts with a second equivalent of silylene to generate a spiro intermediate. The spiro intermediate rearranges giving the product **II-159**.

Roesky *et al.* reported a reaction of the amidinato-stabilized disilylene[134] **II-160** with benzophenone resulting in the activation of the C=O bond of ketone, with the formation of product **II-161** containing a Si_2O_2 four-membered ring (Scheme 58).[135] The suggested mechanism involves a [1+2] cycloaddition followed by rearrangement and hydrogen abstraction from THF. THF-d_8 was used as a solvent to confirm the hydrogen abstraction from the solvent.

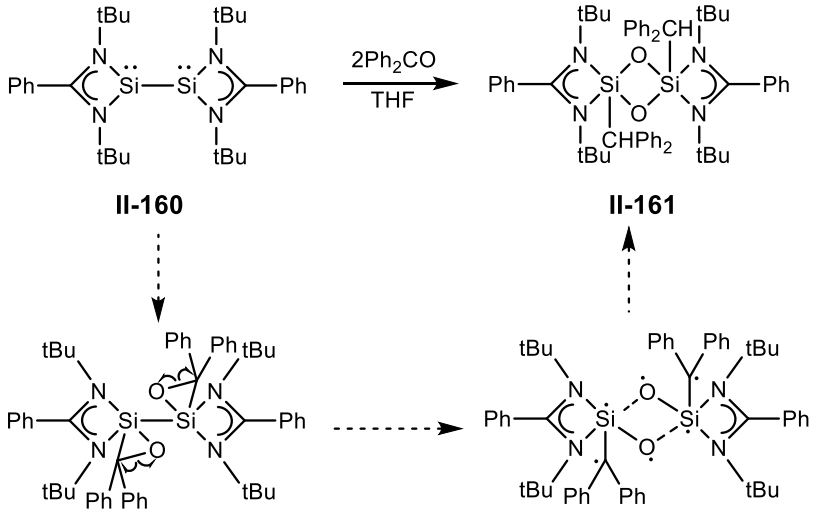

Scheme 58. Reaction of disilylene **II-160** with benzophenone

Carbon dioxide reduction to carbon monoxide was performed using the disilyne bis(phosphine) adduct **II-162** (Scheme 59).[136] The compound **II-162** reacts with four equivalents of CO_2, releasing three molecules of CO and capturing one molecule of CO_2 to

form the aminosilicate **II-163**. The proposed mechanism involves silaketene and silaketone intermediates formed from the cleavage of the C=O bond. Silaketene then releases CO forming an oxadisilirene derivative and then a similar sequence repeats until the fourth molecule of CO_2 is trapped with the formation of **II-163**.

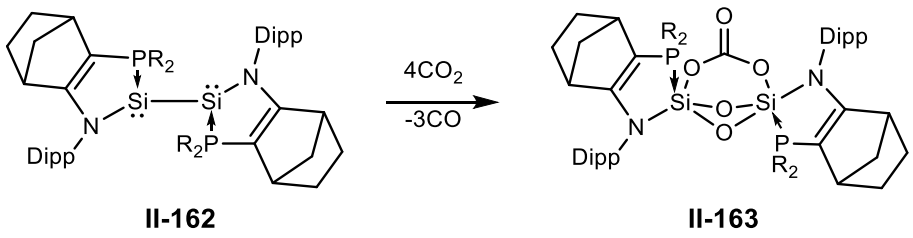

II-162 **II-163**

Scheme 59. Reaction of **II-162** with CO_2.

Kira and co-workers studied the reactivity of dialkylsilylene **II-47**, 2,2,5,5-tetrakis(trimethylsilyl) silacyclopentane-1,1-diyl, towards heterocumulenes (Scheme 60).[137] Treatment of **II-47** with carbon dioxide resulted in the bis(silyl) carbonate **II-164**.

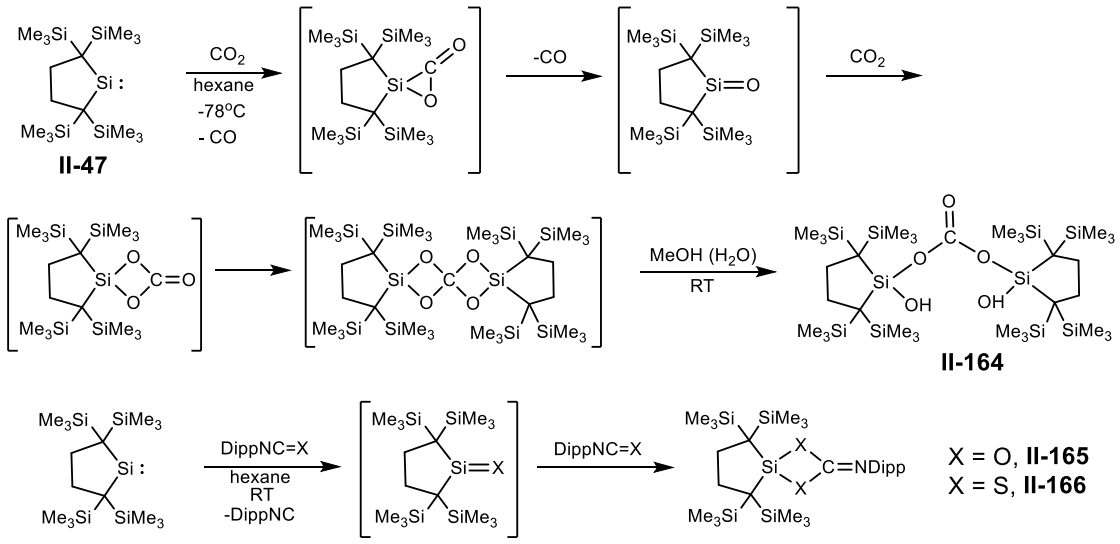

Scheme 60. Reaction of **II-47** with CO_2, DippNCO, and DippNCS.

The mechanism of reaction was proposed to be similar to the reaction of silicocene **II-151** with CO_2.[117] The last step is suggested to be the hydrolysis of a spiro intermediate by traces of moisture in methanol. A reaction of **II-47** with isocyanate and isothiocyanate led to the 4-iminodioxasiletane **II-165** and 4-iminodithiasiletane **II-166**. The proposed mechanism involves the cleavage of the C=X (X=O or X=S) bond forming an intermediate silanone or silanethione which then cyclizes with a second equivalent of DippNCO or DippNCS.

The Driess group reported the reactivity of silylene **II-60** with carbonyl compounds. The silylene **II-60** undergoes a [1+4] cycloaddition with benzophenone forming compound **II-167** with a dearomatized phenyl ring (Scheme 61).[138] The reaction is similar to the cycloaddition of the Al(I) compound (**II-10**) with benzophenone. However, unlike the aluminum-benzophenone adduct **II-109**, the compound **II-167** tautomerizes over the period of one week to restore the aromaticity of the phenyl ring, resulting in the compound **II-168**. Reacting **II-60** with a conjugated ketone resulted in the [1+4] cycloaddition product **II-169**, whereas the α-C-H acidic acetophenone led to the formation of the silyl enol ether **II-170**.

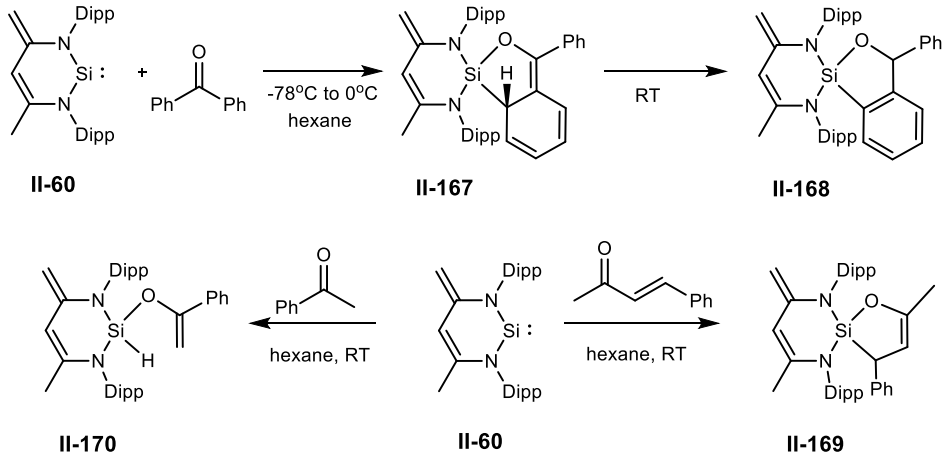

Scheme 61. Reaction of **II-60** with ketones.

Compared to cyclic silylenes, acyclic silylenes have a smaller HOMO-LUMO gap which makes them more reactive towards small molecules. The Aldridge and Jones group prepared two-coordinate acyclic silylene **II-171** which activates H_2 under ambient conditions.[139] The silylene **II-171** also reacts with carbon monoxide and carbon dioxide (Scheme 62).[140] Carbon monoxide undergoes reductive coupling with **II-171** forming a dimeric structure with a $Si_2C_2O_2$ ring (**II-172**), which is suggested to form from the insertion of the C≡C bond of ethynediolate anion $[OCCO]^{2-}$ into the Si-B bond. Treatment of **II-171** with CO_2 led to oxygen abstraction, forming an intermediate silanone, followed by silyl transfer from N to O to furnish the compound **II-173.**

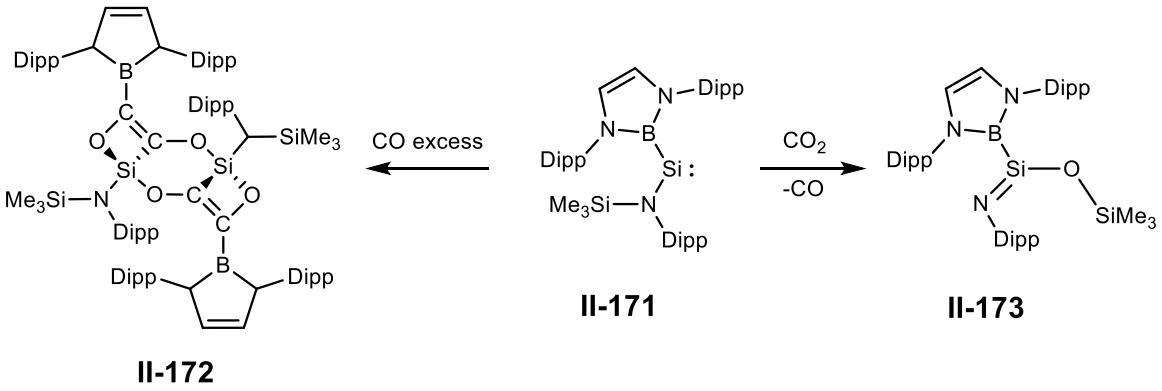

II-172 **II-171** **II-173**

Scheme 62. Reaction of **II-171** with carbon monoxide and carbon dioxide.

Jones et at. showed the reduction of carbon dioxide to carbon monoxide with the amido-substituted digermyne **II-174** (Scheme 63).[141] Spectroscopic and theoretical investigations of the mechanism suggest insertion of CO_2 into the Ge-Ge bond, followed by a rearrangement into a germacarboxylato amide intermediate which subsequently eliminates the CO gas. Similarly, CS_2 and tBuNCO were reacted with **II-174** forming the oxide- or sulfide-bridged dimers **II-175.**

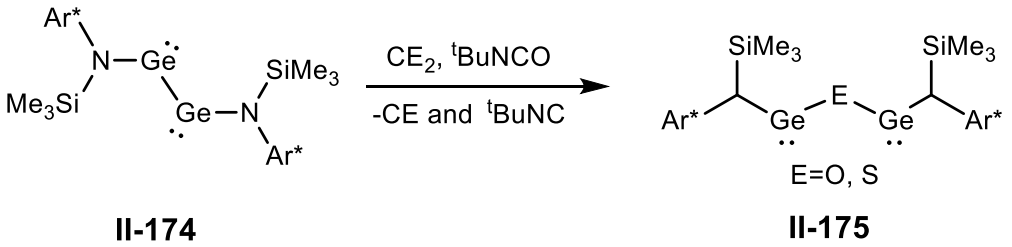

II-174 **II-175**

Scheme 63. Reaction of **II-174** with CO_2, CS_2, ^{t}BuNCO, and N_2O.

Dialkylstannylene **II-176** reacts with CS_2 to produce 3,3′-distanna-2,2′,4,4′-tetrathiabicyclobutylidene **II-177**, which then rearranges into 3,7-distanna-2,4,6,8-tetrathiabicyclo[3.3.0]oct-1(5)-ene **II-178** (Scheme 64).[142] The ratio of products depends on reaction times. The mechanism of the reaction is proposed to go via a [1+2] cycloaddition of CS_2 to **II-177** followed by the formation of a dithiocarbene and dimerization of carbene, resulting in **II-178**. Rearrangement of **II-177** to **II-178** is suggested to be Lewis acid-catalyzed. Thus, the coordination of the Lewis acid **II-176** to sulfur initiates the isomerization of **II-177** to **II-178**.

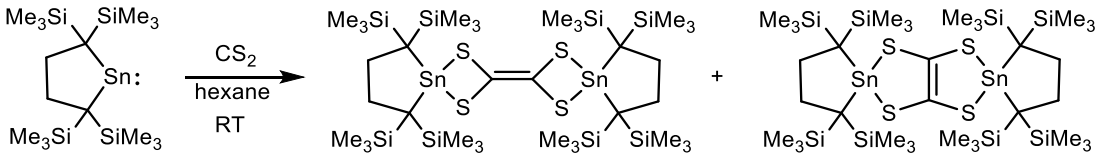

II-176 **II-177** **II-178**

Scheme 64. Reaction of **II-176** with CS_2.

II.1.2.3. Group 15

Nitrenes (NR) are nitrogen analogues of carbenes. *In situ* generated nitrenes are widely applied in organic synthesis for aziridination, C-H insertion, addition to unsaturated bonds, etc.[143] Isolable nitrenes are unknown in the literature because of their high reactivity. The aminonitrenes N-(2,2,5,5-tetramethylpyrrolidyl)nitrene and N-(2,2,6,6-tetramethylpiperidy1)nitrene prepared by Dervan *et al.* are stable at -78°C only long enough for IR and UV-Vis spectroscopic characterization.[144, 145]

Bertrand and co-workers employed a sterically hindered π-donor phosphino group to stabilize the singlet nitrene (Scheme 65).[146] To prepare the compound **II-181**, imidazolidin-2-iminato phosphorus chloride (**II-179**) was converted to an azide **II-180**, which under UV irradiation transformed into the phosphinonitrene **II-181**.

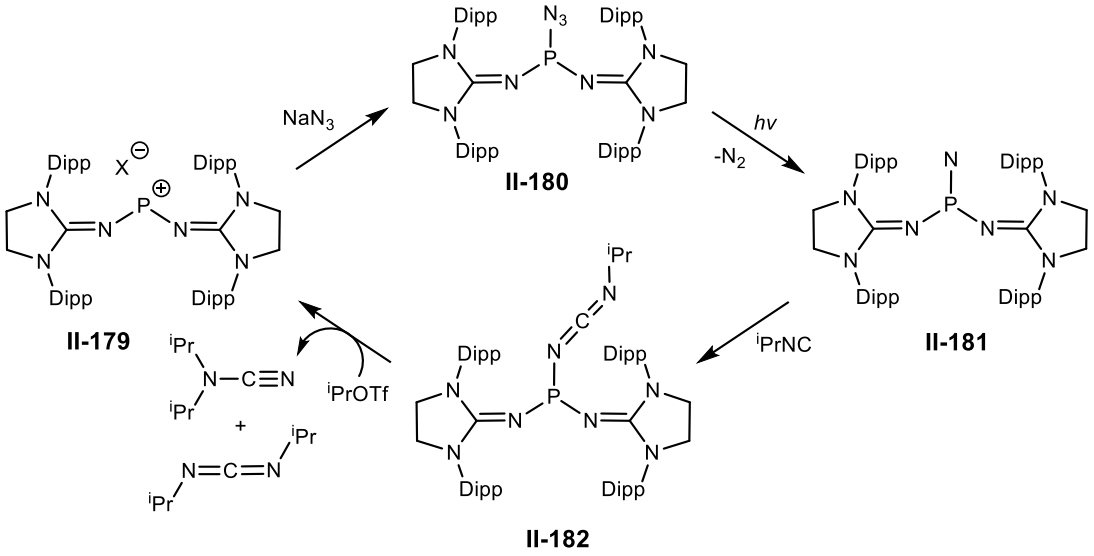

Scheme 65. Formation of nitrene **II-181.**

NBO analysis (NBO – natural bond orbital) showed a large negative charge (-1.22e) on the nitrene nitrogen and a Wiberg bond order of 2.09 for the P-N bond, suggesting the presence of a large polarized double bond. Compound **II-181** is stable at room temperature for several days and when reacted with isopropyl isonitrile produces the nitrogen transfer product carbodiimide **II-181**. Reacting phosphinonitrene **II-181** with isopropyl trifluoromethanesulfonate led to the recovery of the phosphenium salt **II-179**, closing a synthetic cycle depicted in Scheme 65.

Further reactivity studies of the phosphinonitrene **II-181** were performed by the same group (Scheme 66).[147] Compound **II-181** reacts with acetonitrile resulting in an adduct between the nitrene and MeCN (**II-183**) that subsequently gives the ketenimine **II-184** and then diazaphosphete **II-185**. Treatment of **II-181** with carbon dioxide and carbon disulfide resulted in the C=O and C=S bond addition across the N-P bond of phosphinonitrene, giving products **II-186** and **II-187**, respectively.

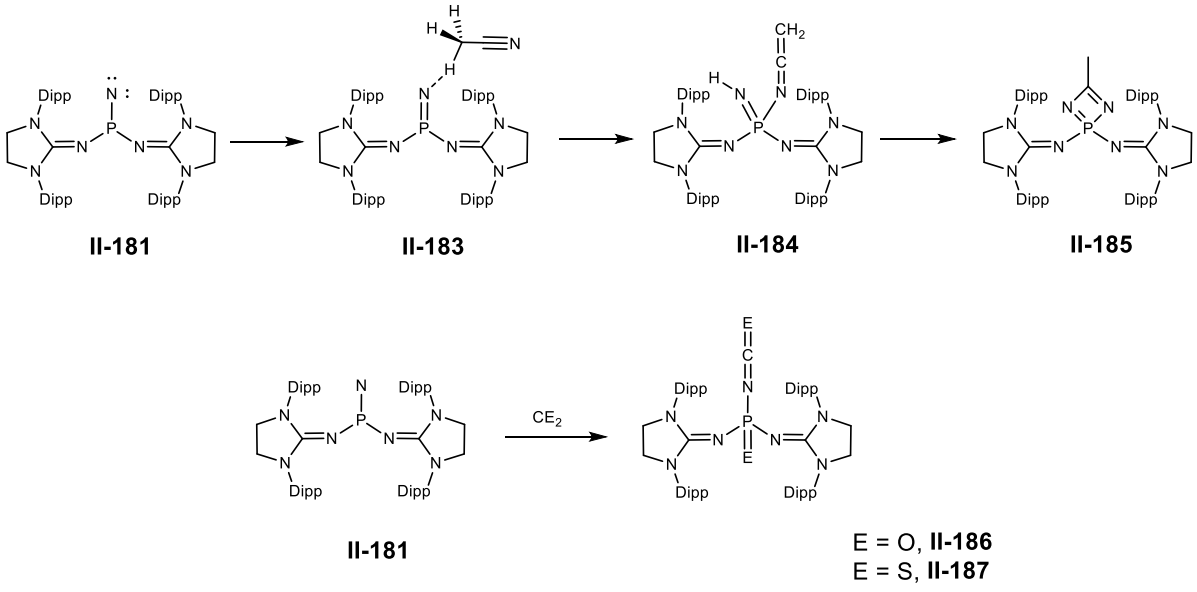

Scheme 66. Reactions of nitrene **II-181** with nitrile, CO_2, and CS2.

The reaction is suggested to proceed via an initial nucleophilic attack of nitrene at the substrate, forming an iminophosphonium intermediate, which then converts to a phosphine oxide or sulfide. The reactivity of **II-181** towards S_8, P_4, and water was also demonstrated. Further application of the phosphinonitrene **II-181** was compromised by the presence of a phosphino group that interferes with its reactivity.

Phosphinidene **II-93** reversibly adds carbon monoxide generating phosphaketene **II-92** (Scheme 67).[111] DFT calculations revealed that the reaction of **II-93** with CO is exergonic by 14.5 ± 1.8 kcal mol^{-1} with a barrier of 16.1 ± 1.9 kcal mol^{-1}. The approach of CO causes the lengthening of the P-P bond. A reverse reaction to form phosphinidene **II-93** is only possible upon UV irradiation.

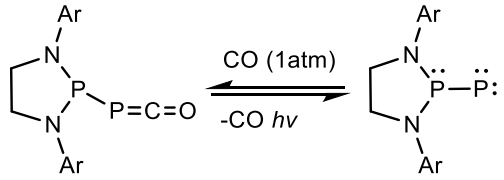

II-92 **II-93**

Scheme 67. Reaction of phosphinidene **II-93** with CO.

Arduengo *et al.* demonstrated that NHC carbenes react with cyclopolyphosphines forming carbene-phosphinidene adducts or phosphaalkenes of the type **II-98**.[148] Treating a carbene-phosphinidene **II-98** with a Lewis acid (e.g. BPh_3) led to extrusion of the phenylphosphinidene forming a cyclopolyphosphines $(PR)_n$ (n=3,4, and 5) without phosphinidene transfer.[149]

The Grützmacher group developed a Lewis acid complex of carbene-phosphinidene to promote the transfer of phosphinidene. Reacting **II-98** with one equivalent of $ZnCl_2$ yielded the soluble adduct **II-188** (Scheme 68).[115] **II-188** was then treated with carbonyl

compounds to induce the transfer of the phenylphosphinidene, PPh. Facile cyclization products of phosphinidene with phenanthrene-9,10-quinone (**II-189**), diphenylketene (**II-190**), and *trans*-chalcone (**II-191**) were isolated. The formation of insoluble polymeric $[MeNHC{\cdot}ZnCl_2]_n$ (**II-192**) was suggested to be the driving force for the PPh transfer reactions.

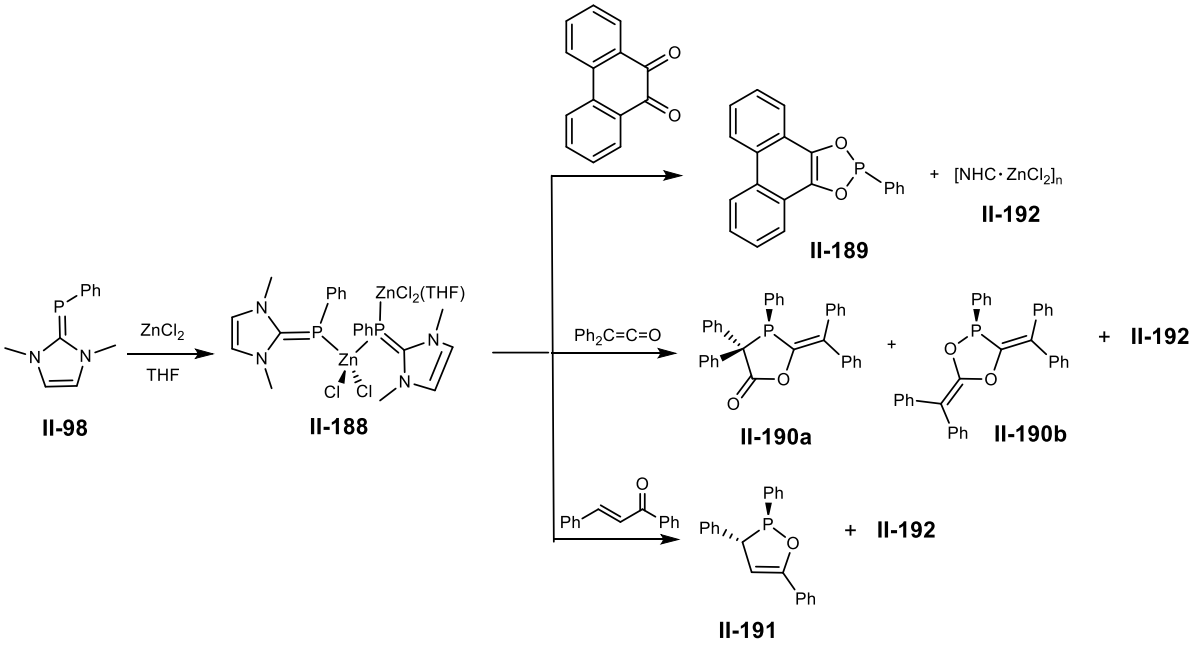

Scheme 68. Reaction of a Zn adduct of phosphaalkene **II-188** with carbonyls.

In this chapter, reactivity of main group reagents towards unsaturated compounds containing carbon-heteroatom bonds was discussed. In particular, cleavage of robust C=X double bonds, selective coupling reactions between unsaturated compounds on main group centers, and catalytic reduction of carbon dioxide were presented.

II.2. Multiple Bonding in Main Group Compounds.

For a long time, multiple bonding between heavier main group elements had been thought to be impossible due to the poor overlap of the p orbitals having a principal quantum number greater than two. The so-called "Double Bond Rule"[150] was broken when a Si–Si double-bonded compound, the disilene $Mes_2Si=SiMes_2$ was synthesized by West *et al.* in 1981.[151] Not long after, compounds containing C=Si[152] and P=P[153] bonds were isolated. These double-bonded compounds were stabilized utilizing sterically hindered supporting ligands. Since then, multiple E-E bonded compounds between the same type of elements have been developed for all p-block elements.[154]

The distinguishing feature of multiple-bonded heavier main group compounds is that they are not planar. Double-bonded compounds adopt the *trans*-bent structure (Scheme 64) with pyramidalization of the main group element center and triple-bonded compounds adopt a bent structure. These geometries are because of the mixing of σ* with π orbitals changes the π bonding orbital to a nonbonding lone pair (Scheme 69). The weak bonding between heavier group elements leads to frontier orbitals with closely spaced energy levels available for interaction with small molecules.[155]

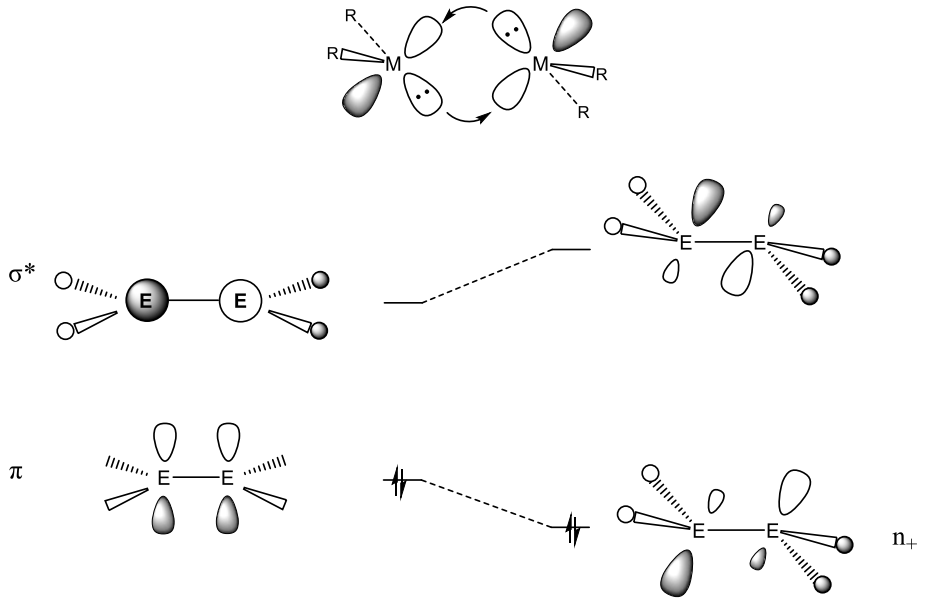

Scheme 69. π-σ* interaction in double-bonded heavier main group elements.

Multiple-bonded main group compounds proved to have transition metal-like reactivity and were applied in activation of strong bonds as demonstrated in Schemes 18, 19, 21, 76 for Al, Ga, and Si analogues of alkene and Si and Ge analogues of alkynes. In fact, the first dihydrogen bond activation on a main group center was performed by a germanium analogue of an alkyne.[22]

Among multiple-bonded main group compounds, the monomeric molecular group 13 element imides and oxides have attracted increased attention as potentially very reactive species. In many cases, their high reactivity prevented their isolation as monomeric species. Chapter II.2 focus on the progress made in the isolation of monomeric oxides and imides of group 13 elements and their reactivity.

II.2.1. Group 13 Imides and Their Reactivity.

Monomeric group 13 imides [E(L)(NR)] (L = supporting ligands) formally containing an element-nitrogen multiple bond have received increased attention as potentially reactive compounds for the activation of strong bonds. However, isolation of monomeric group 13 imides has been a challenging task. The large electronegativity difference between the main group element and nitrogen makes main group imides highly reactive and prone to different side reactions. They tend to undergo aggregation reactions with the formation of dimers and oligomers.[156-158] Another side reaction that hampered the isolation of imides is the intramolecular C-H activation of substituents in the supporting ligand, confirming the high reactivity of the E-N_{imide} moiety.[121, 159] A reaction of monovalent group 13 complexes with organic azides by means of N_2 elimination has proven to be a good strategy for the generation of monomeric group 13 imides. However, another side reaction, a [2+3] cycloaddition of organic azide with group 13 imides forming a tetrazole was also reported.[160-162] To prevent such undesirable reactions, kinetic protection with the use of sterically encumbered ligands has been widely applied.[163] However, the main issue associated with using extremely bulky ligands is that they may hamper further reactivity studies of group 13 imides.

In 2001, Power and Roesky reported the first example of monomeric aluminum (**II-194**) and gallium imides (**II-195**) that were produced from the reaction of bulky azide N_3-2,6-$Trip_2C_6H_3$ (Trip = 2,4,6-$^iPr_3C_6H_2$) with NacNacAl (**II-10**) and NacNacGa (**II-193**) complexes (Scheme 70).[164] A bulky aromatic terphenyl group was used as a steric protection from side reactions, such as dimerization or cycloaddition with a second equivalent of the

azide. Only the gallium imide **II-195** was structurally characterized and the Ga-N_{imide} distance was found to be 1.742(3) Å, which represents one of the shortest Ga-N bonds.[165] Nitrogen adopts a bent geometry, with a Ga-N-C angle of 134.6(3)°, as expected due to the presence of a lone pair on nitrogen. Hartree-Fock calculations on the model gallium imide NacNacGa=NH revealed a weak π-bonding component (48.6 kJ mol^{-1}), which can be explained by the size difference between the Ga and N atoms, the polarity of the bond, and by the weak π-accepting character of NacNacGa.[166]

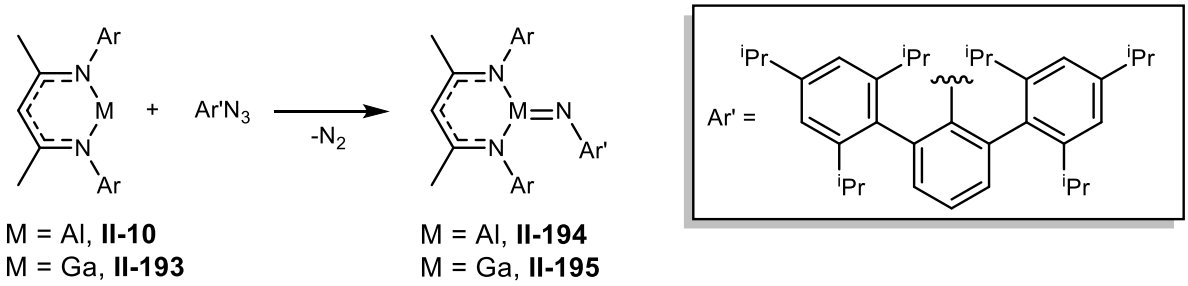

Scheme 70. Terminal Al (**II-194**) and Ga imides (**II-195**).

Similarly, gallium (**II-197**) and indium imides (**II-198**) were synthesized from the reaction of corresponding dimers ArMMAr (Ar = 2,6-$Dipp_2$-C_6H_3; M = Ga **II-41** or In **II-196**) with an azide Ar'N_3 (Ar' = 2,6-(Xyl-4-^{t}Bu)$_2$-C_6H_3) (Scheme 71).[167]

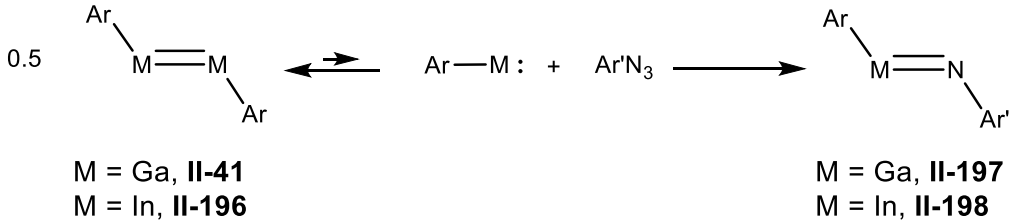

Scheme 71. Terminal Ga (**II-197**) and In imides (**II-198**).

Group 13 dimetallenes ArMMAr are known to dissociate into ArM: monomers in hydrocarbon solvents due to weak M-M bonds.[65] ArM: then reacts with the azide forming a group 13 imide. The Ga-N bond length was found to be 1.701(3) Å, shorter than that in compound **II-194** because gallium in **II-197** is two-coordinate. The In-N distance is 1.928(3) Å, which is the shortest In-N reported in the literature. The CMNC core in compounds **II-197** and **II-198** adopts a *trans*-bent structure consistent with the M–N multiple bond character. Hartree-Fock calculations on the model HM=NH (M = Ga, In) species demonstrated the presence of a M-N π character in the HOMO.

The Power group prepared the first gallium(I) amide $GaN(SiMe_3)Ar$ (**II-199** Ar = 2,6-$MesC_6H_3$), a rare example of a low valent group 13 amide.[168, 169] Treatment of the Ga(I) amide **II-199** with a bulky azide ArN_3 led to the formation of a monomeric imido-gallium amide $ArNGaN(SiMe_3)Ar$ **II-120** (Scheme 72).[168] DFT calculations showed the HOMO of **II-200** to be a polarized Ga-N π bond and the absence of delocalization over N_{amide}-Ga-N_{imide}. The Ga-N_{imide} bond was calculated to have a Wiberg bond order of 1.53, suggesting the presence of a multiple bond character.

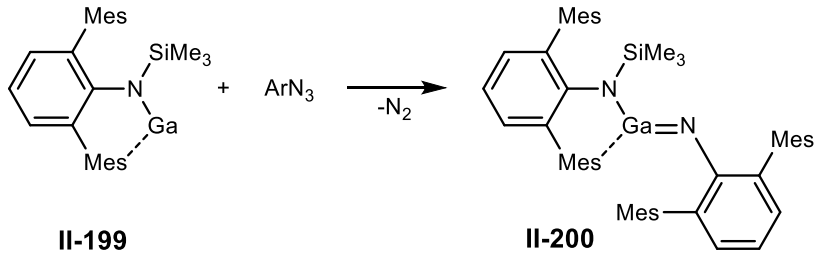

Scheme 72. Synthesis of imido-gallium amide **II-200**.

The first structurally characterized base-stabilized monomeric aluminum imide was prepared by the Cui group in 2012 (Scheme 73).[170] The Al(I) compound **II-201** with the NacNac ligand, having ^{t}Bu groups on the *β*-position of the backbone,[171] was reacted with a N-heterocyclic carbene that led to the cleavage of the C-N bond of the ligand and formation of an NHC adduct of a monomeric aluminum imide **II-202**. X-ray analysis revealed a Al-N_{imide} bond length of 1.705(2) Å, which is shorter than a typical Al-N_{amide} single bond.[165] NBO analysis of the Al-N bond (1.62e) showed a high polarity of the bond (the NBO charges were 1.76135 on Al and -1.20923 on N). Based upon these data, the authors described the bond to be a polar σ bond with an ionic contribution (Al^{+}–N^{-}). Compound **II-202** was reacted with phenyl acetylene and aniline, which resulted in the C-H and N-H bond addition across Al-N_{imide} bond, forming **II-203** and **II-204**, respectively. A reaction of **II-202** with carbon monoxide led to a cyclization product **II-205** through a complicated mechanism.

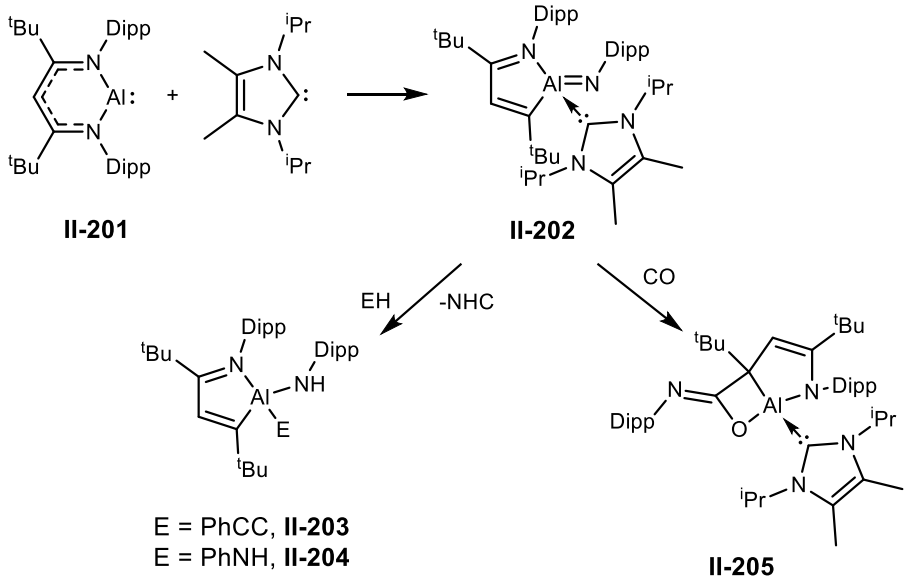

Scheme 73. Base-stabilized monomeric aluminum imide **II-202**.

The first examples of indyl anions have been reported more recently and applied in the synthesis of terminal indium imides.[172] Coles and co-workers used the bis(amidodimethyl)disiloxane ligand NON^{Ar} (NON^{Ar} = $[O(SiMe_2Ndipp)_2]^{2-}$) to form low valent group 13 complexes. The potassium indyl complex K[In(NON^{Ar})] (**II-206**) was reacted with mesityl azide to form the terminal indium imide **II-207** K[In(NONAr)(NMes)] (Scheme 74).[173] Compound **II-207** crystallizes as a dimer with the In-N_{imide} bonds 1.986(2) and 1.999(2) Å found to be shorter than the In-N single bond to amides but longer than that in the neutral indium imide **II-198** (1.928(3) Å). Computational data indicate the presence of a multiple bond character in the In-N_{imide} bond. **II-207** undergoes [2+3] cycloaddition with another equivalent of azide to form the indium tetrazole **II-208**.

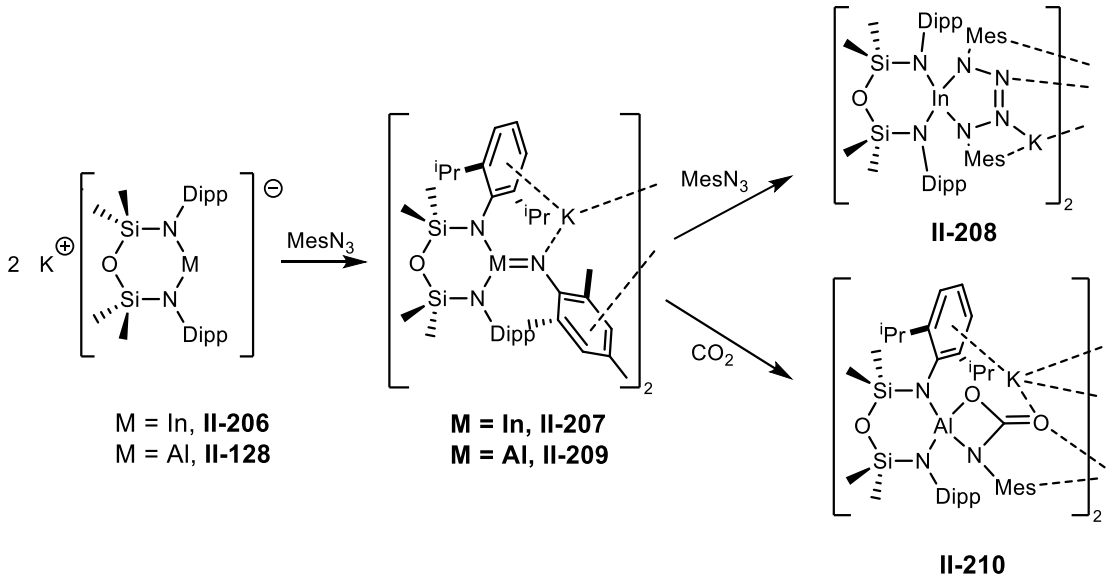

M = In, **II-206**
M = Al, **II-128**

M = In, II-207
M = Al, II-209

II-208

II-210

Scheme 74. Anionic indium (**II-207**) and aluminum (**II-209**) imides.

Similarly, anionic monomeric aluminum imide **II-209** was synthesized from the treatment of the potassium aluminyl K[Al(NON^{Dipp})] complex **II-128** with mesityl azide $MesN_3$.[174] X-ray data show a Al-N_{imide} bond length of 1.7251(11) Å, which is a bit longer

than in the neutral imide **II-202.** Frontier Kohn–Sham MOs revealed a π-symmetric nitrogen lone pair to be in the HOMO. The Wiberg bond index of 0.790 and NPA charges (NPA - natural population analysis, +1.91 on Al and -1.34 on N) suggest the presence of a large ionic component in the Al-N_{imide} bond. Compound **II-209** undergoes [2+2] cyclization with carbon dioxide to form an aluminum carbamate **II-210**.

Aldridge *et al.* reported synthesis of an anionic monomeric aluminum imide **II-211** by the reaction of $K_2[(NON)Al]_2$ **II-18** with azide (Scheme 75).[175] The high reactivity of aluminum imide **II-211** was demonstrated by the cleavage of strong H-H and C≡O bonds. Thus, a reaction of **II-211** with dihydrogen led to the production of the aluminum amido hydride **II-212**. A reaction of **II-211** with CO resulted in the C≡O bond activation and C-C bond formation, resulting in product **II-213**. The mechanism of the reaction involves an isocyanate intermediate that leads to the C-O bond cleavage.

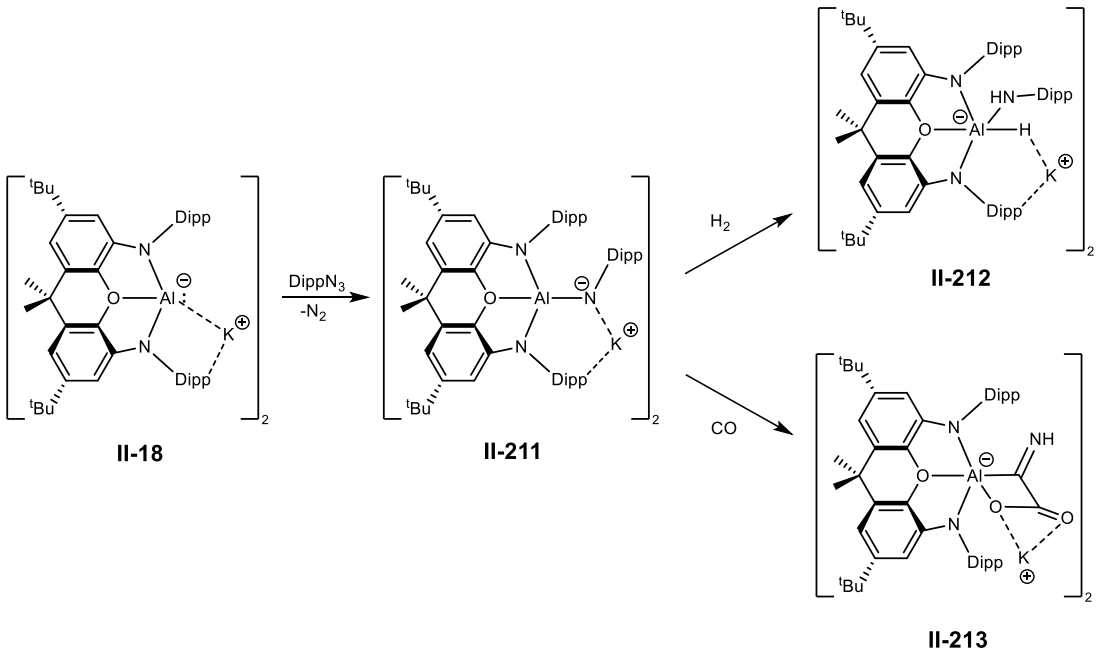

Scheme 75. Anionic aluminum imide (**II-212**).

The Power group has recently synthesized a one-coordinate organoaluminum (I) compound **II-214** stabilized by a sterically encumbered aromatic group.[176] A reaction of **II-214** with terphenyl azide led to the formation of the first example of a two-coordinate aluminum imide **II-215** (Scheme 76).[177] Unlike its heavier analogues **II-197** and **II-198** which are *trans*-bent, the crystal structure of **II-215** revealed a linear geometry with short Al-N_{imide} distances of 1.625(4) and 1.628(3) Å (there were two crystallographically unique molecules), suggestive of an Al–N triple bond. Calculations revealed the σ-donation from Al to N to be the major component of the bonding with two weak π-backdonations from N to Al.

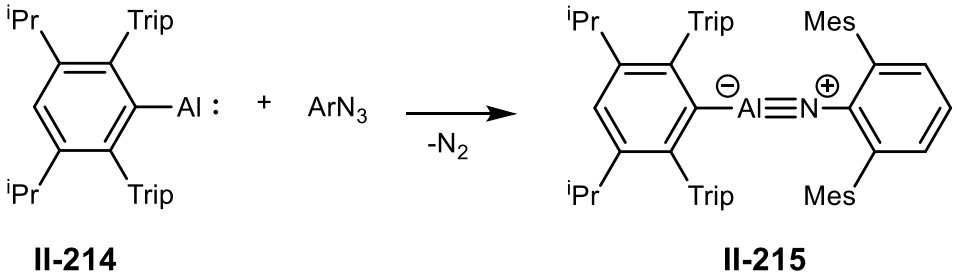

II-214 **II-215**

Scheme 76. Terminal aluminum imide (**II-215**).

II.2.2. Group 13 Oxides and Their Reactivity.

Terminal molecular group 13 oxides [E(L)(NR)] (L = supporting ligands) are challenging compounds for isolation. Similar to related imides, the electronegativity difference between oxygen and group 13 elements also results in aggregation reactions. Different ways of stabilization of monomeric group 13 oxides have been suggested in the literature (Scheme 77).[178] One of them is the kinetic stabilization using very bulky ligands on main group centers. Alternatively, Lewis base and/or Lewis acids can be applied to decrease the electronegativity difference between the main group element and oxygen. A Lewis base coordination to the main group center increases the latter's basicity, while Lewis acid coordination to oxygen quenches the basicity of oxygen.

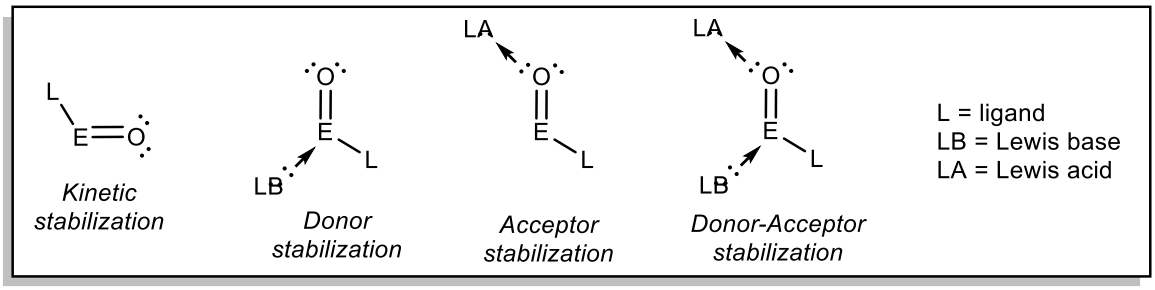

Scheme 77. The ways to stabilize E=O bonded compounds.

A Lewis acid adduct of a monomeric oxoborane LB=O-$AlCl_3$ **II-217** (L = $[C_6F_5NC(Me)CHC(Me)NC_6F_5]^-$) was prepared by the reaction of **II-216** salt with one equivalent of H_2O (Scheme 78).[179] Compound **II-217** has a very short B-O bond length of 1.304(2) Å. The C_6F_5- aromatic group was used in the ligand to prevent C-H bond activation, and $AlCl_3$ coordinates to oxygen stabilizing the compound. DFT calculations on LB=O-$AlCl_3$ and LB=O showed only a small difference in the B-O bond lengths, suggesting

multiple bond character in the compound **II-217.** However, molecular orbital analysis demonstrated considerable difference in the frontier orbitals of the two oxides. The LUMO of both compounds are C-N π^* orbitals in the ligand. The HOMO of the LB=O-$AlCl_3$ is nonbonding orbitals of Al-Cl, whereas the HOMO of LB=O is nonbonding orbitals of Al=O.

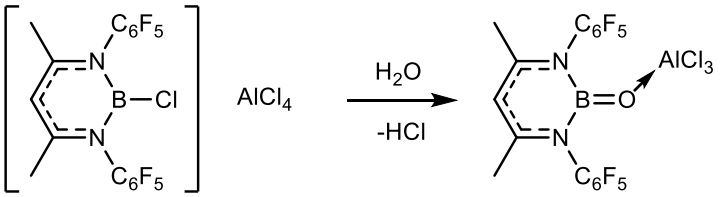

II-216 **II-217**

Scheme 78. Synthesis of oxoborane **II-217**.

Cui *et al*. later reported BCl_3- and $B(C_6F_5)_3$-stabilized *β*-diketiminato oxoboranes (**II-19a,b**) similar to compound **II-217**.[180] An anionic oxoborane **II-213** was prepared by reacting boron hydroxide **III-218** with N-heterocyclic carbene (Scheme 79). DFT calculations on a sterically reduced model compound showed the HOMO-7 contributes towards a B-O π bond; the HOMO is located on two nitrogen atoms and C=C bonds of the ligand, and the LUMO is centered on the imidazolium ring. NBO analysis revealed electron donation from oxygen to boron, supporting the B-O double bond character in **III-219**.

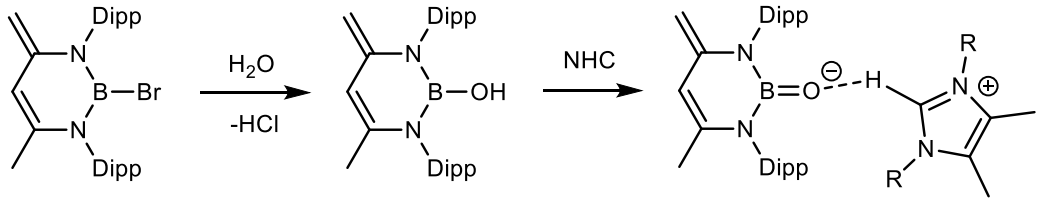

II-218

II-219a, R = Me
II-219b, R = ^{i}Pr

Scheme 79. Synthesis of anionic oxoborane **II-219**.

A Lewis acid and Lewis base-stabilized monoalumoxane was prepared by the Roesky group (Scheme 80).[181] $LAlMe_2$ (**II-220**, L = $Et_2NCH_2CH_2NC(Me)CHC(Me)NCH_2CH_2NEt_2$) was reacted with $H_2O{\cdot}B(C_6F_5)_3$ in toluene giving an aluminum oxide adduct of borane **II-221** as a result of methane evolution. The amine group of the ligand acts as a Lewis base, stabilizing the aluminum oxide thorugh coordination to the aluminum center. The crystal structure of compound **II-221** showed a very short Al-O bond length of 1.659(3) Å.

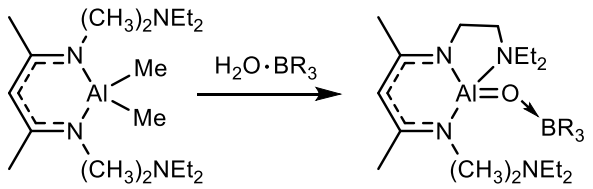

II-220 **II-221**

Scheme 80. Lewis acid and Lewis base stabilized aluminum oxide **II-221.**

Oxidation of the aluminyl anion **II-18** with N_2O in THF resulted in the formation of a THF adduct of aluminum oxide **II-222** (Scheme 81).[123] The choice of solvent is important as the reaction in benzene leads to the formation of a *cis*-hyponitrite complex $K_2[(NON)Al(N_2O_2)]_2$. The crystal structure of **II-222** revealed a very short Al-O distance of 1.676 Å. DFT calculations on $[(NON)AlO(THF)]^-$ and the THF-free anion $[(NON)AlO]^-$ showed similar electronic structures, with the HOMO and HOMO-1 mainly located on the oxide (two pπ-orbitals), whereas the LUMO was on the ligand backbone. The HOMO-LUMO gaps in these compounds were very similar, 4.31 and 4.34 eV, respectively. A scrambling experiment with THF-d_8 suggested coordination of THF to be labile above 0°C. The calculated Al-O bond length in $[(NON)AlO(THF)]^-$ was very close to the

experimentally determined value, which means the K^+ cation has a minimal influence on the Al-O moiety. From these results the authors assigned complex **II-222** as a terminal aluminum oxide. A reaction of **II-222** with H_2 resulted in the cleavage of the H-H bond across the Al-O bond, forming an aluminum hydride hydroxide product **II-223**. The treatment of **II-222** with CO_2 and PhNCO led to [2+2] cycloaddition products **II-126** and **II-127** (Scheme 47).

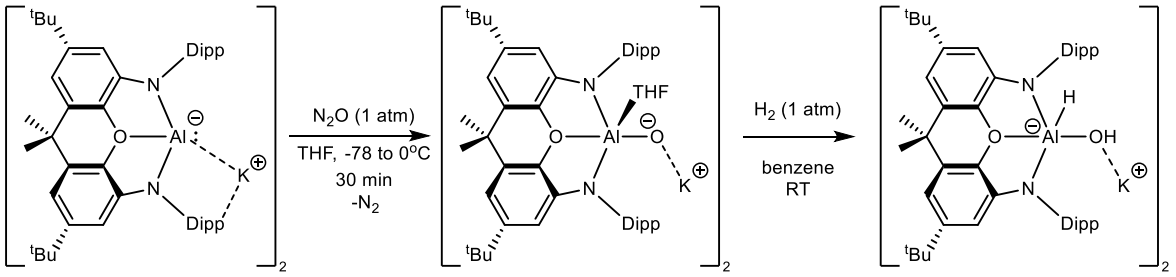

II-18 **II-222** **II-223**

Scheme 81. Synthesis of anionic aluminum oxide **II-222** and its reaction with H_2.

Oxidation of **II-128** with N_2O also resulted in the anionic aluminum oxide complex **II-224** (Scheme 82).[124] Structural data revealed a shorter Al-O bond distance of 1.6362(14) Å, as compared to those in **II-221** and **II-222**, which could be because of a lower coordination number of the aluminum center in the compound **II-224**. The HOMO is localized over an Al-O nonbonding orbital with a π-symmetry according to the composition of the frontier Kohn–Sham orbitals. The rather low Wiberg bond index of 0.86 and NPA charges (Al has +2.03 and O has -1.46) point to an ionic character of the Al-O bond. However, treatment of **II-224** with carbon dioxide led to [2+2] cycloaddition to form **II-129**, showing a double bond-like reactivity of the Al-O bond (Scheme 48).

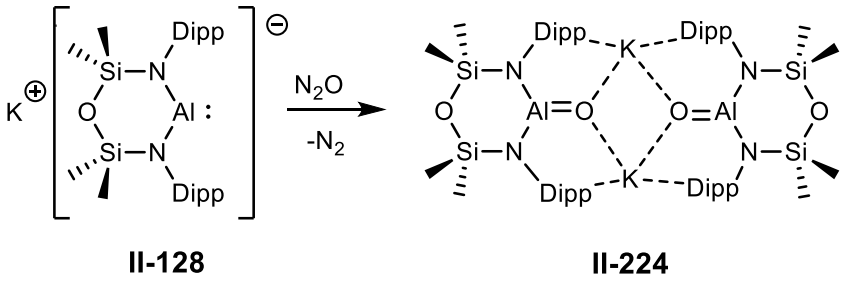

II-128 **II-224**

Scheme 82. Synthesis of anionic aluminum oxide **II-218.**

Multiple bonded main group compounds with particular focus on monomeric group 13 oxides and imides were introduced. Large electronegativity difference between main group center and oxygen or nitrogen makes these reagents highly reactive. Initially kinetically protected oxides and imides were isolated. However, steric protection also prevented from reactivity studies. Only recently base-protected aluminum imide and anionic aluminum oxides/imides have been isolated and their reactivity towards E-H bonds (E = C, N), CO, CO_2 was presented.

III. Reactivity of a Low Valent Gallium Compound.

Low oxidation state compounds of group 13 elements have received increased attention in the last two decades. Among low-valent group 13 compounds, the reactivity of NacNacAl (**II-6**) has been intensively studied in the activation of strong single and multiple-bonded reagents.[23, 120-122, 182] A heavier analogue of **II-6**, the *β*-diketiminato compound of Ga(I), NacNacGa (**III-1**, NacNac = [DippNC(Me)CHC(Me)NDipp]$^-$) is a gallium carbenoid featuring a singlet lone pair of electrons and an empty orbital localized on the gallium center. Power *et al.* reported preparation of **III-1** from the reaction of NacNacLi with "GaI"[183] (Scheme 83).[4]

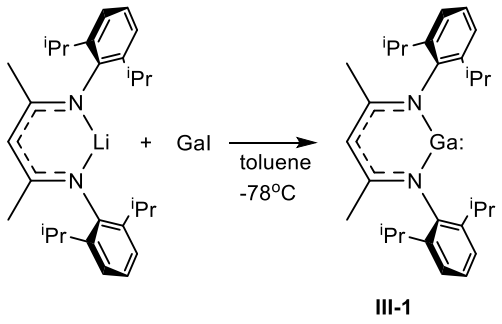

III-1

Scheme 83. Synthesis of NacNacGa.

The ability of **III-1** to activate strong element-hydrogen σ bonds (Si-H, Sn-H, B-H, H-H, N-H, O-H, P-H),[5] group 13 – 15 halides (Ga-Cl, Sn-Cl, SI-Cl, C-Cl, P-Cl, P-Br, As-Cl)[6, 7], oxide (Bi-O)[8], amides (As-N, Bi-N)[7], and alkyls (Ga-Me, In-Et, Bi-Et)[6, 9, 10] has been demonstrated. Reversible insertion of **III-3** into Sb-Sb and Bi-Bi bonds has also been shown.[11] Recently, heterodiatomic compounds containing Ga–E double bonds were prepared: gallaarsene,[12] gallastibene,[13] and gallaphosphene.[14-17]

The electronic structure of Ga(I) and Al(I) complexes **III-1** and **II-6**, respectively, were studied by Power and co-workers.[166] NacNacGa **III-1** was found to have a larger HOMO-LUMO (around 12 kcal/mol difference) gap compared to that of its aluminum congener, primarily due to the lower energy of the gallium lone pair. This makes NacNacGa less reactive than NacNacAl.

The first section of this chapter will discuss the reactions of Ga(I) compound **III-1** with unsaturated substrates. The second and third sections are about the reactivity of transient gallium oxide and imide generated from an *in situ* oxidation of NacNacGa. The last section will present a gallium nitrilimine formed from the reaction of Ga(I) **III-1** with diazomethane and its reactivity.

III.1 Interaction of Multiple Bonds with NacNacGa: Oxidative Cleavage vs Coupling and Cyclization[a]

Bond activation is one of the main steps in catalytic transformations and until recently bond activation reactions have been the exclusive feature of transition metals. Discovery of new classes of main group compounds having transition-metal like properties led to an increased interest in bond activation reactions on main group compounds.[1] There has been a significant development in the oxidative cleavage of strong σ bonds on main group centers.[2] The chemistry of main group element compounds in terms of their reactivity with unsaturated compounds has been less studied. Our group has established the propensity of the Al(I) *β*-diketiminate, NacNacAl (**II-10**), in cleaving the C=S bond of thiourea[122], the P=O of phosphine oxide,[120] the P=S bond of phosphine sulfide,[122] and the C=N bond of a cyclic guanidine.[121] More recently, a reversible olefin addition to **II-10** has been reported.[25, 48] However, very little is known about the reactivity of low-valent gallium compounds towards multiple bonds. Reactivity studies of low valent gallium compounds towards multiple-bonded species are limited to reaction of digallenes with alkenes and alkynes[65, 67, 68], addition of alkynes[71, 72] and cleavage of the C=S bond of isothiocyanate[128] by digallanes, activation of the C=N bond of carbodiimide and the C=O bond of carbon dioxide or isocyanate by anionic gallylene[129, 130].

We decided to probe the reactivity of NacNacGa (**III-1**) towards unsaturated molecules to expand its reaction scope. In this part of the thesis, we investigate the reactivity of Ga(I) toward various heterocumulenes, carbonyls, phosphine oxides, and sulfides.

---

[a]Adapted with permission from Kassymbek, A.; Britten, J. F.; Spasyuk, D.; Gabidullin, B.; Nikonov, G. I. *Inorg. Chem.* **2019**, *58*, 8665−8672 Copyright 2021, American Chemical Society.

The gallium (I) compound **III-1** does not show any sign of olefin coordination in reactions with cyclohexene and ethylene, even at low temperature (−20°C). Neither is there a [1 + 4] cycloaddition with butadiene, which is in contrast to the reactivity of its aluminum congener (**II-10**)[45, 49] and isolobal silylene (**II-60**).[83, 85] On the other hand, the *α,β*-unsaturated aldehyde, methacrolein, easily cyclizes with **III-1** to give the gallium enolate **III-2** (Scheme 84).

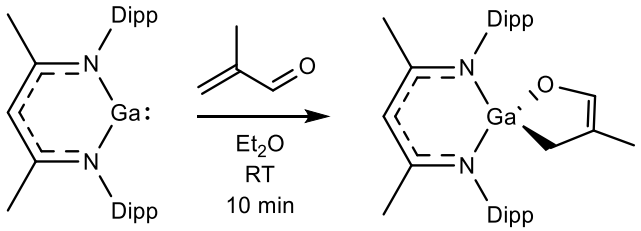

III-1 **III-2**

Scheme 84. Reaction of **III-1** with methacrolein.

The identity of this product was established by NMR spectroscopy and confirmed by X-ray analysis (Figure 1). In particular, the olefinic proton gives rise to a resonance at 6.88 ppm and the backbone methine of NacNac is seen at 4.86 ppm. The methyl signal of the enolate part was observed at 1.45 ppm. X-ray diffraction revealed a spiro structure formed as a result of [1 + 4] cycloaddition. The Ga−O bond of 1.884(2) Å and the Ga−C bond of 1.979(3) Å are normal for the respective single bonds. The C31−C30 distance, corresponding to the C−C double bond in the parent methacrolein, is elongated to 1.516 (5) Å, whereas the C31−C32 distance is contracted to 1.339 (5) Å, indicating the formation of an enolate moiety. Interestingly, the spiro structure is distorted in such a way that the C30−Ga1−N1−N2 fragment is close to planarity (the sum of bond angles around Ga of 345.37°), whereas the oxygen atom forms rather small angles with the GaN_2 fragment, 109.7(1)° and 107.7(1)°.

The C32−Ga1−O1 angle is nearly a right angle, 93.0(1)°. This feature indicates that a significant s character of Ga is spent on the bond to the carbon atom, whereas more p-character goes to the bond with oxygen, in agreement with the relative electronegativity of these two groups.

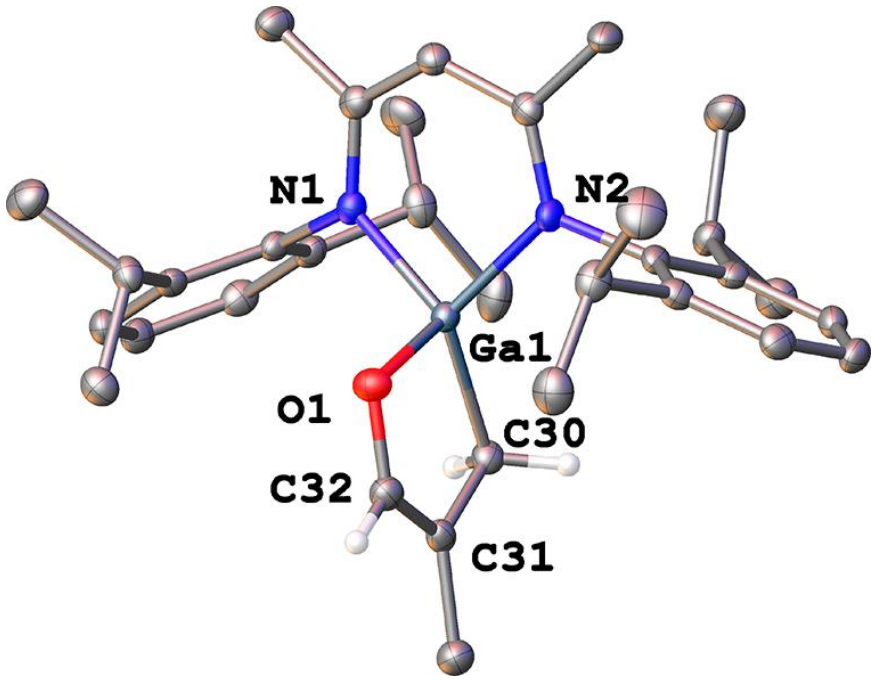

Figure 1. Molecular structure of NacNacGa(-OCH=C(CH_3)-CH_2-) (**III-2**). Hydrogen atoms, except C32-H and C30-H, are omitted for clarity. Thermal ellipsoids are shown at 30%.

Table 2. Selected bond lengths and angles for the compound **III-2**.

Lengths, Å				**Angles, °**	
Ga1−N1	1.942(3)	Ga1− C30	1.979(3)	N1−Ga1−N2	96.3(1)
Ga1−N2	1.943(3)	C31−C32	1.339(5)	O1−Ga1−C30	93.0(1)
Ga1−O1	1.884(2)	C30−C31	1.516(5)	Ga1−O1−C32	105.4(2)
				Ga1−C30−C31	100.3(2)

Unexpectedly, there was no reaction between **III-1** and diphenylketone, which also stands in contrast to the easy addition of this ketone to the aluminum (I) compound **II-10** (Schemes 40 and 42). This difference in reactivity between aluminum and gallium likely stems from the greater stabilization of the lone pair of gallium vs the lone pair of aluminum, which results in a larger singlet-to-triplet gap in **III-1**.[166]

We then looked at the possibility of multiple bond cleavage at gallium. Oxidative addition of a multiple bond X=Y to a group 13 NacNac compound NacNacM is possible if one of the partners, X or Y, is stable in the subvalent state. The possible candidates are, therefore, CO_2, CS_2, isocyanates, isothiocyanates, and diimines, to name a few.

Unlike the reactions of the aluminum analogue **II-10** shown in Schemes 45 and 46, compound **III-1** does not react with cyclic urea, thiourea, guanidine, and phosphine oxides ($Ph_3P=O$ and $Et_3P=O$). Neither was there any cleavage of the P=S bond of $Et_3P=S$, even upon heating to 80 °C. With $Ph_3P=S$, however, a slow reaction (2 days) was observed upon heating the reaction mixture at 80°C to furnish the known sulfide dimer $(NacNacGa\text{-}S)_2$ (**III-3** in Scheme 85).[184] The reaction progress was monitored by ^{31}P NMR spectroscopy.

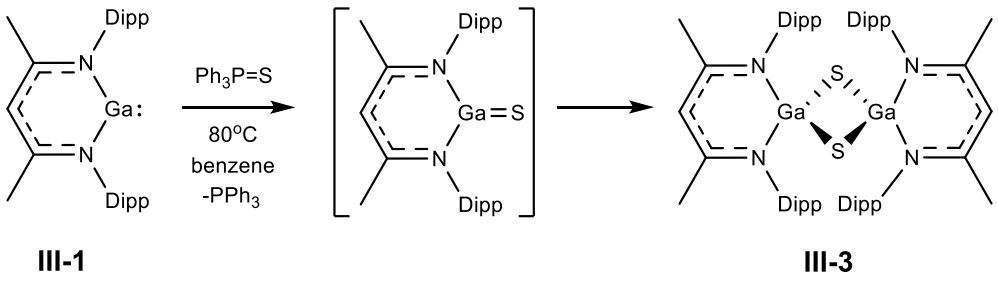

Scheme 85. Reaction of **III-1** with phosphine sulfide.

Nevertheless, **III-1** readily reacts with two equivalents of isothiocyanate PhNCS to give the product of C=S cleavage and cyclization **III-4** and the dimer $(NacNacGa)_2(\mu\text{-}S)(\mu\text{-}CNPh)$ (**III-5**) in the ratio 5:1 (Scheme 86). Dropwise addition of only one equivalent of phenyl isothiocyanate to a toluene solution of **III-3** produced a mixture containing products **III-4** and **III-5** in the ratio 1:1. The reaction likely proceeds via intermediate formation of the sulfide cyanide complex (NacNacGa)(=S)(CNPh) that either reacts with another equivalent of PhNCS to give **III-4** or is intercepted by the starting complex **III-3** to furnish **III-5**. The first reaction is thus analogous to the reaction of aluminum compound **II-10** with isothiocyanate to give NacNacAl(κ^2-S_2C=NPh) (**II-125**).[122]

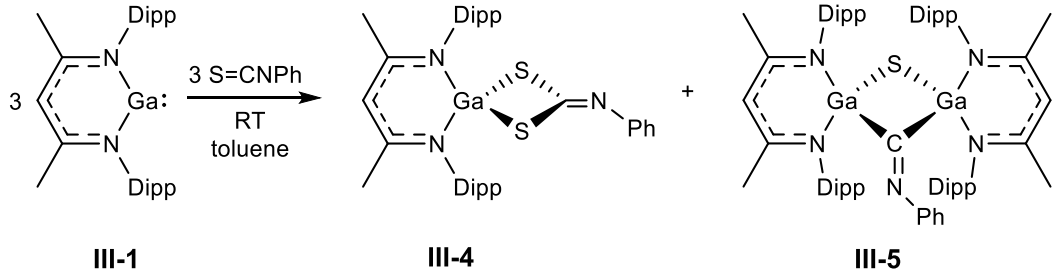

III-1 **III-4** **III-5**

Scheme 86. Cleavage of S=C bond of phenyl isothiocyanate by **III-1**.

In the ^{1}H NMR spectrum, compound **III-4** gives rise to a *Cs* symmetric pattern featuring the backbone signals at 4.79 and 1.51 ppm, two septets (at 3.17 and 3.10 ppm) for the methine part of ^{i}Pr groups, and four doublets for their methyl groups. The imine carbon of the -C=NPh moiety was assigned the resonance at 155.6 ppm by ^{1}H-^{13}C HMBC. Crystals suitable for X-ray diffraction were grown from a 1:2 mixture of toluene and hexanes, and the molecular structure is shown in Figure 2.

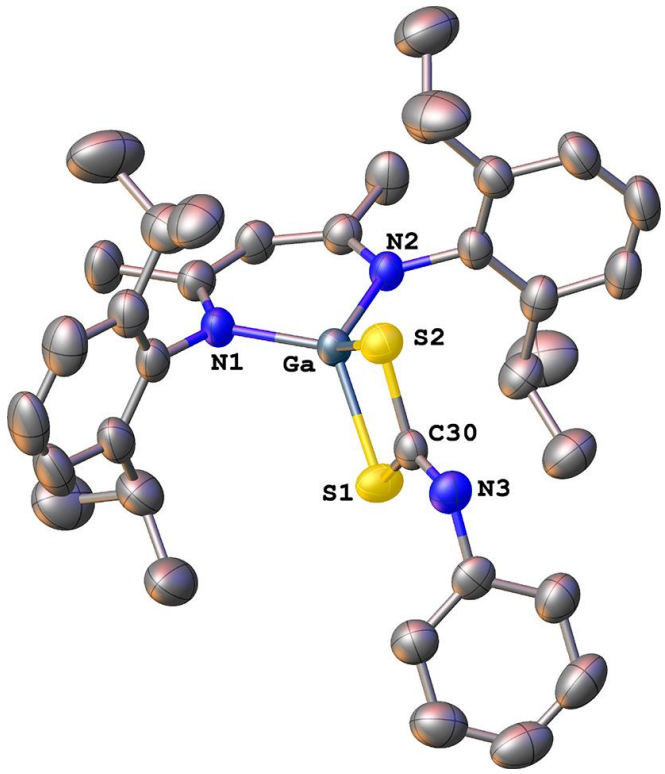

Figure 2. Molecular structure of NacNacAl(κ2-S_2C=NPh) (**III-4**). Thermal ellipsoids are shown at 30%; hydrogen atoms are omitted for clarity.

Table 3. Selected bond lengths and angles for compound **III-4**.

Lengths, Å		**Angles, °**	
Ga1−N1	1.912(3)	N1−Ga1−N2	99.28(8)
Ga1− S2	2.2561(7)	S1−Ga1−S2	81.78(3)
Ga1−N2	1.909(2)	S1−C30−S2	112.5(1)
S1−C30	1.787(2)	Ga1− S1−C30	82.54(8)
Ga1−S1	2.2639(7)	Ga1−S2−C30	83.09(8)
S2−C(30)	1.772(2)		

The gallium atom has a distorted tetrahedral environment comprised of the chelating NacNac ligand and the κ^2(S,S)-coordinated dithioazacarbonate. The Ga−S bonds have

slightly differing distances 2.2639(7) and 2.2561(7) Å and are comparable to the Ga−S distances (2.2511(7) and 2.2736(7) Å) in the sulfide dimer **III-3** produced from the reaction of **III-1** with elemental sulfur.[184] The S− C−S bond angle of 112.5(1)° is significantly wider than angles at sulfur (82.54(9)°) or gallium (81.78(3)°) making the GaS_2C ring kite-shaped. Similar metrics, e.g., the S−C−S bond angle of 112.21(14)° and the S−Al−S bond angle of 82.91(4)°, were found in the aluminum congener **II-114**.[122]

The chemistry of **III-1** (Scheme 86) is reminiscent of the C=S bond cleavage and cyclization observed by Jutzi *et al.* in the reaction of silylene Cp^*_2Si (**II-151**) with MeNCS or PhNCS to give $Cp^*_2Si(S_2CNR)$ (**II-153**, R = Me or Ph, Scheme 55),[117] and to the reaction of Kira's dialkylsilylene, 2,2,5,5-tetrakis- (trimethylsilyl)-silacyclopentane-1,1-diyl **II-47**, with isothiocyanate forming **II-166** (Scheme 60).[137] These authors suggested an initial [2 + 1] cycloaddition of the C=S bond to the silicon center to form a highly strained three-membered ring. Subsequent extrusion of isocyanide generates an intermediate silanthione, which then undergoes a cycloaddition reaction with a second equivalent of isothiocyanate. The groups of Fedushkin and Yang reported on the first instance of the oxidative cleavage of the C=S bond of isothiocyanates on subvalent digallanes **II-135** and **II-45** supported by a non-innocent diimine ligands (Scheme 52).[128]

The formation of dimeric species **III-5**, having the sulfide and cyanide bridges (Figure 3), in the reaction mixture of **III-1** and S=C=NPh serves as indirect evidence that the reaction proceeds via the oxidative addition of the S=C bond of isothiocyanate to low valent gallium center. Compound **III-5** then can be considered as the result of a reaction between the immediate product of C=S oxidative addition, the sulfide

NacNacGa(=S)(CNPh), and the starting NacNacGa. **III-5** was characterized by multinuclear NMR spectroscopy. Two NacNac groups give rise to a separate set of signals. The backbone methine signals appear at 4.85 and 4.79 ppm in ^{1}H NMR spectrum and at 97.5 and 97.3 ppm in ^{13}C NMR spectrum. Red crystals of **III-5**, grown from ether, were manually isolated from the yellow crystals of **III-4**The molecular structure of **III-5** is shown in Figure 3. The structure is nearly symmetric except that the C(1)=N(1) imine moiety has a bent geometry, so that the N-bound phenyl group is oriented to Ga2. Apart from this, the metrics associated with the bridging atoms as well as the coordination of NacNac ligands are very similar for both parts of the dimer. Thus, the Ga−N distances fall in the narrow range 1.989−2.023(2), albeit the bonds to Ga2 appear to be slightly longer, likely in order to accommodate the phenyl group located in the pocket comprised by two bulky Dipp groups attached to N4 and N5. The gallium−sulfide bonds are very similar at 2.2844(6) and 2.2648(6) Å for Ga1 and Ga2, respectively; as are the gallium−cyanide distances to the bridging carbon atom, 2.045(2) and 2.086(2) Å, respectively. The somewhat longer distance from C1 to Ga2 again may reflect the need to accommodate the phenyl substituent of the bridging isocyanide. The central Ga_2SC cycle is almost planar, with the dihedral angle of 0.29(6)°. The Ga1− C1− Ga2 bond angle of 94.98(9) is quite small for an expected sp^2-hybridized carbon, whereas the C1− N1 − C2 angle is normal (122.2(2)°) for an imine, as is the N(1)− C(1) bond length of 1.276(3) Å. On the other hand, the similarly small bond angle at the sulfur atom, Ga2 − S1 − Ga1 of 84.04(2)°, is normal for heavy main group elements and indicative of a high degree of 3p character in the bonds to Ga. The Ga···Ga separation of 3.0452(4) Å is similar to other known gallium sulfide dimers[128, 184] and is significantly larger than the doubled

covalent radius of Ga (2 × 1.22 Å = 2.44 Å),[66] suggesting that there is no interaction between two gallium centers.

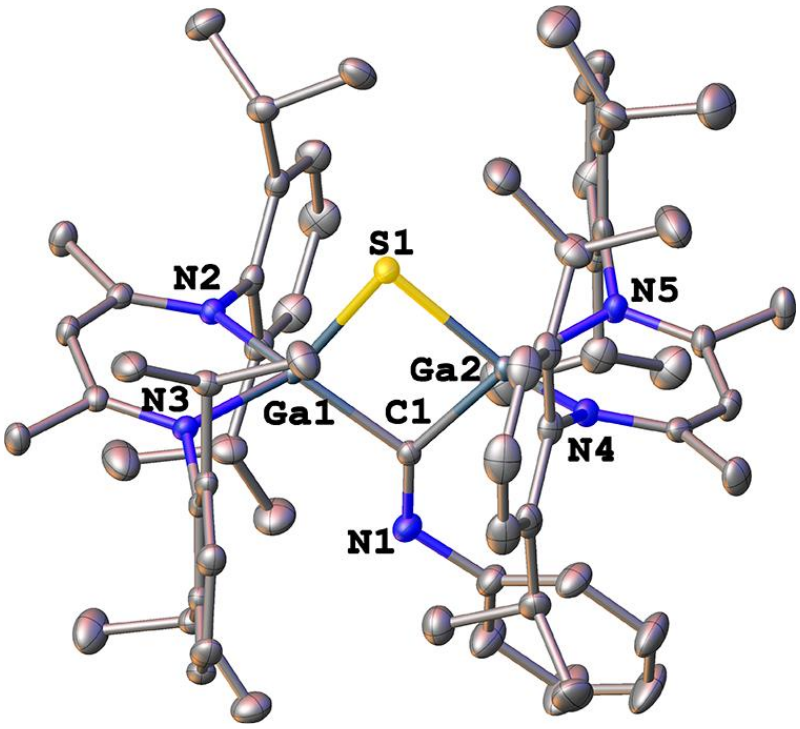

Figure 3. Molecular structure of $(NacNacGa)_2(\mu\text{-}S)(\mu\text{-}CNPh)$ (**III-5**). Thermal ellipsoids for the core elements are shown at 30%; hydrogen atoms are omitted for clarity.

Table 4. Selected bond lengths and angles for the compound **III-5**.

Lengths, Å				**Angles, °**	
Ga1−N2	1.9988(18)	Ga1−C1	2.045(2)	N3−Ga1−N1	93.86(7)
Ga1−N3	1.9890(19)	Ga2−C1	2.086(2)	N5−Ga2−N4	92.95(8)
Ga2−N4	2.0225(18)	Ga1−S1	2.2844(6)	C1−Ga1−S1	90.73(6)
Ga2−N5	2.0099(19)	Ga2−S1	2.2648(6)	C1−Ga2−S1	90.24(6)
		N1−C1	1.276(3)	Ga2−S1−Ga1	84.04(2)
				Ga1−C1−Ga2	94.98(9)

Encouraged by this result, we then studied the possibility of C=O cleavage in isocyanates. An anionic gallium compound reacts with isocyanates forming cyclization products **II-149** and **II-150** as reported by the Fedushkin group (Scheme 54). (3,5-$Me_2C_6H_3$)NCO and PhNCO readily react with **III-3** giving the coupling products shown in Scheme 87. The preservation of the C=O bond agrees well with its strength (799 kJ/mol) and the lack of C=O oxidative addition in the related aluminum chemistry (Scheme 45).

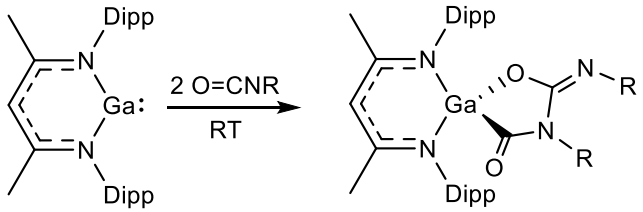

III-1

R = Ph, **III-6**
R = 3,5-Xyl, **III-7**

Scheme 87. Addition of isocyanates to **III-1**.

Crystals of **III-6** suitable for X-ray diffraction could not be obtained, but the xylyl derivative, complex **III-7**, was fully characterized by both multinuclear NMR spectroscopy and X-ray analysis. The ^{1}H NMR spectrum displays a C_s symmetric pattern, with two sets of methine signals at 3.44 and 3.22 ppm and four sets of methyl signals for the ^{i}Pr groups (1.50, 1.36, 1.15, and 1.04 ppm). Methyl groups of the xylyl moiety appear at 2.21 ppm and 1.90 ppm. The molecular structure is shown in Figure 4, which reveals a bicyclic spiro structure with the gallium atom in the bridgehead position. The newly formed OGaCNC ring is almost planar, with the dihedral angle C4− Ga1 − O1 −C16 being 0.5(2)°. The Ga−O distance of 1.886(2) Å and Ga−C distance of 1.997(3) Å are very close to the respective values in the enolate **III-2**. The OGaC bond angle at 87.4(1)° is considerably smaller than other bond angles within the OGaCNC cycle.

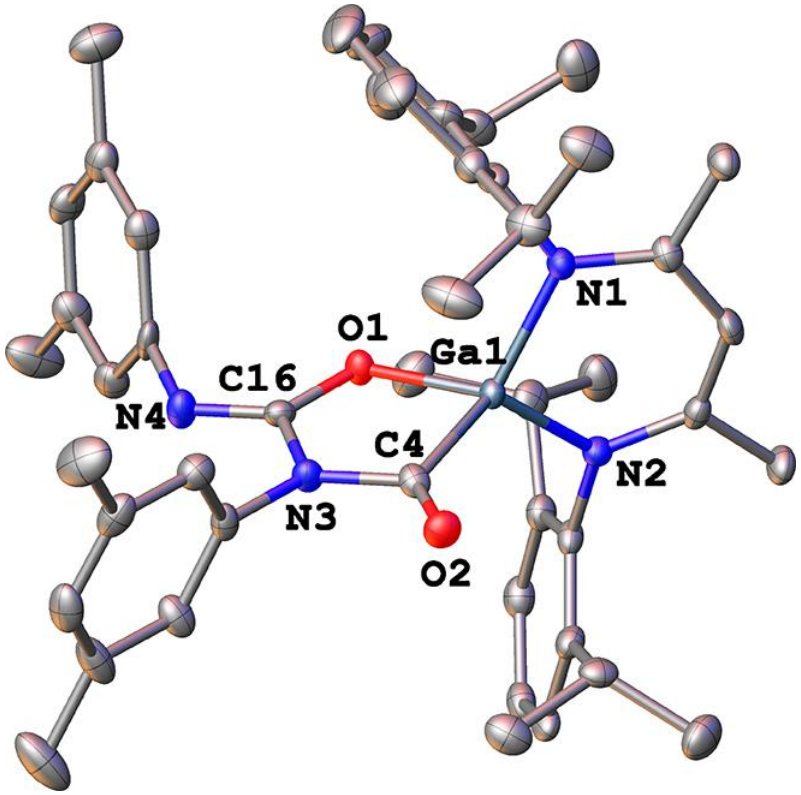

Figure 4. Molecular structure of NacNacGa[(3,5-CH_3)$_2$$C_6H_3$NCO]$_2$ (**III-7**). Thermal ellipsoids for the core elements are shown at 30%; hydrogen atoms are omitted for clarity.

Table 5. Selected bond lengths and angles for the compound **III-7**.

Lengths, Å		**Angles, °**			
Ga1−N1	1.909(2)	N1−Ga1−N2	99.8(1)	Ga1−C4−N3	104.7(2)
Ga1−N2	1.899(2)	O1−Ga1−C4	87.4(1)	O1−C16−N3	115.9(3)
Ga1−O1	1.886(2)	Ga1−O1−C16	112.8(2)	C4−N3−C16	119.1(2)
Ga1−C4	1.997(3)				

The regioselectivity of cyclization is such that the C=N bond of one isocyanate adds to the C=O bond of another isocyanate to form a new C−N bond and a cyclic alkoxy alkyl gallium fragment. While we have no mechanistic data from this reaction, we speculate that the reaction may start by the reaction of the C=N group of isocyanate with the gallium center

acting as a Lewis base, forming the intermediate with a negative charge on nitrogen (Scheme 88). The regioselectivity of subsequent [3 + 2] step is such that the nucleophilic nitrogen atom attacks the carbonyl center of the second isocyanate, resulting in a cyclization product.

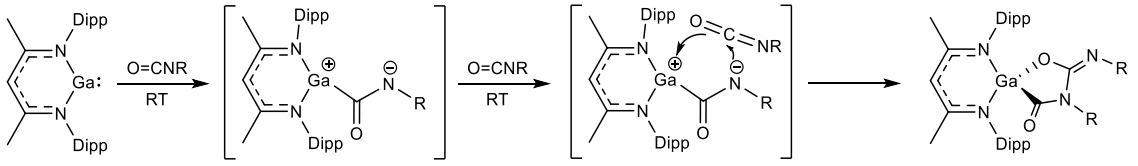

Scheme 88. Possible mechanism of addition of isocyanate to **III-1.**

Given the ability of the aluminum compound **II-10** to cleave the C=N in guanidines but the lack of the corresponding reactivity for the gallium compound **III-1**, we reasoned that the more accessible linear carbodiimides RN=C=NR could be better candidates for oxidative addition of C=N. There has been no reaction between **III-1** and bulky iPrN=C=NPri or (o-Tol)N=C=N(o-Tol), but (p-Tol)N=C=N(p-Tol) reacted at room temperature in the course of five hours to give the coupling product **III-8**, similar to compound **III-7** (Scheme 89).

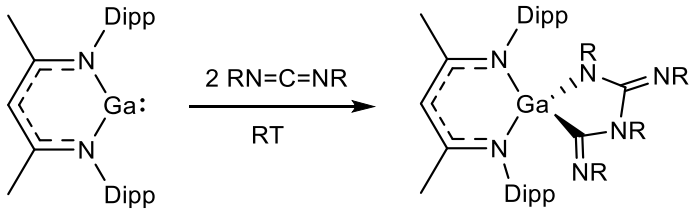

Scheme 89. Reaction of **III-1** with carbodiimide.

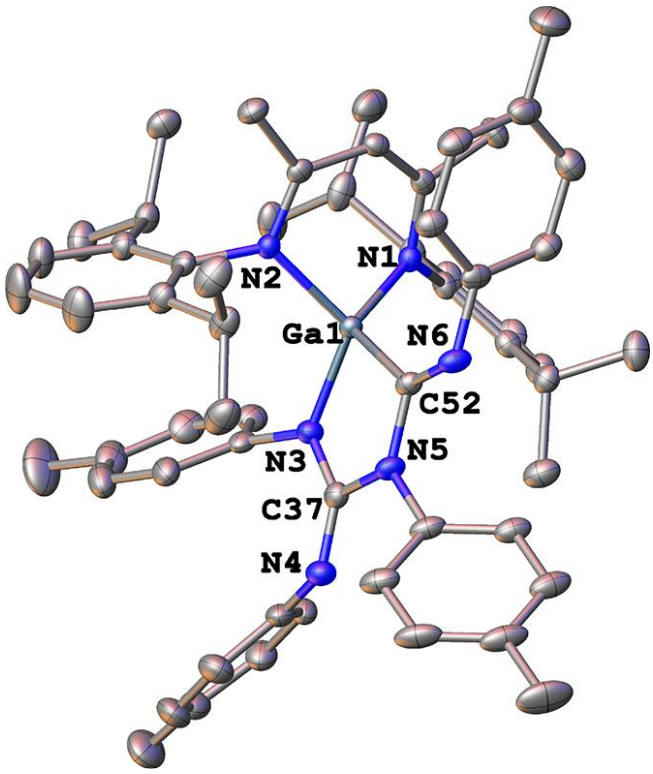

Figure 5. Molecular structure of NacNacGa[4-$CH_3C_6H_4NCN$(4-$CH_3C_6H_4$)]$_2$ (**III-8**). Thermal ellipsoids are shown at 30%; hydrogen atoms are omitted for clarity.

Table 6. Selected bond lengths and angles for the compound **III-8**.

Lengths, Å		**Angles, °**			
Ga1−N1	1.930(2)	N1−Ga1−N2	96.72(7)	Ga1−C52−N5	105.9(1)
Ga1−N2	1.936(2)	N3−Ga1−C52	86.81(8)	N3−C37−N5	113.0(2)
Ga1−N3	1.893(2)	Ga1−N3−C37	114.2(1)	C37−N5−C52	120.1(2)
Ga1−C52	2.004(2)				

The product was characterized by NMR spectroscopy and by X-ray diffraction (Figure 5). As expected, the Ga1−N3 bond of 1.893(2) Å is slightly longer than the Ga1−O1 distance in **III-7**. The Ga1−C52 bond is also slightly longer (2.004(2) Å), likely because of the need to accommodate the more sterically encumbered iminyl-guanidide ligand.

In conclusion, the reactivity of NacNacGa (**III-1**) towards unsaturated substrates was studied. Treatment of compound **III-1** with conjugated carbonyl, methacrolein, resulted in the [4+1] cycloaddition product **III-2**. The reaction of NacNacGa with phenyl isothiocyanate led to cleavage of C=S bond at room temperature. Depending on addition the mode, either the cycloaddition product [NacNacGa(S_2CNPh)] (**III-4**) or the sulfur/isocyanide-bridged dimer **III-5** were obtained. Isocyanate and carbodiimide susbtrates, containing more robust C=O and C=N bonds underwent cycloaddition reactions on Ga(I) forming **III-7** and **III-8**, respectively.

III.2 Sequential Oxidation and C-H Bond Activation at a Gallium(I) Center.[b]

There has been a great interest in the isolation of monomeric group 13 oxides with the potential application in activation of strong bonds. However, the large electronegativity difference between oxygen and group 13 elements has precluded the isolation of reactive group 13 oxides. More recently, Aldridge *et al.* reported the anionic terminal aluminum oxide **II-222**, and its high reactivity was demonstrated in the cyclization reaction with carbon dioxide, activation of the C-H bond of benzene and the addition of dihydrogen.[123] The Coles group has also isolated a related anionic aluminum oxide **II-224**.[174]

The C-H activation reaction is the important way of functionalizing organic compounds to obtain value-added products. For a long time, C-H activation has been exclusively a domain of transition metal complexes. C-H activations on main group centers usually involve intramolecular insertions of reactive low-valent centers into the adjacent C-H bonds of ligands.[185-187] Intermolecular C-H activation reactions are less represented. NacNacAl (**II-10**) was reported to cleave the C-H bond of pentamethylcyclopentadiene[182] and, in the presence of NacNacCaH_2, C-H bonds of benzene, toluene, and p-xylene.[188] Iminoborane and diboryne compounds were shown to perform sp^3C-H activation of acetone.[189]

---

[b]Adapted with permission from Kassymbek A.; Vyboishchikov, S. F.; Gabidullin, B. M.; Spasuyk, D.; Pilkington, M.; Nikonov. G. I. *Angew. Chem. Int. Ed.* **2019**, *58*, 18102 – 18107. Copyright 2021, Wiley-VCH

In this part of the thesis, the *in situ* oxidation of NacNacGa **III-1** in the presence of various substrates that results in C-H activation by an intermediate NacNacGa=O will be presented.

Power *et al.* have previously reported that oxidation of NacNacGa (**III-1**) by N_2O results in the isolation of the oxo-bridged dimer [NacNacGa(μ-O)]$_2$, which is poorly soluble in nonpolar solvents.[184] Attempts to react a suspension of this compound with organic substrates (pyridine and cyclohexanone) did not lead to any noticeable reactivity. However, our attempts to oxidize **III-1** by using pyridine N-oxide unexpectedly resulted in the isolation of unreacted **III-1**, together with the oxopyridyl hydroxide NacNacGa(OH)(η^1(C),κ^1(O)-*o*-C_5H_4N-O) (**III-9**), the product of sequential oxidation and C–H activation in pyridine N-oxide (Scheme 90). With two equivalents of pyridine N-oxide, the products were exclusively **III-9** and free pyridine. A similar reaction between **III-1** and N_2O in the presence of pyridine led to the related product of C–H activation of pyridine, NacNacGa(OH)(o-C_5H_4N) (**III-10**), along with [NacNacGa(μ-O)]$_2$ and some other unidentified compounds. Related to this reaction is the C-H activation of pyridine by the *in situ* generated iminosilane reported by Driess *et al.*[190] Similarly the Aldridge group showed oxidation of an N-heterocyclic germylene with Me_3NO or py-O that resulted in the C-H activation by a transient germanone.[191] Schulz *et al.* reported sp^3C-H activation of ketones by a gallaphosphene in a more recent study.[14]

The compounds **III-9** and **III-10** were characterized by ^{1}H and ^{13}C NMR spectroscopy and the structure of **III-9** was ascertained by single-crystal X-ray diffraction. In the ^{1}H NMR spectrum of **III-9**, the NacNac ligand gives rise to backbone signals at 4.99 (CH) and 1.66 (Me) ppm and the pattern for the ^{i}Pr groups of the Ar substituents indicates

the C_s symmetry. The four protons of the oxo-pyridyl group resonate at δ=7.80 (d, 1H), 6.53 (dd, 1H), and 6.22–6.14 (m, 2H) ppm. The hydroxyl group resonates at -0.03 ppm. The peak assignments were performed on the basis of COSY, HSQC, and HMBC experiments. The ^{1}H NMR spectrum of compound **III-10** shows a similar pattern with four signal of the pyridyl group and the OH signal at 0.26 ppm.

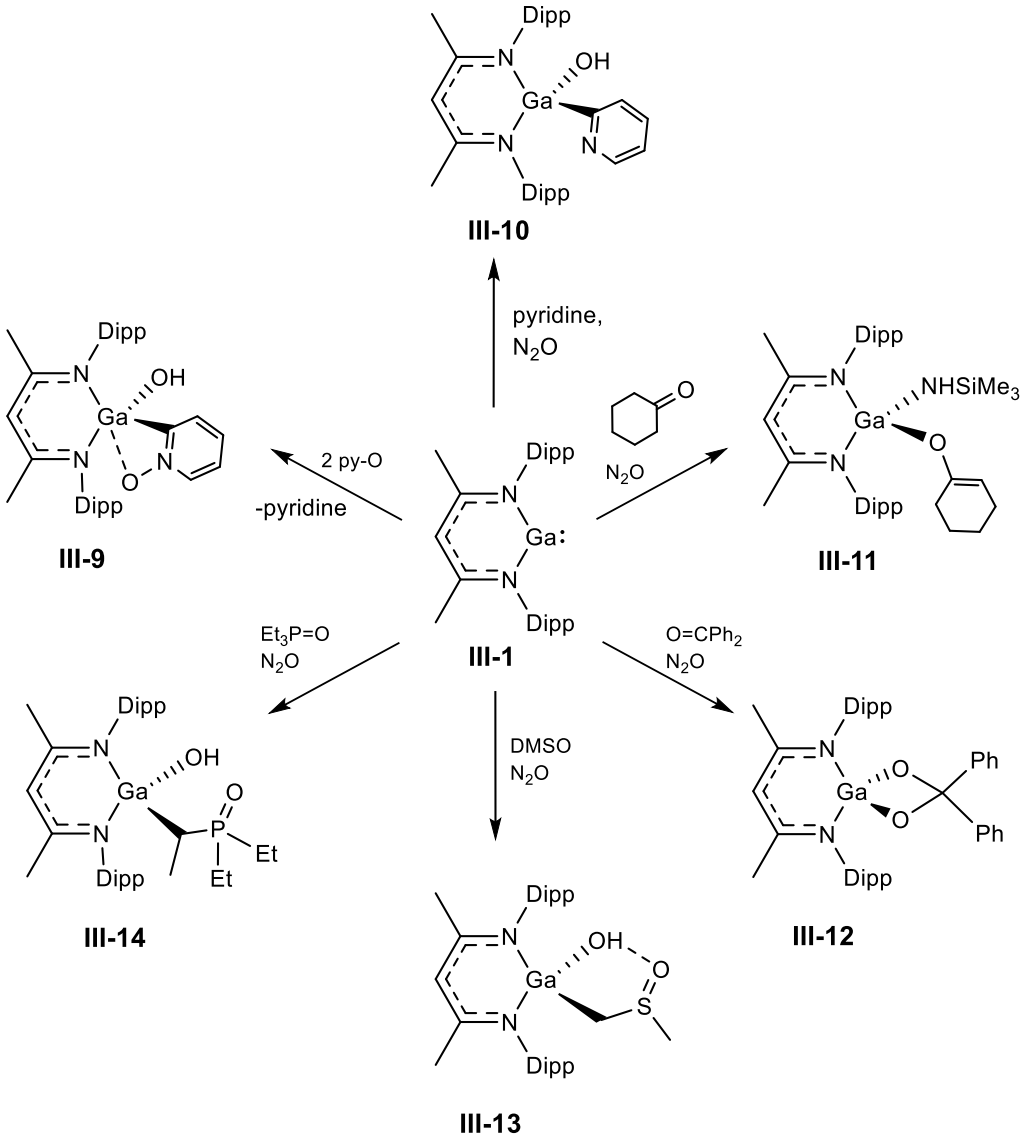

Scheme 90. Sequential oxidation/ C–H activation on Ga(I).

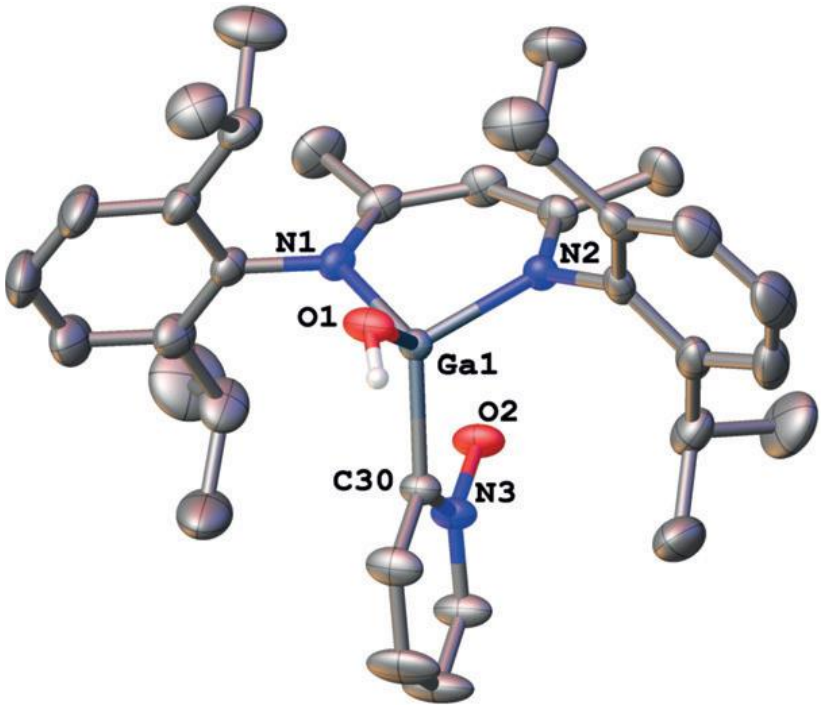

Figure 6. Molecular structure of NacNacGa(py-O)(OH) **III-9**, hydrogen atoms, except OH, are omitted for clarity. Thermal ellipsoids are plotted at 50%.

Table 7. Selected bond lengths and angles for the compound **III-9**.

Lengths, Å				**Angles, °**	
Ga1–O1	1.7975(9)	Ga1–N2	1.9359(11)	N2–Ga1–N1	97.09(5)
Ga1–O2	2.924(1)	Ga1–C30	1.9698(13)	O1–Ga1–N2	108.65(5)
Ga1–N1	1.9411(11)	O2–N3	1.3121(14)	O1–Ga1–N1	107.83(5)
				O1–Ga1–C30	110.59(5)

The molecular structure of **III-9** is presented in Figure 6. It belongs to the small family of NacNac-supported gallium hydroxides. The related aluminum hydroxides have been thoroughly described by Roesky *et al.*, but are also very scarce.[192] The gallium atom adopts a tetrahedral geometry, typical of two-substituted NacNac compounds of gallium. The Ga-OH bond of 1.7963(13) Å is longer than the Al-OH distance (1.731(2) Å) in the

related hydroxide NacNac'Al(OH)($OPEt_3$) containing a deprotonated backbone,[120] but is noticeably shorter than the Ga-OH in NacNacGa(Me)OH (1.831(1) Å)[193] and the average sp^3Ga-O bond of 1.879 Å, and is close to the low end of the range 1.801–1.915 Å previously observed for other NacNacGa(X)OH compounds, where X=C-, O- or P-based substituents.[192, 194-197] The oxopyridyl ligand is attached to gallium at the ortho position, forming a Ga-C single bond of 1.9698(18) Å. The oxo-pyridyl ligand is oriented in such a way that the oxo end is located *trans* to the OH moiety. Although the corresponding Ga···O contact of 2.924(1) Å is smaller than the sum of van der Waals radii (3.39 Å),[198] the short *trans* Ga-OH bond suggests that this Ga···O contact is mostly electrostatic in origin.

Intrigued by the ease of these C–H activations, we decided to check the generality of this oxidation/C–H activation reaction. As discussed in the previous Chapter, **III-1** is amenable to bond cleavage and cyclization of heterocumulenes (S=C=NR, O=C=NR, RN=C=NR) and *α,β*-enones, but does not react with nonconjugated C=O, P=O, and S=O bonds. For the latter class of substrates, the C–H activation can be easily investigated by direct N_2O oxidation of mixtures of **III-1** and substrates. Oxidation of a mixture of **III-1** and cyclohexanone leads to clean generation of the hydroxy enolate, NacNacGa(OH)(OC_6H_9) (**III-11**; Scheme 90). The identity of this compound was established by NMR spectroscopy and its molecular structure was further confirmed by X-ray diffraction. In this respect, the ^{1}H NMR spectrum of **III-11** shows the unique enolate resonance at 4.14 ppm, which is coupled in the COSY spectrum to the methylene signal at 1.90 ppm. The molecular structure of **III-11** is presented in Figure 7. The Ga-OH bond of 1.823(5) Å is slightly longer than its Ga-OH counterpart in **III-9**, whereas the Ga-O bond to the enolate ligand (1.804(5) Å) is almost identical.

In contrast, oxidation of **III-1** in the presence of a nonenolizable ketone, such as $Ph_2C{=}O$, led to the isolation of the product from sequential oxidation and cyclization, that is, NacNacGa(κ^2-O_2CPh_2) (**III-12**; Scheme 90). The ^{1}H NMR spectrum of **III-12** revealed a C_{2v} symmetrical pattern, with one signal for the isopropyl methine group at 3.06 ppm and two doublets for the methyl groups at 1.40 and 1.07 ppm.

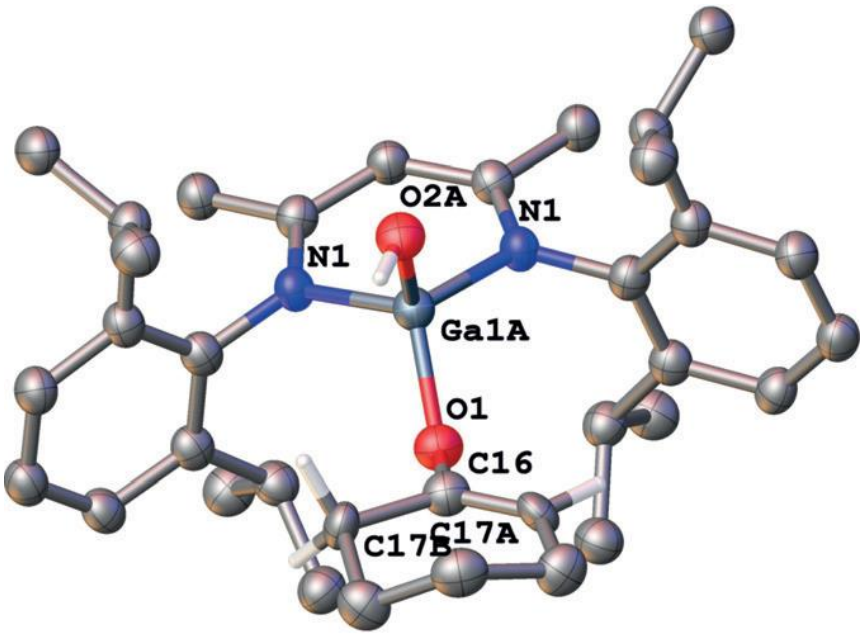

Figure 7 Molecular structure of NacNacGa(OC(=CH(CH_2)$_4$–)(OH) (**III-11**). Thermal ellipsoids are plotted at 50%. Hydrogen atoms, except OH, and those on C17A and C17B are omitted for clarity. The methylene atom C17B and the methine atomC17A are disordered because of a crystallographically imposed mirror plane. Only one component is shown.

Table 8. Selected bond lengths for the compound **III-11**.

Lengths, Å			
Ga1A–N1	1.923(4)	C16–C17A	1.330(10)
Ga1A–O1	1.804(5)	C16–C17B	1.520(13)
Ga1A–O2A	1.823(5)		

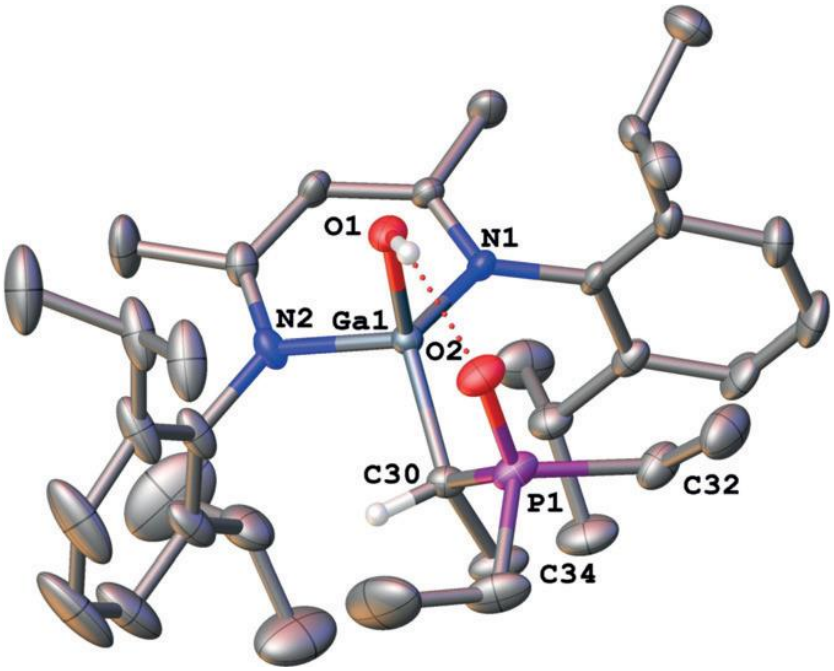

Figure 8. Molecular structure of one of the crystallographically unique molecules of NacNacGa(CH(Me)P(=O)Et_2)OH (**III-14**) in the asymmetric unit. Thermal ellipsoids are plotted at 50%. With the exception of OH and GaCH, the H atoms are omitted for clarity. The CHP(O)(CH_2CH_3)$_2$ moiety is conformationally disordered and only one component is shown.

Table 9. Selected bond lengths and angles for the compound **III-14**.

Lengths, Å				**Angle, °**	
Ga1–N1	1.9541(16)	Ga1–C30	1.988(2)	N1–Ga1–N2	94.51(6)
Ga2–N2	1.9575(16)	P1–O2	1.4970(15)		
Ga1–O1	1.8089(13)				

The *in situ* oxidation of mixtures of **III-1** with the aliphatic main-group element oxides O=SMe_2 and O=PEt_3 resulted in the isolation of compounds NacNacGa(CH_2S(=O)Me)OH (**III-13**) and NacNacGa(CH(Me)P(=O)Et_2)OH (**III-14**),

respectively, formed as the result of $sp^3C–H$ bond cleavage (Scheme 90). Both products were characterized by multinuclear NMR spectroscopy and the structure of **III-14** was further confirmed by single-crystal X-ray diffraction (Figure 8). The overall features of this structure are very similar to those of **III-9** and **III-11**, with the main difference being that the GaOH unit is engaged in a GaOH···OP hydrogen bond with the oxophosphinyl moiety.

In contrast to these easy C-H activations, attempted oxidation of a mixture of **III-1** and NEt_3 by N_2O resulted in the oxo-bridged dimer $[NacNacGa(\mu\text{-}O)]_2$[184] and intact NEt_3. Likewise, sulfurization of a mixture of **III-1** and either pyridine or phosphine oxide by elemental sulfur resulted only in the formation of the known sulphide-bridged dimer $[NacNacGa\text{-}(\mu\text{-}S)]_2$,[184] suggesting that either the NacNacGa=S intermediate does not form in this process or is not amenable to C–H activation.

Our attempts to intercept the putative intermediate oxide NacNacGa=O by performing the oxidation of **III-1** in the presence of N-heterocyclic carbene $:C(NMeCMe=)_2$ resulted in a mixture of products. The main component in this mixture appears to be a species with a deprotonated backbone methyl group, tentatively assigned the following structure NacNac'Ga(OH)(NHC) based on observation the characteristic methylene signals at δ=3.23 ppm and 3.95 ppm in the ^1H NMR spectrum. However, so far this species has eluded isolation.

The possible mechanism for the sequential oxidation and C–H activation of **III-1** was studied by DFT taking into account solvent (toluene) effects (Scheme 91).[199]

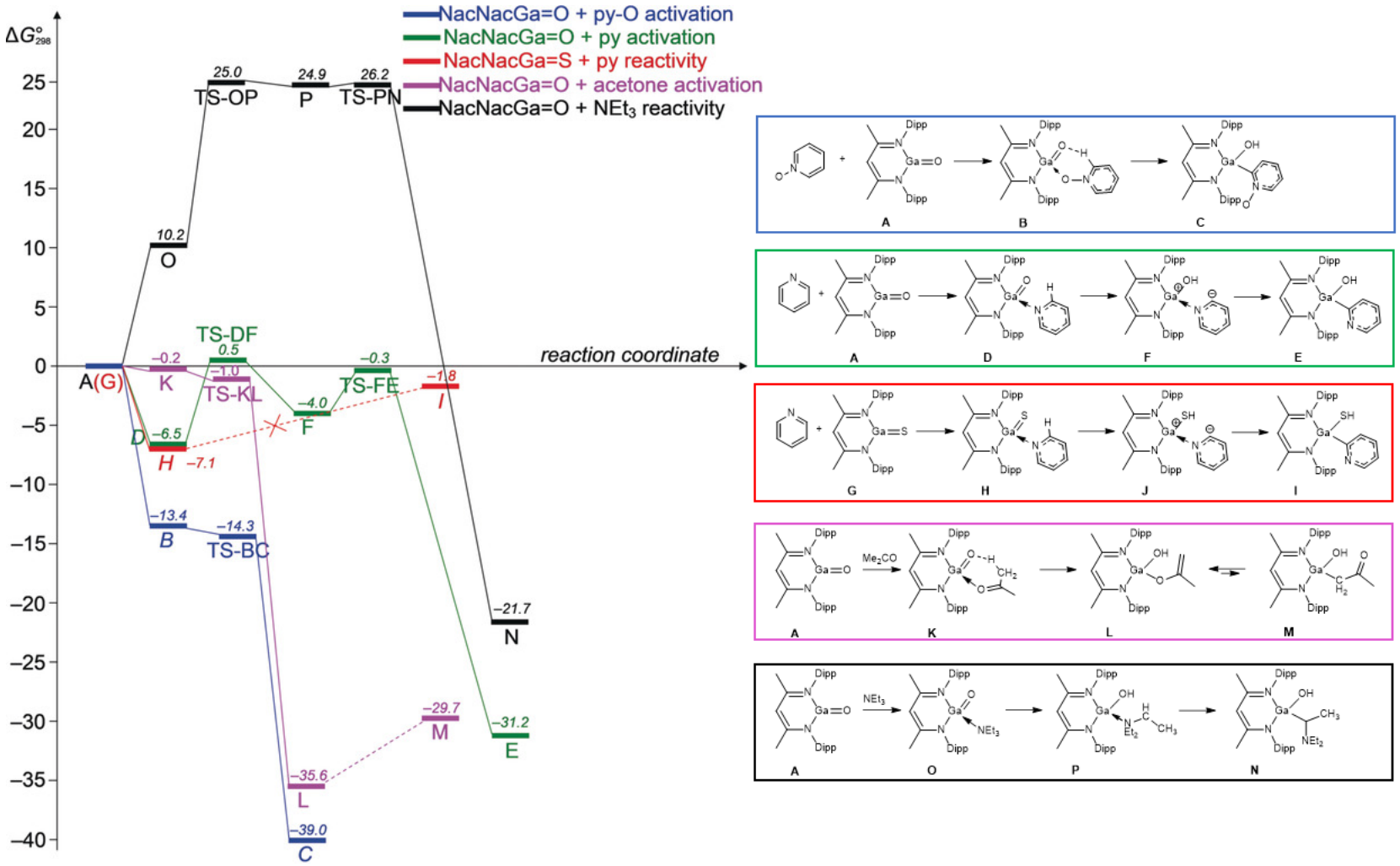

Scheme 91. Energy diagram for C-H activation in various substrates by NacNacGa(O) (A). Calculated free energies $\Delta G°_{298}$ (in kcal mol^{-1}) in toluene are shown.

The calculations were performed by Prof. S. F. Vyboishchikov. Institut de Química Computacional i Catàlisi and Departament de Química, Universitat de Girona, Spain.

According to the calculations, the initial oxidation of **III-1** to give NacNacGa(O) (**A**; Scheme 92) is highly exergonic: $\Delta G°_{298}$ = -48.4 kcal mol^{-1}or -31.6 kcal mol^{-1} when using N_2O or pyridine N-oxide as the oxidizing agents, respectively. The reaction of **A** with pyridine N-oxide starts with a favorable ($\Delta G°_{298}$ = -13.4 kcal mol^{-1}) coordination of pyridine N-oxide to gallium to yield the complex NacNacGa(O)(O-NC_5H_5) (**B**). The latter compound contains an intramolecular interaction between the oxo ligand and the *ortho*-hydrogen atom of the pyridine oxide, evidenced by the presence of a short O-H distance of 1.55 Å and an elongated C–H bond of 1.16 Å. This interaction facilitates subsequent hydrogen transfer towards the oxo ligand, which is virtually barrierless: Δ^*E=0.8 kcal mol^{-1}. During the hydrogen-transfer reaction, the pyridine N-oxide ligand spontaneously rearranges from O to the C coordination to afford the final product **C**.

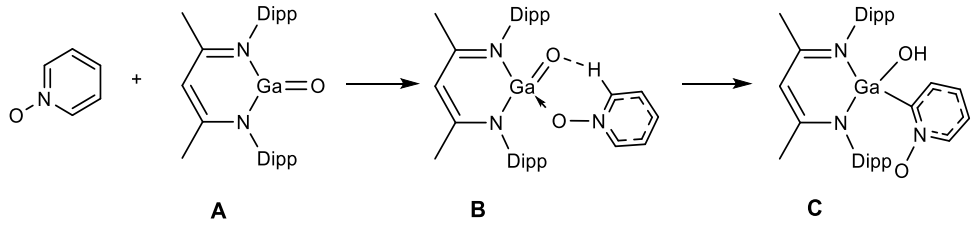

Scheme 92. Key calculated structures for the C–H bond activation in py-O by NacNacGa(O) (**A**).

For comparison, C–H activation in pyridine was also studied (Schemes 91 and 93). Pyridine coordination to **A** to give the adduct NacNacGa(O)(py) (**D**) is exergonic ($\Delta G°_{298}$= -6.5 kcal mol^{-1}). Unlike **B**, this adduct does not feature a CH···O hydrogen bond, but still easily rearranges into a much more stable C–H addition product NacNacGa(OH)-(η^1-C_5H_4N) (**E**), in which the pyridinide ligand is bound to gallium through the *ortho*-carbon atom. The rearrangement occurs via a much less stable N-bound pyridinide intermediate **F**.

The hydrogen transfer from pyridine to the oxo ligand in **D** to form **F** requires a very modest free energy barrier of 6.9 kcal mol^{-1}. The subsequent isomerization of **F** into **E** has an even lower $\Delta G°_{298}$ barrier of just 4.3 kcal mol^{-1}. These rather small kinetic barriers are in accord with a very fast reaction, which was observed experimentally.

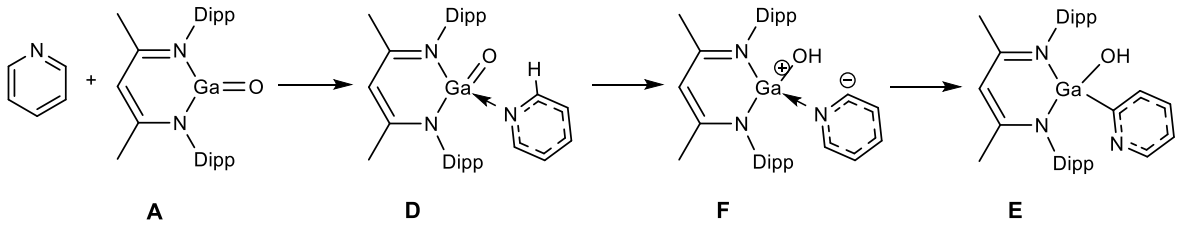

Scheme 93. Key calculated structures for the C–H bond activation in pyridine by NacNacGa(O) (**A**).

Interestingly, calculations of the analogous reaction of sulfide NacNacGa(S) (**G**) with pyridine (Schemes 91 and 94) revealed considerably different thermodynamics with respect to the **A** + py system described above. In this case, the most stable species on the potential energy surface is the pyridine complex **H**. The isomeric pyridinide complex NacNacGa- (SH)(η^1-C_5H_4N) (**I**), analogous to **E**, is about 5.3 kcal mol^{-1} higher in energy. The lower stability of **I** compared to **H** (in contrast to a much higher stability of **E** with respect to **D**) is likely due to the fact that the S-H bond is much weaker than both the O-H and C-H bonds. A possible pathway from **H** to **I** was not found, since the existence of a hypothetical N-bound pyridinide intermediate **J** has not been computationally confirmed. In total, the calculations indicate that no reaction, apart from a plain pyridine coordination is likely for the NacNacGa(S) (**G**) + py system.

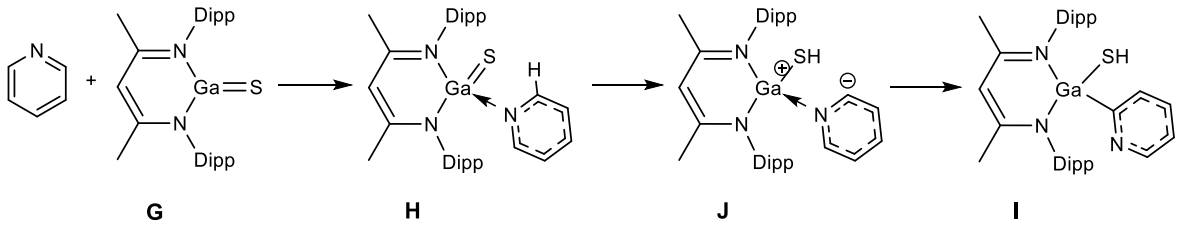

Scheme 94. Key calculated structures for the C-H bond activation in pyridine by NacNacGa(S) (**G**).

C–H bond activation in acetone (as an example of an enolizable ketone) was studied next (Scheme 95). The reaction again starts with the formation of a primary O-coordinated adduct **K**, which is quite weakly bound ($\Delta G°_{298}$ = -0.2 kcal mol^{-1}). Like the pyridine N-oxide system, the adduct shows a weak O–H interaction and exhibits a barrierless hydrogen transfer to form the stable O-coordinated product **L**. Its C-coordinated tautomer **M** was also found, but is 5.9 kcal mol^{-1} less stable on the $\Delta G°_{298}$ scale.

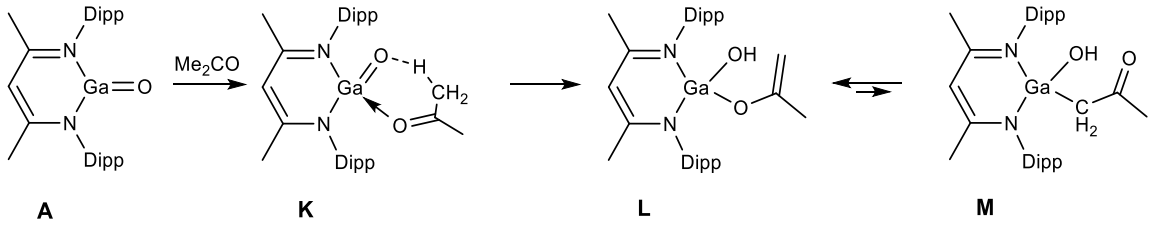

Scheme 95. Key calculated structures for the C-H bond activation in acetone by NacNacGa(O) (**A**).

Finally, we investigated C–H activation in an aliphatic amine, NEt_3 (Scheme 96). Although the hypothetical product **N** was computed to be stable ($\Delta G°_{298}$ = –21.7 kcal mol^{-1} with respect to **A** + NEt_3, Scheme 91), the corresponding reaction pathway exhibits very different energetics when compared to the **A** + py system.

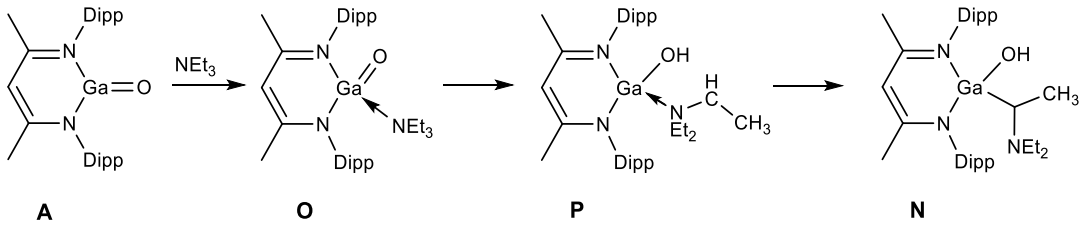

Scheme 96. Key calculated structures for the process of C–H bond activation in NEt_3 by NacNacGa(O) (**A**).

Firstly, NEt_3 coordination to **A** to give **O** is endergonic ($\Delta G°_{298}$ = +10.2 kcal mol^{-1}). Secondly, hydrogen transfer from carbon to oxygen atom leads to an even less favorable complex NacNacGa(OH)(-NEt_2-CH(Me)) (**P**; $\Delta G°_{298}$ = +24.9 kcal mol^{-1}), with a $\Delta G°_{298}$ barrier of 25.0 kcal mol^{-1}. The N-coordinated complex **P** is a very shallow minimum that rearranges easily to yield a much more stable product **N**. The overall $\Delta G°_{298}$ barrier amounts to 26.2 kcal mol^{-1}, corresponding to a kinetically unfavorable reaction. Considering the very easy C–H activation within the heteroaromatic system, this finding is quite remarkable. We propose that the main reason for the difference in reactivity is due to the steric factors from the NEt_3, system which disfavors amine coordination and eventually results in a relatively high barrier.

In conclusion, *in situ* oxidation of NacNacGa (**III-1**) in the presence of substrates with donor sites led to the C–H bond activation by intermediate NacNacGaO forming gallium hydroxides. Substrates employed in this reaction were pyridine N-oxide, pyridine, cyclohexanone, DMSO, and triethylphosphine oxide. DFT calculations revealed formation of NacNacGa(O)(L) adducts in which the oxide abstracts a proton of the closest C–H bond.

III.3 Reactivity of a Transient Gallium Imide.

As discussed in Section II.2.1 in this thesis, there has been great progress in the isolation of monomeric main group imides. Kinetic protection utilizing sterically hindered ligands and large substituents on nitrogen has been applied for this purpose. Anionic aluminum imides (**II-209** and **II-211**) reported by Coles[174] and Aldridge[175] were prepared by reacting aluminyl anions with azides. Treatment of **II-209** with carbon dioxide led to [2+2] cycloaddition. The imide **II-211** was shown to cleave the C-O bond of carbon monoxide and the H-H bond of dihydrogen. The Cui group reported neutral aluminum imide **II-202** produced by ligand rearrangement upon addition of carbene to ^{tBu}NacNacAl[170] .The reactivity of aluminum imide **II-202** towards amine, terminal alkyne, and carbon monoxide was demonstrated.

In an attempt to prepare a gallium imide, Power and co-workers have previously studied the reaction of NacNacGa **III-1** with trimethylsilyl(azide), which resulted in the formation of a gallium tetrazole and amide/azide isomers. These products were proposed to form from the reaction of the monomeric gallium imide (NacNacGa=NSiMe$_3$) intermediate with a second equivalent of azide.[162] Reacting **III-1** with the more sterically crowded azide ArN$_3$ (Ar = 2,6-Trip$_2$-C$_6$H$_3$, Trip = 2,4,6-^{i}Pr$_3$-C$_6$H$_2$) led to the first example of an isolable monomeric gallium imide (**II-195**).[164]

Knowing that the *in situ* generated monomeric oxide NacNacGa=O can easily cleave aliphatic and aromatic C–H bonds (Scheme 90), we decided to extend this approach to a transient gallium imide by treating a mixture of NacNacGa and a substrate of choice with N$_3$SiMe$_3$.

Reaction of NacNacGa (**III-1**) with N_3SiMe_3 in the presence of pyridine resulted in the ortho C–H activation of pyridine at room temperature (Scheme 97). The reaction is proposed to proceed via the monomeric gallium imide NacNacGa($NSiMe_3$)(py) intermediate that undergoes C–H activation of pyridine. In contrast to the activation of pyridine with the transient gallium oxide NacNacGa=O (25% yield, not selective), gallium imide effects selective and quantitative C-H activation of pyridine. The product of the reaction, NacNacGa($NHSiMe_3$)(*o*-C_5H_4N) (**III-15**), was characterized by NMR spectroscopy and its molecular structure was confirmed by X-ray diffraction. The most notable feature of the ^1H NMR spectrum of compound **III-15** is the presence of four resonances of the dearomatized pyridine ring at 8.65, 7.92, 7.08, and 6.69 ppm. The upfield signal at 0.04 is assigned to the $SiMe_3$ group and a broad signal of NH is observed at -0.58 ppm.

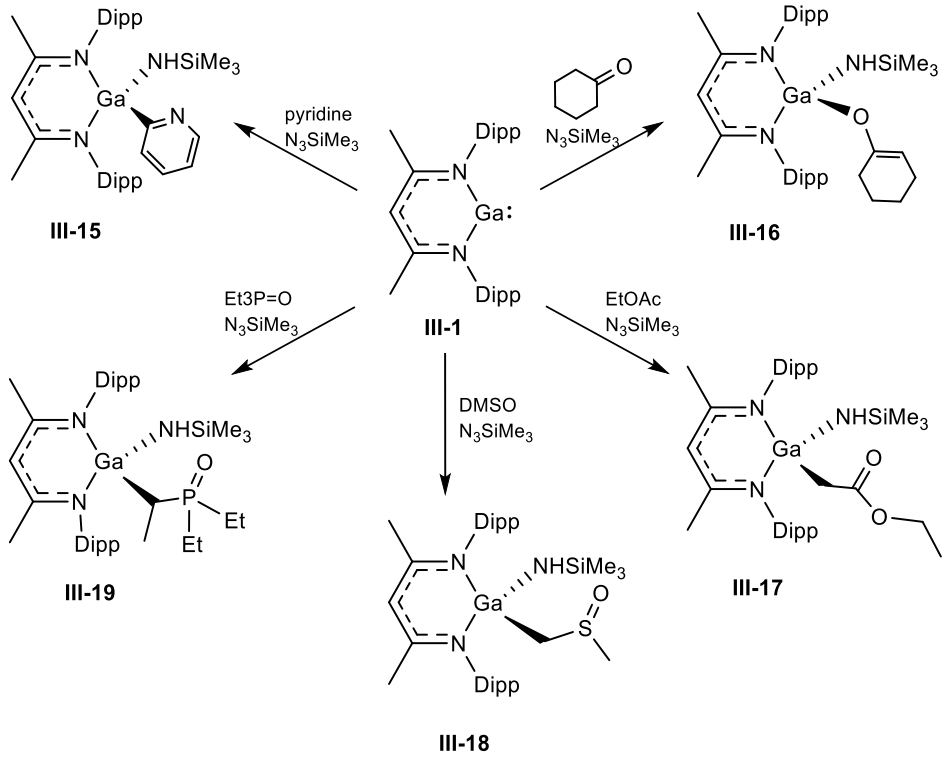

Scheme 97. C-H activation by an intermediate gallium imide.

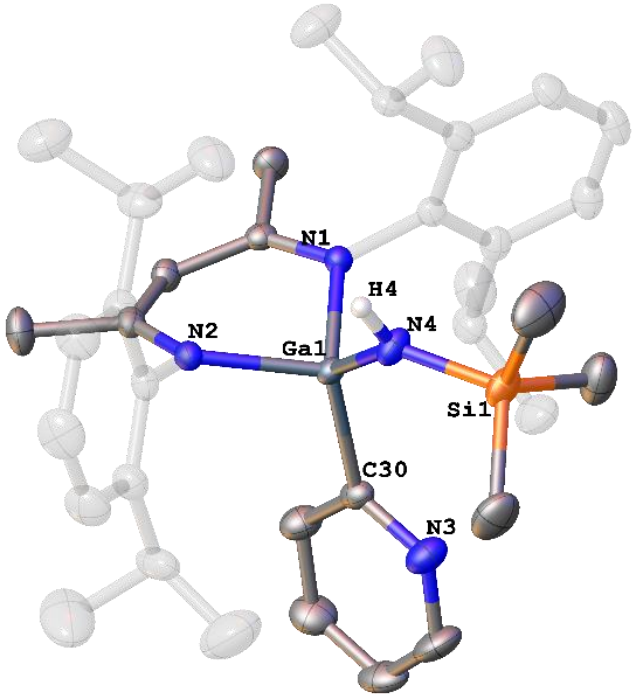

Figure 9. Molecular structure of NacNacGa(py)(NHSiMe$_3$) (**III-15**). The bulk of 2,6-diisopropylphenyl group is dimmed and the hydrogen atoms, except NH, are omitted for clarity. Thermal ellipsoids are plotted at 50%.

Table 10. Selected bond lengths and angles for the compound **III-15**.

Lengths, Å		**Angles, °**	
Ga1–N4	1.8497(15)	N2–Ga1–N1	97.09(5)
Ga1–N1	1.9811(14)	N4–Ga1–N2	107.15(6)
Ga1–N2	1.9707(14)	N4–Ga1–C31	119.83(7)
Ga1–C30	1.9903(17)		

The molecular structure of compound **III-15** is shown in Figure 9. The gallium center adopts a distorted tetrahedral environment comprised of the NacNac ligand, amido and pyridyl groups. The Ga-N bond lengths to the NacNac ligand are 1.9811(14) and 1.9707(14) Å. The gallium amide (Ga1-N4) bond length is, however, short (1.8497(15) Å), which is

typical for related β-diketiminate gallium amides.[162, 197] The gallium carbon bond length to the pyridyl ligand is 1.9903(17) Å, akin to the Ga-C bond of 1.9698(18) Å to the oxopyridyl group in **III-9**.

To determine the scope of the reaction, the same substrates employed in C-H activation by a gallium oxide were tested for C-H activation by the gallium imide (Scheme 97). Treatment of the Ga(I) compound **III-1** and cyclohexanone mixture with N_3SiMe_3 resulted in an amido enolate product NacNacGa(NHSiMe$_3$(OC$_6$H$_9$) (**III-16**)**.** As in the case of the gallium enolate hydroxide **III-11**, the oxygen-bonded tautomer must be more stable than the carbon-bonded form (Scheme 95) for the gallium amide.

In the ^{1}H NMR spectrum of **III-16** the unique enolate signal appears at 4.53 ppm and correlates with the carbon signal at 96.3 ppm in the ^{1}H-^{13}C HSQC spectrum. The quaternary carbon of enolate is observed at 155.5 ppm in ^{1}H-^{13}C HMBC. Other cyclohexenyl signals are assigned at 2.32, 1.81, and 1.71 ppm in the ^{1}H NMR spectrum. A broad NH resonance is seen at -0.80 ppm. The molecular structure of **III-16** is presented in Figure 10. The gallium-amide bond distance of 1.8387(15) Å is similar to that of **III-15**. The Ga1-O1 bond to the enolate is 1.8242(12) Å comparable to the corresponding Ga–O bond in the gallium hydroxide enolate **III-11**. The C30–C35 bond of 1.335(2) Å is shorter than C(30)-C(31) bond of 1.507(2) as expected from the enolization forming a C-C double bond.

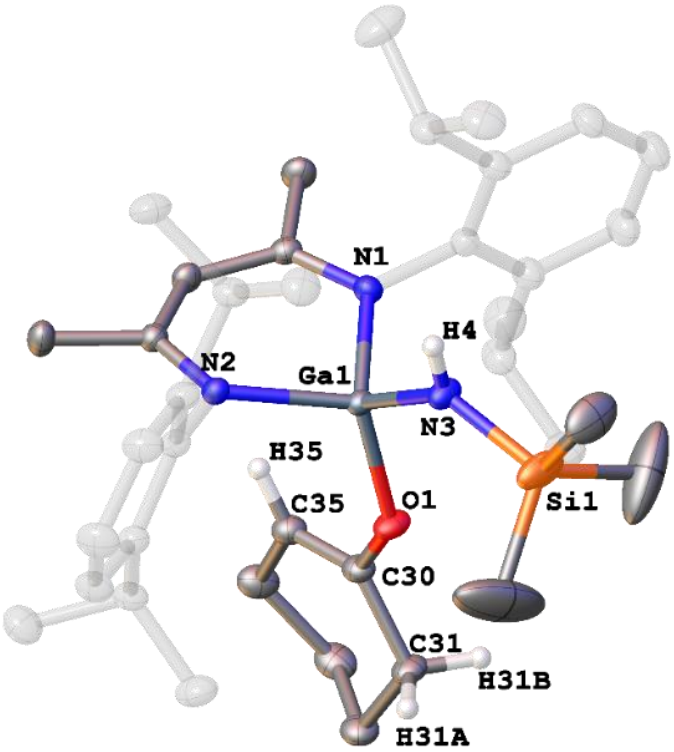

Figure 10. Molecular structure of NacNacGa(OC(=CH(CH$_2$)$_4$ –)(NHSiMe$_3$) **III-16**. The bulk of 2,6-diisopropylphenyl group is dimmed and hydrogen atoms, except NH, and those on C31 and C35 are omitted for clarity. Thermal ellipsoids are plotted at 50%.

Table 11. Selected bond lengths and angles for the compound **III-16**.

Lengths, Å				**Angles, °**	
Ga1–O1	1.824(1)	O1–C30	1.352(2)	N2–Ga1–N1	96.56(6)
Ga1–N3	1.839(1)	C30–C31	1.507(2)	N3–Ga1–N1	114.91(7)
Ga1–N2	1.947(1)	C30–C35	1.335(2)	N3–Ga1–N2	115.63(7)
				N3–Ga1–O1	104.07(6)

Unlike cyclohexanone, C–H activation of ethyl acetate with the gallium imide led to a Ga-C bonded product **III-17** without an enolization (Scheme 97). ^{1}H NMR signals of the ethyl group appear at 4.01 and 1.07 ppm and the methylene group bound to the gallium center shows a resonance at 1.90 ppm. A broad signal at -0.59 ppm was assigned to the NH

signal of the amide. The crystal structure of compound **III-17** (Figure 11) revealed a Ga1-N3 bond length of 1.848(1) Å and a Ga1-C30 distance of 2.012(1), normal for a gallium-carbon single bond. The O1-C31 bond length of 1.210(2) is in the double bond range, as expected for a carbonyl group.

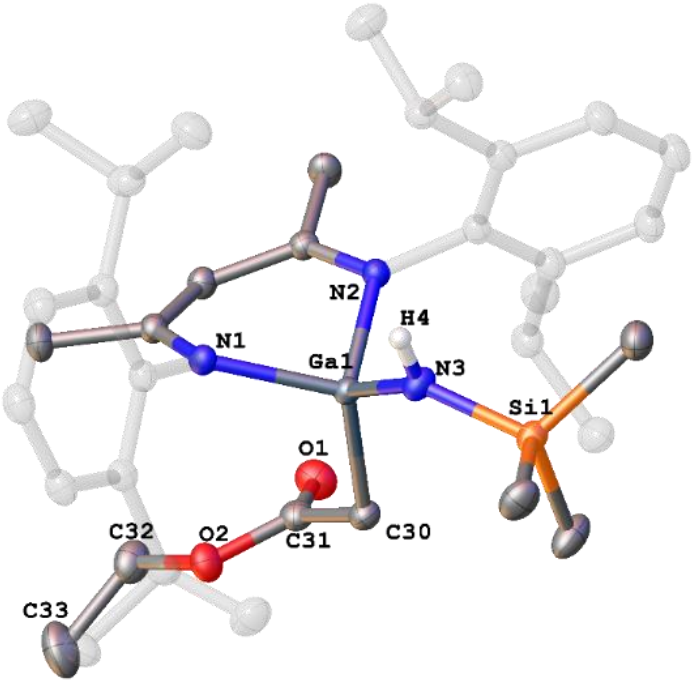

Figure 11. Molecular structure of NacNacGa($CH_2CO_2CH_2CH_3$)($NHSiMe_3$) (**III-17**). The bulk of 2,6-diisopropylphenyl group is dimmed and hydrogen atoms, except NH, are omitted for clarity. Thermal ellipsoids are plotted at 50%.

Table 12. Selected bond lengths and angles for the compound **III-17**.

Lengths, Å				**Angles, °**	
Ga1–N3	1.848(1)	Ga1–C30	2.012(1)	N2–Ga1–N1	97.65(4)
Ga1–N1	1.948(1	O1-C31	1.210(2)	N3–Ga1–N1	112.12(5)
Ga1–N2	1.982(1)			N3-Ga1-N2	112.35(5)
				N3–Ga1–C30	118.69(5)

$Me_2S{=}O$ and $Et_3P{=}O$ were probed in the gallium imide-mediated C-H activation (Scheme 97). Reacting mixture of **III-1** and $Me_2S{=}O$ with N_3SiMe_3 resulted in the formation of NacNacGa($CH_2S(=O)Me$)($NHSiMe_3$) (**III-18**). **III-18** was characterized by multinuclear NMR spectroscopy. The ^{1}H NMR spectrum of **III-18** showed a pattern consistent with the C_1 symmetry of the product due to the presence of a chiral sulfur center. The prochiral methylene group attached to gallium gives rise to two signals, at 2.28 and 1.81 ppm, which correlate with the ^{13}C signal at 41.1 ppm in ^{1}H-^{13}C HSQC. The -SMe_3 group gives rise to a resonance at 2.12 ppm and a ^{13}C signal at 45.3 ppm. The NH signal of the formed amide group is observed at -0.27 ppm.

Similarly, C-H activation of $Et_3P{=}O$ by the transient gallium imide resulted in NacNacGa($CH(Me)P(=O)Et_2$)($NHSiMe_3$) (**III-19**). The ^{1}H NMR spectrum of **III-19** shows a C_1 symmetric pattern, with four quartets and eight doublets of the ^{i}Pr groups of the NacNac ligand. The gallium-bound methine proton appears at 1.01 ppm as a quartet coupled to the methyl group at 0.51 ppm. A singlet signal of NH was observed at 2.20 ppm.

In conclusion, a reaction of NacNacGa with trimethylsilyl azide produces an intermediate monomeric gallium imide that can cleave C-H bonds of aromatic and aliphatic substrates. The C-H bonds of pyridine, cyclohexanone, ethyl acetate, DMSO, and triethylphosphine oxide adjacent to a donor site were cleaved and the corresponding gallium amide products were isolated.

III.4 An Isolable Gallium-substituted Nitrilimine.[c]

Diazoalkanes are important reagents in organic and organometallic chemistry. One of the established applications of diazoalkane reagents is in the preparation of transition metal alkylidene complexes that are used in olefin metathesis.[200] The reactivity of low-valent main group compounds with diazoalkane reagents has been reported more recently. Thus, a reaction of NacNacAl (**II-10**) with diphenyl diazomethane afforded the diiminylaluminum compound NacNacAl(N=CPh_2)$_2$.[201] Likewise, treatment of the silylene, NacNac′Si (**II-60**, DippNC(Me)CHC(=CH_2)NDipp]$^{2-}$) with Ph_2CN_2 resulted in the diiminylsilane NacNac'Si(N=CPh_2).[202] The hydrido germylene NacNacGe-H was shown to undergo an end-on nitrogen insertion of diazoalkanes into the Ge-H bond with the formation of a germanium(II)-substituted hydrazone derivative,[203] whereas backbone-deprotonated germylene NacNac'Ge forms a diazogermylene upon the treatment with trimethylsilyl diazomethane.[204] Metallated diazomethanes can also exist in the isomeric nitrilimine form. Nitrilimines (R-CNN-R') are unstable organic compounds that were first observed from the thermal decomposition of 2,5-disubstituted tetrazoles.[205] Due to their high reactivity, nitrilimines have been isolated only as metal complexes (Scheme 98). Calculations and experimental results on a lithiated diazo species showed the nitrilimine to be one of the stable isomeric forms.[206, 207] Some main group examples of nitrilimines include germanium-[208] and aluminium-[209] substituted nitrilimines. More recently, transition metal complexes of nitrilimines, i.e. scandium[210] and iron[211] nitrilimines were reported.

---

[c]Adapted with permission from Kassymbek, A.; Gusev, D. G.; Dmitrienko, A.; Pilkington. M.; Nikonov, G. I. *Chem. Eur. J.* **2022**, *28*, e2021034. Copyright 2022, Wiley-VCH.

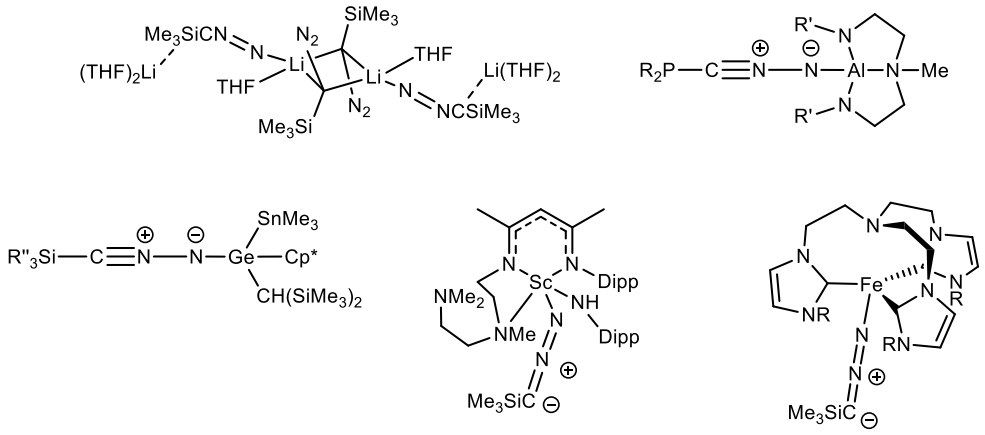

Scheme 98. Examples of isolable nitrilimines.

Here we report a crystallographically characterized terminal gallium nitrilimine **III-20** and gallium diazomethane **III-24**. The reactivity of gallium nitrilimine **III-20** towards borane, silane, and diborane will be demonstrated.

We decided to try the reaction of a low-valent gallium compound **III-1** with diazolakane with the initial motivation to prepare the alkylidene NacNacGa=CR_2 that would be isolobal to the transient oxide NacNacGa=O and imide NacNacGa=$NSiMe_3$ discussed in Chapters III.2 and III.4. Treatment of NacNacGa (**III-1**) with one equivalent of $N_2CHSiMe_3$ resulted in a 1:1 mixture of the starting compound and a new product (**III-20**) having two inequivalent $SiMe_3$ groups. Performing this reaction with two equivalents of $N_2CHSiMe_3$ led to the exclusive formation of compound **III-20** (Scheme 99). ^{1}H NMR spectrum of the reaction mixture revealed the formation of a C_s symmetric species of the type NacNacGaXY, where the group X was identified as CH_2SiMe_3, and the group Y had the $CSiMe_3$ moiety. X-ray diffraction then revealed that compound **III-20** is a gallium-substituted nitrilimine (Figure 12).

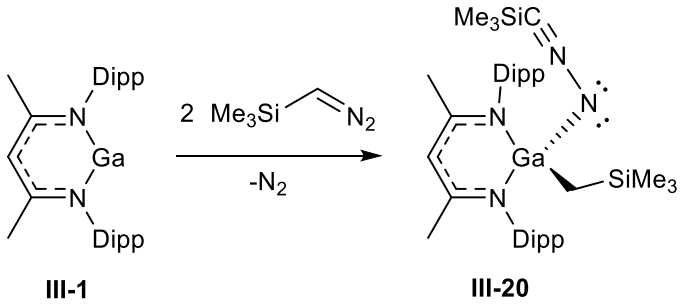

Scheme 99. Reaction of NacNacGa **III-1** with $N_2CHSiMe_3$.

The gallium center of **III-20** adopts a distorted tetrahedral geometry. The nitrilimine moiety in **III-20** is almost linear, with the bond angles N3-N4-C34 of 174.6(4)° and Si2-C34-N4 of 161.6(4)°. The Ga-N distance to the nitrilimine (1.908(3) Å) is slightly shorter than the Ga-N bonds within the NacNacGa fragment and is typical for a Ga-amide bond. The N4-C34 distance of 1.179(5) Å is only slightly longer than a triple bond (1.16 Å) and the N3-N4 bond of 1.235(4) Å in **III-20** is shorter than N-N single bond. Therefore, the bonding situation in **III-20** can be described as a resonance hybrid of propargylic and allenic canonical forms (Scheme 100), with the preference for the propargylic. As such, **III-20** can be viewed as an adduct of a galanitrene with a nitrile.

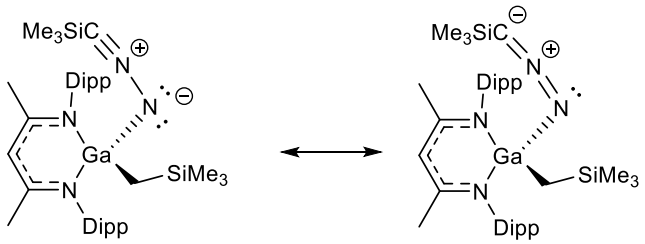

Scheme 100. Valence bond description of bonding in **III-20**.

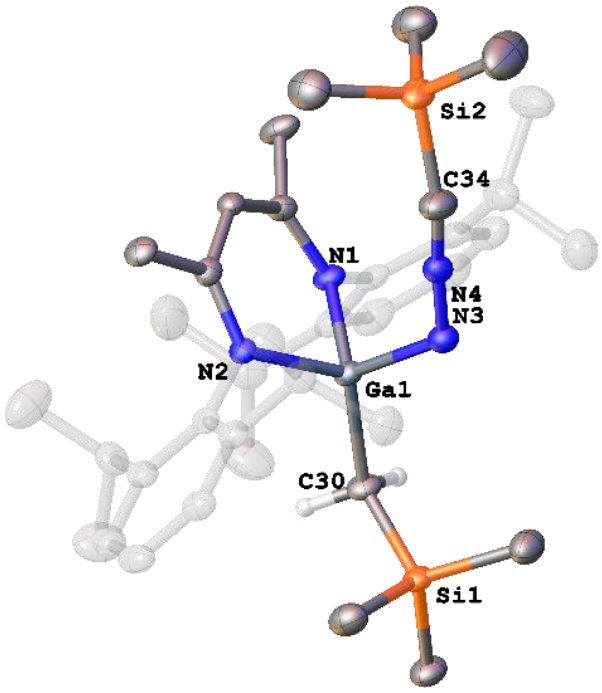

Figure 12. Molecular structure of NacNacGa(CH_2SiMe_3)($NNCSiMe_3$) (**III-20**). The bulk of 2,6-diisopropylphenyl group is dimmed and hydrogen atoms are omitted for clarity. Thermal ellipsoids are plotted at 50%.

Table 13. Selected bond lengths and angles for compound **III-20**.

Lengths, Å				**Angles, °**			
Ga1–N1	1.975(2)	Ga1–C30	1.959(4)	N2–Ga1–N1	95.0(1)	N3-N4-C34	174.6(4)
Ga1–N2	1.958(3)	N3-N4	1.235(4)	N1–Ga1–N3	106.3(1)	Si2-C34-N4	161.6(4)
Ga1–N3	1.908(3)	N4-C34	1.179(5)	N1–Ga1–C30	113.8(1)		

DFT studies at the MN15-L/Def2-QZVP level provided further insight into the electronic structure of **III-20**. The calculated geometry of **III-20** is in a very good agreement with that obtained from X-ray diffraction studies (Figure 12).

The calculations were performed by Prof. D. G. Gusev.
Department of Chemistry and Biochemistry, Wilfrid Laurier University, Canada.

The HOMO at -4.82 eV is localized on the nitrogen and the carbon termini of the nitrilimine ligand and is the non-bonding (or weakly antibonding) π-orbital of the pseudo-allylic NNC fragment (Figure 13).The LUMO is a NacNac-based orbital, whereas the LUMO+5 at -0.52 eV is a π* antibonding orbital of the nitrilimine.

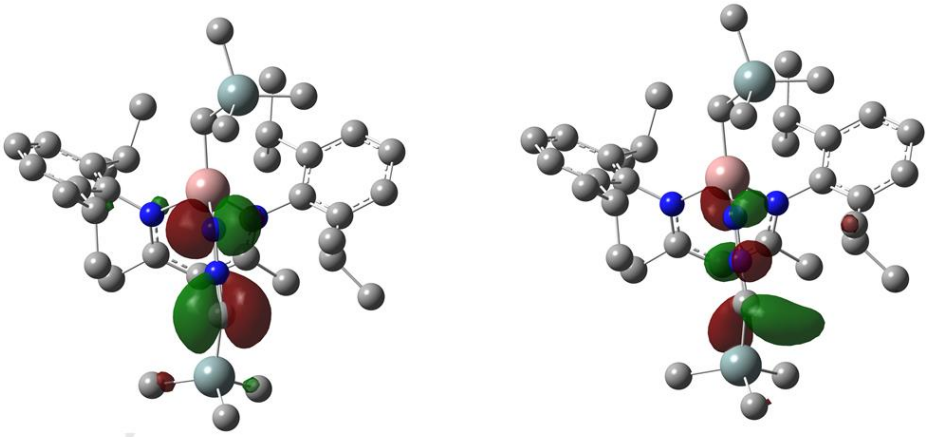

Figure 13. The HOMO (left) and LUMO+5 (right) of nitrilimine compound **III-20**.

Addition of $N_2CHSiMe_3$ to **III-1**, leading to the nitrilimine **III-20**, was modelled as the two-step process of Scheme 101a. In the first step, a low-lying transition-state $TS_{III\text{-}1/III\text{-}21}$ was located at $\Delta G‡ = 16.0$ kcal/mol, exhibiting a Ga-C bond of 2.07 Å and the C-N-N angle of 140°. Dinitrogen elimination from $TS_{III\text{-}1/III\text{-}21}$ leads to the alkylidene $NacNacGa{=}CHSiMe_3$ (**III-21**) at -40.4 kcal/mol vs. **III-1** + $N_2CHSiMe_3$. The alkylidene adds $N_2CHSiMe_3$ in the second step, via $TS_{III\text{-}21/III\text{-}20}$ at -33.5 kcal/mol. The incoming diazomethane is aligned parallel with the Ga=C bond in $TS_{III\text{-}21/III\text{-}}$20, which is characterized by the C-H distances of 1.25 and 1.72 Å, the latter being to the alkylidene carbon. On the gallium side, the Ga-N distance is 2.38 Å, and the C-N-N fragment is bent (157°). From $TS_{III\text{-}21/III\text{-}20}$, the H-transfer gives the kinetic product at -79.2 kcal/mol, which differs from

III-20 (ΔG = -84.7 kcal/mol) by the orientation of the nitrilimine fragment. This fragment is *syn* with the Ga-C bond in the kinetic product, whereas it is *anti* in the structure of **III-20** in Figure 12. The nitrilimine fragment must flip in the kinetic product to complete the reaction. This rearrangement, presumably, is facile.

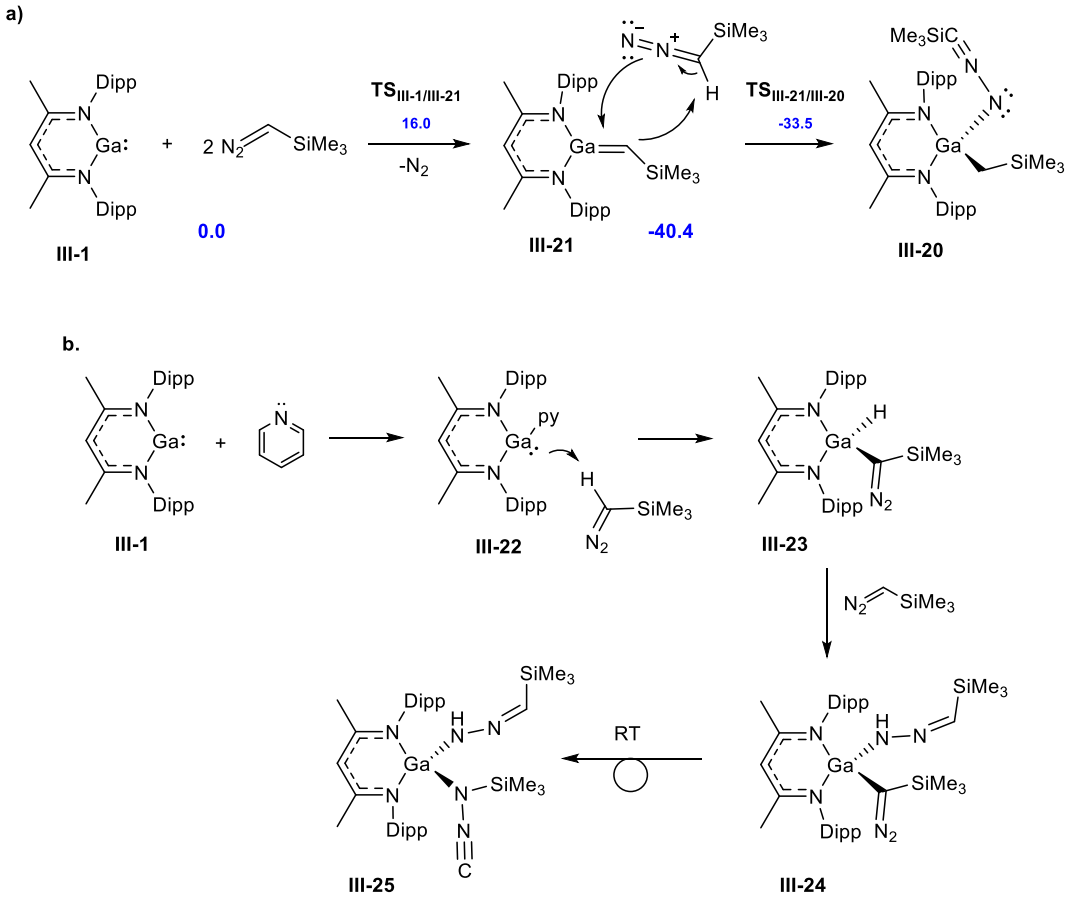

Scheme 101. Possible mechanisms for the reaction of NacNacGa with $N_2CHSiMe_3$ (a) in the absence of pyridine, ΔG (blue) in kcal/mol (b) in the presence of pyridine.

The formation of the CH_2SiMe_3 moiety directly attached to gallium in **III-20** granted further credibility to our assumption that the reaction proceeds via the intermediate formation of alkylidene NacNacGa=$CHSiMe_3$ (**III-21**) amenable to C–H bond activation

(Scheme 101a). To test this hypothesis, the reaction between **III-1** and $N_2CHSiMe_3$ was performed in the presence of pyridine. To our surprise, the pyridine remained unreacted, but the only gallium product formed was the metallated diazo compound **III-24** shown in Scheme 101b. Our rationale for this divergent reactivity is that **III-I** reacts with pyridine faster than with $N_2CHSiMe_3$ to give the adduct **III-22** that then deprotonates the diazomethane to give a gallium diazomethyl hydride intermediate **III-23**. Insertion of the second equivalent of $N_2CHSiMe_3$ into the Ga-H bond completes the process. Compound **III-24** was characterized by NMR spectroscopy. In particular, the singlet at 6.64 ppm in the ^1H NMR spectrum correlating with the carbon resonance at 138.6 ppm was assigned to the imine $N=CHSiMe_3$ moiety and a broad signal at 6.23 ppm was attributed to NH. The $SiMe_3$ signal at 0.28 ppm shows correlation with the imine carbon, whereas the $SiMe_3$ resonance at -0.11 ppm correlates in the HMBC spectrum with a quaternary signal at 41.9 ppm that can be assigned to the metallated diazomethane. Attempts to use pyridine in a catalytic amount resulted in a mixture of **III-20** and **III-24**.

Compound **III-24** is metastable and at room temperature rearranges into the N-silylated compound **III-25** over the course of several days. Analogous rearrangement into a isonitrilesilyl amide has been previously observed by Roesky and co-workers for a germylated diazomethane.[204] Compound **III-25** was characterized by multinuclear NMR spectroscopy and by X-ray diffraction. The imine C-H gives rise to a singlet at 6.48 ppm that correlates in ^1H-^{13}C HSQC with the carbon signal at 140.6 ppm. The hydrazonide NH signal shifts upfield to 5.57 ppm. The $SiMe_3$ signal of the rearranged diazomethane at 0.06 ppm loses correlation to any quaternary carbon. The bond connectivity of **III-25** was finally ascertained by an X-ray diffraction study (Figure 14).

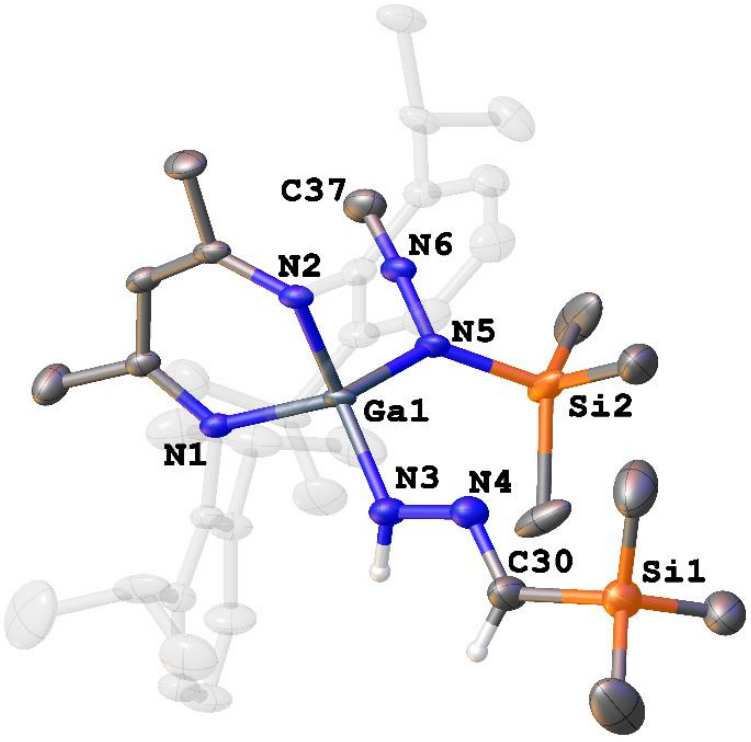

Figure 14. Molecular structure of NacNacGa(NHNCHSiMe$_3$)(N(NC)(SiMe$_3$)) (**III-25**). The bulk of 2,6-diisopropylphenyl group is dimmed and hydrogen atoms are omitted for clarity. Thermal ellipsoids are plotted at 50%.

Table 14. Selected bond lengths and angles for the compound **III-25**.

Lengths, Å				**Angles, °**			
Ga1-N1	1.930(3)	N4-C30	1.282(6)	N1-Ga1-N2	97.5(1)	C30-N4-N3	119.4(4)
Ga1-N2	1.941(3)	N5-N6	1.353(5)	N3-Ga1-N5	108.9(2)	N6-N5-Ga1	112.7(3)
Ga1-N3	1.861(4)	N5-Si2	1.773(10)	N4-N3-Ga1	121.3(3)	N6-N5-Si2	113.1(5)
Ga1-N5	1.911(3)	N6-C37	1.156(6)	N6-N5-Ga1	112.7(3)		
N3-N4	1.358(5)			C37-N6-N5	176.9(4)		

The Ga1-N5 amide bond of 1.911 Å is in the typical Ga-N single bond range, whereas the Ga-N distance to the hydrazonide ligand is short at 1.860(3) Å. The isonitrile amide moiety is almost linear with the N5-N6-C37 bond angle of 176.9(4)°. The N6-C37 distance in the

isonitrile (1.156(6) Å) is in the triple bond region, whereas the N5-N6 bond of 1.353(5) Å is shorter than a typical N-N single bond (1.47 Å), likely because of the sp hybridization of N6. The imine N4-C30 distance of 1.282(6) Å is typical for a double bond.

With the nitrile imine **III-20** in hand, we were intrigued whether this species could serve as a synthon for a nitrene. To test its ability to activate single bonds, **III-20** was reacted with the borane HBcat (cat = catechol). A reaction of **III-20** with HBcat in benzene resulted in the product of 1,3-addition to the nitrilimine fragment (**III-26**, Scheme 102). The salient NMR features of the product are the appearance of an aldimine resonance in the ^{1}H NMR spectrum at 8.60 ppm and the carbonyl signal at 169.2 ppm in ^{13}C NMR spectrum.

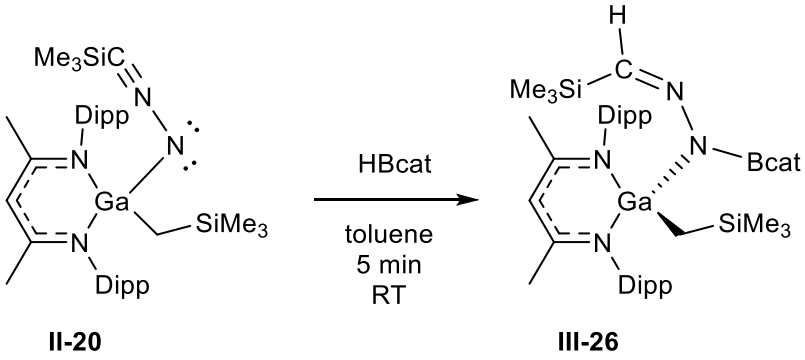

II-20 **III-26**

Scheme 102. Reaction between nitrilimine **III-20** and HBcat.

The X-ray diffraction of **III-26** (Figure 15) established that the boryl is attached to the former nitrene atom to give a N3-B1 bond having a length of 1.397(8) Å. The corresponding Ga1-N3 distance of 1.929(4) Å does not change upon addition of the borane (cf. 1.908(3) Å in **III-20**), whereas the N3-N4 distance elongates from 1.235(4) Å to 1.421(6) Å, consistent with the change of hybridization of N4 from sp to sp^{2}. The latter is also seen in the decrease of the bond angle at N4 from 174.6(4) to 119.4(4)°. The N4-C34 bond elongates from 1.179(5) Å in **III-20** to 1.20(1) Å, because of the decrease of in bond order

from three to two. This regioselectivity of borane addition reflects the presence of a formal negative change on nitrogen in the Lewis structure of **III-20** (Scheme 100) and the known nitrophilicity of boron.

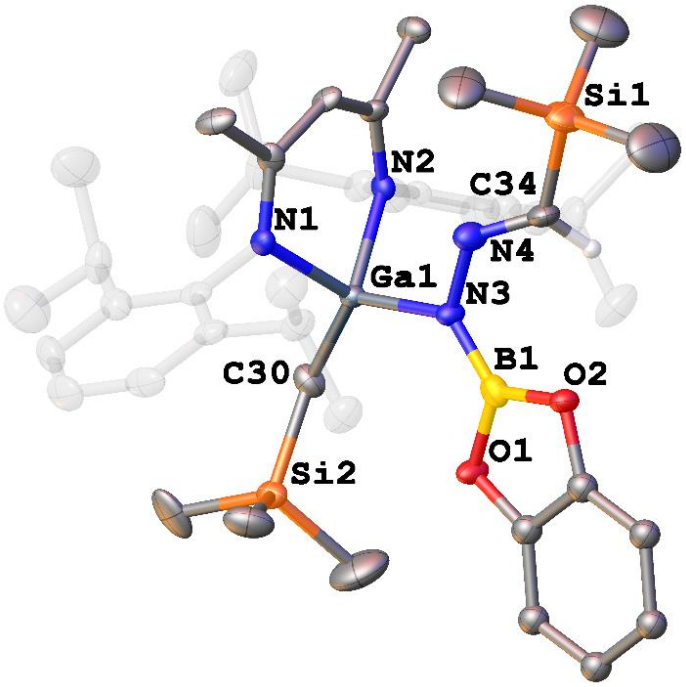

Figure 15. Molecular structure of NacNacGa(CH_2SiMe_3)(N(Bcat)(N=$CHSiMe_3$)) (**III-26**). The bulk of 2,6-diisopropylphenyl group is dimmed and hydrogen atoms except C34-H are omitted for clarity. Thermal ellipsoids are plotted at 50%.

Table 15. Selected bond lengths and angles for the compound **III-26**.

Lengths, Å				**Angles, °**	
Ga1-N1	1.967(4)	N3-B1	1.397(8)	N1-Ga1-N2	94.7(2)
Ga1-N2	1.972(4)	N3-N4	1.421(6)	N1-Ga1-N3	103.6(2)
Ga1-N3	1.929(4)	N4-C34	1.20(1)	N3-Ga1-C30	126(1)
Ga1-C30	1.96(2)			N4-N3-B1	119.7(5)
				N3-N4-C30	119.4(4)

Similar to the addition of borane, a reaction of **III-20** with silane H_3SiPh produced a 1,3-addition product **III-27**. The ^1H NMR spectrum showed the presence of two isomeric species in a 2:1 ratio (Scheme 103). As for **III-26**, the aldimine group gives rise to characteristic signals at 8.10 and 7.80 ppm (for two distinct conformers), whereas the NacNac and CH_2SiMe_3 fragments show their expected signals. ^1H NOE experiments established that the major isomer has the SiH_2Ph moiety oriented towards the NacNac ligand, whereas in the minor one it is the imine group that is oriented towards the ligand. Apparently, these two conformers are formed because of the restricted rotation around the Ga-N bond imposed by the bulky Dipp substituents in NacNac.

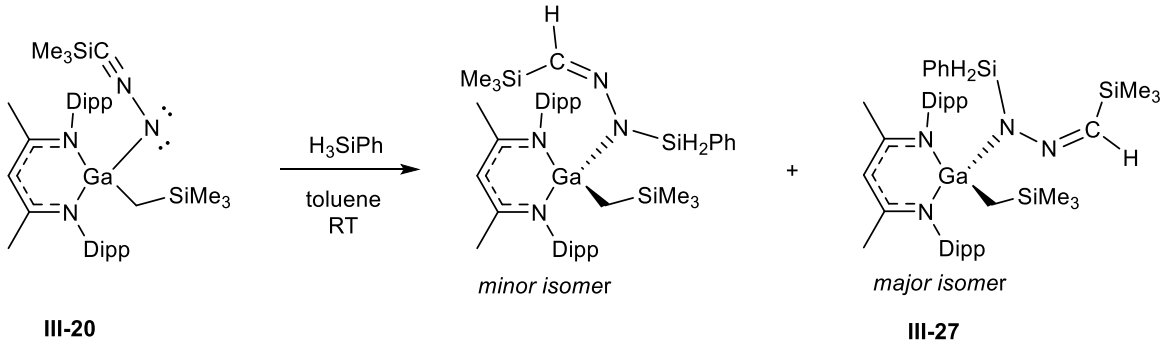

Scheme 103. Reaction between nitrilimine **III-20** and silane H_3SiPh.

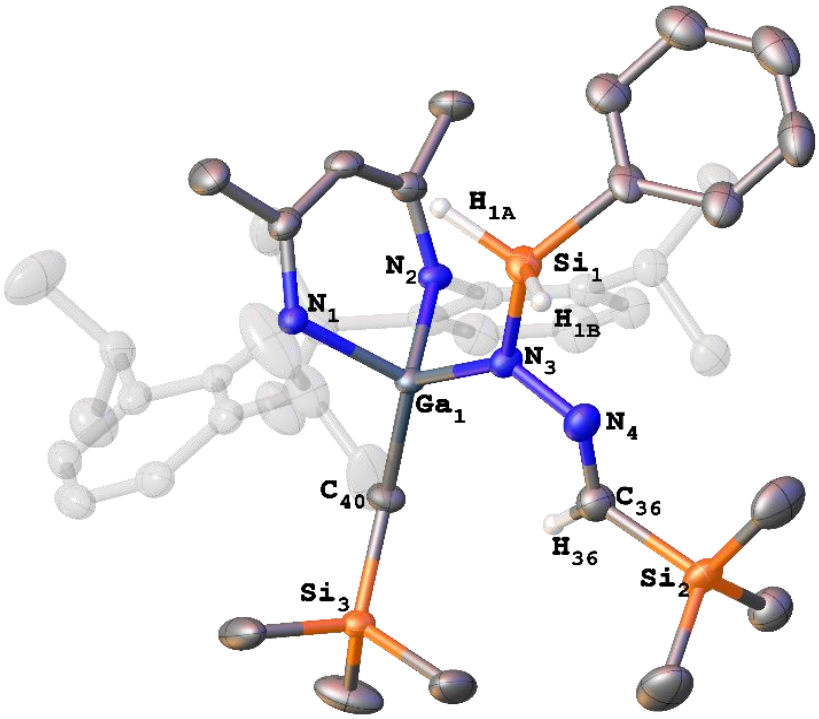

Figure 16. Molecular structure of compound NacNacGa(CH_2SiMe_3)(N(SiH_2Ph)(N=$CHSiMe_3$)) (**III-27**). The bulk of 2,6-diisopropylphenyl group is dimmed and hydrogen atoms except C36-H are omitted for clarity. Thermal ellipsoids are plotted at 50%.

Table 16. Selected bond lengths and angles for the compound **III-27**.

Lengths, Å				**Angles, °**	
Ga1-N1	1.975(3)	N3-N4	1.4202(4)	N1-Ga1-N2	94.3(1)
Ga1-N2	1.984(3)	Si1-1N3	1.744(3)	N1-Ga1-N3	103.4(1)
Ga1-N3	1.935(3)	N4-C36	1.272(5)	N3-Ga1-C40	127.2 (1)
Ga1-C40	1.969(3)			Si1-N3-N4	101.7(2)
				N3-N4-C36	121.8(3)

III-20 was then reacted with diborane and disilane to test if the addition reaction is feasible for non-hydrogen atoms. No reaction between **II-20** and Si_3Me_6 was observed. The

reaction of B_2cat_2 with **III-20**, however, resulted in the formation of a $NacNaGa(CH_2SiMe_3)X$ species and a free nitrile $NCSiMe_3$. The ^1H NMR spectrum features for the catechol fragment suggested that the two boryl groups are inequivalent. An X-ray diffraction study of this product finally revealed the formation of a bis(boryl)amide of gallium **III-28** (Figure 17), the product of a formal insertion of a galanitrene across the B-B bond (Scheme 104).

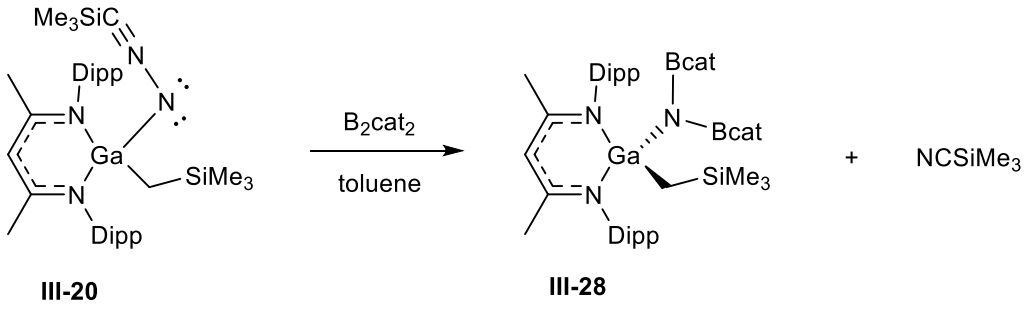

Scheme 104. Reaction between nitrilimine **III-20** and diborane.

Monitoring the reaction by NMR spectroscopy at low temperatures showed formation of an intermediate at -30°C which then converts to **III-28** at 10°C. The ^1H NMR spectrum of this intermediate showed two septets and four doublets for the isopropyl groups of the ligand, consistent with the C_s symmetry. The most telling feature is a correlation in ^1H-^{13}C HMBC spectrum between a $SiMe_3$ signal and a carbonyl carbon signal at 171.0 ppm, suggesting the presence of an imine group. Based on these data, we propose that this species is the product of 1,3-addition of diborane to the nitrilimine moiety (Scheme 105). Upon warming above 10°C this intermediate converts into the compound **III-28** with concurrent formation of free $NCSiMe_3$.

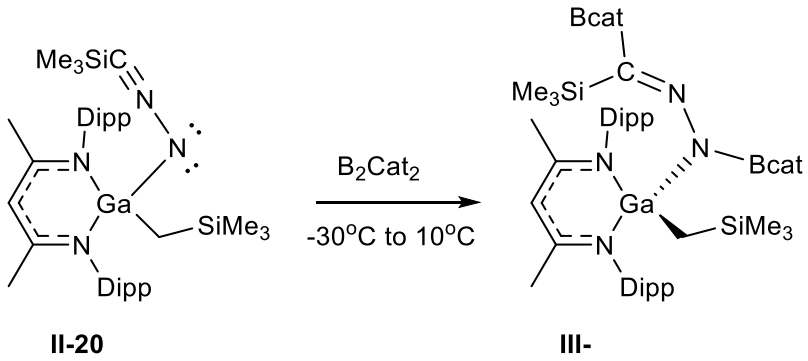

II-20 **III-**

Scheme 105. 1,3-addition intermediate from the reaction between nitrilimine **III-20** and diborane.

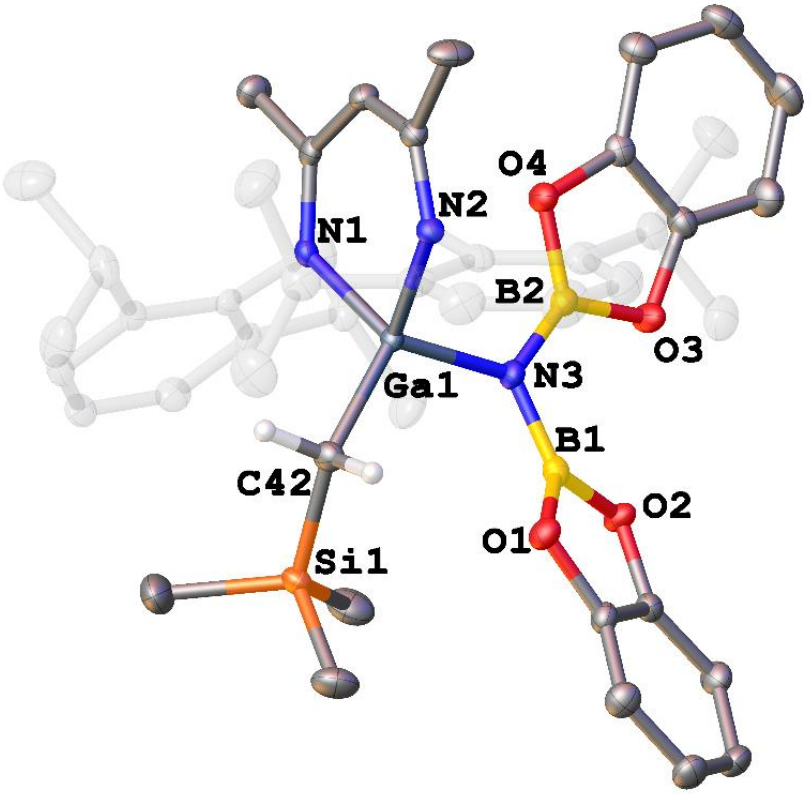

Figure 17. Molecular structure of NacNacGa(CH_2SiMe_3)(N(Bcat)$_2$) (**III-28**). The bulk of 2,6-diisopropylphenyl group is dimmed; hydrogen atoms are omitted for clarity. Thermal ellipsoids are plotted at 50%.

Table 17. Selected bond lengths and angles for the compound **III-28**.

Lengths, Å		**Angles, °**	
Ga1-N1	1.957(2)	N1-Ga1-N2	94.71(9)
Ga1-N2	1.983(2)	N1-Ga1-N3	109.43(9),
Ga1-N3	1.934(2)	N3-Ga1-C42	112.5 (1),
Ga1-C42	1.964(2)	Ga1-N3-B1	120.5(2)
N3-B1	1.416(4)	B1-N3-B2	118.4(2)
N3-B2	1.399(4)		

To the best of our knowledge, this is the first example of the nitrene-like reactivity of a nitrilimine. The molecular structure of **III-28** is shown in Figure 17. The Ga-NB_2 bond of 1.934(2) Å is similar to the Ga-N distances to the NacNac ligand nitrogen atoms, 1.957(2) and 1.983(2) Å. The bis(boryl) amido fragment adopts a planar geometry as the result of a π-interaction between the amide lone pair and vacant orbitals on boron atoms. The N-B bonds of 1.416(4) and 1.399(4) Å are comparable that of the single N-B bond in the monoboryl **III-26**.

We attempted DFT modelling of the addition of diborane B_2cat_2 to **III-20**. Unfortunately, **III-20** is lacking symmetry and there are multiple computationally distinct addition pathways. Computational exploration of all of these pathways on the bulky system of **III-20** + B_2cat_2 is prohibitively expensive. Along one pathway, the addition of diborane to **III-20** affords a labile Lewis acid-base adduct **III-29** (ΔG = -3.0 kcal/mol) where the B-N bond length is 1.68 Å. From this adduct, there is a direct path to the products, bis(boryl)amide **III-28** and $NCSiMe_3$, via a $TS_{III\text{-}29/III\text{-}28}$ (Scheme 106). The calculated Gibbs energy of $TS_{III\text{-}29/III\text{-}28}$, however, is 27.2 kcal/mol vs **III-20** + B_2cat_2, or 30.2 kcal/mol above the initial adduct. Assuming no major computational error, the calculated barrier is

inconsistent with the experimentally observed formation of **III-28** at 10 °C. Along another addition pathway, a different Lewis acid-base adduct **III-30** was located at +6.5 kcal/mol (Scheme 106). Although unstable, it works as an entry point for the 1,3-addition of diborane, via $TS_{III\text{-}30/III\text{-}31}$ at $\Delta G^{\ddagger}$ = 19.1 kcal/mol. The $TS_{III\text{-}30/III\text{-}31}$ is characterized by a B-N bond of 1.62 Å and a nascent B···C bonding interaction at 2.21 Å; the N-N-C fragment is bent (136.5°). From $TS_{III\text{-}30/III\text{-}31}$, the energy drops precipitously towards the 1,3-adduct **III-31**, at -37.1 kcal/mol. Along the way, the B-B bond is cleaved, whereas the B-N and B-C bonds are fully formed, at 1.43 and 1.57 Å, respectively. The N-N-C angle of the 1,3-adduct is 122° and the N-N and N-C bond distances are 1.38 and 1.31 Å, respectively. From this adduct, there is another large energy drop towards the final products, **III-28** and $NCSiMe_3$. The calculated overall reaction Gibbs energy is ΔG = -93.2 kcal/mol. It remains an open question whether the 1,3-adduct is connected with **III-28**. Our calculations found no low-energy stationary points connected with the 1,3-adduct that could lead to the formation of **III-28**.

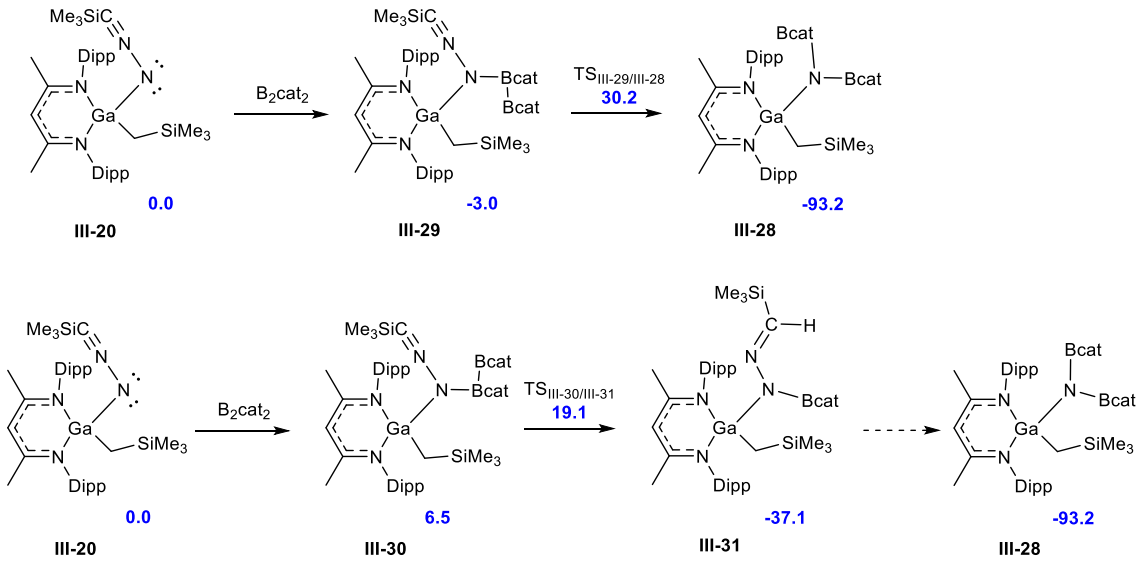

Scheme 106. Two calculated pathways for the addition of diborane to nitrilimine **III-20**. ΔG (blue) in kcal/mol.

In conclusion, we prepared a gallium nitrilimine (**III-20**) from the reaction of NacNacGa with trimethylsilyl diazomethane. A gallium diazomethane (**III-24**) was obtained from the reaction of **III-1** with N_2CSiMe_3 in the presence of pyridine. The gallium diazomethane compound **III-24** rearranges into the gallium isonitrile amide **III-25** at room temperature. The gallium nitrilimine showed 1,3-addition reactions with catecholborane and phenylsilane with the formation of products **III-26** and **III-27**, respectively. In contrast, a 1,1-addition was observed upon the reaction with diborane yielding the gallium diborylamide **III-28.**

IV. Conclusion and Future Work

The reactivity of low-valent gallium complex (**III-1**) with a variety of unsaturated substrates was investigated. As expected from the lower lying HOMO of gallium, **III-1** proved to be less reactive compared to its aluminum analogue **II-10**. Thus, there were no reactions between Ga(I) and alkenes, urea, thiourea and phosphine oxides. The cleavage of the P=S bond of triphenylphosphine sulfide was observed only at elevated temperatures. **III-1** also does not react with ketones but undergoes a [1+4] cycloaddition with a conjugated aldehyde, resulting in **III-2**. In contrast, the oxidative addition of the C=S bond of phenyl isothiocyanate to **III-1** was facile, resulting in the formation of cycloaddition products, the gallium sulfide-isothiocyanate (**III-4**) and the sulfide/isocyanide-bridged dimer (**III-5**). Related reactions of **III-1** with isocyanates and carbodiimides led to [1+2+3] cycloaddition products **III-7** and **III-8**, respectively. Given the low reactivity of NacNacGa **III-1**, its mixture with various electrophilic substrates should be reacted with isocyanates. Based on the proposed mechanism of the reaction between NacNacGa **III-1** and isocyanates in Scheme 88, other coupling products with unsaturated substrates or bond activation reactions can be achieved (Scheme 107).

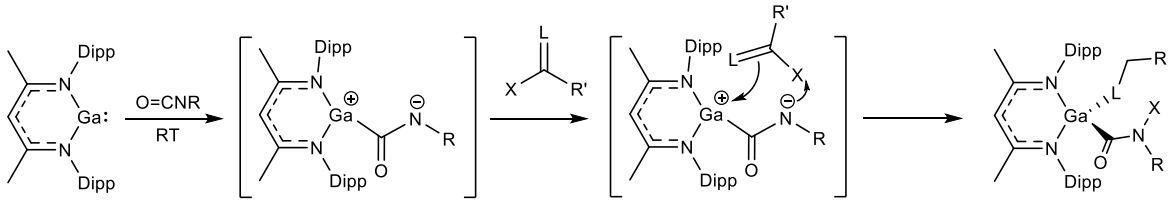

Scheme 107. Possible reaction of an intermediate gallium isocyanate adduct with reagents containing a donor site.

The oxidation of Ga(I) compound **III-1** with pyridine N-oxide resulted in the ortho C-H activation of pyridine oxide. DFT calculations on the mechanism of this reaction revealed that monomeric NacNacGa(O)(L) forms during the reaction and can easily activate C-H bonds. Fortunately, NacNacGa (**III-1**) is not very reactive and can easily be mixed with variety of substrates. Therefore, the reaction was extended to different aromatic and aliphatic substates with donor sites by the *in situ* oxidation of **III-1** with N_2O. Thus, the C-H activation of pyridine, cyclohexanone, DMSO, and $Et_3P{=}O$ was demonstrated. In contrast, the C–H activation in an aliphatic amine, NEt_3 by NacNacGa(O) is kinetically disfavored. Experimental and DFT results show that C–H activation by the related sulfide NacNacGa(S) is not possible either. The imide NacNacGa=$NSiMe_3$, generated *in situ* from the reaction of **III-1** with N_3SiMe_3 also activates C-H bonds of pyridine, cyclohexanone, ethyl acetate, DMSO, and $Et_3P{=}O$. Future work should focus on the isolation of monomeric gallium oxide and imide. To this purpose ligand modification will be required, as an attempt to intercept the gallium oxide in the presence of N-heterocyclic carbene resulted in the deprotonation of the backbone methyl group. Methyl group of the ligand can be replaced with tert-butyl group, in analogy with the known Al(I) compound **II-201** prepared by the Cui group (Scheme 108).[171]

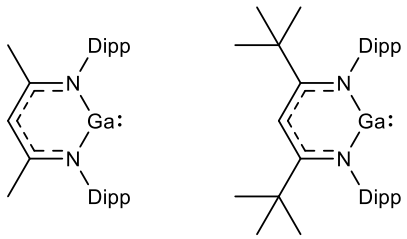

Scheme 108. Modification of NacNac ligand.

With the intent to generate a transient gallium alkylidene NacNacGa=CR_2, **III-1** was reacted with trimethylsilyl diazomethane. Instead, the reaction resulted in the gallium nitrilimine **III-20** or gallium diazomethane **III-25** in the presence of pyridine. The reactivity of gallium nitrilimine **III-20** was then studied. **III-20** undergoes a 1,3-addition of Si-H and B-H bonds of silane and borane to furnish the metallated hydrazonides **III-26** and **III-27**, respectively. In contrast, treatment of **III-20** with a diborane, B_2cat_2, led to a product of formal nitrene insertion into the B-B bond, the gallium diboryl amide **III-28**. DFT calculations ruled out a direct carbene-like insertion of nitrilimine into B-B and indicated a viable reaction pathway via a 1,3-addition of the B-B bond to the nitrilimine fragment. However, a trajectory for the rearrangement of this 1,3-adduct to the final amide has not been located. Reactivity of **III-20** with unsaturated substrates including isocyanates, carbodiimides, and carbon dioxide should be studied in the future work. As for the preparation of gallium alkylidene, Wittig reagents should be reacted with NacNacGa **III-1**.

Finally, catalytic application of main group reagents should be a focus of future research in the field. For low valent gallium compounds reductive elimination step has been a challenging task (Scheme 109). Application of redox active ligands and use of photoactivation could be a potential solution for this issue. Moreover C-H activation reaction on transient gallium oxide/imide should be developed further. Functionalization N-heterocycles and preparation of conjugated carbonyls could be possible routes for the future studies.

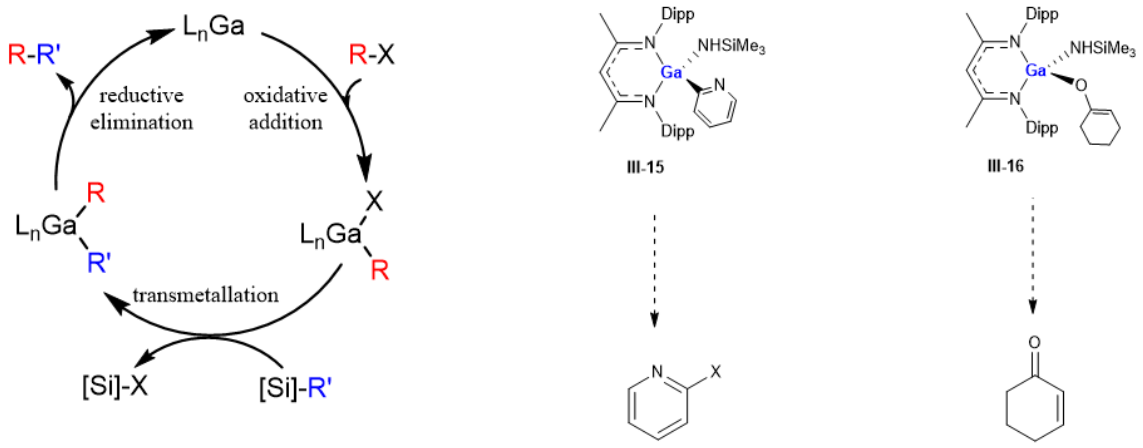

Scheme 109. Generic redox Ga(I)/Ga(III) catalytic cycle. Functionalization of pyridine and cyclohexanone

V. Experimental

V.1 General Methods and Solvents

Unless stated otherwise, all manipulations were performed using standard inert atmosphere (N_2 gas) glovebox and Schlenk techniques. All glassware was rinsed with organic solvents and stored in a 190 °C oven for a minimum of 2 hours before immediate transfer to the glovebox or assembly or evacuation on the vacuum line. Liquid nitrogen (−196 °C) and dry ice/acetone (−78 °C) baths were used to maintain low temperature conditions during reactions, when required. Benzene, toluene, hexanes, diethyl ether, tetrahydrofuran, and dichloromethane were dried and purified using a Grubbs-type solvent purification system. Benzene-d_6 and toluene-d_8 were dried and distilled from a K/Na alloy and stored in a glass vessel equipped with a Teflon stopcock in the glovebox.

V.2 Instrumentation and Analysis

NMR spectra were obtained with a Bruker DPX-300, AVANCE III HD 400 MHz, and DPX-600 spectrometers (^{1}H 400 and 600 MHz; ^{13}C 101 and 151 MHz; ^{11}B 128 and 193 MHz; ^{31}P 162 and 243 MHz) at room temperature, unless stated otherwise, then processed and analyzed with the MestReNova software (v10.0.2-15465).. Elemental analyses were performed by the ANALEST laboratory at the University of Toronto.

X-ray crystallographic analyses were performed on suitable crystals coated in perfluoropolyether oil and mounted on a glass fiber. Crystallographic data were collected on Bruker APEX-II CCD diffractometer equipped with an Oxford Cryosystems low-

temperature device operating at T = 100.0(1)/150.0(1)/200.0(1) K. Full details can be found in the individual tables for each crystal structure (Appendix).

V.3 Starting Materials

2,6-Diisopropyl aniline, acetylacetone, methyllithium (1.6 M in diethyl ether), Ga metal, triphenylphosphine oxide, triethylphosphine oxide, 1,3-dimethyl-2-imidazolidinone, methacrolein, phenyl isothiocyanate, phenyl isocyanate, 3.5-dimethylphenyl isocyanate, di-isopropylcarbodiimide, di-p-tolylcarbodiimide, di-o-tolylcarbodiimide, triphenylphosphine sulfide, triethylphosphine sulfide, pyridine N-oxide, N_2O gas, pyridine, cyclohexanone, benzophenone, ethyl acetate, DMSO, (trimethylsilyl)azide, (trimethylsilyl)diazomethane (0.5M in hexanes), catecholborane, biscatecholato diboron, were purchased from Sigma Aldrige or Alfa Aesar and used as received. Compound **III-1** was prepared according to a literature procedure.[4]

V.4 Experimental Procedures Pertaining to Chapter III

Section III.1

Preparation of NacNacGa(-OCH=C(CH_3)-CH_2-) (III-2)

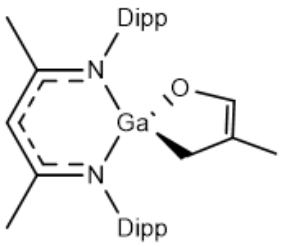

III-2

To a solution of NacNacGa (0.099 g, 0.20 mmol) in Et_2O was added methacrolein (0.017 ml, 0.20 mmol). The reaction mixture was stirred for 10 min at room temperature. Volatiles were removed. The resulting yellow solid was washed with hexanes to give NacNacGa(-OCH=C(CH_3)-CH_2-) (0.084 g, 0.15 mmol,

74%). The product was dissolved in a minimum amount of Et_2O and recrystallized at -30°C to give white crystals (0.019g, 0.034 mmol).

^{1}H NMR (600 MHz, C_6D_6): δ 7.10 – 7.01 (m, 6H, C_6H_3), 6.88 (s, 1H, OC*H*C(CH_3)CH_2), 4.86 (s, 1H, CH), 3.69 (hept, 2H, C*H*(CH_3)$_2$, $^3J_{H-H}$ = 6.7 Hz), 3.18 (hept, 2H, C*H*(CH_3)$_2$, $^3J_{H-H}$ = 6.8 Hz), 1.56 (s, 6H, NCCH_3), 1.45 (s, 3H, OCHC(C*H*$_3$)CH_2), 1.43 (d, 6H, CH(C*H*$_3$)$_2$, $^3J_{H-H}$ = 6.7 Hz), 1.29 (d, 6H, CH(C*H*$_3$)$_2$, $^3J_{H-H}$ = 6.8 Hz), 1.16 (d, 6H, CH(C*H*$_3$)$_2$, $^3J_{H-H}$ = 6.7 Hz), 1.11 (d, 6H, CH(C*H*$_3$)$_2$, $^3J_{H-H}$ = 6.8 Hz), 0.66 (s, 2H, OCHC(CH_3)C*H*$_2$).

^{13}C{^{1}H} NMR (151 MHz, C_6D_6): δ 169.6 (N*C*CH_3), 148.4 (O*C*HC(CH_3)CH_2), 145.7, 142.6, 140.38, 127.8, 125.3, 123.7 (C_6H_3), 105.5 (OCH*C*(CH_3)CH_2), 96.3 (CH), 29.0, 28.1 (*C*H(CH_3)$_2$), 25.8, 24.6, 24.6, 24.2 (CH(*C*H_3)$_2$), 23.4 (NC*C*H_3), 19.4 (OCHC(*C*H_3)CH_2), 7.1 (OCHC(CH_3)*C*H_2).

Elemental Analysis: Calculated for $C_{33}H_{47}GaN_2O$: C, 71.10; H, 8.50; N, 5.03. Found: C, 70.87; H, 8.51; N, 4.93.

Preparation of NacNacGa(κ^2-S_2C=NPh) (III-4)

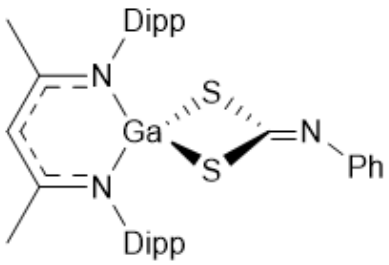

III-4

To a solution of phenyl isothiocyanate (0.046 mL, 0.38 mmol) in toluene was slowly added a toluene solution of NacNacGa (0.093 g, 0.19 mmol). The reaction was stirred for 10 minutes at room temperature. Volatiles were removed under vacuo. A pale orange solid produced was washed with cold hexanes to yield NacNacGa(κ^2-S_2C=NPh) (0.114 g, 0.21 mmol, 91%). The product was recrystallized from

a 1:2 mixture of toluene and hexanes at −30°C to give white crystals of NacNacGa(κ^2-S_2C=NPh) (0.024 g, 0.037 mmol, 19%).

^{1}H NMR (600 MHz, C_6D_6): δ 7.18-7.14 (m, 2H, C_6H_3), 7.13 – 7.08 (m, 4H, C_6H_3), 6.99 (t, 2H, C_6H_5, $^3J_{H-H}$ =), 6.80 (d, 2H, C_6H_5, $^3J_{H-H}$ = 7.3 Hz), 6.74 (t, 1H, C_6H_5, $^3J_{H-H}$ = 7.3 Hz), 4.79 (s, 1H, CH), 3.17 (hept, 2H, C*H*$(CH_3)_2$ $^3J_{H-H}$ = 6.7 Hz), 3.10 (hept, 2H, C*H*$(CH_3)_2$ $^3J_{H-H}$ = 6.7 Hz), 1.51 (s, 6H, NCCH_3), 1.46 (d, 6H, CH(C*H*$_3)_2$, $^3J_{H-H}$ = 6.7 Hz), 1.36 (d, 6H, CH(C*H*$_3)_2$, $^3J_{H-H}$ = 6.7 Hz), 1.07 (d, 6H, CH(C*H*$_3)_2$, $^3J_{H-H}$ = 6.7 Hz),1.04 (d, 6H, CH(C*H*$_3)_2$, $^3J_{H-H}$ = 6.7 Hz).

^{13}C{^{1}H} NMR (151 MHz, C_6D_6): δ 171.9 (N*C*CH_3), 155.6 (NCS), 144.3, 144.3, 138.7, 128.6, 128.4, 125.0, 125.0 (C_6H_3), 152.5, 128.7, 123.3, 121.3 (C_6H_5), 97.1 (CH), 29.3, 29.0 (*C*H$(CH_3)_2$), 25.3, 25.1, 25.0, 25.0 (CH(*C*$H_3)_2$), 23.9 (NC*C*H_3).

Elemental Analysis: Calculated $C_{36}H_{46}GaN_3S_2$·0.6 toluene: C, 68.01; H, 7.21; N, 6,03.H, 7.08; N, 6.42. Found: C, 67.94; H, 7.15; N, 5.69.

Preparation of (NacNacGa)$_2$(μ-S)(μ-PhNC) (III-5)

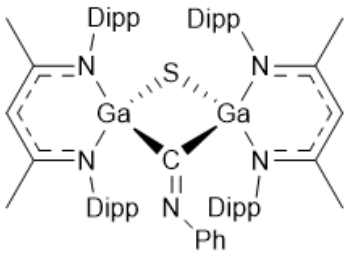

III-5

A toluene solution of phenyl isothiocyanate (0.023 mL, 0.19 mmol) was slowly added to a solution of NacNacGa (0.095 g, 0.19 mmol). The reaction mixture was stirred for 10 min at room temperature. Volatiles were removed under reduced pressure. The orange residue was dissolved in Et_2O and crystallized by slow evaporation. Red crystals of (NacNacGa)$_2$(μ-S)(μ-PhNC) (0.030 g, 0.028 mmol, 44%) were manually separated from the NacNacGa(S_2CNPh) powder.

^{1}H NMR (400 MHz, C_6D_6): δ 7.78 (d, 2H, C_6H_5,$^{3}J_{H\text{-}H}$ = 8.1 Hz), 7.27 (t, 2H, C_6H_5, $^{3}J_{H\text{-}H}$ = 8.1 Hz), 7.10 (m, 6H, C_6H_3 and C_6H_5), 7.04 (m, 3H, C_6H_3), 6.91 (dd, 2H, C_6H_3, *J* = 7.8 Hz, *J*=1.5 Hz), 6.80 (t, 2H, C_6H_3, $^{3}J_{H\text{-}H}$ = 4.5 Hz), 4.85 (s, 1H, CH), 4.79 (s, 1H, CH), 3.73 (hept, 2H, C*H*$(CH_3)_2$, $^{3}J_{H\text{-}H}$ = 6.7 Hz), 3.68 (hept, 2H, C*H*$(CH_3)_2$, $^{3}J_{H\text{-}H}$ = 6.8 Hz), 3.22 (hept, 2H, C*H*$(CH_3)_2$, $^{3}J_{H\text{-}H}$ = 6.7 Hz), 2.30 (hept, 2H, C*H*$(CH_3)_2$, $^{3}J_{H\text{-}H}$ = 6.8 Hz), 1.71 (d, 6H, CH(C*H*$_3)_2$, $^{3}J_{H\text{-}H}$ = 6.8 Hz), 1.62 (d, 6H, CH(C*H*$_3)_2$, $^{3}J_{H\text{-}H}$ = 6.7 Hz) 1.34 (s, 6H, NCC*H*$_3$), 1.22 (s, 6H, NCC*H*$_3$), 1.15 (d, 6H, CH(C*H*$_3)_2$, $^{3}J_{H\text{-}H}$ = 6.8 Hz), 1.11 (d, 6H, CH(C*H*$_3)_2$, $^{3}J_{H\text{-}H}$ = 6.7 Hz), 1.07 (d, 6H, CH(C*H*$_3)_2$, $^{3}J_{H\text{-}H}$ = 6.7 Hz), 0.74 (d, 6H, CH(C*H*$_3)_2$, $^{3}J_{H\text{-}H}$ = 6.8 Hz), 0.57 (d, 6H, CH(C*H*$_3)_2$, $^{3}J_{H\text{-}H}$ = 6.7 Hz), -0.04 (d, 6H, CH(C*H*$_3)_2$, $^{3}J_{H\text{-}H}$ = 6.8 Hz).

^{13}C{^{1}H} NMR (101 MHz, C_6D_6): δ 169.7 (N*C*CH_3), 169.0 (N*C*CH_3), 151.5 (CN), 146.1, 145.0, 143.8, 143.8, 143.4, 127.4, 127.3, 124.8, 124.7, 124.2, 123.9 (C_6H_3), 143.9, 129.0, 126.4, 120.3 (C_6H_5), 97.5 (CH), 97.3 (CH), 29.4, 29.2, 27.9, 27.7 (*C*H$(CH_3)_2$), 27.1, 25.4, 25.3, 24.5, 24.3, 24.3, 23.4 (CH(*C*$H_3)_2$), 24.9, 24.8 (NC*C*H_3).

Elemental Analysis: Calculated for $C_{65}H_{87}Ga_2N_5S$·toluene C, 71.94; H, 7.97; N, 5.83. . Found: C, 72.72; H, 7.34; N, 5.85.

Preparation of NacNacGa[(3,5-$CH_3)_2C_6H_3$NCO]$_2$ (III-7)

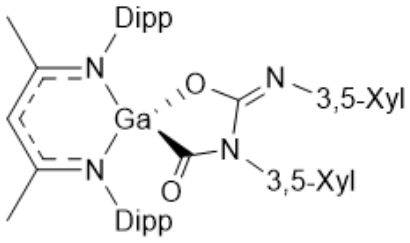

III-7

To a solution of NacNacGa (0.094 g, 0.19 mmol) in diethyl ether (5 mL) was added 3,5-dimethylphenyl isocyanate (0.054 mL, 0.39 mmol) and the mixture was left overnight at room temperature. The resulting yellow solution was concentrated to give yellow crystals of NacNacGa[(3,5-$CH_3)_2C_6H_3$NCO]$_2$ (0.012 g, 0.015 mmol). The remaining

solution was placed in a −30 °C freezer to give a yellow precipitate that was filtered to yield the product (0.115 g, 0.15 mmol, 76%).

^{1}H NMR (400 MHz, C_6D_6): δ 7.14 (s, 1H, C_6H_3), 7.11 (m, 5H, $C_6H_3(CH_3)_2$ and C_6H_3), 7.06 (dd, J = 6.6, 2.6 Hz, 2H, C_6H_3), 6.63 (s, 1H, $C_6H_3(CH_3)_2$), 6.62 (s, 2H, $C_6H_3(CH_3)_2$), 6.59 (s, 1H, $C_6H_3(CH_3)_2$), 4.75 (s, 1H, CH), 3.44 (hept, 2H, $CH(CH_3)_2$ $^3J_{H\text{-}H}$ = 6.8 Hz), 3.22 (hept, 2H, $CH(CH_3)_2$ $^3J_{H\text{-}H}$ = 6.8 Hz), 2.21 (s, 6H, $C_6H_3(CH_3)_2$), 1.90 (s, 6H, $C_6H_3(CH_3)_2$), 1.50 (d, 6H, $CH(CH_3)_2$, $^3J_{H\text{-}H}$ = 6.7 Hz), 1,48 (s, 6H, $NCCH_3$), 1.36 (d, 6H, $CH(CH_3)_2$, $^3J_{H\text{-}H}$ = 6.8 Hz), 1.15 (d, 6H, $CH(CH_3)_2$, $^3J_{H\text{-}H}$ = 6.8 Hz), 1.04 (d, 6H, $CH(CH_3)_2$, $^3J_{H\text{-}H}$ = 6.8 Hz).

^{13}C{^{1}H} NMR (101 MHz, C_6D_6): δ 171.8 ($NCCH_3$), 153.1 (NCO), 148.8 (NCO), 145.0, 143.5, 138.7, 125.1, 124.8 (C_6H_3), 138.4, 137.4, 136.8, 128.7, 128.7, 123.7, 123.3 ($C_6H_3(CH_3)_2$), 97.8 (CH), 29.4, 28.5 ($CH(CH_3)_2$), 25.6, 24.7, 24.6, 24.4 ($CH(CH_3)_2$), 23.3 ($NCCH_3$), 21.7, 21.1 ($C_6H_3(CH_3)_2$).

Elemental Analysis: Calculated for $C_{47}H_{59}GaN_4O_2$: C, 72.21; H, 7.61; N, 7.17. Found: C, 72.03; H, 7.54; N, 7.09.

Preparation of NacNacGa[4-$CH_3C_6H_4$NCN4-$CH_3C_6H_4$]$_2$ (III-8)

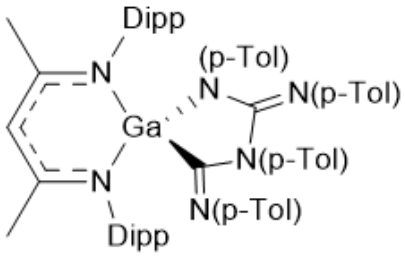

III-8

To a solution of NacNacGa (0.094 g, 0.19 mmol) in Et_2O (5 mL) was added 1,3-di-p-tolylcarbodiimide (0.054 mL, 0.39 mmol). The reaction mixture was left overnight at room temperature, after which time yellow crystals of NacNacGa[(3,5-CH_3)$_2C_6H_3$NCO]$_2$ started to form. After collecting the crystals (0.015 g, 0.016 mmol) for X-ray analysis, the remaining solution was

dired and the residue was washed with cold hexanes to give 0.126 g (0.13 mmol, 70%) of product.

^{1}H NMR (400 MHz, C_6D_6): δ 7.71 (d, 2H, $C_6H_4CH_3$, $^{3}J_{H\text{-}H}$ = 8.3 Hz), 7.21 (m, 2H, C_6H_3), 6.10 (d, 2H, $C_6H_4CH_3$, $^{3}J_{H\text{-}H}$ = 8.3 Hz), 6.99, (m, 2H, C_6H_3) 6.96 (d, 2H, $C_6H_4CH_3$, $^{3}J_{H\text{-}H}$ = 8.2 Hz), 6.91 (d, 2H, $C_6H_4CH_3$, $^{3}J_{H\text{-}H}$ = 8.2 Hz), 6.41 (d, 2H, $C_6H_4CH_3$, $^{3}J_{H\text{-}H}$ = 8.0 Hz), 6.30 (d, 2H, $C_6H_4CH_3$, $^{3}J_{H\text{-}H}$ = 8.0 Hz), 6.26 (d, 2H, $C_6H_4CH_3$, $^{3}J_{H\text{-}H}$ = 8.1 Hz), 5.92 (d, 2H, $C_6H_4CH_3$, $^{3}J_{H\text{-}H}$ = 8.1 Hz), 4.25 (s, 1H, CH), 3.69 (hept, 2H, C*H*$(CH_3)_2$, $^{3}J_{H\text{-}H}$ = 6.7 Hz), 2.69 (hept, 2H, C*H*$(CH_3)_2$, $^{3}J_{H\text{-}H}$ = 6.7 Hz), 2.17 (s, 3H, $C_6H_4CH_3$), 2.08 (s, 3H, $C_6H_4CH_3$), 1.95 (s, 3H, $C_6H_4CH_3$), 1.89 (s, 3H, $C_6H_4CH_3$), 1.78 (d, 6H, CH$(CH_3)_2$, $^{3}J_{H\text{-}H}$ = 6.7 Hz), 1.36 (s, 6H, $NCCH_3$), 1.28 (d, 6H, CH$(CH_3)_2$, $^{3}J_{H\text{-}H}$ = 6.7 Hz), 0.91 (d, 6H, CH$(CH_3)_2$, $^{3}J_{H\text{-}H}$ = 6.7 Hz), 0.79 (d, 6H, CH$(CH_3)_2$, $^{3}J_{H\text{-}H}$ = 6.7 Hz).

^{13}C{^{1}H} NMR (101 MHz, C_6D_6): δ 172.2 (N*C*CH_3), 153.8, 150.3 (NCN), 145.6, 143.6, 140.4, 125.2, 124.6 (C_6H_3), 147.2, 142.6, 138.7, 134.8, 132.6, 130.5, 129.4, 128.7, 126.8, 121.7, 121.5 (*C*$_6H_4CH_3$), 100.9 (CH), 28.9, 28.8 (*C*H$(CH_3)_2$), 26.3, 25.6, 24.8, 24.4 (CH(*C*$H_3)_2$), 23.9 (NC*C*H_3), 21.1, 20.8, 20.7, 20.7 ($C_6H_4CH_3$).

Elemental Analysis: Calculated for $C_{59}H_{69}GaN_6$: C, 76.04; H, 7.46; N, 9.02. Found: C, 76.29; H, 6.09; N, 8.63

Section III.2

Preparation of NacNacGa(py-O)(OH) (III-9)

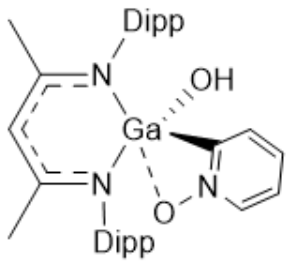

III-9

NacNacGa (0.097 g, 0.20 mmol) in toluene was treated with two equivalents of pyridine oxide (0.038 g, 0.40 mmol) at room temperature. The reaction mixture was stirred for 10 minutes. Volatiles were removed under reduced pressure. The orange solid produced was washed with cold hexanes to yield 0.101 g (0.17 mmol, 85%) of of NacNacGa(py-O)(OH). The product was recrystallized from Et_2O at -30°C to give orange crystals of NacNacGa(py-O)(OH) (0.052 g, 0.09 mmol, 45%).

^{1}H NMR (400 MHz, C_6D_6) δ 7.80 (d, 1H, C_5H_4N,$^3J_{H-H}$ = 6.0 Hz), 7.19-7.12 (m, 4H, C_6H_3), 7.04 (dd, 2H, C_6H_3, $^3J_{H-H}$ = 7.3 Hz, $^3J_{H-H}$ =2 Hz), 6.53 (dd, 1H, C_5H_4N, $^3J_{H-H}$ = 7.0 Hz, $^4J_{H-H}$ = 2.4 Hz), 6.22-6.14 (m, 2H, C_5H_4N), 4.99 (s, 1H, CH), 3.75 (hept, 2H, C*H*$(CH_3)_2$ $^3J_{H-H}$ = 6.8 Hz), 3.66 (hept, 2H, C*H*$(CH_3)_2$ $^3J_{H-H}$ = 6.8 Hz), 1.66 (s, 6H, NCCH_3), 1.58 (d, 6H, CH(C*H*$_3)_2$, $^3J_{H-H}$ = 6.8 Hz), 1.23 (d, 6H, CH(C*H*$_3)_2$, $^3J_{H-H}$ = 6.8 Hz), 1.22 (d, 6H, CH(C*H*$_3)_2$, $^3J_{H-H}$ = 6.8 Hz), 0.65 (d, 6H, CH(C*H*$_3)_2$, $^3J_{H-H}$ = 6.8 Hz), -0.03 (s, 1H, OH).

^{13}C{^{1}H} NMR (101 MHz, C_6D_6) δ 169.3 (N*C*CH_3), 145.2, 144.9, 141.3, 127.3, 124.5, 124.2 (C_6H_3), 137.3, 134.8, 125.5, 122.4 (C_5H_4N), 97.5 (CH), 28.8, 27.2 (*C*H$(CH_3)_2$), 25.3, 25.1, 25.0, 23.9 (CH(*C*$H_3)_2$), 23.6 (NC*C*H_3).

Elemental Analysis: Calculated for $C_{34}H_{46}GaN_3O_2$: C, 68.23; H, 7.75; N, 7.02. Found: C, 68.04; H, 7.78; N, 6.94.

Preparation of NacNacGa(py)(OH) (III-10)

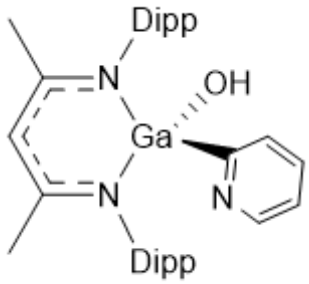

III-10

A mixture of NacNacGa (0.056 g, 0.11 mmol) and pyridine (0.009 mL, 0.11 mmol) in hexane was freeze-pump degassed and filled with the N_2O gas. The mixture was allowed to react over 10 min at room temperature. The solution was concentrated and recrystallized from hexanes at -30°C to give yellow crystals of NacNacGa(py)(OH) (0.016 g, 0.027 mmol, 25%).

^{1}H NMR (400 MHz, C_6D_6) δ 8.46 (m, 1H, C_5H_4N), 7.12 (m, 4H, C_6H_3), 7.02 (dd, 1H, $^3J_{H-H}$ = 7.3 Hz, $^3J_{H-H}$ = 1.8 Hz, C_6H_3), 6.92 (dt, 1H, $^3J_{H-H}$ = 8.6 Hz, $^3J_{H-H}$ =1.2 Hz, C_5H_4N), 6.73 (td, 1H, $^3J_{H-H}$ = 7.4 Hz, $^3J_{H-H}$ = 1.8 Hz, C_5H_4N), 6.47 (m, 1H, C_5H_4N), 4.85 (s, 1H, CH), 3.80 (hept, 2H, C*H*$(CH_3)_2$ $^3J_{H-H}$ = 6.8 Hz), 3.39 (hept, 2H, C*H*$(CH_3)_2$ $^3J_{H-H}$ = 6.7 Hz), 1.64 (s, 6H, $NCCH_3$), 1.54 (d, 6H, $CH(CH_3)_2$, $^3J_{H-H}$ = 6.8 Hz), 1.24 (d, 6H, $CH(CH_3)_2$, $^3J_{H-H}$ = 6.8 Hz), 1.15 (d, 6H, $CH(CH_3)_2$, $^3J_{H-H}$ = 6.7 Hz), 0.67 (d, 6H, $CH(CH_3)_2$, $^3J_{H-H}$ = 6.7 Hz), 0.26 (s, 1H, OH).

^{13}C NMR (101 MHz, C_6D_6) δ 169.4 ($NCCH_3$), 145.1, 144.2, 141.2, 127.2, 124.5, 124.3 (C_6H_3), 150.0, 132.6, 132.3, 122.0 (C_5H_4N), , 96.4 (CH), 28.6, 28.4 ($CH(CH_3)_2$), 25.4, 24.9, 24.8, 23.7, 23.5 ($CH(CH_3)_2$), 23.1 (NC*C*H).

Elemental Analysis: Calculated for $C_{34}H_{46}GaN_3O_2$*0.5Et_2O: C, 69.79; H, 8.24; N, 6.78. Found: C, 68.75; H, 8.85; N, 7.24.

Preparation of NacNacGa(OC(=CH(CH$_2$)$_4$ –)(OH) (III-11)

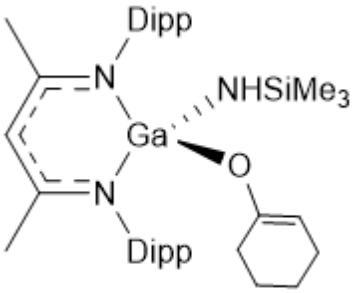

III-11

A solution of NacNacGa (0.090 g, 0.18 mmol) and cyclohexanone (0.018 mL, 0.18 mmol) in toluene was freeze-pump degassed and filled with the N_2O gas. The mixture was allowed to react over 10 min at room temperature. Volatiles were removed under reduced pressure. The solid residue was washed with cold hexane to yield NacNacGa(OC(=CH(CH$_2$)$_4$ –)(OH) (0.010 g, 0.17 mmol, 92%). The product was recrystallized from a 1:2 mixture of toluene and hexanes at -30°C to give colorless crystals of NacNacGa(OC(=CH(CH$_2$)$_4$ –)(OH) (0.064 g, 0.12 mmol, 64%).

^{1}H NMR (400 MHz, C_6D_6) 7.17-7.12 (m, 6H, C_6H_3), 4.82 (s, 1H, CH), 4.14 (m, 1H, OC_6H_9), 3.55 (hept, 2H, C*H*$(CH_3)_2$, $^3J_{H\text{-}H}$ = 6.9 Hz), 3.42 (hept, 2H, C*H*$(CH_3)_2$, $^3J_{H\text{-}H}$ = 6.8 Hz), 1.90 (m, 2H, OC_6H_9), 1.80 (m, 2H, OC_6H_9), 1.56 (s, 6H, $NCCH_3$), 1.48 (d, 6H, CH(C*H*$_3)_2$, $^3J_{H\text{-}H}$ = 6.8 Hz and 2H, OC_6H_9), 1.45 (d, 6H, CH(C*H*$_3)_2$, $^3J_{H\text{-}H}$ = 6.9 Hz), 1.38 (m, 2H, OC_6H_4), 1.18 (d, 6H, CH(C*H*$_3)_2$, $^3J_{H\text{-}H}$ = 6.8 Hz), 1.14 (d, 6H, CH(C*H*$_3)_2$, $^3J_{H\text{-}H}$ = 6.9 Hz), 0.49 (s, 1H, OH).

^{13}C{^{1}H}NMR (101 MHz, C_6D_6) δ 170.6 (N*C*CH_3), 155.6 (O*C*(=CH)$(CH_2)_4$), 144.8, 144.7, 139.9, 124.6, 124.4 (C_6H_3), 98.1 (OC(=*C*H)$(CH_2)_4$), 95.6 (CH), 31.1 (CH_2), 28.8, 28.3 (*C*H$(CH_3)_2$), 25.2, 24.9, 24.8, 24.8 (CH(*C*$H_3)_2$), 24.1 (CH_2), 23.4 (NC*C*H_3), 23.4 (CH_2).

Elemental Analysis: Calculated for $C_{35}H_{51}GaN_2O_2$: C, 69.89; H, 8.55; N, 4.66. Found: C, 69.82; H, 8.58; N, 4.60.

Preparation of NacNacGa(κ^2-O_2CPh_2) (III-12)

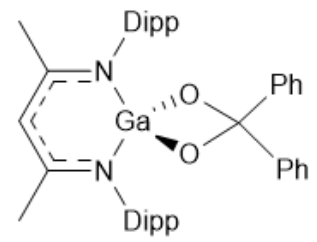

III-12

A solution of NacNacGa (0.084 g, 0.17 mmol) and benzophenone (0.027 g, 0.17 mmol) in toluene was freeze-pump degassed and filled with the N_2O gas. The reaction mixture was allowed to react over 10 min at room temperature. Volatiles were removed under reduced pressure. The residue was washed with cold hexanes to yield NacNacGa(κ^2-O_2CPh_2) (0.072 g, 0.10 mmol, 61%).

^{1}H NMR (400 MHz, C_6D_6) δ 7.29 (m, 4H, C_6H_5), 7.13 (d, 2H, C_6H_3, $^3J_{H\text{-}H}$ = 7.7 Hz), 7.01 (d, 4H, C_6H_3, $^3J_{H\text{-}H}$ = 7.7 Hz), 6.96 (m, 6H, C_6H_5), 4.87 (s, 1H, CH), 3.06 (hept, 4H, C*H*$(CH_3)_2$, $^3J_{H\text{-}H}$ = 6.8 Hz), 1.56 (s, 6H, NCCH_3), 1.40 (d, 12H, CH(C*H*$_3)_2$, $^3J_{H\text{-}H}$ = 6.8 Hz)), 1.07 (d, 12H, CH(C*H*$_3)_2$, $^3J_{H\text{-}H}$ = 6.8 Hz)

^{13}C{^{1}H}NMR (101 MHz, C_6D_6) δ 172.4 (N*C*CH_3), 143.6, 138.6, 124.6 (C_6H_3), 150.4, 127.0, 126.6, 125.3 (C_6H_5) 105.4 (O*C*Ph_2), 96.6 (CH), 29.1 (*C*H$(CH_3)_2$), 24.7, 23.8 (CH(*C*$H_3)_2$), 23.5 (NC*C*H_3).

Elemental Analysis: Calculated for $C_{42}H_{51}GaN_2O_2$: C, 73.58; H, 7.50; N, 4.09. Found: C, 72.82; H, 7.54; N, 4.10.

Preparation of NacNacGa($CH_2S(=O)Me$)(OH) (III-13)

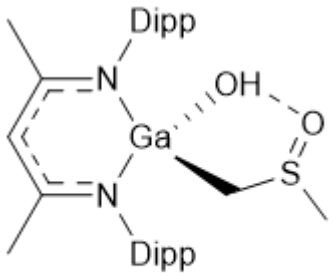

III-13

A solution of NacNacGa (0.079 g, 0.18 mmol) and DMSO (0.012 mL, 0.16 mmol) in toluene was freeze-pump degassed and filled with N_2O gas. The reaction mixture was allowed to react over 10 min at room temperature. Volatiles were removed under reduced pressure. The residue was washed with cold hexane to yield NacNacGa($CH_2S(=O)Me$)(OH) (0.079 g, 0.14 mmol, 84%). The product was recrystallized from a 1:2 mixture of toluene and hexanes at -30°C to give colorless crystals of NacNacGa($CH_2S(=O)Me$)(OH) (0.063 g, 0.11 mmol, 67%).

^{1}H NMR (400 MHz, C_6D_6) δ 7.19-7.13 (m, 3H, C_6H_3), 7.09 (t, 1H, C_6H_3, $^3J_{H-H}$ = 7.6 Hz), 7.03 (dd, 1H, C_6H_3, $^3J_{H-H}$ = 7.4 Hz, $^4J_{H-H}$ = 1.9 Hz), 6.98 (dd, 1H, C_6H_3, $^3J_{H-H}$ = 7.6 Hz, $^4J_{H-H}$ = 1.6 Hz), 4.79 (s, 1H, CH), 3.87 (hept, 1H, C*H*$(CH_3)_2$, $^3J_{H-H}$ = 6.8 Hz), 3.79 (hept, 1H, C*H*$(CH_3)_2$, $^3J_{H-H}$ = 6.8 Hz), 3.06 (m, 2H, C*H*$(CH_3)_2$), 1.95 (d, 1H, SCH_2, $^2J_{H-H}$ = 12.9 Hz), 1.85 (s, 1H, OH), 1.61 (s, 3H, SCH_3), 1.57 (s, 3H, NC*C*H_3), 1.57 (s, 3H, NCCH_3), 1.54 (d, 1H, SCH_2), 1.52 (d, 3H, CH(C*H*$_3)_2$, $^3J_{H-H}$ = 6.8 Hz), 1.51 (d, 3H, CH(C*H*$_3)_2$, $^3J_{H-H}$ = 6.8 Hz), 1.21 – 1.14 (m, 12H, CH(C*H*$_3)_2$), 1.06 (d, 3H, CH(C*H*$_3)_2$, $^3J_{H-H}$ = 6.8 Hz), 1.02 (d, 3H, CH(C*H*$_3)_2$, $^3J_{H-H}$ = 6.8 Hz).

^{13}C{^{1}H} NMR (101 MHz, C_6D_6) δ 169.3, 169.1 (N*C*CH_3), 146.2, 146.1, 142.6, 142.5, 140.7, 140.6, 127.7, 127.6, 125.6, 125.6, 123.8, 96.2 (CH), 41.9 (SCH_3), 37.4 (SCH_2), 29.0, 28.8, 27.9 (*C*H$(CH_3)_2$), 25.8, 25.8, 24.9, 24.9, 24.8, 24.7, 24.1, 23.8 (CH(*C*$H_3)_2$), 23.4, 23.4 (NC*C*H_3).

Elemental Analysis: Calculated for $C_{32}H_{50}GaN_2O_2S$: C, 64.43; H, 8.45; N, 4.70. Found: C, 63.83; H, 8.06; N, 4.72.

Preparation of NacNacGa(CH(Me)P(=O)Et$_2$)(OH) (III-14)

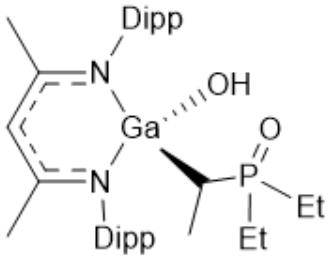

III-14

A solution of NacNacGa (0.087 g, 0.18 mmol) and triethylphosphine oxide (0.024 g, 0.18 mmol) in toluene was freeze-pump degassed and filled with the N_2O gas. The mixture was allowed to react over 10 min at room temperature. Volatiles were removed under reduced pressure. The solid residue was washed with cold hexanes to yield NacNacGa(OP(CHCH$_3$)(CH$_2$CH$_3$)$_2$)(OH) (0.101 g, 0.16 mmol, 89%). The product was recrystallized from Et_2O at -30°C to give colorless crystals of NacNacGa(CH(Me)P(=O)Et$_2$)(OH) (0.088g, 0.14 mmol, 77%).

^{1}H{^{31}P} NMR (400 MHz, C_6D_6) δ 7.20-7.17 (m, 2H, C_6H_3), 7.13 (m, 1H, C_6H_3), 7.10 (d, 1H, C_6H_3, $^3J_{H\text{-}H}$ = 7.7 Hz), 7.03 (m, 2H, C_6H_3), 4.89 (s, 1H), 4.23 (hept, 2H, C*H*(CH$_3$)$_2$, $^3J_{H\text{-}H}$ = 6.8 Hz), 3.93 (hept, 2H, C*H*(CH$_3$)$_2$, $^3J_{H\text{-}H}$ = 6.8 Hz), 3.28 (m, 2H, C*H*(CH$_3$)$_2$), 2.99 (s, 1H, OH), 1.64 (s, 6H, NCCH$_3$), 1.63-1.61 (m, 6H, CH(C*H*$_3$)$_2$), 1.61 (s, 6H, NCCH$_3$), 1.28 (m, 6H, CH(C*H*$_3$)$_2$), 1.20 (m, 6H, CH(C*H*$_3$)$_2$), 1.12 (d, 3H, CH(C*H*$_3$)$_2$, $^3J_{H\text{-}H}$ = 6.8 Hz), 1.07 (d, 3H, CH(C*H*$_3$)$_2$, $^3J_{H\text{-}H}$ = 6.8 Hz), 1.09-0.96 (m, 2H, PC*H*$_2$C*H*$_3$), 0.93 (q, 1H, PC*H*CH$_3$, $^3J_{H\text{-}H}$ = 7.9 Hz), 0.73 – 0.58 (m, 11H, PC*H*$_2$C*H*$_3$).

^{13}C{^{1}H} NMR (101 MHz, C_6D_6) δ 169.2, 169.1 (N*C*CH$_3$), 146.7, 146.3, 143.2, 142.9, 142.3, 141.7, 127.3, 127.2, 125.8, 125.6, 123.6, 123.5 (C_6H_3), 96.8 (CH), 29.3, 29.0, 27.9, 27.8 (*C*H(CH$_3$)$_2$), 23.9, 23.6 (NC*C*H$_3$), 25.7, 25.5, 25.2, 25.0, 24.98, 24.8 (NC*C*H$_3$), 23.4, 18.77

(PCH_2CH_3), 18.75 (PCH_2CH_3), 16.9 ($PCHCH_3$), 9.7 (PCH_2CH_3), 6.3 (PCH_2CH_3), 6.0 (PCH_2CH_3).

$^{31}P\{^1H\}$ NMR (162 MHz, C_6D_6) δ 54.91.

Elemental Analysis: Calculated for $C_{35}H_{56}GaN_2O_2P$: C, 65.94; H, 8.85; N, 4.39. Found: C, 66.18; H, 9.26; N, 4.38.

Section III.3

Preparation of NacNacGa(py)(NHSiMe$_3$) (III-15)

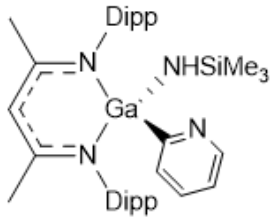

III-15

To a solution of NacNacGa (0.063 g, 0.13 mmol) in toluene was added pyridine (0.010 mL, 0.13 mmol) and the mixture was treated with N_3SiMe_3 (0.015 mL, 0.13 mmol). The reaction was allowed to stir for 10 min at room temperature. Volatiles were removed and NacNacGa(py)(NHSiMe$_3$) was obtained in quantitative yield. Colorless crystals of **2** were obtained from toluene solution at -30^{0}C.

^{1}H NMR (400 MHz, C_6D_6) δ 8.65 (m, 1H C_5H_4N), 7.92 (d, 1H, C_5H_4N), 7.11 (m, 4H, C_6H_3), 7.08 (m, 1H, C_5H_4N) 7.02 (m, 2H, C_6H_3), 6.69 (m, 1H, C_5H_4N), 4.85 (s, 1H, CH), 3.59 (hept, 2H, $CH(CH_3)_2$ $^3J_{H\text{-}H}$ = 6.8 Hz), 3.05 (hept, 2H, $CH(CH_3)_2$ $^3J_{H\text{-}H}$ = 6.7 Hz), 1.62 (s, 6H, $NCCH_3$), 1.50 (d, 6H, $CH(CH_3)_2$, $^3J_{H\text{-}H}$ = 6.8 Hz),), 1.16 (d, 6H, $CH(CH_3)_2$, $^3J_{H\text{-}H}$ = 6.8 Hz), 1.05 (d, 6H, $CH(CH_3)_2$, $^3J_{H\text{-}H}$ = 6.7 Hz), 0.52 (d, 6H, $CH(CH_3)_2$, $^3J_{H\text{-}H}$ = 6.7 Hz), 0.04 (s, 9H, $Si(CH_3)_3$), -0.58 (s, 1H, NH).

^{13}C{1H} NMR (101 MHz, C_6D_6) δ 169.4 (N*C*CH_3), 145.0, 143.6, 141.6, 127.1, 124.7, 124.0 (C_6H_3), 179.5, 149.5, 132.9, 132.2, 121.8 (C_5H_4N), 96.6 (CH), 29.0, 28.1 (*C*H$(CH_3)_2$), 25.0, 24.7, 24.5, 24.4 (CH(*C*$H_3)_2$), 23.9 (NC*C*H_3), 3.6 (Si$(CH_3)_3$).

Elemental analysis: Calculated for tol* $C_{37}H_{55}GaN_4Si$: C, 70.86; H, 8.51; N, 7.51. Found: C, 70.57; H, 9.04; N, 7.07.

Preparation of NacNacGa(OC(=CH$(CH_2)_4$ –)(NHSiMe_3) (III-16)

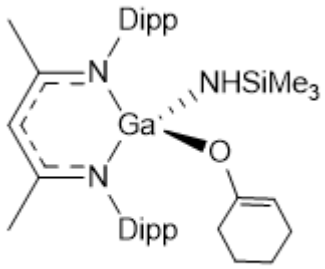

III-16

To a solution of NacNacGa (0.078 g, 0.16 mmol) in toluene was added cyclohexanone (0.017 mL, 0.16 mmol) and the mixture was treated with N_3SiMe_3 (0.021 mL, 0.16 mmol). The reaction was allowed to stir for 10 min at room temperature. Volatiles were removed and NacNacGa(OC(=CH$(CH_2)_4$ –)(NHSiMe_3) was obtained as a white powder in quantitative yield. Colorless crystals of **3** obtained from toluene solution at -30^{0}C.

1H NMR (400 MHz, C6D6) δ 7.17-7.01 (m, 6H, C_6H_3), 4.87 (s, 1H, CH), 4.53 (m, 1H, OC_6H_9), 3.56 (hept, 2H, C*H*$(CH_3)_2$ $^3J_{H\text{-}H}$ = 6.8 Hz), 3.18 (hept, 2H, C*H*$(CH_3)_2$ $^3J_{H\text{-}H}$ = 6.9 Hz), 2.32 (m, 4H, OC_6H_9), 1.81 (m, 2H, OC_6H_9), 1.71 (m, 2H, OC_6H_9), 1.49 (s, 6H, NCCH_3), 1.44 (d, 6H, CH(C*H*$_3)_2$, $^3J_{H\text{-}H}$ = 6.8 Hz), 1.37 (d, 6H, CH(C*H*$_3)_2$, $^3J_{H\text{-}H}$ = 6.9 Hz), 1.25 (d, 6H, CH(C*H*$_3)_2$, $^3J_{H\text{-}H}$ = 6.8 Hz), 1.08 (d, 6H, CH(C*H*$_3)_2$, $^3J_{H\text{-}H}$ = 6.9 Hz), -0.10 (s, 9H, Si$(CH_3)_3$), -0.89 (s, 1H, NH).

^{13}C{^{1}H} NMR (101 MHz, C6D6) δ 169.7 (N*C*CH_3), 155.5 (O*C*(=CH)$(CH_2)_4$), 145.6, 143.3, 140.8, 127.6, 124.9, 123.9, 96.7 (CH), 96.3 (OC(=*C*H)$(CH_2)_4$), 29.0, 28.4

(*C*H(CH$_3$)$_2$), 31.6, 25.63, 24.8, 24.1 (CH$_2$), 25.6, 24.9, 24.8, 24.6 (CH(*C*H$_3$)$_2$), 23.7 (NC*C*H$_3$), 2.9 (Si(CH$_3$)$_3$).

Elemental analysis: Calculated for 0.5 tol* $C_{38}H_{60}GaN_3OSi$: C, 69.35; H, 8.97; N, 5.85. Found: C, 69.16; H, 9.09; N, 5.62.

Preparation of NacNacGa(CH$_2$CO$_2$CH$_2$CH$_3$)(NHSiMe$_3$) (III-17)

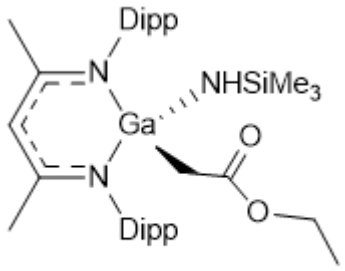

III-17

To a solution of NacNacGa (0.078 g, 0.16 mmol) in toluene was added ethyl acetate (0.016 mL, 0.16 mmol) and the mixture was treated with N_3SiMe_3 (0.021 mL, 0.16 mmol). The reaction was allowed to stir for 10 min at room temperature. Volatiles were removed and NacNacGa(CH$_2$S(=O)Me)(NHSiMe$_3$) was obtained as a white powder in quantitative yield. Colorless crystals of **4** were obtained from toluene solution at -30^{0}C.

^{1}H NMR (400 MHz, C6D6) δ 7.19-7.08 (m, 6H, C$_6$H$_3$), 4.72 (s, 1H, CH), 4.01 (q, 2H, O*C*H$_2$CH$_3$, $^3J_{H\text{-}H}$ = 7.14 Hz), 3.96 (hept, 2H, C*H*(CH$_3$)$_2$ $^3J_{H\text{-}H}$ = 6.7 Hz), 3.45 (hept, 2H, C*H*(CH$_3$)$_2$ $^3J_{H\text{-}H}$ = 6.8 Hz), 1.90 (s, 2H, CH$_2$), 1.56 (s, 6H, NCCH$_3$), 1.47 (d, 6H, CH(C*H*$_3$)$_2$, $^3J_{H\text{-}H}$ = 6.7 Hz), 1.37 (d, 6H, CH(C*H*$_3$)$_2$, $^3J_{H\text{-}H}$ = 6.8 Hz), 1.33 (d, 6H, CH(C*H*$_3$)$_2$, $^3J_{H\text{-}H}$ = 6.7 Hz), 1.12 (d, 6H, CH(C*H*$_3$)$_2$, $^3J_{H\text{-}H}$ = 6.8 Hz), 1.07 (t, 3H, OCH$_2$C*H*$_3$, $^3J_{H\text{-}H}$ = 7.14 Hz), -0.20 (s, 9H, Si(CH$_3$)$_3$), -0.59 (s, 1H, NH).

^{13}C{^{1}H} NMR (101 MHz, C6D6) δ 175.2 (CO), 170.2 (N*C*CH$_3$), 145.7, 144.0, 141.1, 127.3, 125.2, 124.3 (C$_6$H$_3$), 97.6 (CH), 59.4 (O*C*H$_2$CH$_3$), 28.7, 26.9 (*C*H(CH$_3$)$_2$), 26.1,

25.12, 25.06, 24.9 (CH(CH_3)$_2$), 23.9 (NCCH_3), 20.9 (CH_2), 14.8 (OCH_2CH_3), 3.2 (Si(CH_3)$_3$).

Elemental analysis: Calculated for $C_{36}H_{58}GaN_3O_2Si$*0.6Et2O: C, 65.22; H, 9.12; N 5.94. Found: C, 65.45; H, 9.65, N, 6.37.

Preparation of NacNacGa(CH_2S(=O)Me)(NHSiMe_3) (III-18)

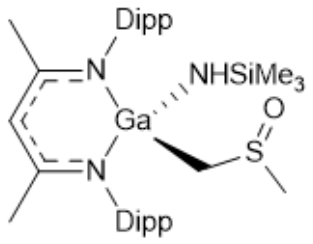

III-18

To a solution of NacNacGa (0.071 g, 0.15 mmol) in toluene was added DMSO (0.010 mL, 0.15 mmol) and the mixture was treated with N_3SiMe_3 (0.019 mL, 0.15 mmol). The reaction was allowed to stir for 10 min at room temperature. Volatiles were removed and NacNacGa(CH_2S(=O)Me)(NHSiMe_3) was obtained as a white powder in quantitative yield.

^{1}H NMR (400 MHz, C6D6) δ 7.19-7.05 (m, 6H, C_6H_3), 4.91 (s, 1H, CH), 4.10 (hept, 1H, C*H*(CH_3)$_2$ $^3J_{H\text{-}H}$ = 6.8 Hz), 3.55 (m, 2H, C*H*(CH_3)$_2$), 3.39 (hept, 1H, C*H*(CH_3)$_2$ $^3J_{H\text{-}H}$ = 6.8 Hz), 2.28 (d, 1H, SCH_2, $^2J_{H\text{-}H}$ = 12.8 Hz), 2.12 (s, 3H, SCH_3), 1.81 (d, 1H, SCH_2, $^2J_{H\text{-}H}$ = 12.8 Hz), 1.62 (s, 3H, NCCH_3), 1.54 (s, 3H, NCCH_3), 1.44 (d, 3H, CH(C*H*$_3$)$_2$, $^3J_{H\text{-}H}$ = 6.9 Hz), 1.42 (d, 6H, CH(C*H*$_3$)$_2$, $^3J_{H\text{-}H}$ = 6.8 Hz), 1.36 (d, 6H, CH(C*H*$_3$)$_2$, $^3J_{H\text{-}H}$ = 6.8 Hz), 1.18 (d, 6H, CH(C*H*$_3$)$_2$, $^3J_{H\text{-}H}$ = 6.8 Hz), 1.13(d, 3H, CH(C*H*$_3$)$_2$, $^3J_{H\text{-}H}$ = 6.9 Hz), 1.12 (d, 3H, CH(C*H*$_3$)$_2$, $^3J_{H\text{-}H}$ = 6.9 Hz), -0.13 (s, 9H, Si(CH_3)$_3$), -0.27 (s, 1H, NH).

^{13}C{^{1}H} NMR (101 MHz, C_6D_6) δ 170.8, 168.6 (N*C*CH_3), 145.3, 144.2, 144.0, 143.8, 140.9, 140.8, 126.94, 126.87, 124.7, 124.3, 123.9 (C_6H_3), 98.2 (CH), 45.3 (SCH_3), 41.1

(SCH_2), 28.4, 28.3, 27.1, 26.5 ($CH(CH_3)_2$), 26.0, 25.3, 24.8, 24.7, 24.6, 24.4, 23.9, 23.4 ($NCCH_3$), 3.1 ($Si(CH_3)_3$).

Elemental analysis: Calculated for $C_{34}H_{56}GaN_3OSSi$: C, 62.57; H, 8.65; N, 6.44. Found: C, 62.51; H, 8.75; N, 6.10.

Preparation of NacNacGa(CH(Me)P(=O)Et$_2$)(NHSiMe$_3$) (III-19)

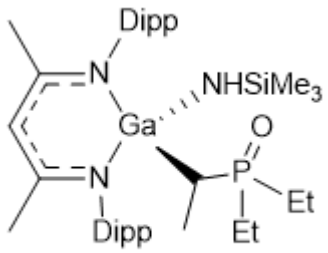

III-19

To a solution of NacNacGa (0.064 g, 0.13 mmol) in toluene was added $Et_3P{=}O$ (0.018 g, 0.13 mmol) and the mixture was treated with N_3SiMe_3 (0.017 mL, 0.13 mmol). The reaction was allowed to stir for 10 min at room temperature. The reaction mixture was concentrated and crystallized at -30^{0}C. Colorless crystals of NacNacGa(CH(Me)P(=O)Et$_2$)(NHSiMe$_3$) was obtained (0.066 g, 0.09 mmol, 72%).

^{1}H {^{31}P} NMR (400 MHz, C6D6) δ 7.21-7.03 (m, 6H, C_6H_3), 4.94 (s, 1H, CH), 4.03 (hept, 1H, C*H*$(CH_3)_2$ $^3J_{H\text{-}H}$ = 6.7 Hz), 3.96 (hept, 1H, C*H*$(CH_3)_2$ $^3J_{H\text{-}H}$ = 6.7 Hz), 3.29 (hept, 1H, C*H*$(CH_3)_2$ $^3J_{H\text{-}H}$ = 6.7 Hz), 3.24 (hept, 1H, C*H*$(CH_3)_2$ $^3J_{H\text{-}H}$ = 6.7 Hz), 2.20 (s, 1H, NH), 1.65 (s, 3H, $NCCH_3$), 1.64 (d, 3H, $CH(CH_3)_2$, $^3J_{H\text{-}H}$ = 6.7 Hz),1.62 (s, 3H, $NCCH_3$), 1.61 (d, 3H, $CH(CH_3)_2$, $^3J_{H\text{-}H}$ = 6.7 Hz), 1.28 (m, 12H, $CH(CH_3)_2$), 1.12 (d, 3H, $CH(CH_3)_2$, $^3J_{H\text{-}H}$ = 6.7 Hz), 1.07 (d, 3H, $CH(CH_3)_2$, $^3J_{H\text{-}H}$ = 6.7 Hz), 1.03 (m, 1H, PCH_2CH_3), 1.01 (q, 1H, $PCHCH_3$, $^3J_{H\text{-}H}$ = 7.6 Hz), 0.86 (m, 1H, PCH_2CH_3), 0.78 (t, 3H, PCH_2CH_3, $^3J_{H\text{-}H}$ = 7.2 Hz), 0.75 (t, 3H, PCH_2CH_3, $^3J_{H\text{-}H}$ = 7.3 Hz), 0.69 (m, 1H, PCH_2CH_3), 0.56 (m, 1H, PCH_2CH_3), 0.51 (d, 3H, $PCHCH_3$, $^3J_{H\text{-}H}$ = 7.6 Hz), 0.40 (s, 9H, $Si(CH_3)_3$).

$^{13}C\{^{1}H\}$ NMR (101 MHz, C6D6) δ 169.6, 169.4 (N*C*CH_3), 146.4, 146.2, 143.3, 143.2, 143.0, 142.1, 127.04, 127.0125.9, 125.7, 124.2, 124.0 (C_6H_3), 98.7 (CH), 28.9, 28.7, 27.8, 27.7 (*C*H$(CH_3)_2$), 26.4, 25.9, 25.8, 25.31, 25.29, 25.0, 24.9, 24.4 (CH(*C*$H_3)_2$), 24.33, 24.29 (NC*C*H_3), 18.4 (P*C*H_2CH_3), 16.7 (P*C*HCH_3), 19.7, 10.7 (PCH*C*H_3), 19.1, 19.0, 5.8 (PCH_2*C*H_3), 4.3 (Si$(CH_3)_3$).

$^{31}P\{^{1}H\}$ NMR (162 MHz, C_6D_6) δ 52.86 ppm.

Elemental analysis: Calculated for $C_{38}H_{65}GaN_3OPSi$: C, 64.40; H, 9.24, N, 5.93. Found: C, 64.87; H, 9.76; N, 5.97.

Section III.4

Preparation of NacNacGa(CH_2SiMe_3)(NNC$SiMe_3$) (III-20)

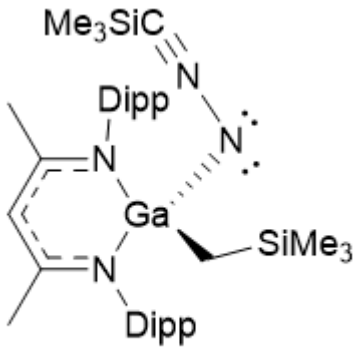

III-20

NacNacGa (0.082 g, 0.17 mmol) was treated with two equivalents of a trimethylsilyl diazomethane (0.6M solution in hexane, 0.561 mL, 0.34 mmol) in toluene. The reaction mixture was stirred for 20 min at room temperature. The color of the solution was bright yellow. Volatiles were removed under reduced pressure and the residue was recrystallized from toluene at -35°C. After several days light yellow crystals of NacNacGa(CH_2SiMe_3)(NNC$SiMe_3$) (0.072 g, 0.11 mmol, 62%) were obtained.

^{1}H NMR (600 MHz, C_6D_6) δ 7.22 (m, 2H, C_6H_3),7.16 (m, 2H, C_6H_3), 7.08 (m, 2H, C_6H_3), 4.73 (s, 1H, CH), 3.71 (hept, 2H, C*H*$(CH_3)_2$ $^3J_{H\text{-}H}$ = 6.7 Hz), 3.29 (hept, 2H, C*H*$(CH_3)_2$ $^3J_{H\text{-}H}$ = 6.8 Hz), 1.73 (d, 6H, CH(C*H*$_3)_2$, $^3J_{H\text{-}H}$ = 6.8 Hz), 1.69 (s, 6H, NCCH_3), 1.40 (d, 6H,

$CH(CH_3)_2$, $^3J_{H\text{-}H}$ = 6.7 Hz), 1.34 (d, 6H, $CH(CH_3)_2$, $^3J_{H\text{-}H}$ = 6.7 Hz), 1.09 (d, 6H, $CH(CH_3)_2$, $^3J_{H\text{-}H}$ = 6.8 Hz), 0.22 (s, 9H, $Si(CH_3)_3$), -0.21 (s, 9H, $Si(CH_3)_3$), -0.81 (s, 2H, $CH_2Si(CH_3)_3$).

$^{13}C\{^1H\}$ NMR (151 MHz, C_6D_6) δ 169.2 ($NCCH_3$),145.7, 142.9, 141.3, 127.5, 125.3, 123.9 (C_6H_3), 97.0 (CH), 29.1, 27.7 ($CH(CH_3)_2$), 25.3 25.1, 25.0, 23.8 ($CH(CH_3)_2$), 23.3 ($NCCH_3$), 1.1 ($Si(CH_3)_3$), -0.6 ($Si(CH_3)_3$), -6.7 ($CH_2Si(CH_3)_3$).

$SiMe_3$ at 0.22 ppm in ^{1}H NMR shows correlation with signal at 44.0 ppm in HMBC. Longer scans did not show signal of quaternary carbon in ^{13}C NMR.

Elemental Analysis: Calculated for 0.4 tol*C37H61GaN4Si2: C, 65.94; H, 8.93; N, 7.74. Found C, 66.55; H, 8.88; N, 8.13.

Preparation of NacNacGa(NHNCHSiMe$_3$)(C(N$_2$)(SiMe$_3$)) (III-24)

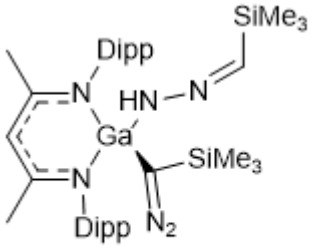

III-24

A mixture of NacNacGa (0.084 g, 0.17 mmol) with pyridine in toluene was treated with two equivalents of trimethylsilyl diazomethane (0.6M solution in hexane, 0.57 mL, 0.34 mmol). The reaction mixture was stirred for one hour at room temperature during which color of the solution turned orange. Volatiles were removed under reduced pressure and the residue was recrystallized in toluene at -35°C. Crystals of NacNacGa(NHNCHSiMe$_3$)(C(N$_2$)(SiMe$_3$)) (0.070g, 0.10 mmol, 57%) were obtained after two days. They were of poor quality and crystal structure was not recorded.

^{1}H NMR (400 MHz, C6D6) δ 7.17-7.17 (m, 6H, C_6H_3) 6.64 (s, 1H, $NCHSiMe_3$), 6.23 (s, 1H, NH), 4.82 (s, 1H, CH), 3.47 (hept, 2H, $CH(CH_3)_2$ $^3J_{H\text{-}H}$ = 6.8 Hz), 3.33 (hept, 2H,

C*H*(CH_3)$_2$ $^3J_{H\text{-}H}$ = 6.8 Hz), 1.61 (d, 6H, CH(C*H*$_3$)$_2$, $^3J_{H\text{-}H}$ = 6.7 Hz), 1.56 (s, 6H, NCCH_3), 1.31 (d, 6H, CH(C*H*$_3$)$_2$, $^3J_{H\text{-}H}$ = 6.8 Hz),), 1.25 (d, 6H, CH(C*H*$_3$)$_2$, $^3J_{H\text{-}H}$ = 6.8 Hz),), 1.17 (d, 6H, CH(C*H*$_3$)$_2$, $^3J_{H\text{-}H}$ = 6.8 Hz),), 0.28 (s, 9H, Si(CH_3)$_3$), -0.11 (s, 9H, Si(CH_3)$_3$).

^{13}C{^{1}H} NMR (101 MHz, C6D6) δ 169.9 (N*C*CH_3), 138.6 (N*C*HSiMe$_3$), 144.9, 144.6, 140.3, 124.8, 124.4 (C_6H_3), 96.0 (CH), 29.2, 26.9 (*C*H(CH_3)$_2$), 25.0, 24.9, 24.7, 24.6 (CH(*C*H_3)$_2$), 23.1 (NC*C*H_3), 0.2 (Si(CH_3)$_3$), -1.1 (Si(CH_3)$_3$).

SiMe$_3$ at -0.11 ppm in ^{1}H NMR shows correlation with signal at 41.9 ppm in HMBC. Longer scans did not show signal of quaternary carbon in ^{13}C NMR.

Preparation of NacNacGa(NHNCHSiMe$_3$)(N(NC)(SiMe$_3$)) (III-25)

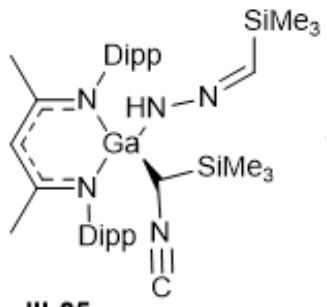

III-25

To grow X-ray quality crystals of NacNacGa(NHNCHSiMe$_3$)(CN_2SiMe$_3$) a concentrated solution in toluene was stored at room temperature to allow for slow evaporation. Color change from orange to yellow was observed. After one week, yellow crystals of the rearranged product NacNacGa(NHNCHSiMe$_3$)(N(NC)(SiMe$_3$)) (0.052 g, 0.073 mmol) were obtained.

^{1}H NMR (400 MHz, C6D6) δ 7.14-7.17 (m, 4H, C_6H_3) 7.07 (m, 2H, C_6H_3), 6.48 (s, 1H, NCHSiMe$_3$), 5.57 (s, 1H, NH), 4.85 (s, 1H, CH), 3.69 (hept, 2H, C*H*(CH_3)$_2$ $^3J_{H\text{-}H}$ = 6.8 Hz), 3.30 (hept, 2H, C*H*(CH_3)$_2$ $^3J_{H\text{-}H}$ = 6.8 Hz), 1.61 (d, 6H, CH(C*H*$_3$)$_2$, $^3J_{H\text{-}H}$ = 6.7 Hz), 1.59 (s, 6H, NCCH_3), 1.31 (d, 6H, CH(C*H*$_3$)$_2$, $^3J_{H\text{-}H}$ = 6.8 Hz), 1.27 (d, 6H, CH(C*H*$_3$)$_2$, $^3J_{H\text{-}H}$ = 6.7 Hz), 1.08 (d, 6H, CH(C*H*$_3$)$_2$, $^3J_{H\text{-}H}$ = 6.8 Hz), 0.07 (s, 9H, Si(CH_3)$_3$), 0.06 (s, 9H, Si(CH_3)$_3$).

^{13}C NMR (101 MHz, C6D6) δ 171.7 (N*C*CH$_3$), 140.6 (N*C*HSiMe$_3$), 145.1, 143.9, 140.73, 124.9, 124.5 (C$_6$H$_3$), 98.0 (CH), 28.4, 28.4 (*C*H(CH$_3$)$_2$), 25.2, 25.2, 25.0, 24.1 (CH(*C*H$_3$)$_2$), 23.9 (NC*C*H$_3$), 0.2 (Si(CH$_3$)$_3$), -1.3 (Si(CH$_3$)$_3$).

Elemental Analysis: Calculated for $C_{37}H_{61}GaN_6Si_2$ C, 62.08; H, 8.59; N, 11.74. Found: C, 62.43; H, 8.63; N, 11.37.

Preparation of NacNacGa(CH$_2$SiMe$_3$)(NBcatNHCSiMe$_3$) (III-26)

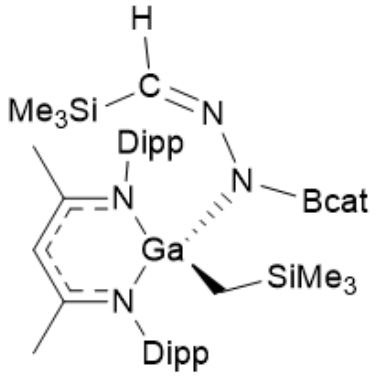

III-26

A solution of NacNacGa (0.064 g, 0.13 mmol) in toluene was treated with two equivalents of trimethylsilyl diazomethane (0.6M in hexane, 0.44 mL, 0.26 mmol). After stirring the mixture for 20 min at room temperature, one equivalent of catecholborane (0.014 mL, 0.13 mmol) was added. The color of the solution changed from yellow to colorless. Volatiles were removed and the residue was recrystallized from toluene at -35°C to afford colorless crystals of NacNacGa(CH$_2$SiMe$_3$)(NBcatNHCSiMe$_3$) (0.077 g, 0.10 mmol, 73%).

^{1}H NMR (400 MHz, C$_6$D$_6$) δ 8.60 (s, 1H, NC*H*Si(CH$_3$)$_3$), 7.10 (m, 6H, C$_6$H$_3$), 7.01 (m, 2H, C$_6$H$_4$O$_2$), 6.70 (m, 2H, C$_6$H$_4$O$_2$B), 4.94 (s, 1H, CH), 3.64 (hept, 2H, C*H*(CH$_3$)$_2$ $^3J_{H\text{-}H}$ = 6.7 Hz), 3.36 (hept, 2H, C*H*(CH$_3$)$_2$ $^3J_{H\text{-}H}$ = 6.8 Hz), 1.64 (s, 6H, NCCH$_3$), 1.46 (d, 6H, CH(C*H*$_3$)$_2$, $^3J_{H\text{-}H}$ = 6.8 Hz), 1.19 (d, 6H, CH(C*H*$_3$)$_2$, $^3J_{H\text{-}H}$ = 6.7 Hz), 1.17 (d, 6H, CH(C*H*$_3$)$_2$, $^3J_{H\text{-}H}$ = 6.7 Hz), 1.13 (d, 6H, CH(C*H*$_3$)$_2$, $^3J_{H\text{-}H}$ = 6.8 Hz), 0.33 (s, 9H, Si(CH$_3$)$_3$), -0.10 (s, 9H, Si(CH$_3$)$_3$), -0.37 (s, 2H, C*H*$_2$Si(CH$_3$)$_3$).

$^{13}C\{^{1}H\}$ NMR (101 MHz, C_6D_6) δ 169.2 (N*C*CH_3), 164.5 (N*C*H$Si(CH_3)_3$), 145.7, 143.3, 142.4, 127.4, 125.2, 124.2 (C_6H_3), 148.9, 121.8, 111.8 ($C_6H_4O_2B$), 99.0 (CH), 29.1, 26.8 (*C*H$(CH_3)_2$), 25.4, 25.2, 24.5 (CH(*C*$H_3)_2$), 24.1 (NC*C*H_3), 3.0 ($Si(CH_3)_3$), -1.7 ($Si(CH_3)_3$), -5.8 (*C*$H_2Si(CH_3)_3$).

^{11}B NMR (128 MHz, C_6D_6) δ 25.4.

Elemental analysis: Calculated for $C_{43}H_{66}BGaN_4O_2Si_2$: C, 63.94; H, 8.24; N, 6.94. Found: C, 64.23; H, 8.38; N, 6.75.

Preparation of NacNacGa(CH_2SiMe_3)($NSiH_2PhNHCSiMe_3$) (III-27)

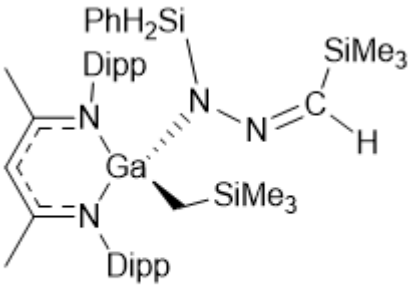

III-27

A solution of NacNacGa (0.092 g, 0.19 mmol) in toluene was treated with two equivalents of trimethylsilyl diazomethane (0.6M in hexane, 0.63 mL, 0.38 mmol). After stirring the mixture for 20 min at room temperature, one equivalent of phenylsilane (0.036 mL, 0.19 mmol) was added. Volatiles were removed and the residue was recrystallized from toluene at -35°C to afford yellow crystals of two isomers of NacNacGa(CH_2SiMe_3)($NSiH_2PhNHCSiMe_3$) (0.084 g, 0.11 mmol, 56%).

^{1}H NMR (400 MHz, C6D6) δ 8.10 and 7.80 (s, 1H, NC*H*$Si(CH_3)_3$), 7.97 – 7.86 (m, 2H, C_6H_5), 7.29-7.20 (m, 3H, C_6H_5), 7.10 (m, 6H, C_6H_3), 5.44 and 5.35 (s, 2H, SiH_2Ph), 5.06 and 5.03 (s, 1H, CH), 3.55 – 3.29 (m, 4H, C*H*$(CH_3)_2$), 1.63 and 1.58 (s, 6H, $NCCH_3$), 1.43

– 0.96 (m, 24H, CH(C*H*$_3$)$_2$), 0.31 and 0.27 (s, 9H, Si(CH$_3$)$_3$), -0.13 and -0.17 (s, 9H, Si(CH$_3$)$_3$), -0.45 and -0.57 (s, 2H, C*H*$_2$Si(CH$_3$)$_3$).

^{13}C NMR (101 MHz, C6D6) δ 169.40, 168.90 (NC*C*H$_3$), 151.16, 148.64 (NC*H*Si(CH$_3$)$_3$), 137.34, 136.96, 136.35, 136.30, 129.71, 129.52 (C$_6$H$_5$),145.70, 145.52, 143.47, 143.37, 142.90, 142.23, 127.35, 127.27, 125.28, 125.13, 124.27, 124.22 (C$_6$H$_3$), 99.18, 98.77 (CH), 29.21, 28.96, 28.92, 27.47 (*C*H(CH$_3$)$_2$), 25.94, 25.88, 25.49, 25.17, 25.07, 24.96, 24.83, 24.73 (CH(*C*H$_3$)$_2$), 24.42, 24.31 (NC*C*H$_3$), 3.17, 2.38, -0.83, -1.27 (Si(CH$_3$)$_3$), -4.67, -5.30 (*C*H$_2$Si(CH$_3$)$_3$).

Elemental analysis: Calculated for C$_{43}$H$_{69}$GaN$_4$Si$_3$: C, 64.88; H, 8.74; N, 7.04. Found: C, 64.78; H, 9.02; N, 6.84.

Preparation of NacNacGa(CH$_2$SiMe$_3$)(N(Bcat)$_2$) (III-28)

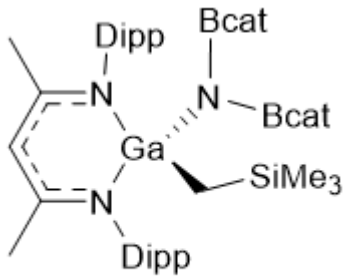

III-28

A solution of NacNacGa (0.064 g, 0.13 mmol) in toluene was treated with two equivalents of trimethylsilyl diazomethane (0.6M in hexane, 0.63 mL, 0.38 mmol). After stirring the mixture for 20 min at room temperature, one equivalent of bis(catecholato)diboron (0.036 mL, 0.19 mmol) was added. Volatiles were removed and the residue was recrystallized from toluene at -35°C to afford colorless crystals of NacNacGa(CH$_2$SiMe$_3$)(N(Bcat)$_2$) (0.071 g, 0.09 mmol, 65%).

^{1}H NMR (400 MHz, C$_6$D$_6$) δ 7.09 (m, 6H, C$_6$H$_3$), 7.07 (m, 2H, C$_6$H$_4$O$_2$B), 7.02 (m, 6H, C$_6$H$_3$), 6.91 (m, 2H, C$_6$H$_4$O$_2$B), 6.82 (m, 2H, C$_6$H$_4$O$_2$B), 6.67 (m, 2H, C$_6$H$_4$O$_2$B), 5.07 (s,

1H, CH), 3.61 (hept, 2H, C*H*(CH_3)$_2$ $^3J_{H-H}$ = 6.7 Hz), 3.37 (hept, 2H, C*H*(CH_3)$_2$ $^3J_{H-H}$ = 6.7 Hz), 1.62 (s, 6H, NCCH_3), 1.46 (d, 6H, CH(C*H*$_3$)$_2$, $^3J_{H-H}$ = 6.7 Hz), 1.21 (d, 6H, CH(C*H*$_3$)$_2$, $^3J_{H-H}$ = 6.7 Hz), 1.13 (d, 6H, CH(C*H*$_3$)$_2$, $^3J_{H-H}$ = 6.7 Hz), 0.95 (d, 6H, CH(C*H*$_3$)$_2$, $^3J_{H-H}$ = 6.7 Hz), -0.17 (s, 2H, C*H*$_2$Si(CH_3)$_3$), -0.23 (s, 9H, Si(CH_3)$_3$).

^{13}C{^{1}H} 8NMR (101 MHz, C_6D_6) δ 169.9 (N*C*CH_3), 145.8, 143.5, 142.2, 127.6, 125.1, 124.4 (C_6H_3), 149.7, 149.1, 122.1, 122.0, 112.1, 111.7 ($C_6H_4O_2B$), 98.6 (CH), 29.1, 27.9 (*C*H(CH_3)$_2$), 25.3, 24.9, 24.8, 24.4 (CH(*C*H_3)$_2$), 24.4 (NC*C*H_3), 2.7 (Si(CH_3)$_3$), -4.4 (*C*H_2Si(CH_3)$_3$).

^{11}B NMR (128 MHz, C_6D_6) δ 30.4.

Elemental analysis: Calculated for $C_{45}H_{60}B_2GaN_3O_4Si$: C, 65.40; H, 7.32; N, 5.08. Found: 65.38; H, 7.66; N, 4.99.

VI. Appendix

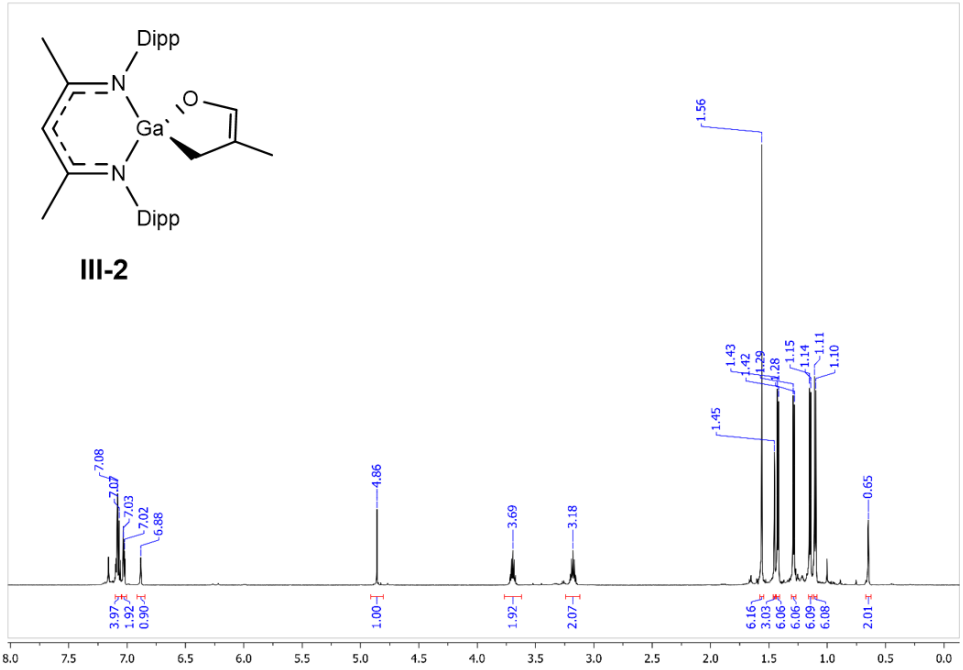

Figure 18. ^{1}H NMR (600 MHz, C_6D_6) spectrum of **III-2**.

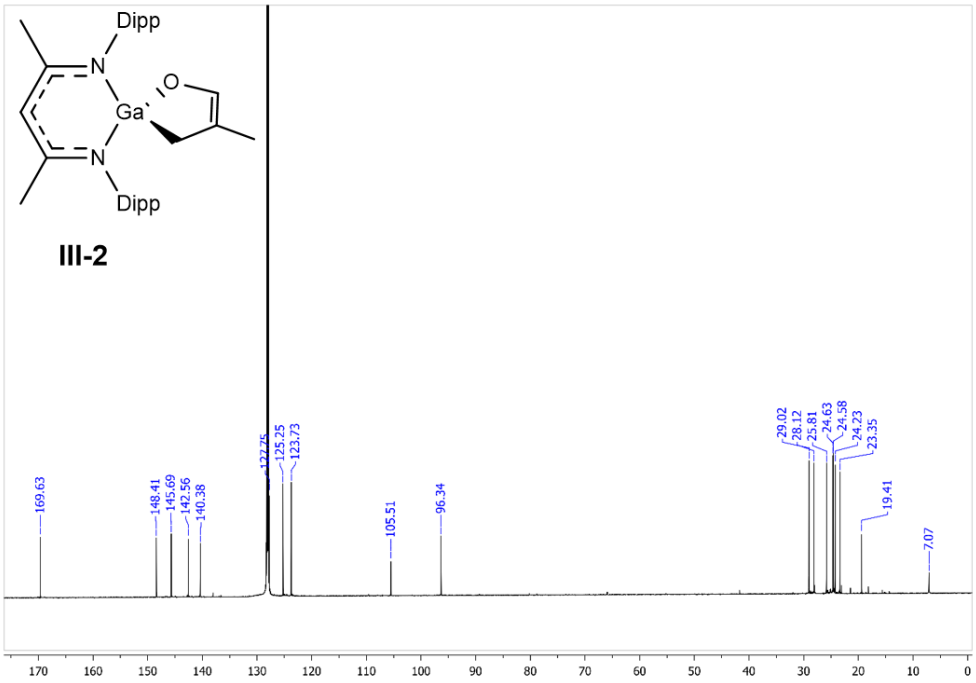

Figure 19. $^{13}C\{^{1}H\}$ NMR (151 MHz, C_6D_6) spectrum of **III-2**.

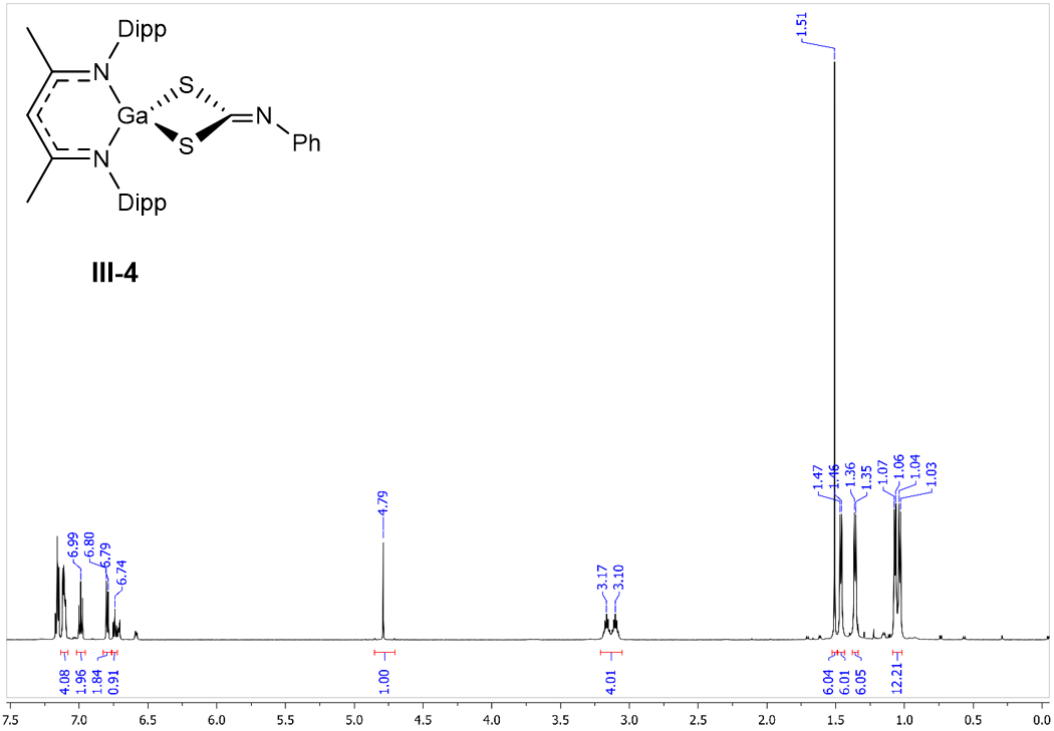

Figure 20. ^{1}H NMR (600 MHz, C_6D_6) spectrum of **III-4**.

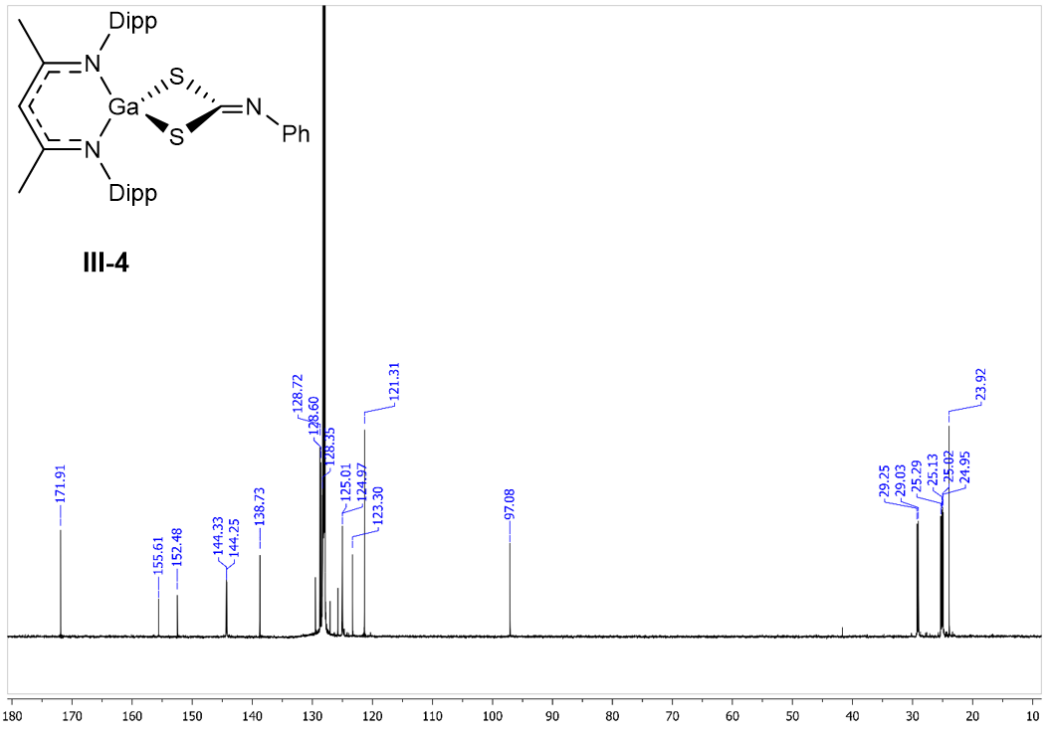

Figure 21. $^{13}C\{^{1}H\}$ NMR (151 MHz, C_6D_6) spectrum of **III-4**.

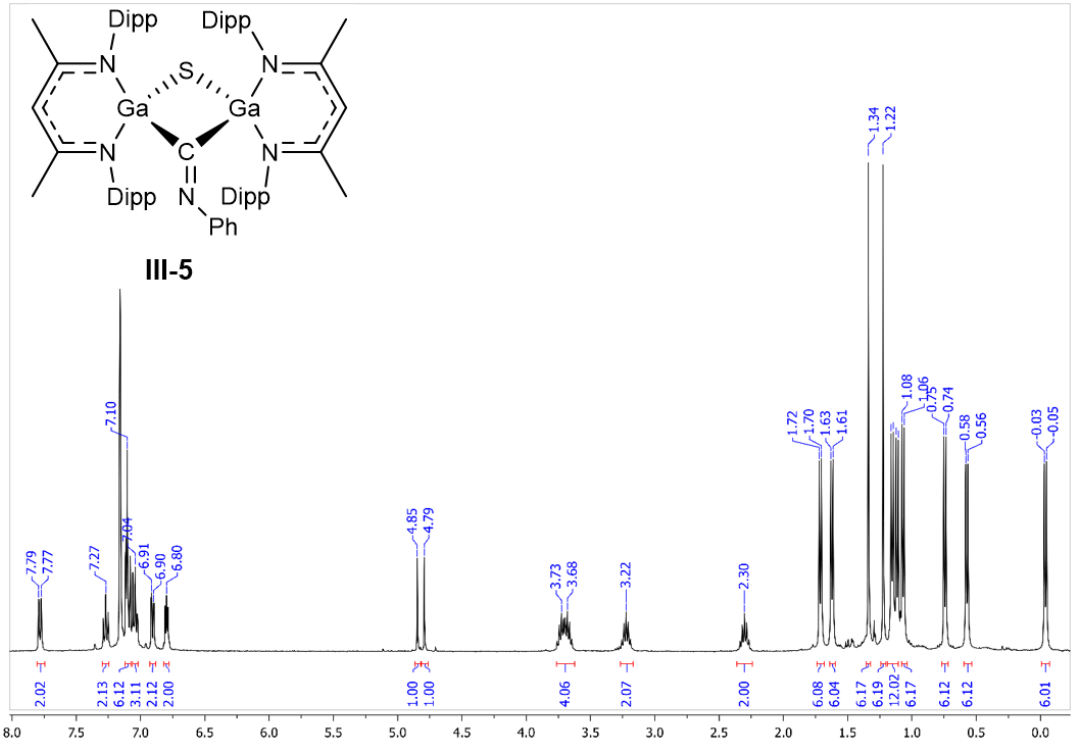

Figure 22. ^{1}H NMR (400 MHz, C_6D_6) spectrum of **III-5**.

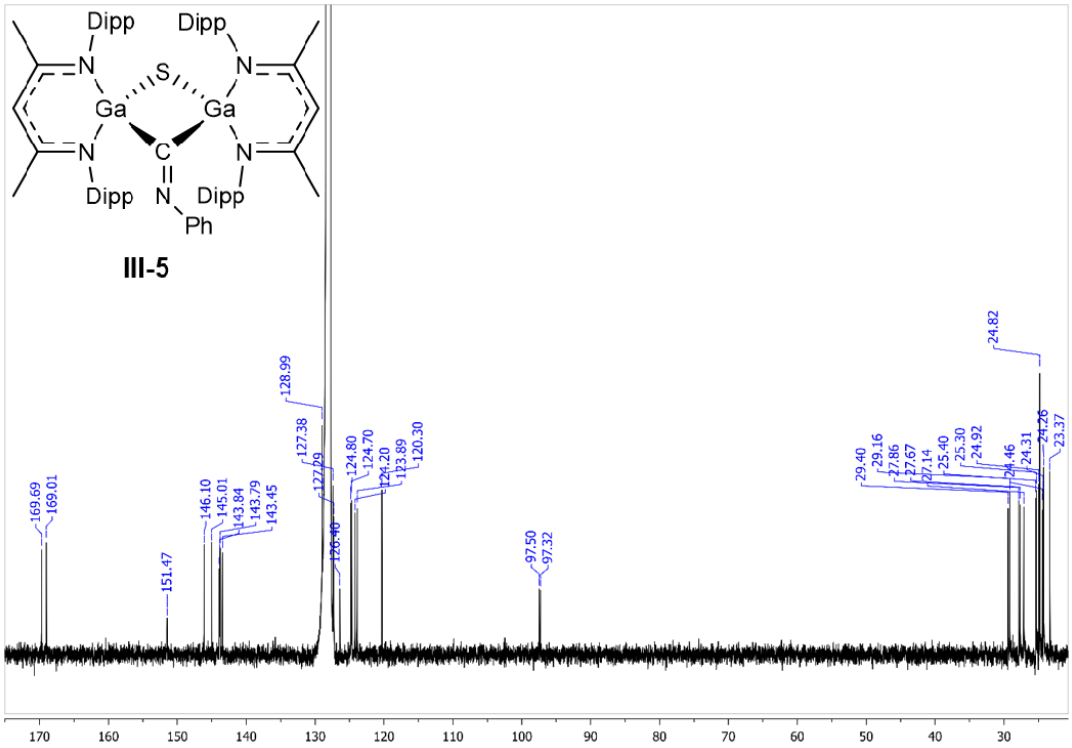

Figure 23. $^{13}C\{^{1}H\}$ NMR (101 MHz, C_6D_6) spectrum of **III-5**.

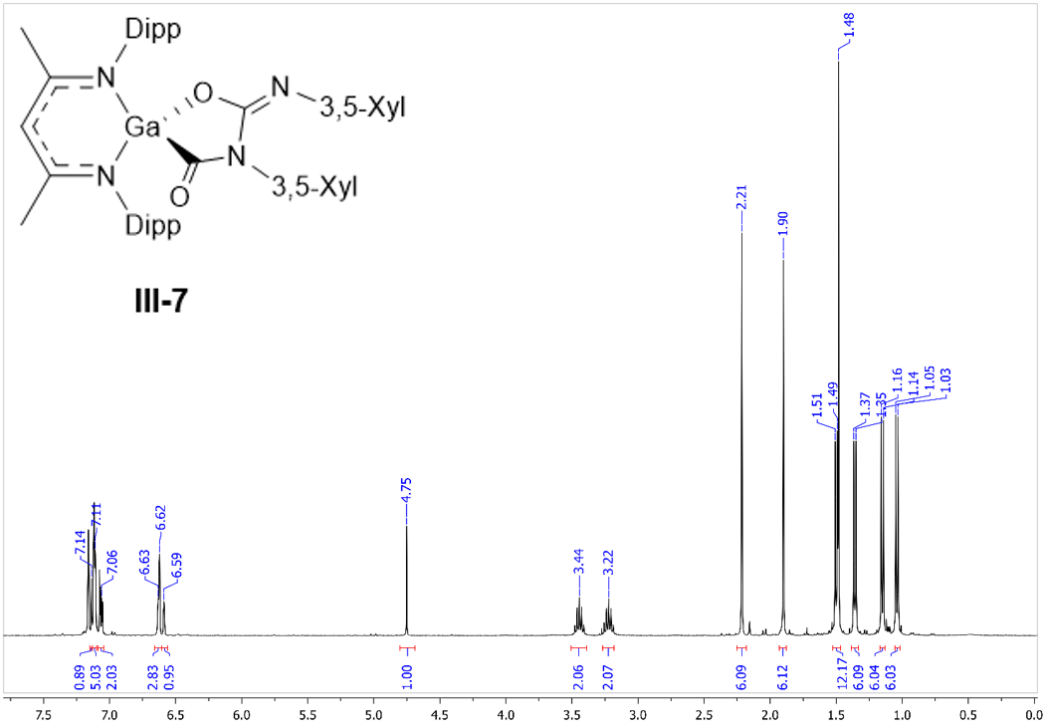

Figure 24. ^{1}H NMR (400 MHz, C_6D_6) spectrum of **III-7**.

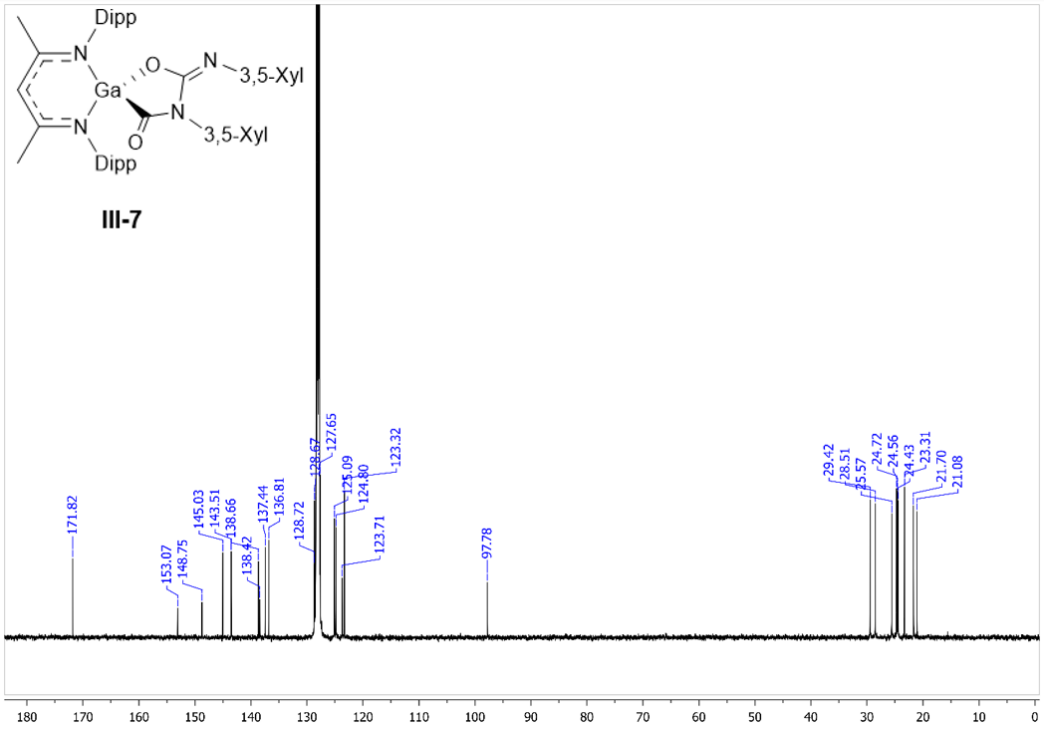

Figure 25. $^{13}C\{^{1}H\}$ NMR (101 MHz, C_6D_6) spectrum of **III-7**.

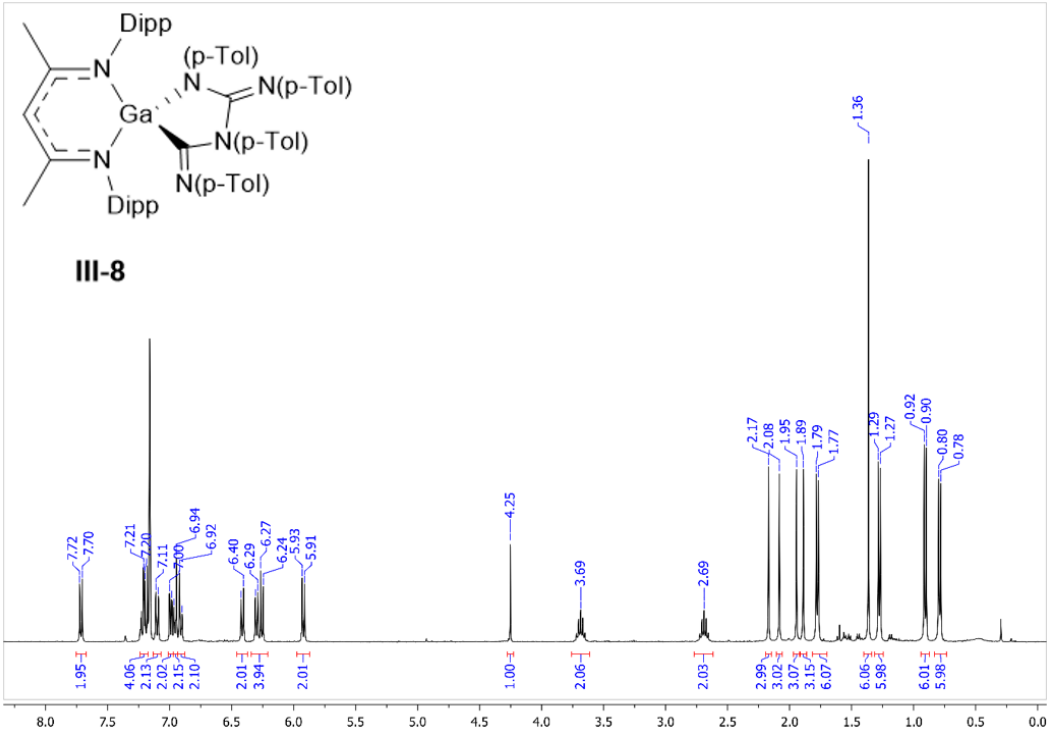

Figure 26. ^{1}H NMR (400 MHz, C_6D_6) spectrum of **III-8**.

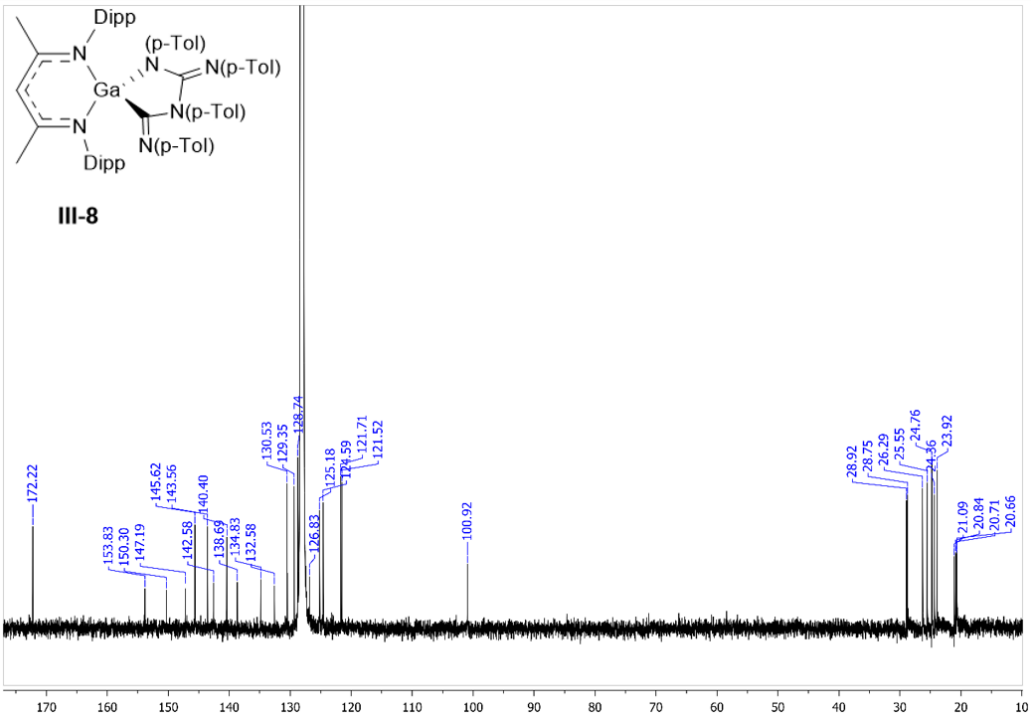

Figure 27. ^{13}C{^{1}H} NMR (101 MHz, C_6D_6) spectrum of **III-8**.

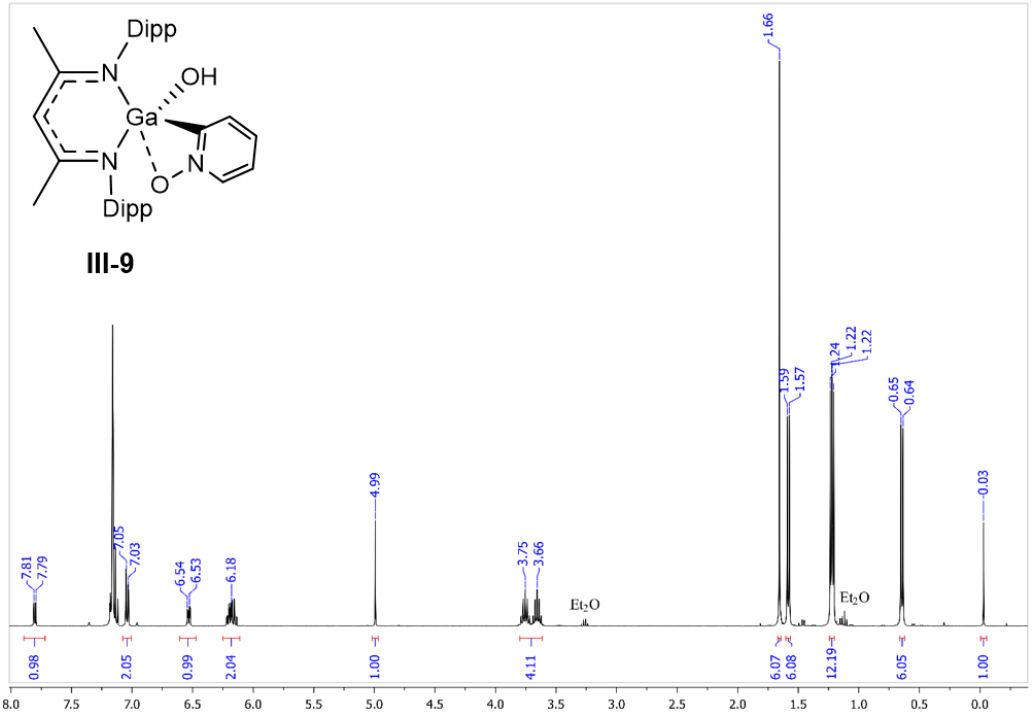

Figure 28. ^{1}H NMR (400 MHz, C_6D_6) spectrum of **III-9**.

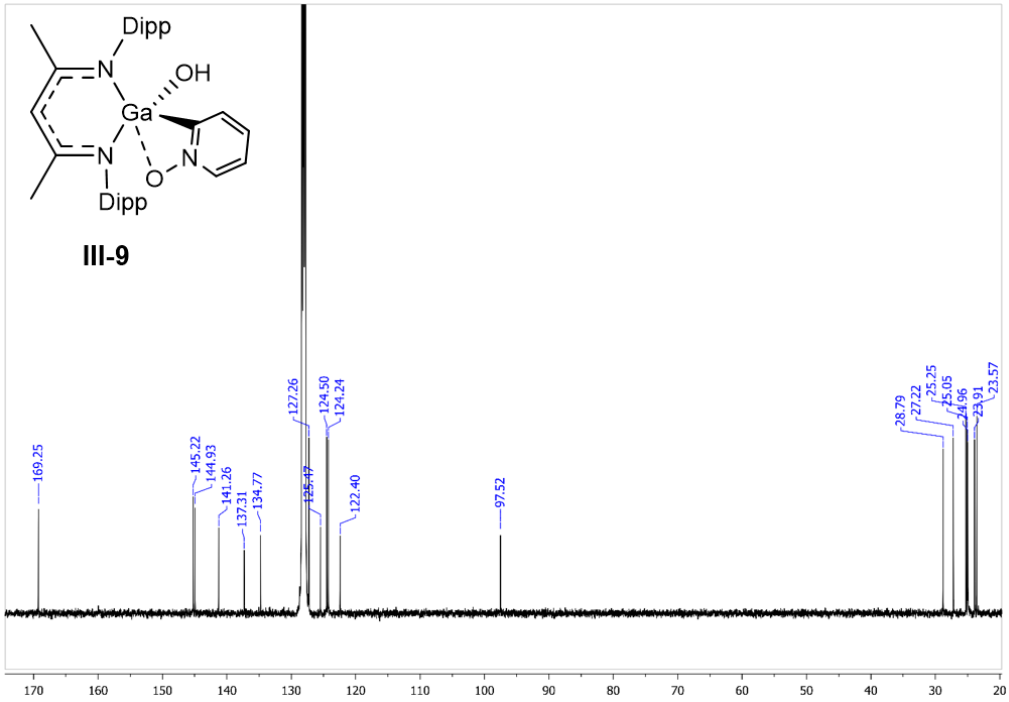

Figure 29. $^{13}C\{^{1}H\}$ NMR (101 MHz, C_6D_6) spectrum of **III-9**.

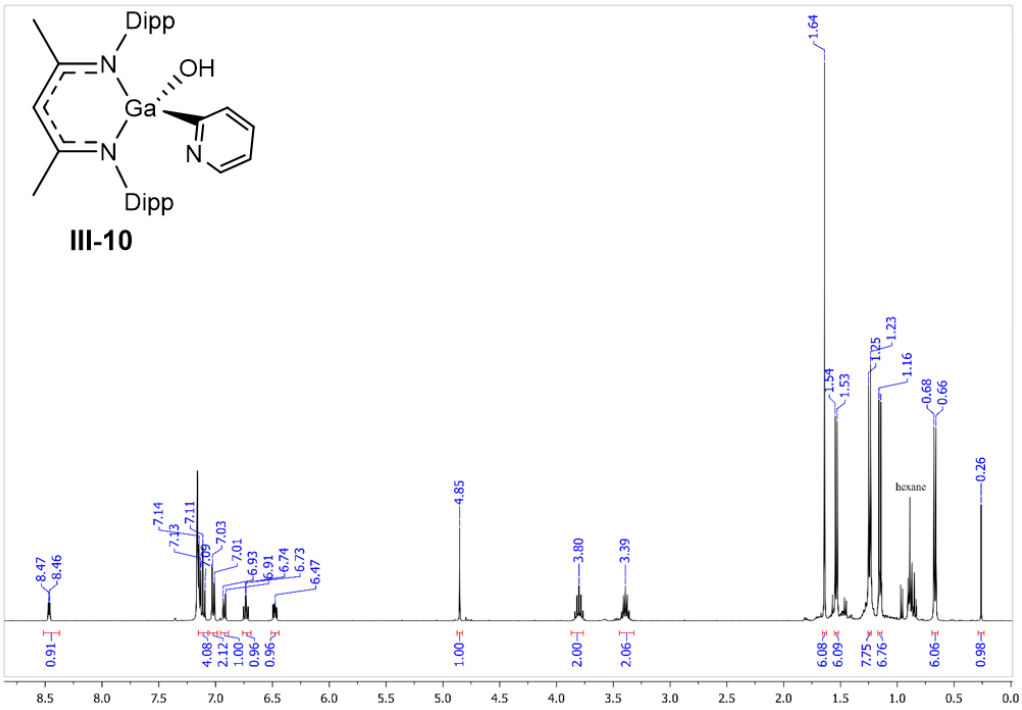

Figure 30. ^{1}H NMR (400 MHz, C_6D_6) spectrum of **III-10**.

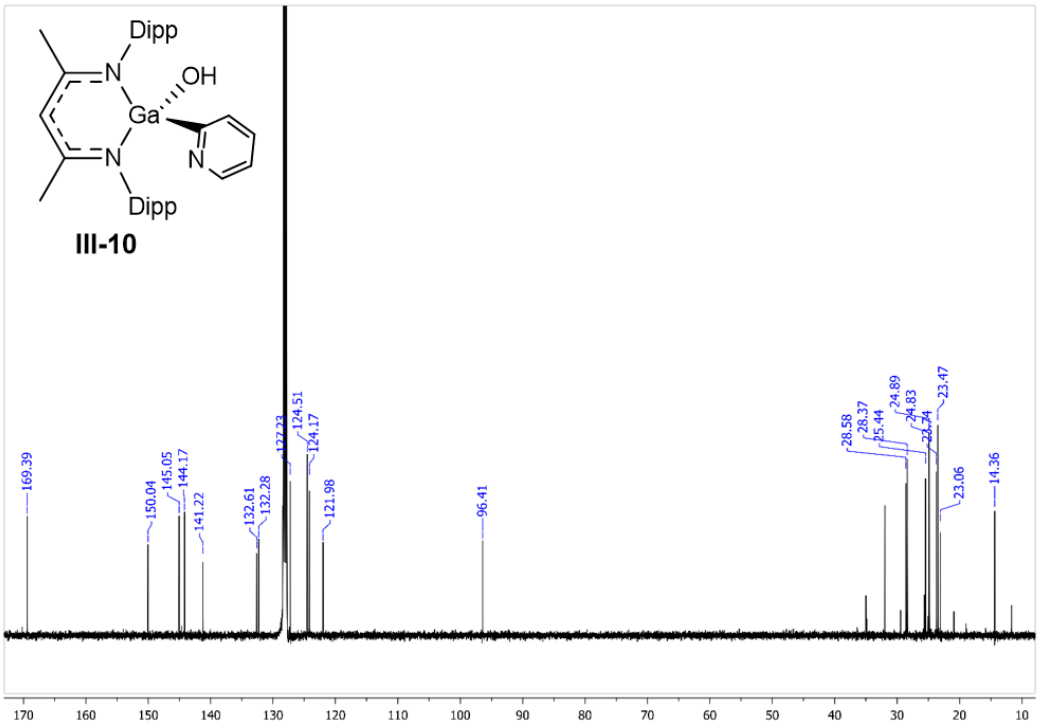

Figure 31. $^{13}C\{^{1}H\}$ NMR (101 MHz, C_6D_6) spectrum of **III-10**.

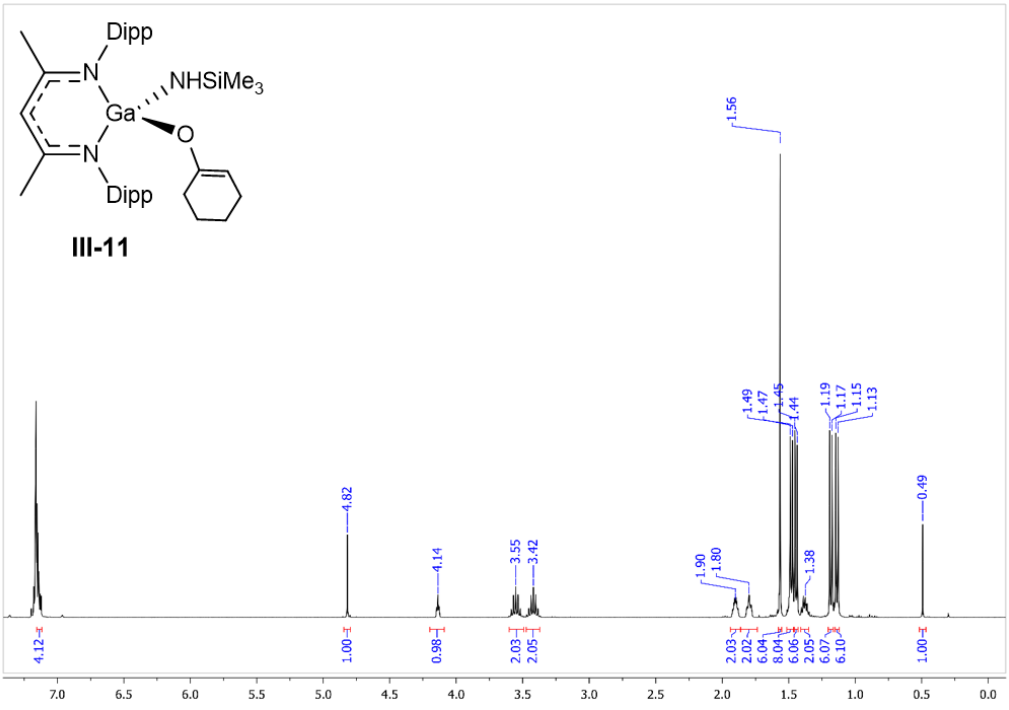

Figure 32. ^{1}H NMR (400 MHz, C_6D_6) spectrum of **III-11**.

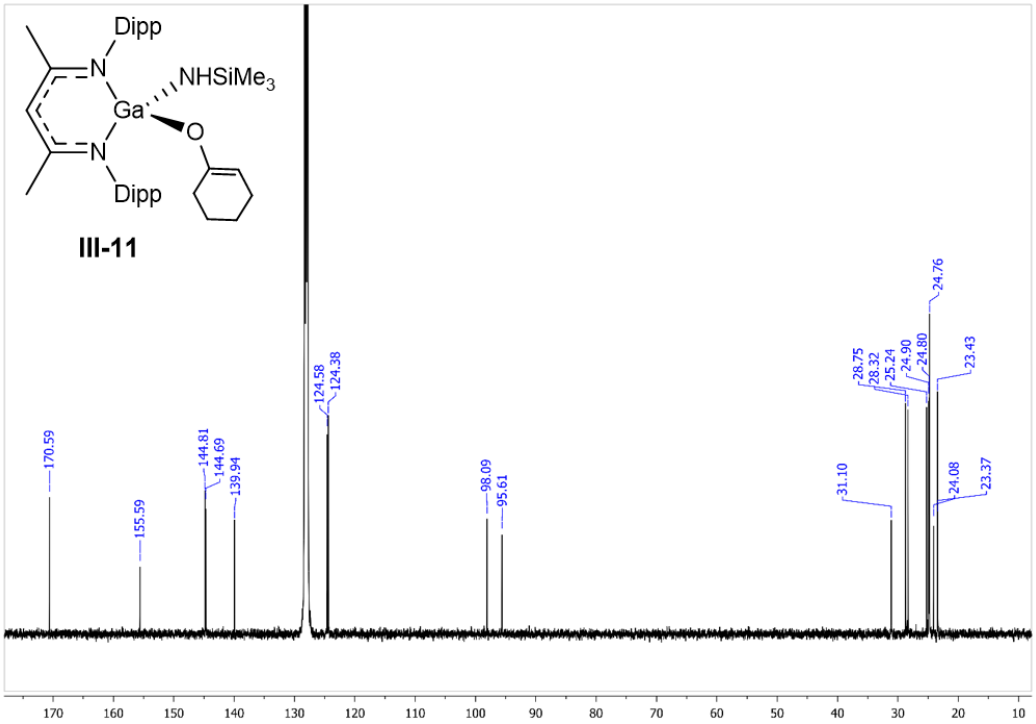

Figure 33. $^{13}C\{^{1}H\}$ NMR (101 MHz, C_6D_6) spectrum of **III-11**.

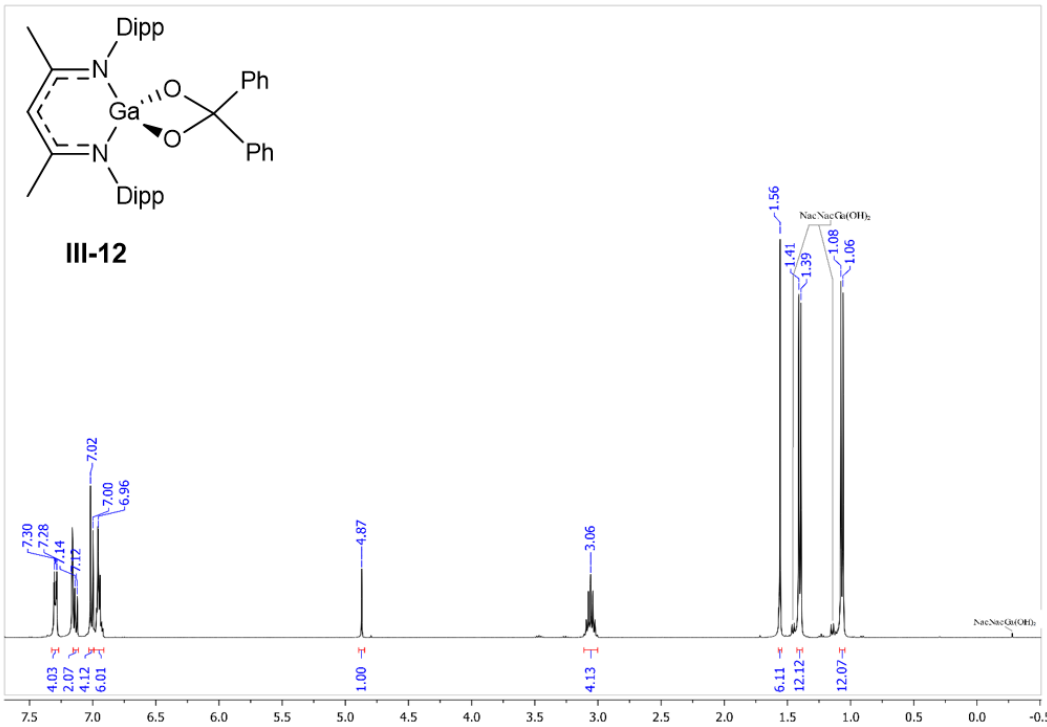

Figure 34. ^{1}H NMR (400 MHz, C_6D_6) spectrum of **III-12**.

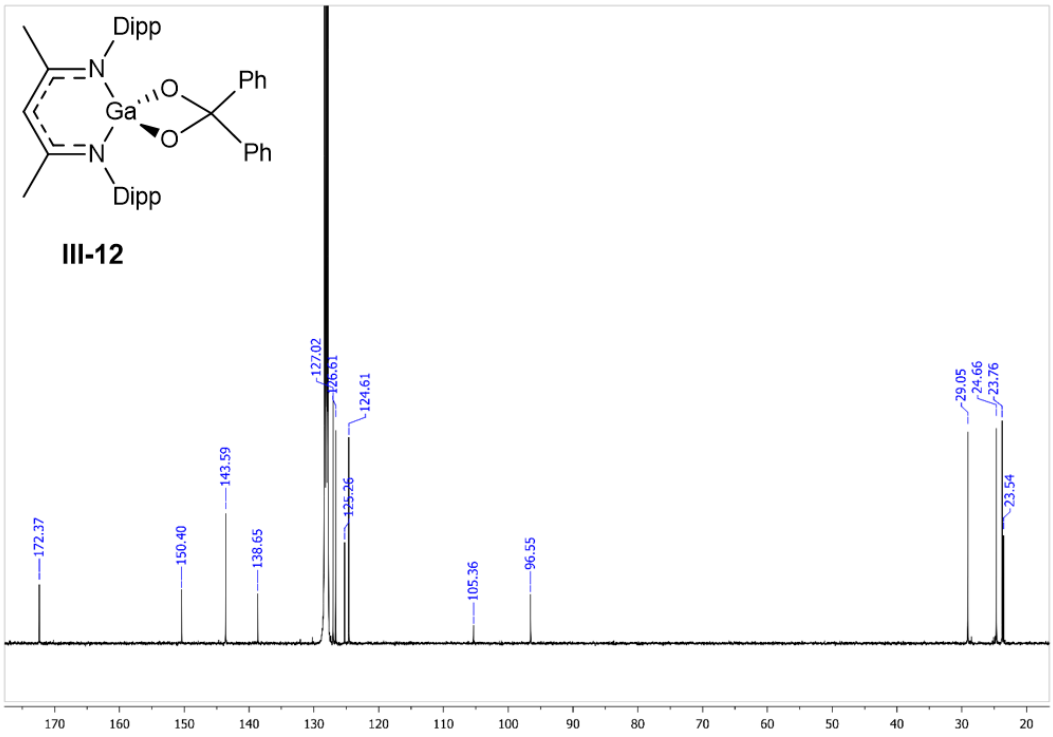

Figure 35. $^{13}C\{^{1}H\}$ NMR (101 MHz, C_6D_6) spectrum of **III-12**.

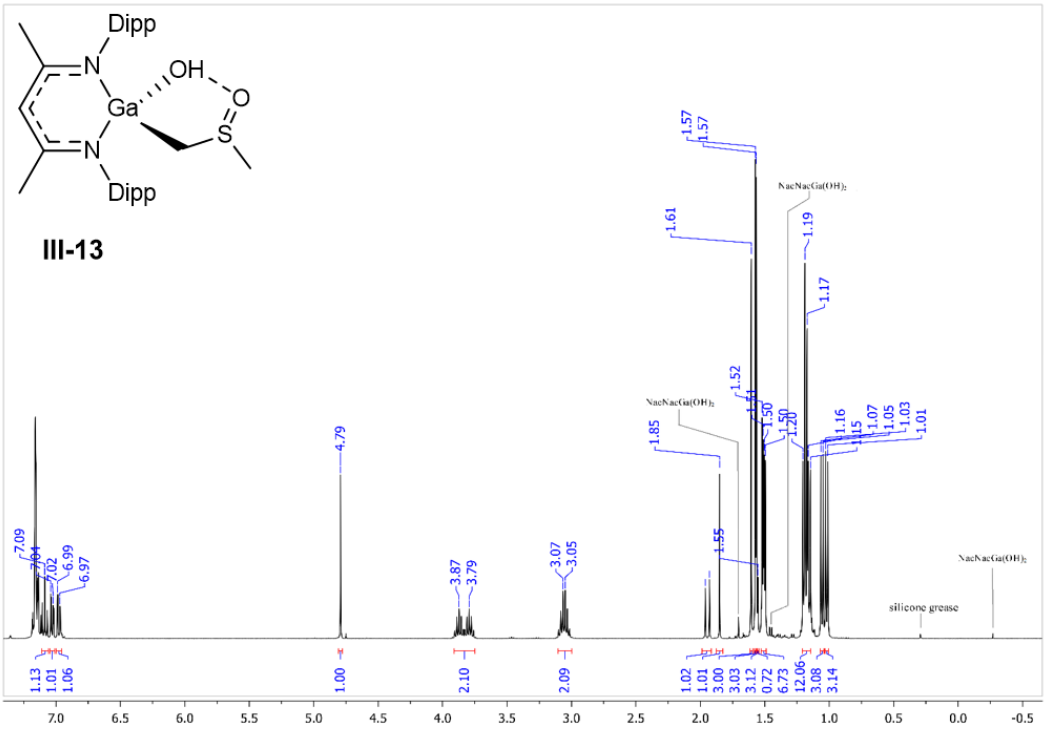

Figure 36. ^{1}H NMR (400 MHz, C_6D_6) spectrum of **III-13**.

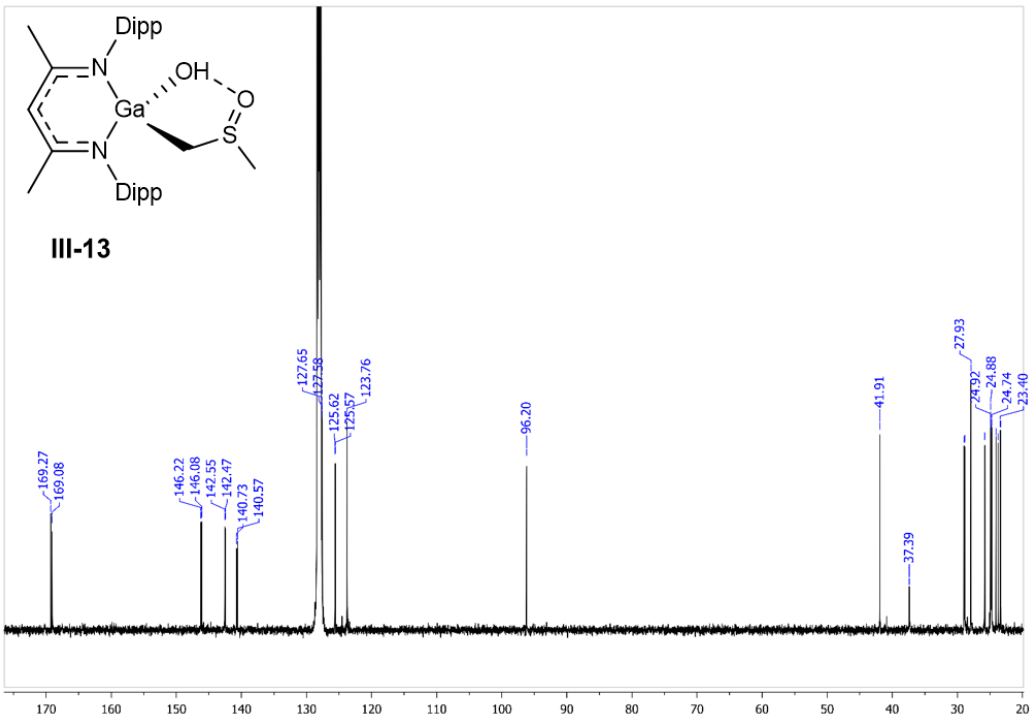

Figure 37. $^{13}C\{^{1}H\}$ NMR (101 MHz, C_6D_6) spectrum of **III-13**.

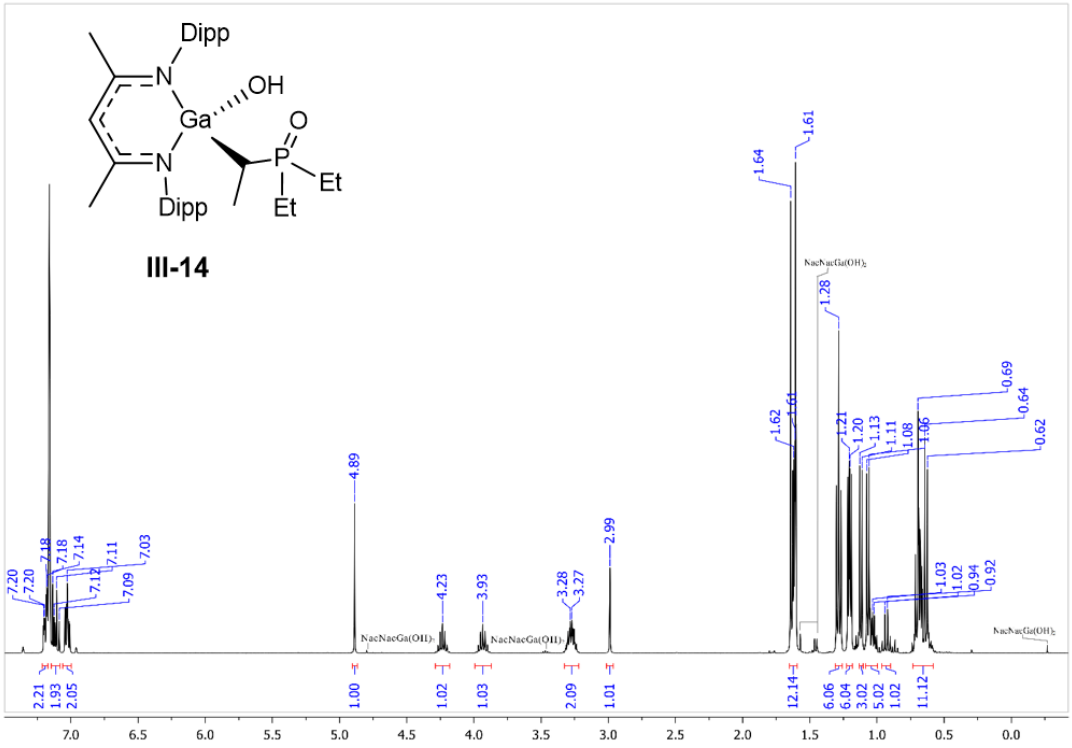

Figure 38. ^{1}H NMR (400 MHz, C_6D_6) spectrum of **III-14**.

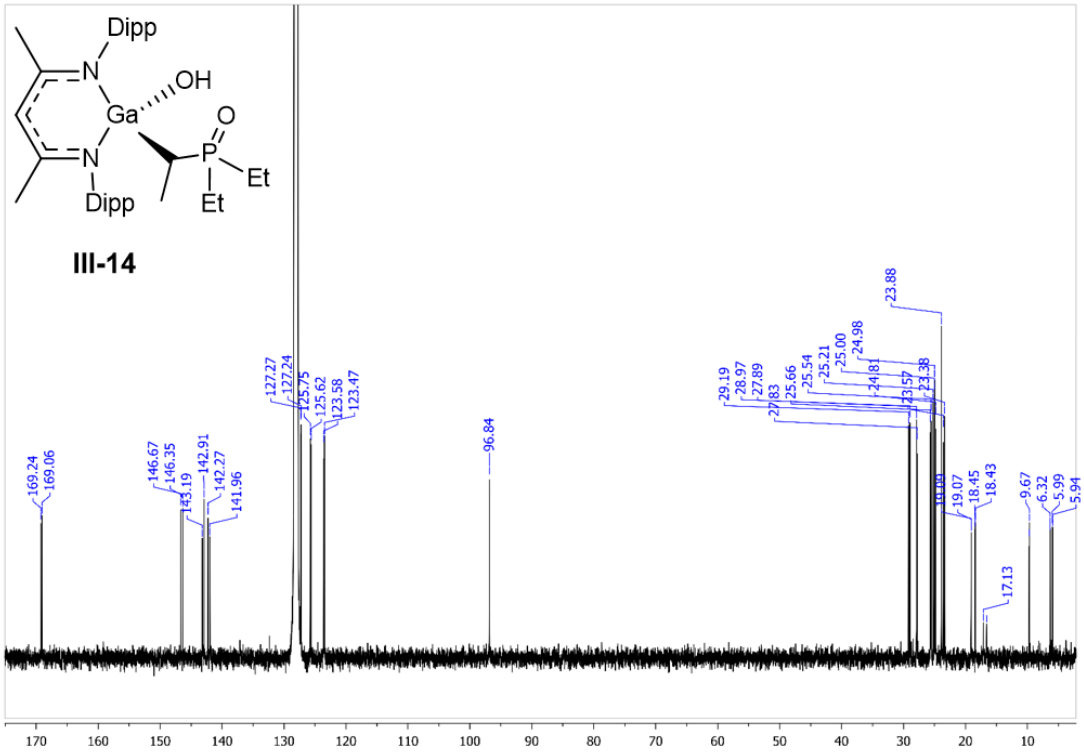

Figure 39. ^{13}C{^{1}H} NMR (101 MHz, C_6D_6) spectrum of **III-14**.

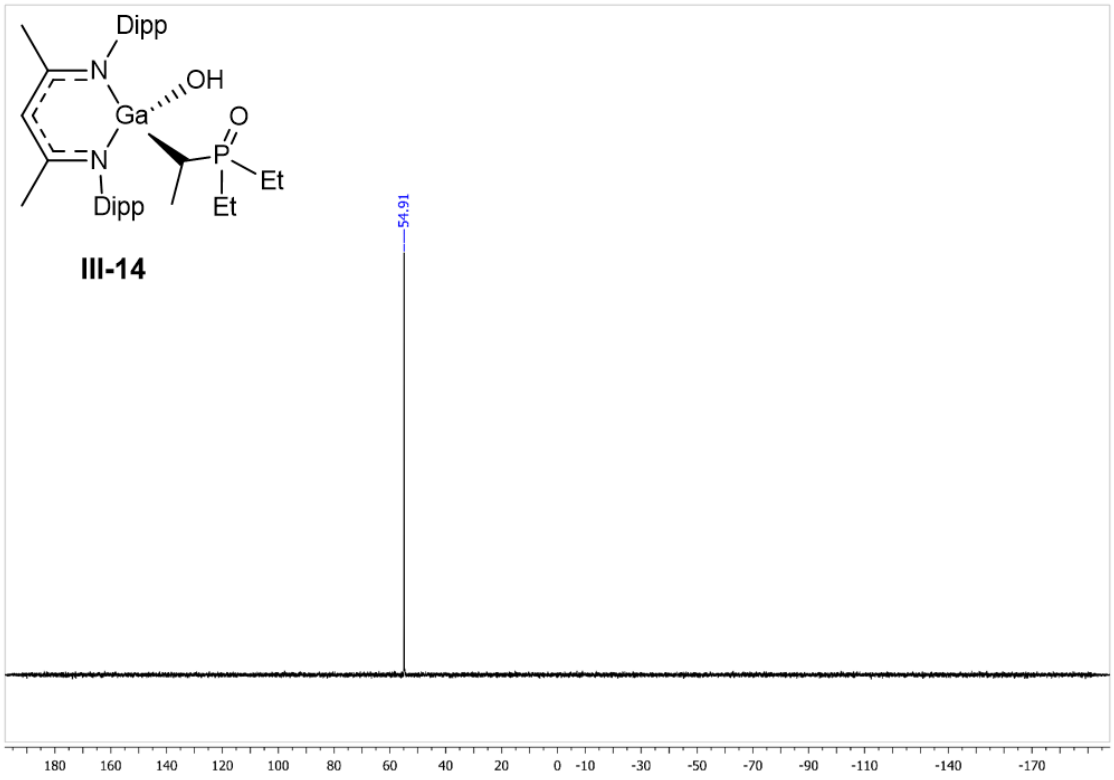

Figure 40. $^{31}P\{^{1}H\}$ NMR (162 MHz, C_6D_6) spectrum of **III-14**.

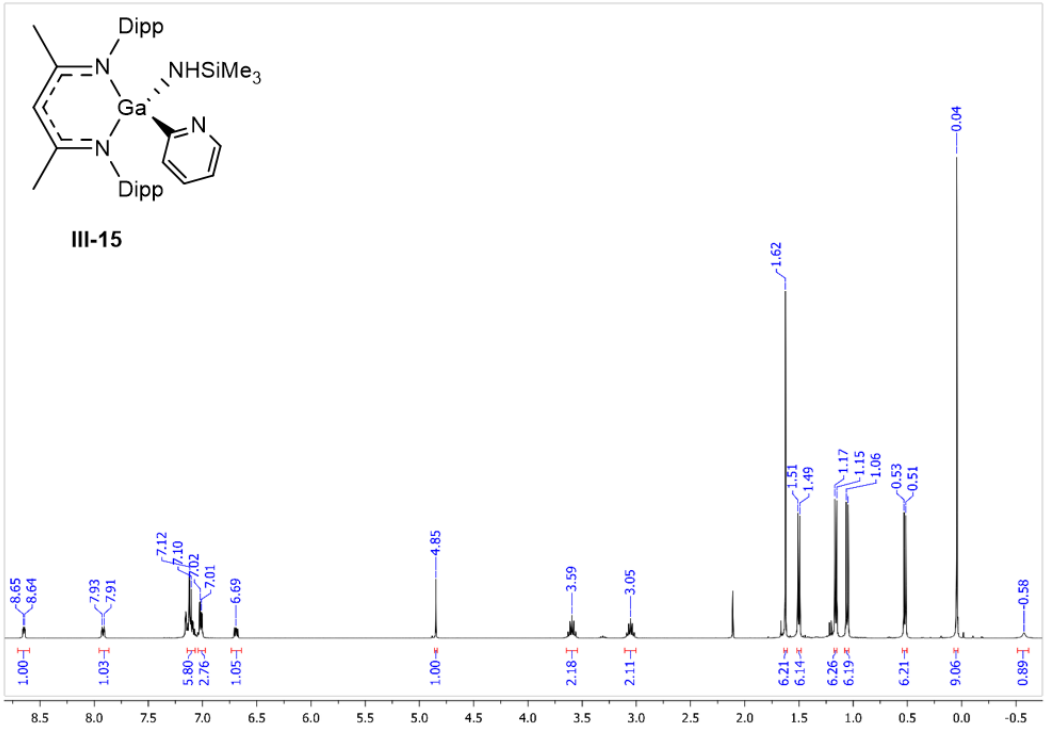

Figure 41. ^{1}H NMR (400 MHz, C_6D_6) spectrum of **III-15**.

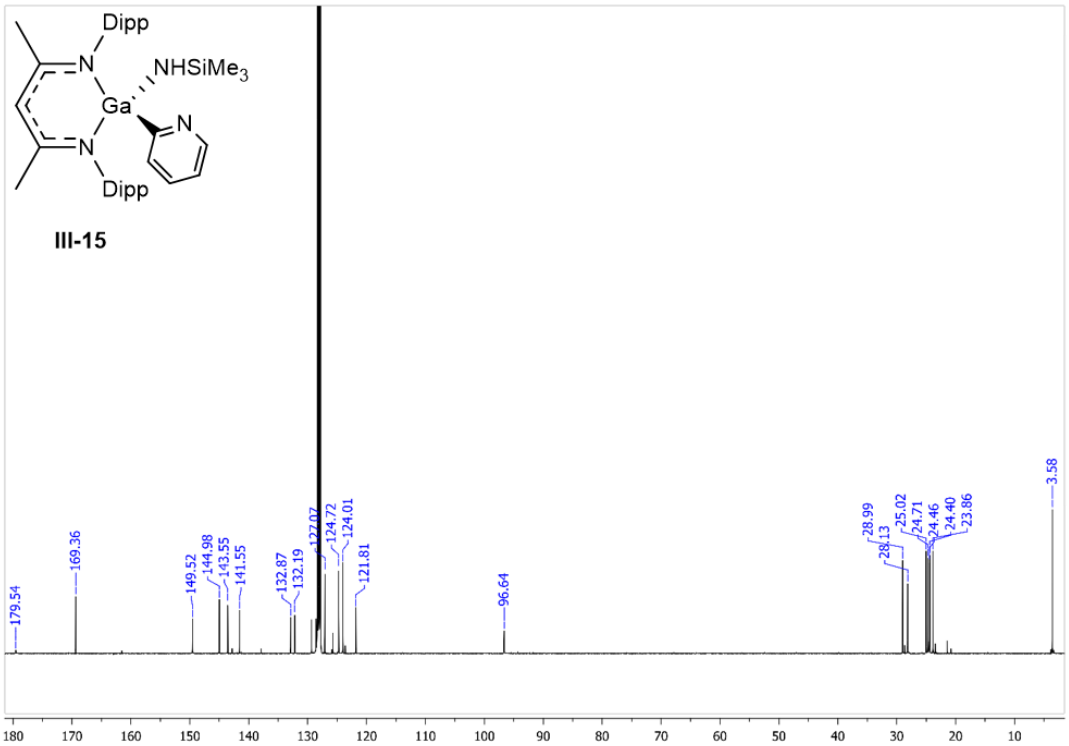

Figure 42. $^{13}C\{^{1}H\}$ NMR (101 MHz, C_6D_6) spectrum of **III-15**.

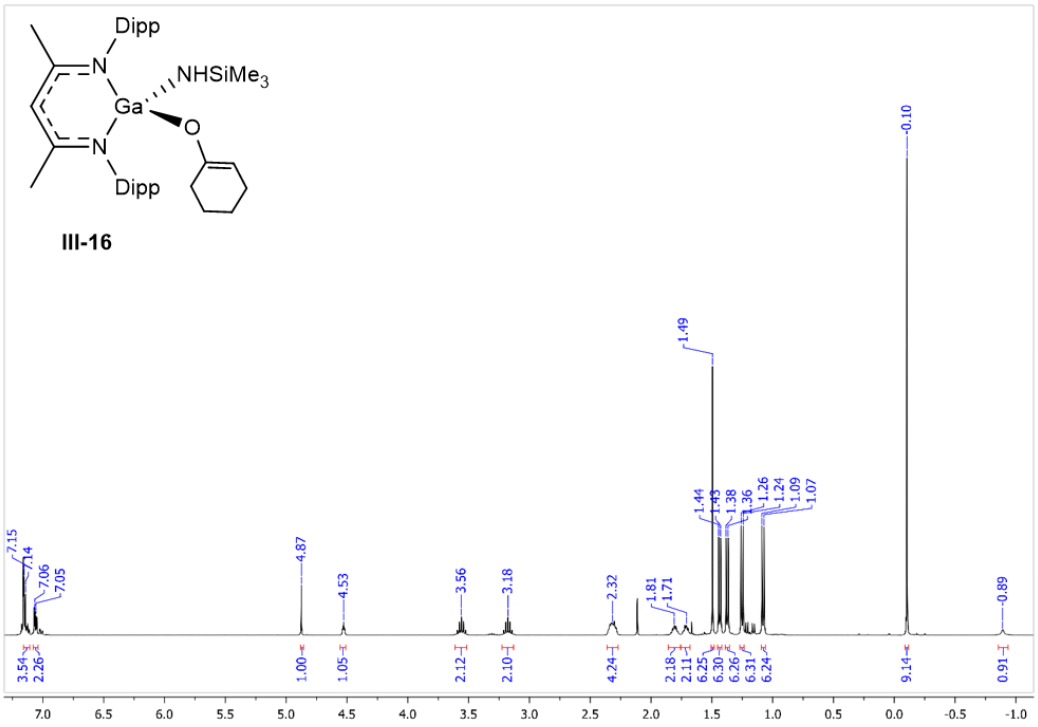

Figure 43. ^{1}H NMR (400 MHz, C_6D_6) spectrum of **III-16**.

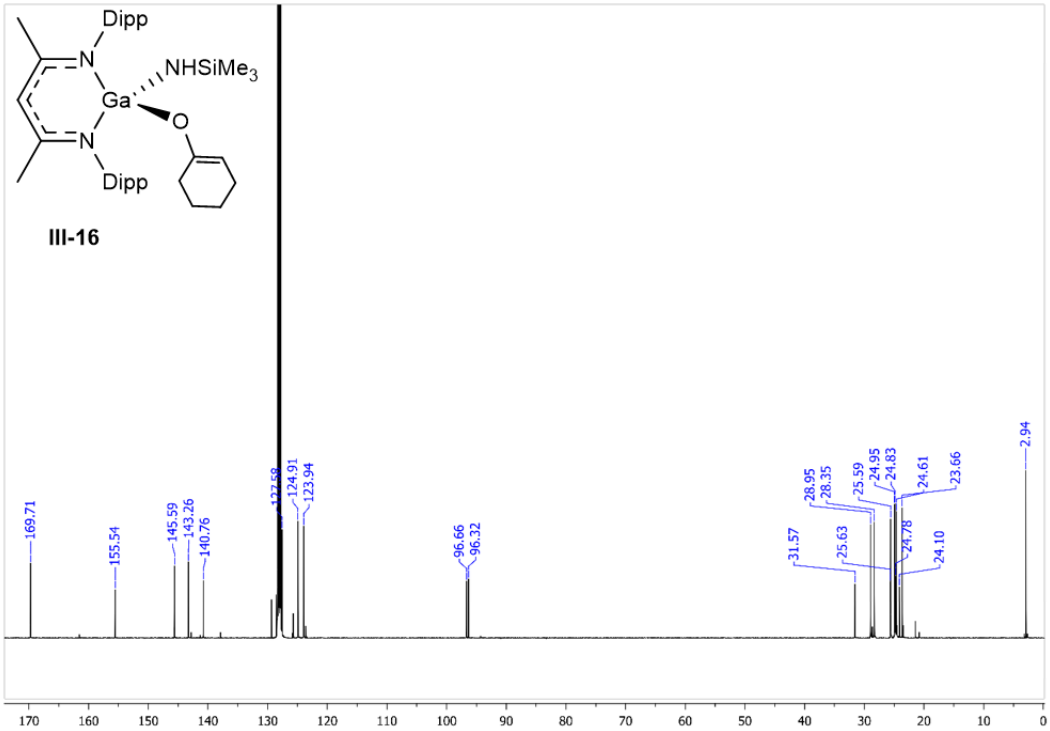

Figure 44. $^{13}C\{^{1}H\}$ NMR (101 MHz, C_6D_6) spectrum of **III-16**.

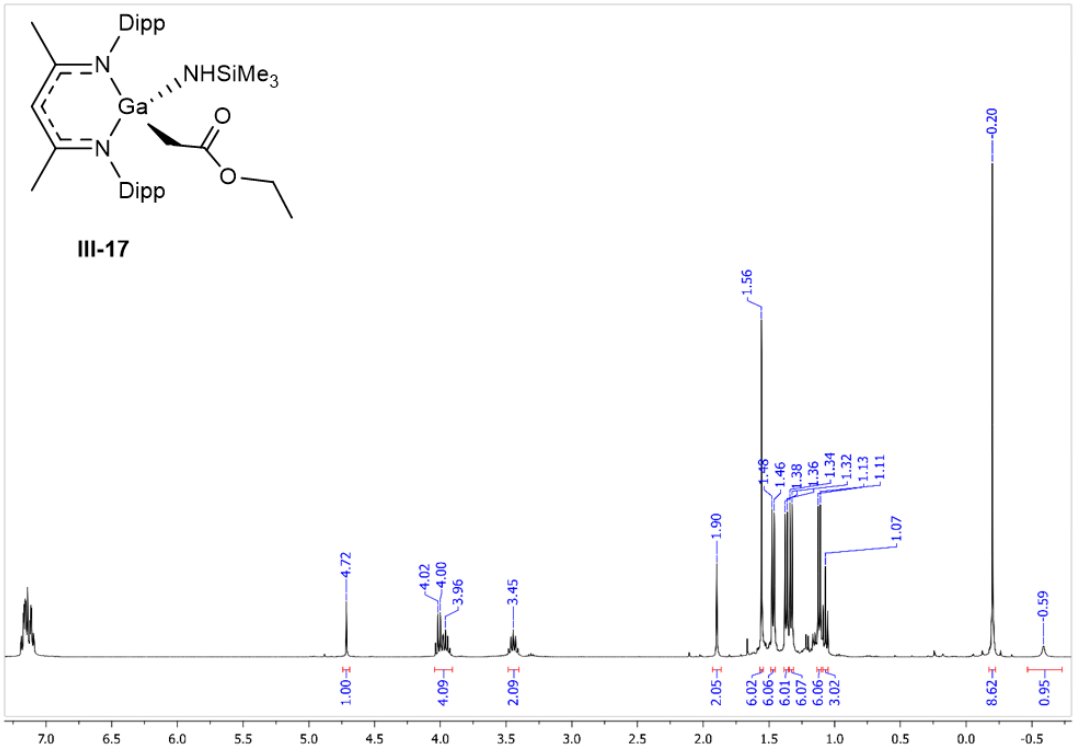

Figure 45. ^{1}H NMR (400 MHz, C_6D_6) spectrum of **III-17**.

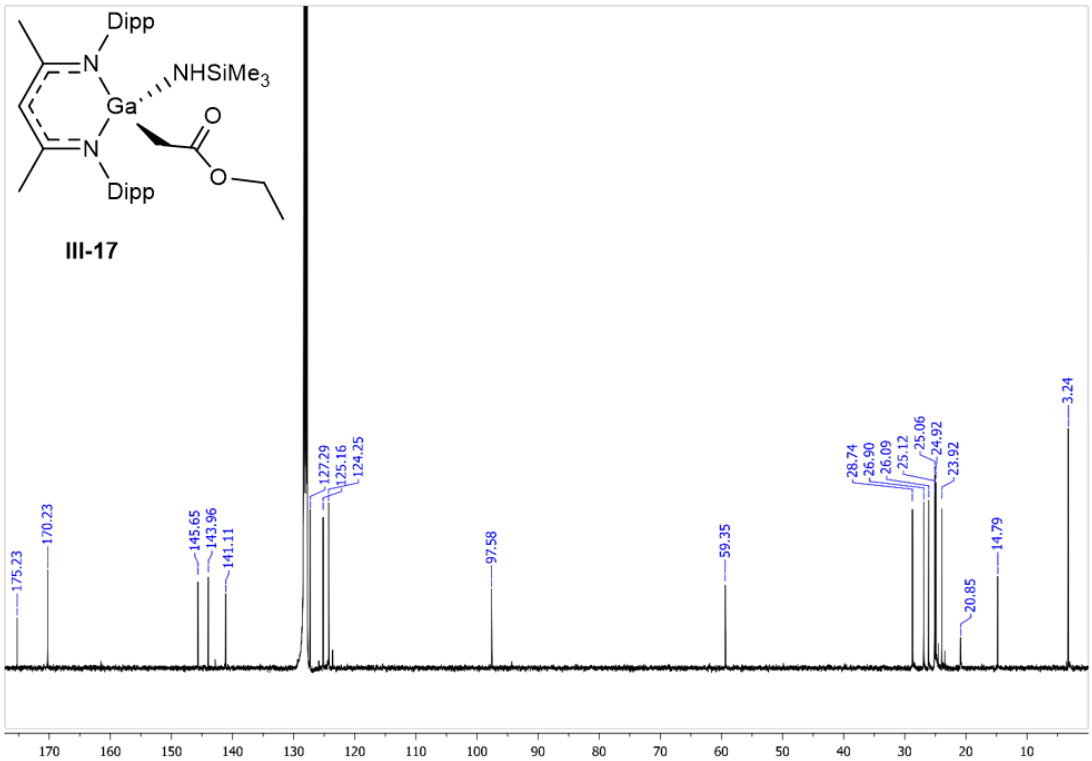

Figure 46. $^{13}C\{^{1}H\}$ NMR (101 MHz, C_6D_6) spectrum of **III-17**.

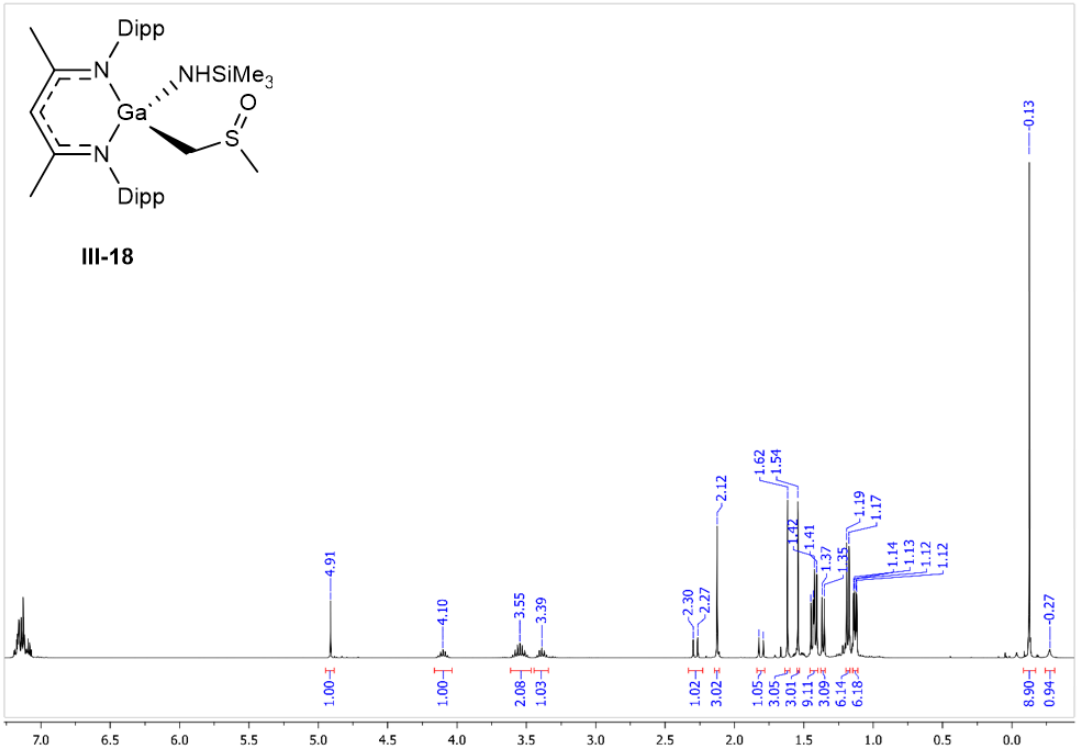

Figure 47. ^{1}H NMR (400 MHz, C_6D_6) spectrum of **III-18**.

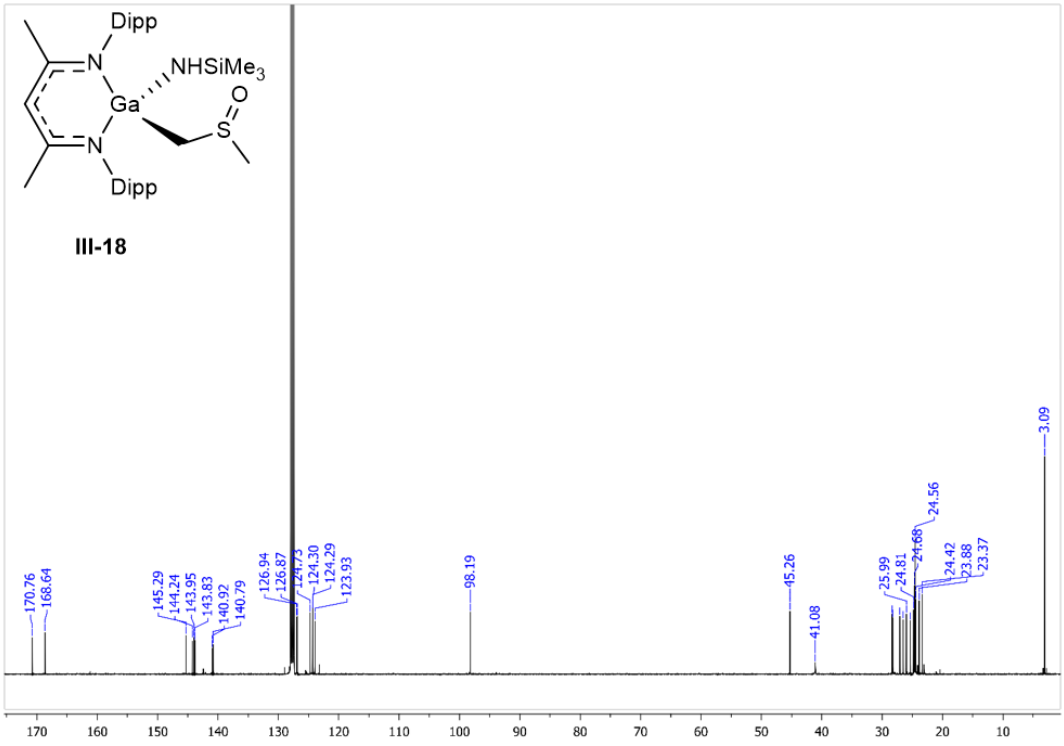

Figure 48. $^{13}C\{^{1}H\}$ NMR (101 MHz, C_6D_6) spectrum of **III-18**.

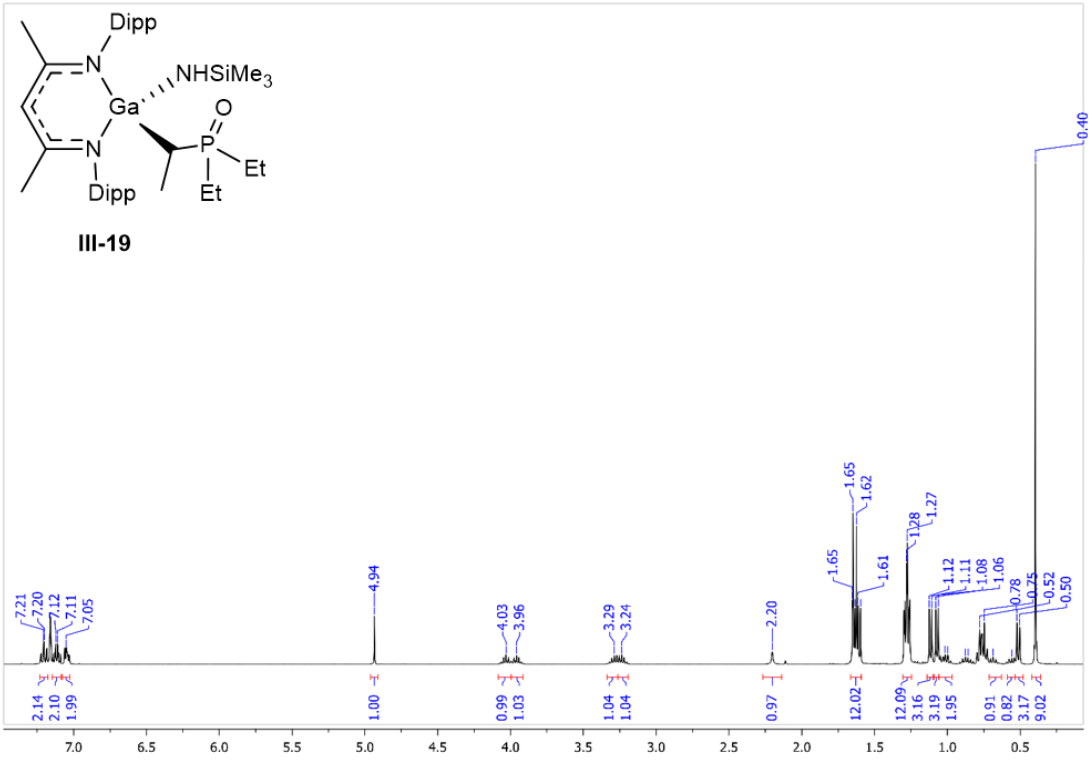

Figure 49. $^{1}H\{^{31}P\}$NMR (400 MHz, C_6D_6) spectrum of **III-19**.

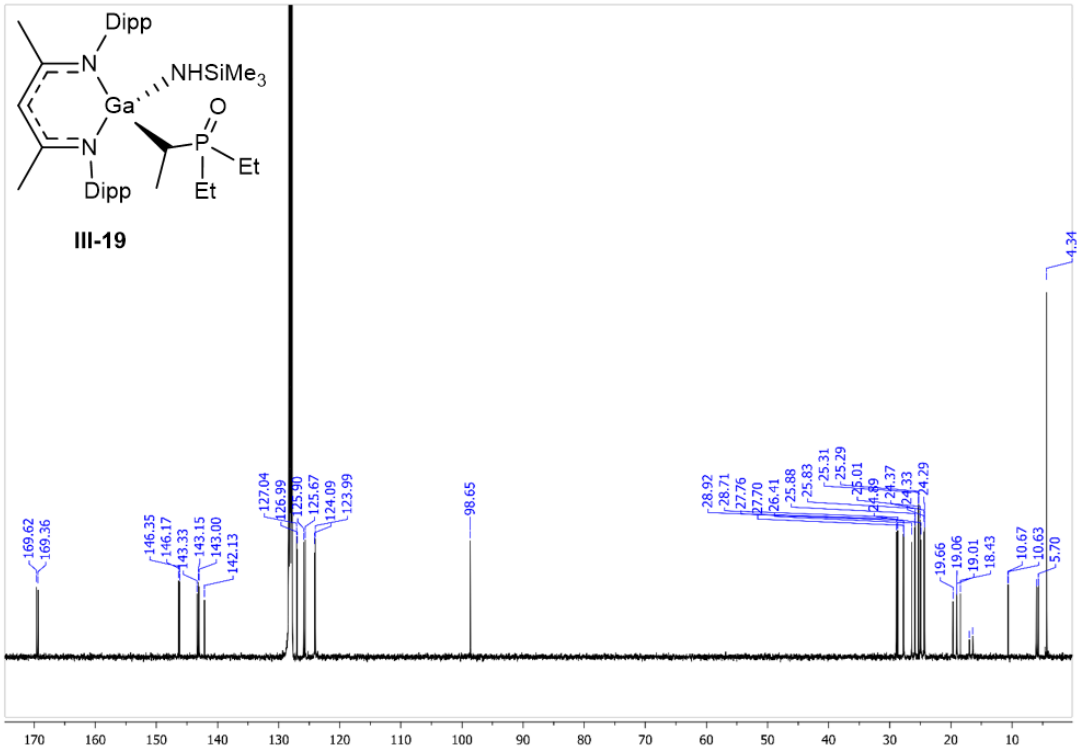

Figure 50. $^{13}C\{^{1}H\}$ NMR (101 MHz, C_6D_6) spectrum of **III-19**.

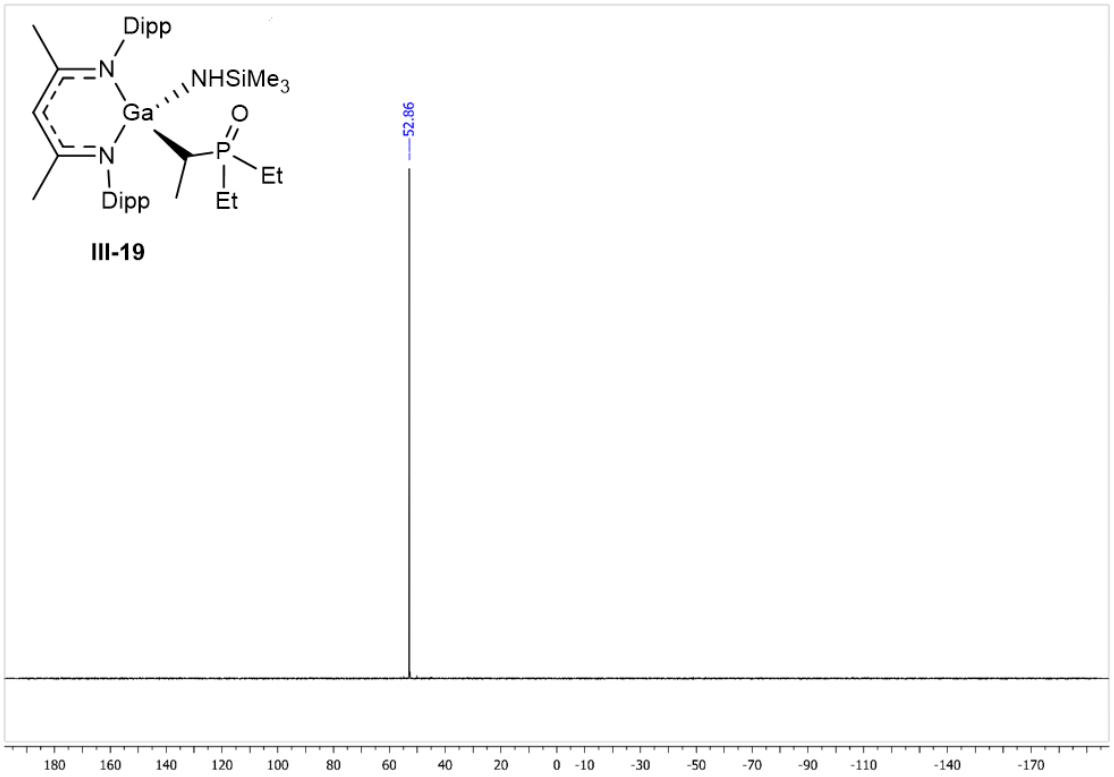

Figure 51. $^{31}P\{^{1}H\}$NMR (162 MHz, C_6D_6) spectrum of **III-19**.

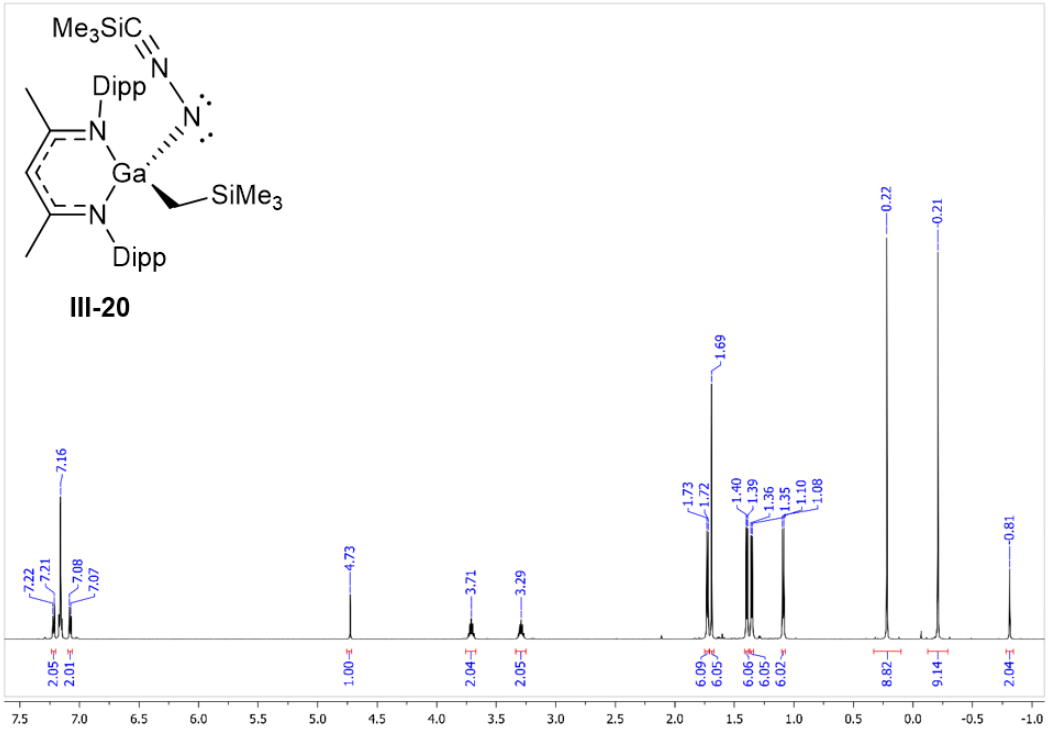

Figure 52. ^{1}H NMR (600 MHz, C_6D_6) spectrum of **III-20**.

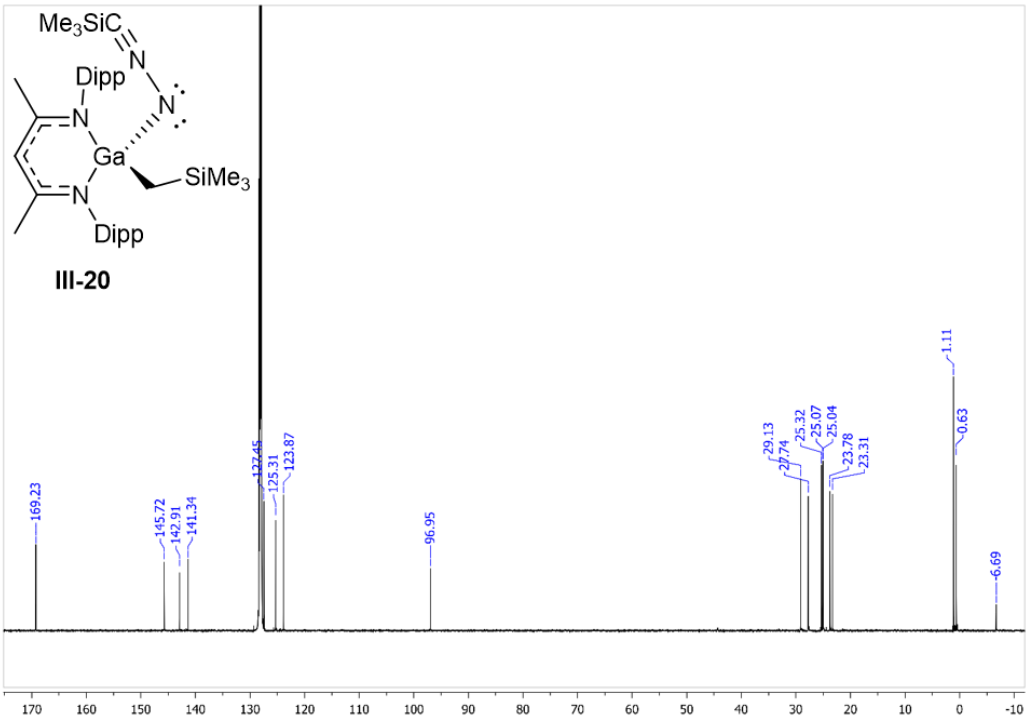

Figure 53. $^{13}C\{^{1}H\}$ NMR (151 MHz, C_6D_6) spectrum of **III-20**.

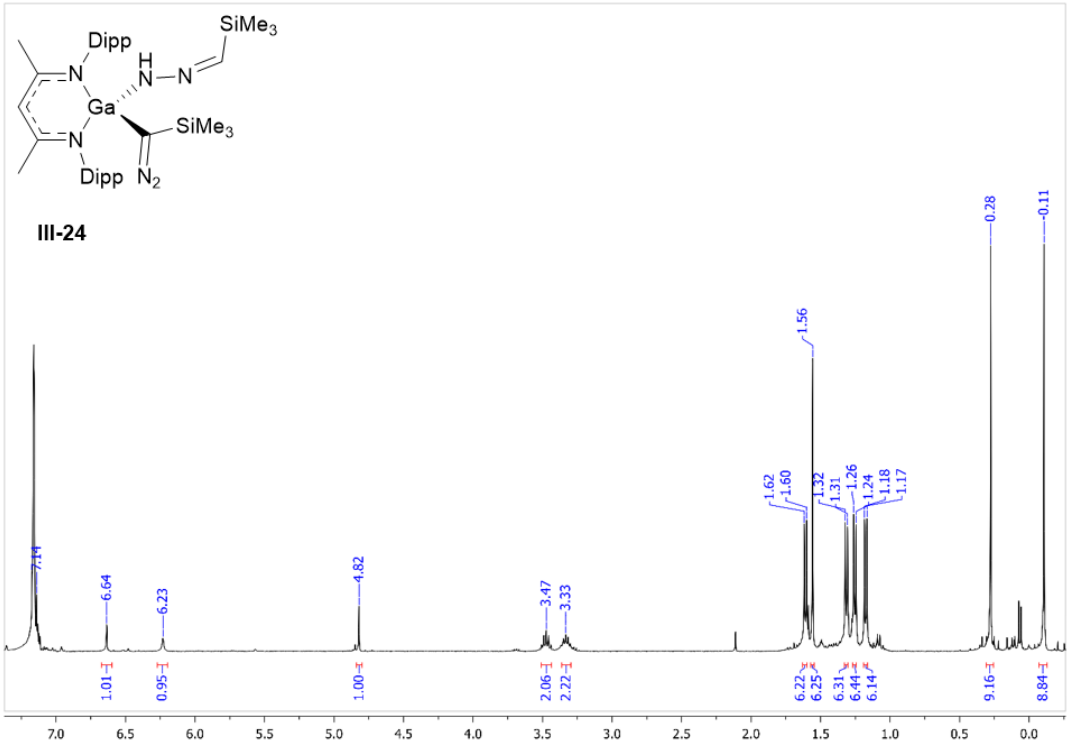

Figure 54. ^{1}H NMR (400 MHz, C_6D_6) spectrum of **III-24**.

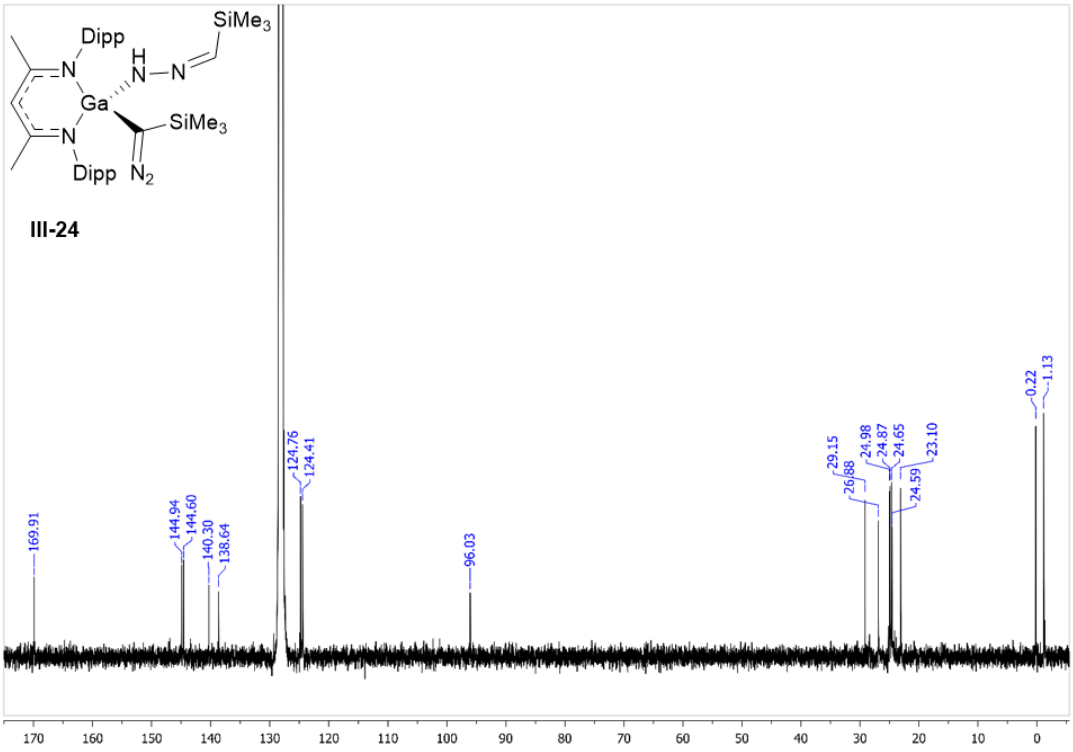

Figure 55. $^{13}C\{^{1}H\}$ NMR (101 MHz, C_6D_6) spectrum of **III-24**.

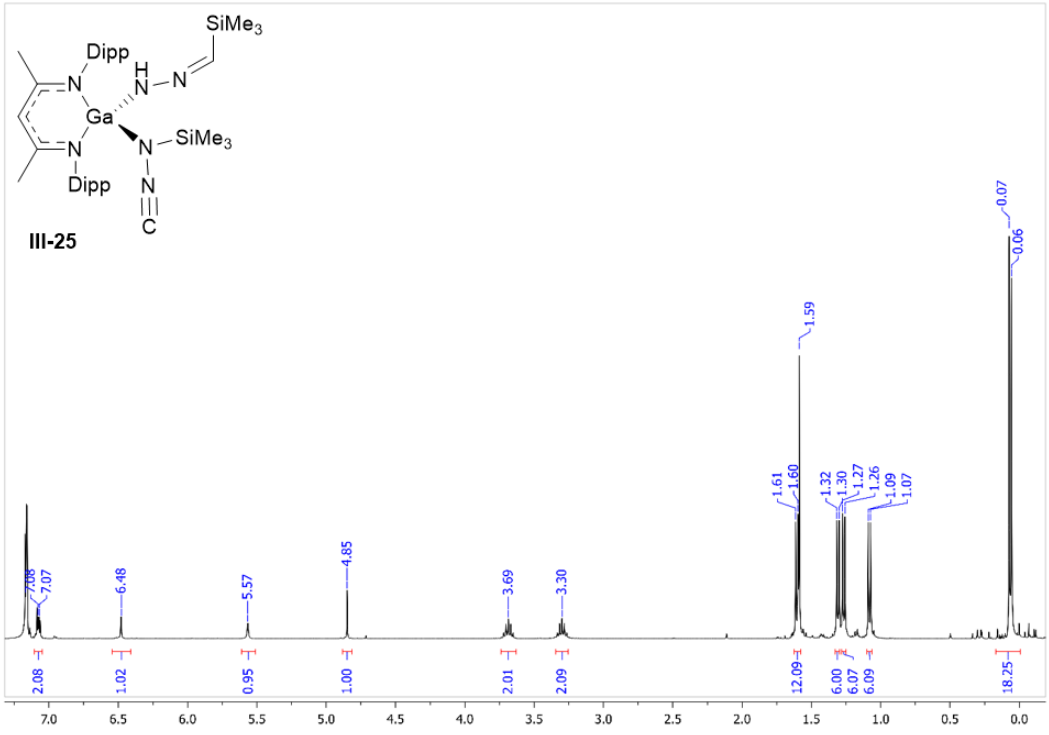

Figure 56. ^{1}H NMR (400 MHz, C_6D_6) spectrum of **III-25**.

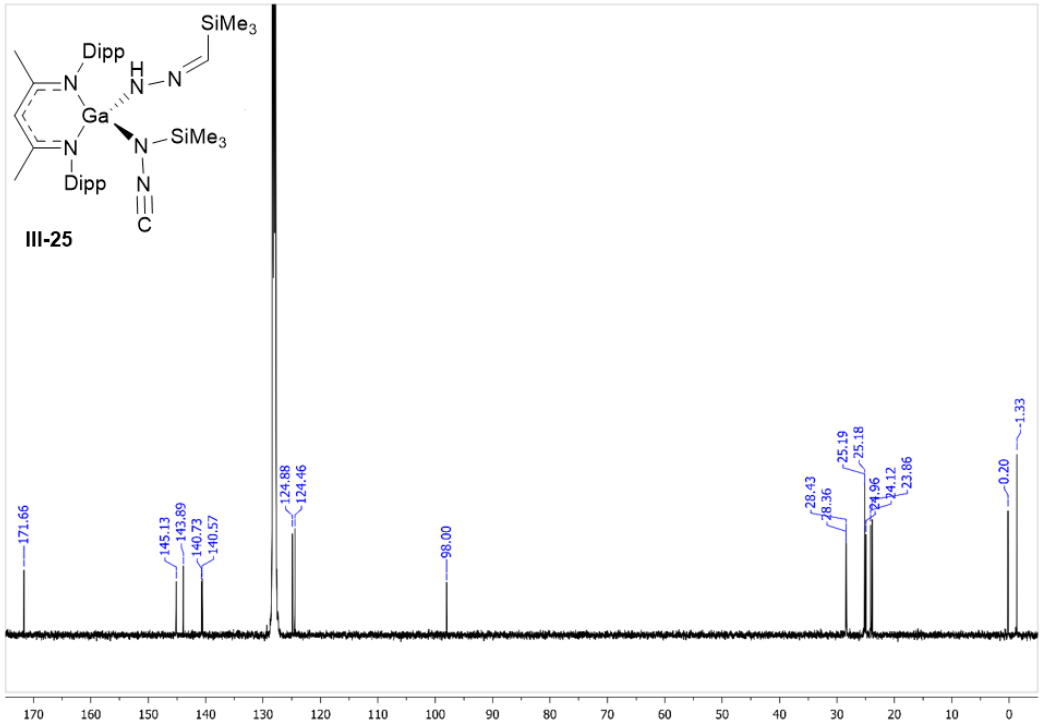

Figure 57. $^{13}C\{^{1}H\}$ NMR (101 MHz, C_6D_6) spectrum of **III-25**.

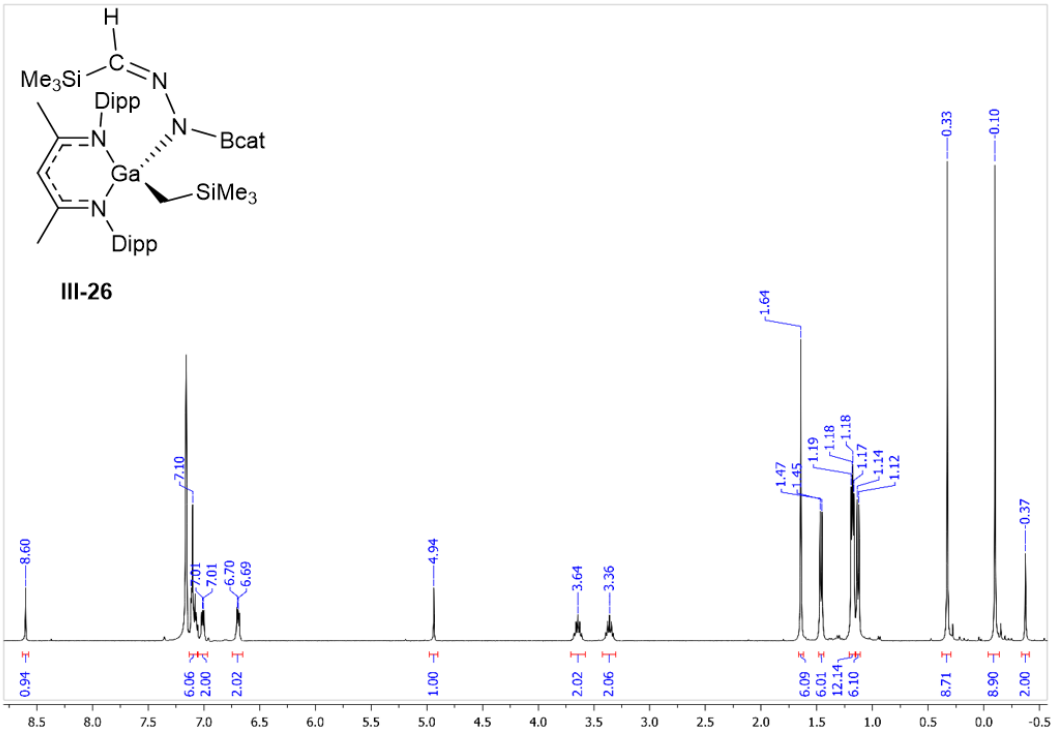

Figure 58. ^{1}H NMR (400 MHz, C_6D_6) spectrum of **III-26**.

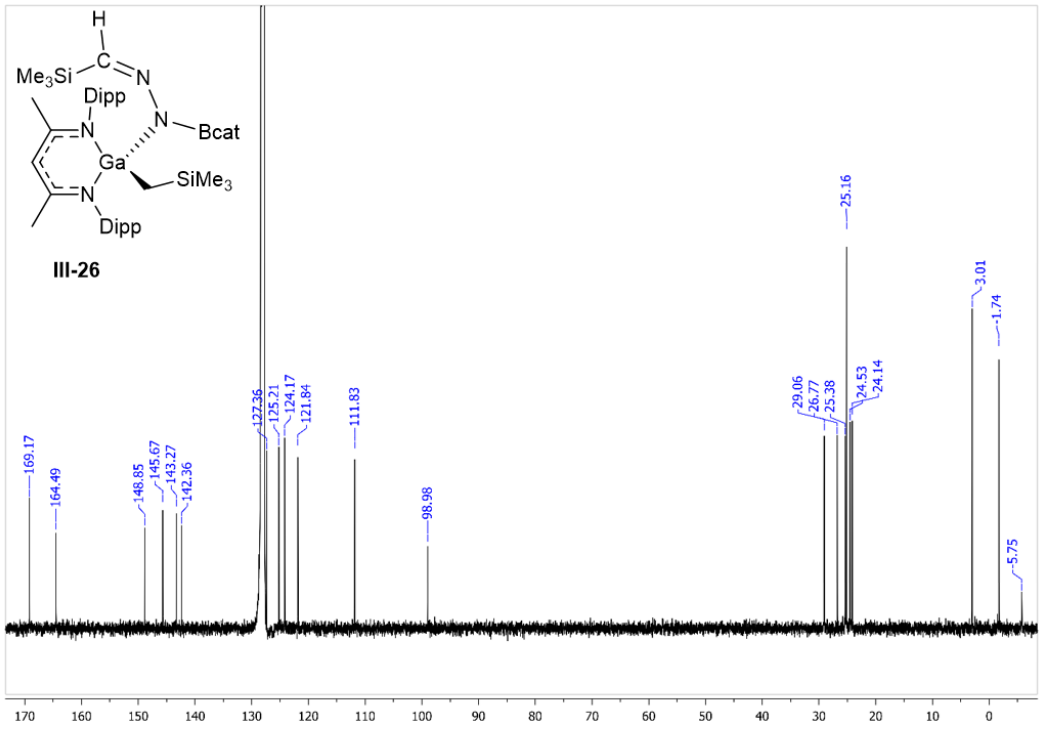

Figure 59. $^{13}C\{^{1}H\}$ NMR (101 MHz, C_6D_6) spectrum of **III-26**.

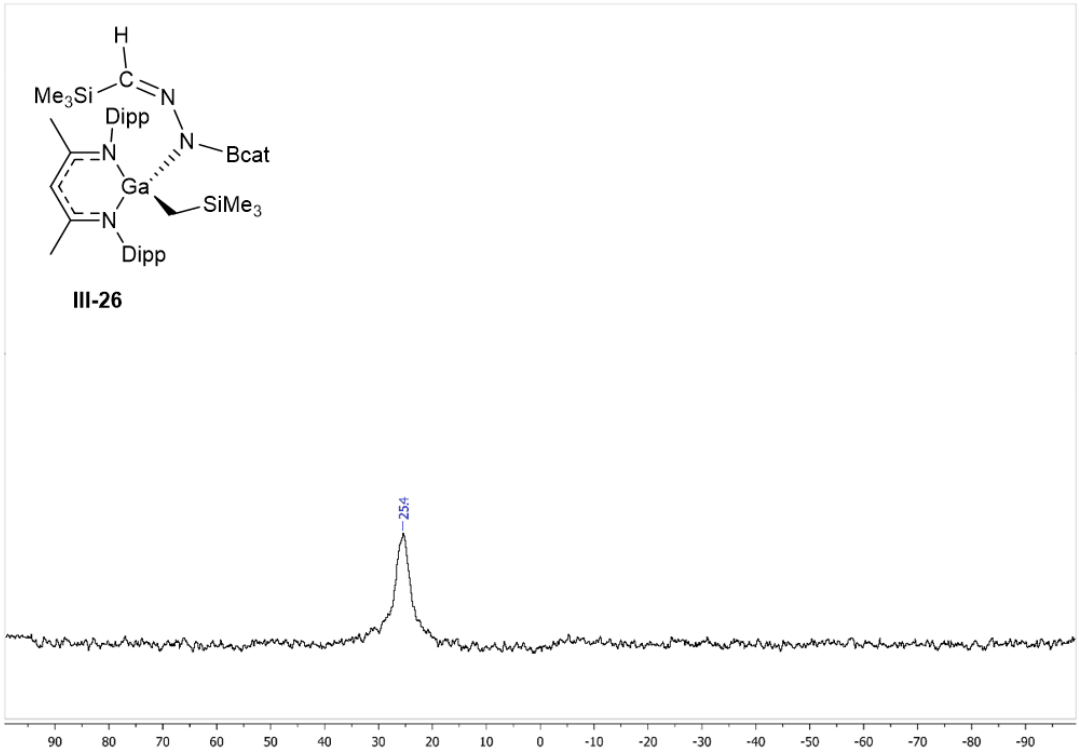

Figure 60. ^{11}B NMR (128 MHz, C_6D_6) spectrum of **III-26**.

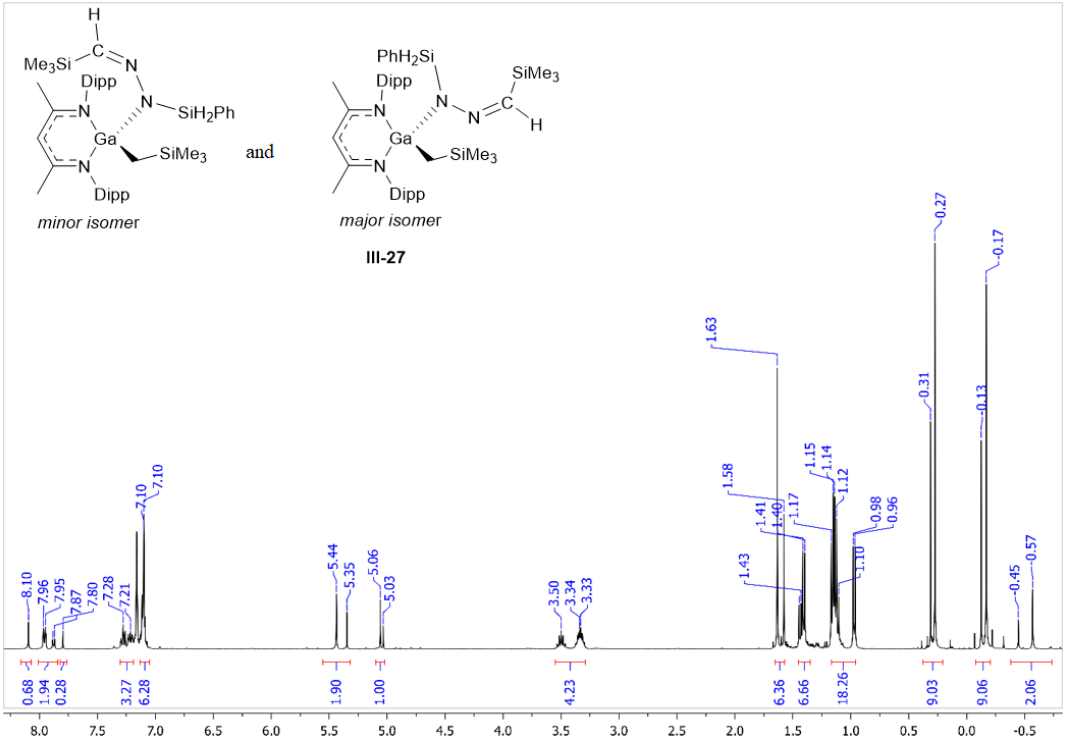

Figure 61. ^{1}H NMR (400 MHz, C_6D_6) spectrum of **III-27**.

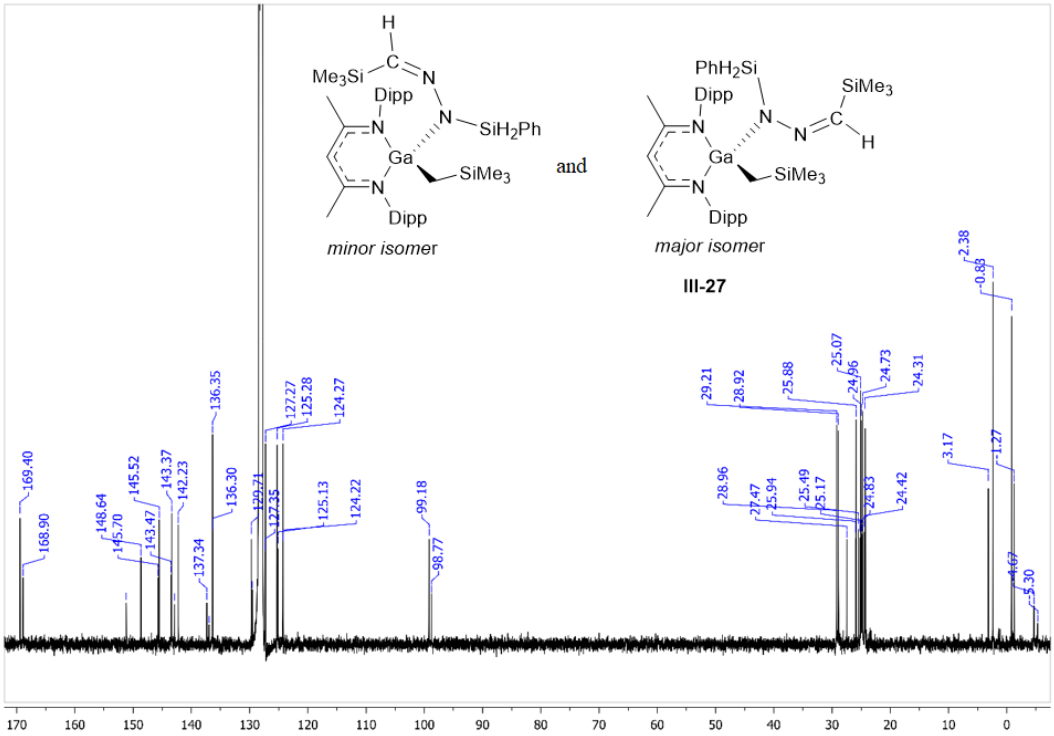

Figure 62. $^{13}C\{^{1}H\}$ NMR (101 MHz, C_6D_6) spectrum of **III-27**.

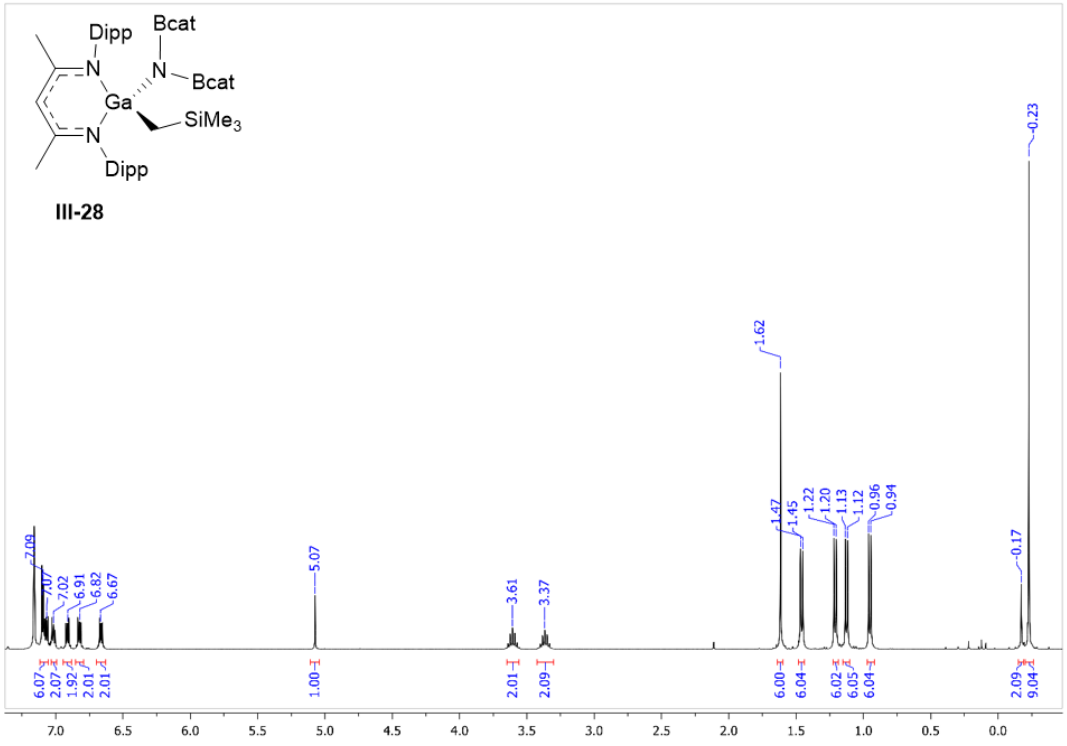

Figure 63. ^{1}H NMR (400 MHz, C_6D_6) spectrum of **III-28**.

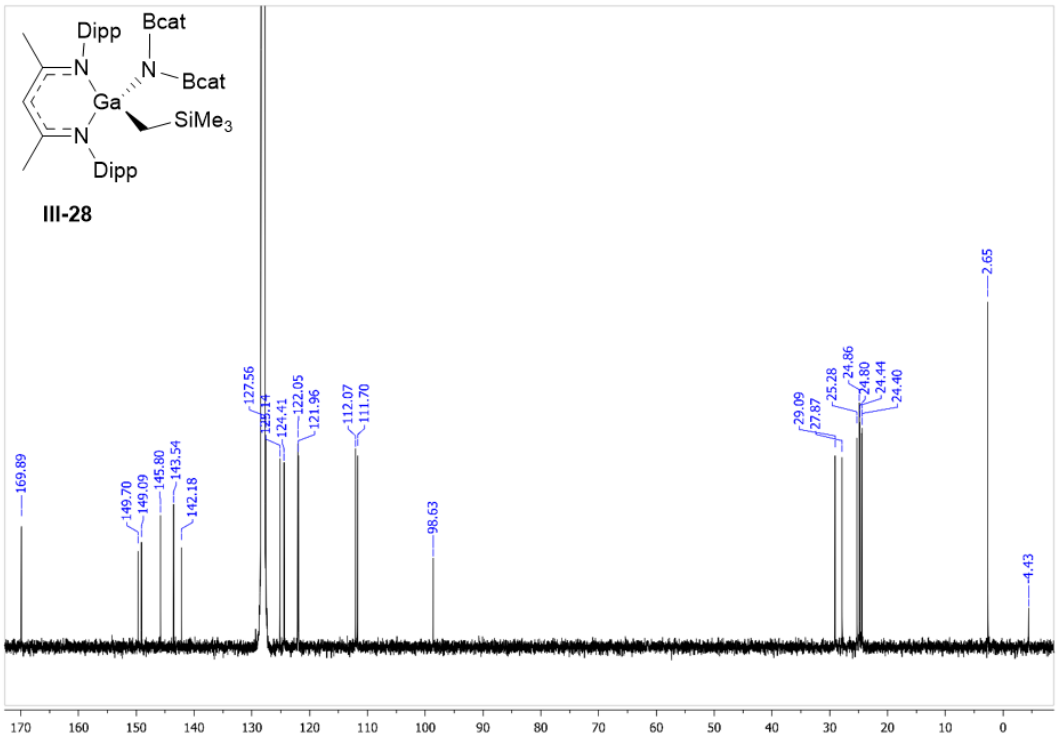

Figure 64. $^{13}C\{^{1}H\}$ NMR (101 MHz, C_6D_6) spectrum of **III-28**.

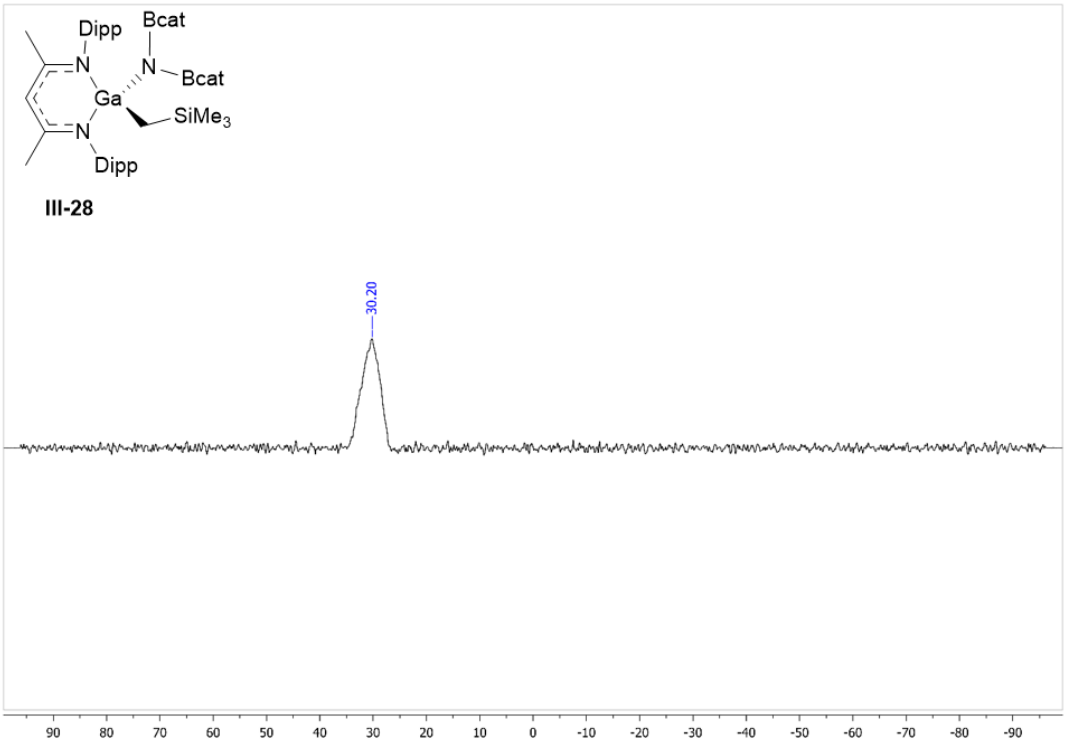

Figure 65. ^{11}B NMR (128 MHz, C_6D_6) spectrum of **III-28**.

VII. Appendix

Table 18. Crystal structure determination parameters for **III-2**.

Empirical formula		$C_{33}H_{47}GaN_2OGa$	
Formula weight		557.45	
Crystal habit		block	
Crystal color		light yellow	
Temperature		173.2 K	
Wavelength		0.71073 Å	
Crystal system		orthorhombic	
Space group		$P2_12_12$	
Unit cell dimensions:			
a	17.548(4) Å	α	90.00°
b	17.574(4) Å	β	90.00°
c	9.958(2) Å	γ	90.00°
Volume		3070.7(12) $Å^3$	
Z		4	
Density (calc)		1.206 mg/m^3	
Absorption coefficient		0.922 mm^{-1}	
F(000)		1192.0	
Crystal size		0.24 × 0.2 × 0.18 mm^3	
θ range for data collection		3.28 to 60.96	
Index ranges		-24≤ h≤22, -19≤ k≤25, -14≤ l≤13	
Reflections collected		20746	
Independent reflections		9281 [R_{int} = 0.0477, R_{sigma} = 0.0477]	
Absorption correction		multi-scan	
Max./min. transmission		0.759 / 0.862	
Refinement method		full-matrix least-squares on F^2	
Data / restraints / parameters		9281/0/346	
Goodness-of-fit on F^2		0.977	
Final R indices [I>2σ(I)]		R_1 = 0.0446, wR_2 = 0.0839	
R indices (all data)		R_1 = 0.0761, wR_2 = 0.0919	
Largest diff. peak and hole, e. $Å^{-3}$		0.55/-0.41	

Table 19. Crystal structure determination parameters for **III-4**.

Empirical formula		$C_{40.2}H_{50.8}GaN_3S_2$	
Formula weight		709.88	
Crystal habit		block	
Crystal color		light yellow	
Temperature		200.0 K	
Wavelength		0.71073 Å	
Crystal system		monoclinic	
Space group		C2/c	
Unit cell dimensions:			
a	25.677(6) Å	α	90.00°
b	17.866(3) Å	β	123.753(5)°
c	21.214(5) Å	γ	90.00°
Volume		8092(3) $Å^3$	
Z		8	
Density (calc)		1.165 mg/m^3	
Absorption coefficient		0.810 mm^{-1}	
F(000)		3008.0	
Crystal size		0.651 × 0.298 × 0.158 mm^3	
θ range for data collection		3.04 to 51.56	
Index ranges		-31≤ h≤31, -21≤ k≤21, -25≤ l≤25	
Reflections collected		115878	
Independent reflections		7735 [R_{int} = 0.0449, R_{sigma} = 0.0180]	
Absorption correction		multi-scan	
Max./min. transmission		0.620 / 0.882	
Refinement method		full-matrix least-squares on F^2	
Data / restraints / parameters		7735/46/434	
Goodness-of-fit on F^2		1.093	
Final R indices [I>2σ(I)]		R_1 = 0.0365, wR_2 = 0.1085	
R indices (all data)		R_1 = 0.0494, wR_2 = 0.1204	
Largest diff. peak and hole, e. $Å^{-3}$		0.53/-0.56	

Table 20. Crystal structure determination parameters for **III-5**.

Empirical formula		$C_{67}H_{92}Ga_2N_5O_{0.5}S$	
Formula weight		1146.96	
Crystal habit		block	
Crystal color		light yellow	
Temperature		173.2 K	
Wavelength		0.71073 Å	
Crystal system		monoclinic	
Space group		C2/c	
Unit cell dimensions:			
a	22.1525(6) Å	α	90.00°
b	14.8569(4) Å	β	101.310(2)°
c	39.0059(11) Å	γ	90.00°
Volume		12588.2(6) $Å^3$	
Z		8	
Density (calc)		1.210 mg/m^3	
Absorption coefficient		0.933 mm^{-1}	
F(000)		4888.0	
Crystal size		0.3 × 0.2 × 0.1 mm^3	
θ range for data collection		3.32 to 56.56	
Index ranges		-29≤ h≤29, -19≤ k≤19, -52≤ l≤52	
Reflections collected		137290	
Independent reflections		15617 [R_{int} = 0.0764, R_{sigma} = 0.0536]	
Absorption correction		multi-scan	
Max./min. transmission		0.766 / 0.862	
Refinement method		full-matrix least-squares on F^2	
Data / restraints / parameters		15617/0/716	
Goodness-of-fit on F^2		1.120	
Final R indices [I>2σ(I)]		R_1 = 0.0443, wR_2 = 0.0991	
R indices (all data)		R_1 = 0.0658, wR_2 = 0.1064	
Largest diff. peak and hole, e. $Å^{-3}$		0.76/-0.33	

Table 21. Crystal structure determination parameters for **III-7**.

Empirical formula		$C_{47}H_{59}GaN_4O_2$	
Formula weight		781.70	
Crystal habit		block	
Crystal color		light yellow	
Temperature		100.15 K	
Wavelength		1.54178 Å	
Crystal system		monoclinic	
Space group		P-1	
Unit cell dimensions:			
a	10.2946(5) Å	α	81.4190°
b	10.8735(5) Å	β	87.6810°
c	19.2723(9) Å	γ	80.8880°
Volume		2105.93(17) $Å^3$	
Z		2	
Density (calc)		1.233 mg/m^3	
Absorption coefficient		1.211 mm^{-1}	
F(000)		832	
Crystal size		0.25 × 0.2 × 0.2 mm^3	
θ range for data collection		4.35 to 72.18	
Index ranges		-12≤ h≤12, -13≤ k≤13, -22≤ l≤22	
Reflections collected		52457	
Independent reflections		8283 [R_{int} = 0.0266, R_{sigma} = 0.0165]	
Absorption correction		multi-scan	
Max./min. transmission		0.659 / 0.746	
Refinement method		full-matrix least-squares on F^2	
Data / restraints / parameters		8283/0/501	
Goodness-of-fit on F^2		0.993	
Final R indices [I>2σ(I)]		R_1 = 0.0262, wR_2 = 0.0696	
R indices (all data)		R_1 = 0.0280, wR_2 = 0.0710	
Largest diff. peak and hole, e. $Å^{-3}$		0.32/-0.32	

Table 22. Crystal structure determination parameters for **III-8**.

Empirical formula		$C_{63}H_{79}GaN_6O$	
Formula weight		1006.04	
Crystal habit		block	
Crystal color		light yellow	
Temperature		173.2 K	
Wavelength		0.71073 Å	
Crystal system		monoclinic	
Space group		$P2_1/c$	
Unit cell dimensions:			
a	11.4736(14) Å	α	90.00°
b	24.067(3) Å	β	97.526(2)°
c	20.824(3) Å	γ	90.00°
Volume		5700.8(12) $Å^3$	
Z		4	
Density (calc)		1.172 mg/m^3	
Absorption coefficient		0.528 mm^{-1}	
F(000)		2152	
Crystal size		0.49 × 0.39 × 0.31 mm^3	
θ range for data collection		3.38 to 61.05	
Index ranges		-16≤ h≤16, -34≤ k≤34, -29≤ l≤29	
Reflections collected		101528	
Independent reflections		17207 [R_{int} = 0.0597, R_{sigma} = 0.552]	
Absorption correction		multi-scan	
Max./min. transmission		0.659 / 0.746	
Refinement method		full-matrix least-squares on F^2	
Data / restraints / parameters		17207/10/664	
Goodness-of-fit on F^2		1.069	
Final R indices [I>2σ(I)]		R_1 = 0.0517, wR_2 = 0.1270	
R indices (all data)		R_1 = 0.0781, wR_2 = 0.1395	
Largest diff. peak and hole, e. $Å^{-3}$		0.91/-0.89	

Table 23. Crystal structure determination parameters for **III-9**.

Empirical formula		$C_{34}H_{46}GaN_3O_2$	
Formula weight		598.46	
Temperature		200.0 K	
Wavelength		0.71073 Å	
Crystal system		orthorhombic	
Space group		$P2_12_12_1$	
Unit cell dimensions:			
a	12.2418(4) Å	α	90.00°
b	13.2598(5) Å	β	90.00°
c	20.3373(7) Å	γ	90.00°
Volume		3301.2(2) $Å^3$	
Z		4	
Density (calc)		1.204 mg/m^3	
Absorption coefficient		0.866 mm^{-1}	
F(000)		1272.0	
Crystal size		0.3 × 0.4 × 0.8 mm^3	
Reflections collected		150419	
Independent reflections		11468 [R_{int} = 0.0468]	
Absorption correction		Bruker SADABS	
Data / restraints / parameters		11468/0/372	
Goodness-of-fit on F^2		1.027	
Final R indices [I>2σ(I)]		R_1 = 0.0287, wR_2 = 0.0625	
R indices (all data)		R_1 = 0.0404, wR_2 = 0.0666	
Largest diff. peak and hole, e. $Å^{-3}$		0.36/-0.39	

Table 24. Crystal structure determination parameters for **III-11**.

Empirical formula		$C_{35}H_{51}GaN_2O_2$	
Formula weight		601.50	
Temperature		100.15 K	
Wavelength		0.65250 Å	
Crystal system		orthorhombic	
Space group		Pnma	
Unit cell dimensions:			
a	16.253(3) Å	α	90.00°
b	20.624(4) Å	β	90.00°
c	9.7280(19) Å	γ	90.00°
Volume		3260.8(11) $Å^3$	
Z		4	
Density (calc)		1.225 mg/m^3	
Absorption coefficient		0.685 mm^{-1}	
F(000)		1288.0	
Crystal size		0.05 × 0.04 × 0.04 mm^3	
Reflections collected		24683	
Independent reflections		2935 [R_{int} = 0.0650]	
Absorption correction		Bruker SADABS	
Data / restraints / parameters		2935/35/219	
Goodness-of-fit on F^2		1.281	
Final R indices [I>2σ(I)]		R_1 = 0.0532, wR_2 = 0.1400	
R indices (all data)		R_1 = 0.0825, wR_2 = 0.1845	
Largest diff. peak and hole, e. $Å^{-3}$		0.56/-0.57	

Table 25. Crystal structure determination parameters for **III-14**.

Empirical formula		$C_{35}H_{56}GaN_2O_2P$	
Formula weight		637.50	
Temperature		150 K	
Wavelength		0.71073 Å	
Crystal system		monoclinic	
Space group		$P2_{1/n}$	
Unit cell dimensions:			
a	11.900(2) Å	α	90.00°
b	28.400(6) Å	β	92.25°
c	20.850(4) Å	γ	90.00°
Volume		3260.8(11) $Å^3$	
Z		8	
Density (calc)		1.207 mg/m^3	
Absorption coefficient		0.861 mm^{-1}	
F(000)		2736.0	
Crystal size		0.5 × 0.4 × 0.2 mm^3	
Reflections collected		122190	
Independent reflections		2935 [R_{int} = 0.0650]	
Absorption correction		Bruker SADABS	
Data / restraints / parameters		21806/0/791	
Goodness-of-fit on F^2		1.10	
Final R indices [I>2σ(I)]		R_1 = 0.047, wR_2 = 0.091	
R indices (all data)		R_1 = 0.0623, wR_2 = 0.0913	
Largest diff. peak and hole, e. $Å^{-3}$		0.72/-0.69	

Table 26. Crystal structure determination parameters for **III-15**.

Empirical formula		$C_{74}H_{109}Ga_2N_8Si_2$	
Formula weight		1306.31	
Temperature		150 K	
Wavelength		0.71073 Å	
Crystal system		monoclinic	
Space group		P-1	
Unit cell dimensions:			
a	9.8888(6) Å	α	109.708(3)°
b	20.6827(13) Å	β	93.827(3)°
c	21.1123(12) Å	γ	97.512(3)°
Volume		4001.7(4) $Å^3$	
Z		2	
Density (calc)		1.084 mg/m^3	
Absorption coefficient		0.744 mm^{-1}	
F(000)		1398.0	
Crystal size		0.18 × 0.23 × 0.3 mm^3	
Reflections collected		136414	
Independent reflections		24752 [R_{int} = 0.0494, R_{sigma} = 0.0407]	
Absorption correction		Bruker SADABS	
Max./min. transmission		0.746 / 0.6677	
Data / restraints / parameters		24752/0/791	
Goodness-of-fit on F^2		1.053	
Final R indices [I>2σ(I)]		R_1 = 0.0482, wR_2 = 0.0994	
R indices (all data)		R_1 = 0.0623, wR_2 = 0.0994	
Largest diff. peak and hole, e. $Å^{-3}$		0.72/-0.69	

Table 27. Crystal structure determination parameters for **III-20.**

Empirical formula		$C_{37}H_{61}GaN_4Si_2$	
Formula weight		687.79	
Crystal habit		block	
Crystal color		yellow	
Temperature		150.0(1) K	
Wavelength		0.71073 Å	
Crystal system		monoclinic	
Space group		$P2_1/n$	
Unit cell dimensions:			
a	12.0898(8) Å	α	90°
b	15.6108(9) Å	β	103.021(3)°
c	21.9844(13) Å	γ	90°
Volume		4042(4) $Å^3$	
Z		4	
Density (calc)		1.130 mg/m^3	
Absorption coefficient		0.768 mm^{-1}	
F(000)		1480.00	
Crystal size		0.45 × 0.42 × 0.22 mm^3	
θ range for data collection		3.804 to 56.564	
Index ranges		-16≤ h≤16, -20≤ k≤20, -29≤ l≤29	
Reflections collected		57681	
Independent reflections		10020 [R_{int} = 0.0683, R_{sigma} = 0.0436]	
Absorption correction		multi-scan	
Max./min. transmission		0.431 / 0.746	
Refinement method		full-matrix least-squares on F^2	
Data / restraints / parameters		10020/18/413	
Goodness-of-fit on F^2		1.082	
Final R indices [I>2σ(I)]		R_1 = 0.0640, wR_2 = 0.1388	
R indices (all data)		R_1 = 0.0832, wR_2 = 0.1523	
Largest diff. peak and hole, e. $Å^{-3}$		1.68/-1.53	

Table 28. Crystal structure determination parameters for **III-25.**

Empirical formula		$C_{37}H_{61}GaN_6Si_2$	
Formula weight		715.81	
Crystal habit		block	
Crystal color		yellow	
Temperature		150.0(1) K	
Wavelength		0.71073 Å	
Crystal system		triclinic	
Space group		P-1	
Unit cell dimensions:			
a	10.9476(9)) Å	α	74.448(3)°
b	11.9669(10) Å	β	84.074(3)°
c	16.9360(13) Å	γ	73.037(3)°
Volume		2043.8(3) $Å^3$	
Z		2	
Density (calc)		1.163 mg/m^3	
Absorption coefficient		0.763 mm^{-1}	
F(000)		768.0	
Crystal size		0.41 × 0.40 × 0.31 mm^3	
θ range for data collection		3.676 to 56.876	
Index ranges		-14≤ h≤14, -15≤ k≤15, -22≤ l≤22	
Reflections collected		50190	
Independent reflections		10149[R_{int} = 0.0629, R_{sigma} = 0.0413]	
Absorption correction		multi-scan	
Max./min. transmission		0.456 / 0.746	
Refinement method		full-matrix least-squares on F^2	
Data / restraints / parameters		10149/427/456	
Goodness-of-fit on F^2		1.231	
Final R indices [I>2σ(I)]		R_1 = 0.0738, wR_2 = 0.1755	
R indices (all data)		R_1 = 0.0839, wR_2 = 0.1809	
Largest diff. peak and hole, e. $Å^{-3}$		0.88/-0.83	

Table 29. Crystal structure determination parameters for **III-26.**

Empirical formula		$C_{50}H_{74}BGaN_4Si_2$	
Formula weight		899.84	
Crystal habit		prism	
Crystal color		yellow	
Temperature		150.0(1) K	
Wavelength		0.71073 Å	
Crystal system		orthorhombic	
Space group		Pccn	
Unit cell dimensions:			
a	24.1141(15) Å	α	90°
b	24.7292(14) Å	β	90°
c	17.5338(11) Å	γ	90°
Volume		10449.2(11) $Å^3$	
Z		8	
Density (calc)		1.144 mg/m^3	
Absorption coefficient		0.612 mm^{-1}	
F(000)		3856.00	
Crystal size		0.102 × 0.046 × 0.045 mm^3	
θ range for data collection		3.313 to 49	
Index ranges		-28≤ h≤28, -28≤ k≤28, -20≤ l≤20	
Reflections collected		39958	
Independent reflections		8702 [R_{int} = 0.1448, R_{sigma} = 0.0985]	
Absorption correction		multi-scan	
Max./min. transmission		0.642 / 0.746	
Refinement method		full-matrix least-squares on F^2	
Data / restraints / parameters		8702/40/518	
Goodness-of-fit on F^2		1.088	
Final R indices [I>2σ(I)]		R_1 = 0.0888, wR_2 = 0.1510	
R indices (all data)		R_1 = 0.1427, wR_2 = 0.1719	
Largest diff. peak and hole, e. $Å^{-3}$		0.43/-0.46	

Table 30. Crystal structure determination parameters for **III-27.**

Empirical formula		$C_{43}H_{69}GaN_4Si_3$	
Formula weight		796.03	
Crystal habit		block	
Crystal color		colorless	
Temperature		150.0(1) K	
Wavelength		0.71073 Å	
Crystal system		orthorhombic	
Space group		Pbca	
Unit cell dimensions:			
a	22.1768(12) Å	α	90°
b	18.1072(12) Å	β	90°
c	22.8370(12) Å	γ	90°
Volume		9170.4(9) $Å^3$	
Z		8	
Density (calc)		1.1531 mg/m^3	
Absorption coefficient		0.711 mm^{-1}	
F(000)		3424.00	
Crystal size		0.48 × 0.45 × 0.24 mm^3	
θ range for data collection		4.3 to 56.8	
Index ranges		-24≤ h≤30, -25≤ k≤12, -29≤ l≤31	
Reflections collected		58462	
Independent reflections		11485 R_{int} = 0.0849, R_{sigma} = 0.0713]	
Absorption correction		multi-scan	
Max./min. transmission		0.513 / 0.746	
Refinement method		full-matrix least-squares on F^2	
Data / restraints / parameters		11485/6/505	
Goodness-of-fit on F^2		1.058	
Final R indices [I>2σ(I)]		R_1 = 0.0677, wR_2 = 0.1330	
R indices (all data)		R_1 = 0.0965, wR_2 = 0.1502	
Largest diff. peak and hole, e. $Å^{-3}$		1.32/-1.18	

Table 31. Crystal structure determination parameters for **III-28.**

Empirical formula		$C_{45}H_{60}B_2GaN_3Si$	
Formula weight		826.39	
Crystal habit		prism	
Crystal color		yellow	
Temperature		150.0(1) K	
Wavelength		0.71073 Å	
Crystal system		monoclinic	
Space group		$P2_1/n$	
Unit cell dimensions:			
a	11.7176(7) Å	α	90°
b	19.6529(11) Å	β	98.455(2)°
c	19.5053(11) Å	γ	90°
Volume		4443.0(4) $Å^3$	
Z		4	
Density (calc)		1.235 mg/m^3	
Absorption coefficient		0.690 mm^{-1}	
F(000)		1752.00	
Crystal size		0.19 × 0.12 × 0.10 mm^3	
θ range for data collection		4.08 to 56.564	
Index ranges		-15≤ h≤15, -26≤ k≤26, -24≤ l≤24	
Reflections collected		62494	
Independent reflections		11034 R_{int} = 0.0817, R_{sigma} = 0.0618]	
Absorption correction		multi-scan	
Max./min. transmission		0.597 / 0.746	
Refinement method		full-matrix least-squares on F^2	
Data / restraints / parameters		11034/456/518	
Goodness-of-fit on F^2		1.078	
Final R indices [I>2σ(I)]		R_1 = 0.0599, wR_2 = 0.1050	
R indices (all data)		R_1 = 0.0818, wR_2 = 0.1128	
Largest diff. peak and hole, e. $Å^{-3}$		0.40/-0.38	

VIII. References

1. Power, P. P., Main-group elements as transition metals. *Nature* **2010,** *463* (7278), 171-7.
2. Chu, T.; Nikonov, G. I., Oxidative Addition and Reductive Elimination at Main-Group Element Centers. *Chem Rev* **2018,** *118* (7), 3608-3680.
3. Weetman, C.; Inoue, S., The Road Travelled: After Main-Group Elements as Transition Metals. *Chemcatchem* **2018,** *10* (19), 4213-4228.
4. Hardman, N. J.; Eichler, B. E.; Power, P. P., Synthesis and characterization of the monomer Ga{(NDippCMe)(2)CH} (Dipp = C6H3Pr2i-2,6): a low valent gallium(I) carbene analogue. *Chem Commun* **2000,** (20), 1991-1992.
5. Seifert, A.; Scheid, D.; Linti, G.; Zessin, T., Oxidative Addition Reactions of Element-Hydrogen Bonds with Different Polarities to a Gallium(I) Compound. *Chem-Eur J* **2009,** *15* (44), 12114-12120.
6. Kempter, A.; Gemel, C.; Fischer, R. A., Oxidative addition of group 13 and 14 metal halides and alkyls to Ga(DDP) (DDP = bulky bisimidinate). *Inorg Chem* **2008,** *47* (16), 7279-7285.
7. Tuscher, L.; Helling, C.; Wolpe, C.; Frank, W.; Nizovtsev, A. S.; Schulz, S., A General Route to Metal-Substituted Dipnictenes of the Type L(X)M (2)E-2. *Chem-Eur J* **2018,** *24* (13), 3241-3250.
8. Prabusankar, G.; Gemel, C.; Parameswaran, P.; Flener, C.; Frenking, G.; Fischer, R. A., A Short Bi = Bi Bond Supported by a Metalloid Group 13 Ligand. *Angewandte Chemie-International Edition* **2009,** *48* (30), 5526-5529.
9. Ganesamoorthy, C.; Blaser, D.; Wolper, C.; Schulz, S., Sequential Bi-C bond activation reactions of BiEt3 via insertion reactions of RE {R = HC[C(Me)N(2,6-i-Pr2C6H3)](2); E = Al, Ga, In}. *Chem Commun* **2014,** *50* (82), 12382-12384.
10. Ganesamoorthy, C.; Blaser, D.; Wolper, C.; Schulz, S., Synthesis of Heterobimetallic Group 13 Compounds via Oxidative Addition Reaction of Gallanediyl LGa and InEt3. *Organometallics* **2015,** *34* (12), 2991-2996.
11. Ganesamoorthy, C.; Blaser, D.; Wolper, C.; Schulz, S., Temperature-Dependent Electron Shuffle in Molecular Group 13/15 Intermetallic Complexes. *Angewandte Chemie-International Edition* **2014,** *53* (43), 11587-11591.
12. Helling, C.; Wolper, C.; Schulz, S., Synthesis of a Gallaarsene {HC C(Me)N-2,6-i-Pr-2-C6H3 (2)}GaAsCp* Containing a Ga=As Double Bond. *J Am Chem Soc* **2018,** *140* (15), 5053-5056.
13. Ganesamoorthy, C.; Helling, C.; Wolper, C.; Frank, W.; Bill, E.; Cutsail, G. E.; Schulz, S., From stable Sb- and Bi-centered radicals to a compound with a Ga=Sb double bond. *Nat. Commun.* **2018,** *9*, 8.
14. Sharma, M. K.; Wolper, C.; Haberhauer, G.; Schulz, S., Multi-Talented Gallaphosphene for Ga-P-Ga Heteroallyl Cation Generation, CO2 Storage, and C(sp(3))-H Bond Activation. *Angewandte Chemie-International Edition* **2021,** *60* (12), 6784-6790.
15. Li, B.; Wolper, C.; Haberhauer, G.; Schulz, S., Synthesis and Reactivity of Heteroleptic Ga-P-C Allyl Cation Analogues. *Angewandte Chemie-International Edition* **2021,** *60* (4), 1986-1991.
16. Wilson, D. W. N.; Feld, J.; Goicoechea, J. M., A Phosphanyl-Phosphagallene that Functions as a Frustrated Lewis Pair. *Angewandte Chemie-International Edition* **2020,** *59* (47), 20914-20918.
17. Feld, J.; Wilson, D. W. N.; Goicoechea, J. M., Contrasting E-H Bond Activation Pathways of a Phosphanyl-Phosphagallene. *Angewandte Chemie-International Edition* **2021,** *60* (40), 22057-22061.

18. Hartwig, J. F., *Organotransition Metal Chemistry: From Bonding to Catalysis*. University Science Books: Sausalito, California, 2010.
19. Power, P. P., Reactions of heavier main-group compounds with hydrogen, ammonia, ethylene and related small molecules. *Chem Rec* **2012,** *12* (2), 238-255.
20. Asay, M.; Jones, C.; Driess, M., N-Heterocyclic Carbene Analogues with Low-Valent Group 13 and Group 14 Elements: Syntheses, Structures, and Reactivities of a New Generation of Multitalented Ligands. *Chemical Reviews* **2011,** *111* (2), 354-396.
21. Yadav, S.; Saha, S.; Sen, S. S., Compounds with Low-Valent p-Block Elements for Small Molecule Activation and Catalysis. *Chemcatchem* **2016,** *8* (3), 486-501.
22. Spikes, G. H.; Fettinger, J. C.; Power, P. P., Facile activation of dihydrogen by an unsaturated heavier main group compound. *J Am Chem Soc* **2005,** *127* (35), 12232-12233.
23. Chu, T.; Boyko, Y.; Korobkov, I.; Nikonov, G. I., Transition Metal-like Oxidative Addition of C-F and C-O Bonds to an Aluminum(I) Center. *Organometallics* **2015,** *34* (22), 5363-5365.
24. Swamy, V. S. V. S. N.; Parvin, N.; Raj, K. V.; Vanka, K.; Sen, S. S., C(sp(3))-F, C(sp(2))-F and C(sp(3))-H bond activation at silicon(II) centers. *Chem Commun* **2017,** *53* (71), 9850-9853.
25. Bakewell, C.; White, A. J. P.; Crimmin, M. R., Reactions of Fluoroalkenes with an Aluminium(I) Complex. *Angewandte Chemie-International Edition* **2018,** *57* (22), 6638-6642.
26. Kysliak, O.; Gorls, H.; Kretschmer, R., Cooperative Bond Activation by a Bimetallic Main-Group Complex. *J Am Chem Soc* **2021,** *143* (1), 142-148.
27. Dewar, J. S., A Review of the Pi-Complex Theory. *B Soc Chim Fr* **1951,** *18* (3-4), C71-C79.
28. Chatt, J.; Duncanson, L. A., Olefin Co-Ordination Compounds .3. Infra-Red Spectra and Structure - Attempted Preparation of Acetylene Complexes. *J Chem Soc* **1953,** (Oct), 2939-2947.
29. Soleilhavoup, M.; Bertrand, G., Borylenes: An Emerging Class of Compounds. *Angewandte Chemie-International Edition* **2017,** *56* (35), 10282-10292.
30. Nomoto, M.; Okabayashi, T.; Klaus, T.; Tanimoto, M., Microwave spectroscopic study of the BBr molecule. *J Mol Struct* **1997,** *413*, 471-476.
31. Bettinger, H. F., Phenylborylene: Direct spectroscopic characterization in inert gas matrices. *J Am Chem Soc* **2006,** *128* (8), 2534-2535.
32. Thompson, C. A.; Andrews, L.; Martin, J. M. L.; Elyazal, J., Infrared-Spectra of Boron Atom-Ammonia Reaction-Products in Solid Argon. *J Phys Chem-Us* **1995,** *99* (38), 13839-13849.
33. Timms, P. L., Boron-Fluorine Chemistry .I. Boron Monofluoride and Some Derivatives. *J Am Chem Soc* **1967,** *89* (7), 1629-&.
34. Timms, P. L., Boron-Fluorine Chemistry .2. Reaction of Boron Monofluoride with Acetylenes. *J Am Chem Soc* **1968,** *90* (17), 4585-&.
35. Timms, P. L., Chemistry of Boron and Silicon Subhalides. *Accounts Chem Res* **1973,** *6* (4), 118-123.
36. Cowley, A. H.; Lomeli, V.; Voigt, A., Synthesis and characterization of a terminal borylene (boranediyl) complex. *J Am Chem Soc* **1998,** *120* (25), 6401-6402.
37. Braunschweig, H.; Kollann, C.; Englert, U., Synthesis and structure of the first terminal borylene complexes. *Angewandte Chemie-International Edition* **1998,** *37* (22), 3179-3180.
38. Kinjo, R.; Donnadieu, B.; Celik, M. A.; Frenking, G.; Bertrand, G., Synthesis and Characterization of a Neutral Tricoordinate Organoboron Isoelectronic with Amines. *Science* **2011,** *333* (6042), 610-613.
39. Dahcheh, F.; Martin, D.; Stephan, D. W.; Bertrand, G., Synthesis and Reactivity of a CAAC-Aminoborylene Adduct: A Hetero-Allene or an Organoboron Isoelectronic with Singlet Carbenes. *Angewandte Chemie-International Edition* **2014,** *53* (48), 13159-13163.

40. Wang, Y.; Quillian, B.; Wei, P.; Wannere, C. S.; Xie, Y.; King, R. B.; Schaefer, H. F.; Schleyer, P. V.; Robinson, G. H., A stable neutral diborene containing a B = B double bond. *J Am Chem Soc* **2007,** *129* (41), 12412-+.
41. Arrowsmith, M.; Bohnke, J.; Braunschweig, H.; Celik, M. A.; Claes, C.; Ewing, W. C.; Krummenacher, I.; Lubitz, K.; Schneider, C., Neutral Diboron Analogues of Archetypal Aromatic Species by Spontaneous Cycloaddition. *Angewandte Chemie-International Edition* **2016,** *55* (37), 11271-11275.
42. Bissinger, P.; Braunschweig, H.; Celik, M. A.; Claes, C.; Dewhurst, R. D.; Endres, S.; Kelch, H.; Kramer, T.; Krummenacher, I.; Schneider, C., Synthesis of cyclic diborenes with unprecedented cis-configuration. *Chem Commun* **2015,** *51* (88), 15917-15920.
43. Bohnke, J.; Braunschweig, H.; Ewing, W. C.; Horl, C.; Kramer, T.; Krummenacher, I.; Mies, J.; Vargas, A., Diborabutatriene: An Electron-Deficient Cumulene. *Angewandte Chemie-International Edition* **2014,** *53* (34), 9082-9085.
44. Cui, C. M.; Kopke, S.; Herbst-Irmer, R.; Roesky, H. W.; Noltemeyer, M.; Schmidt, H. G.; Wrackmeyer, B., Facile synthesis of cyclopropene analogues of aluminum and an aluminum pinacolate, and the reactivity of LA1[eta(2)-C-2(SiMe3)(2)] toward unsaturated molecules (L = HC[(CMe)(NAr)](2), Ar=2,6-i-Pr2C6H3). *J Am Chem Soc* **2001,** *123* (37), 9091-9098.
45. Cui, C. M.; Roesky, H. W.; Schmidt, H. G.; Noltemeyer, M.; Hao, H. J.; Cimpoesu, F., Synthesis and structure of a monomeric aluminum(I) compound [{HC(CMeNAr)(2)}Al] (Ar=2,6-iPr(2)C(6)H(3)): A stable aluminum analogue of a carbene. *Angewandte Chemie-International Edition* **2000,** *39* (23), 4274-+.
46. Zhu, H. P.; Chai, J. F.; Fan, H. J.; Roesky, H. W.; He, C.; Jancik, V.; Schmidt, H. G.; Noltemeyer, M.; Merrill, W. A.; Power, P. R., A stable aluminacyclopropene LA1(eta(2)-C2H2) and its end-on azide insertion to an aluminaazacyclobutene. *Angewandte Chemie-International Edition* **2005,** *44* (32), 5090-5093.
47. Zhu, H. P.; Oswald, R. B.; Fan, H. J.; Roesky, H. W.; Ma, Q. J.; Yang, Z.; Schmidt, H. G.; Noltemeyer, M.; Starke, K.; Hosmane, N. S., Aluminacyclopropene: Syntheses, characterization, and reactivity toward terminal alkynes. *J Am Chem Soc* **2006,** *128* (15), 5100-5108.
48. Bakewell, C.; White, A. J. P.; Crimmin, M. R., Reversible alkene binding and allylic C-H activation with an aluminium(i) complex. *Chem Sci* **2019,** *10* (8), 2452-2458.
49. Kong, R. Y.; Crimmin, M. R., Reversible insertion of CO into an aluminium-carbon bond. *Chem Commun* **2019,** *55* (44), 6181-6184.
50. Schmidt, E. S.; Jockisch, A.; Schmidbaur, H., A carbene analogue with low-valent gallium as a heteroatom in a quasi-aromatic imidazolate anion. *J Am Chem Soc* **1999,** *121* (41), 9758-9759.
51. Baker, R. J.; Farley, R. D.; Jones, C.; Kloth, M.; Murphy, D. M., The reactivity of diazabutadienes toward low oxidation state Group 13 iodides and the synthesis of a new gallium(I) carbene analogue. *J Chem Soc Dalton* **2002,** (20), 3844-3850.
52. Fedushkin, I. L.; Lukoyanov, A. N.; Tishkina, A. N.; Fukin, G. K.; Lyssenko, K. A.; Hummert, M., Reduction of Digallane [(dpp-bian)Ga-Ga(dpp-bian)] with Group 1 and 2 Metals. *Chem-Eur J* **2010,** *16* (25), 7563-7571.
53. Hicks, J.; Vasko, P.; Goicoechea, J. M.; Aldridge, S., Synthesis, structure and reaction chemistry of a nucleophilic aluminyl anion. *Nature* **2018,** *557* (7703), 92-+.
54. Hicks, J.; Vasko, P.; Goicoechea, J. M.; Aldridge, S., The Aluminyl Anion: A New Generation of Aluminium Nucleophile. *Angewandte Chemie-International Edition* **2021,** *60* (4), 1702-1713.
55. Hicks, J.; Vasko, P.; Goicoechea, J. M.; Aldridge, S., Reversible, Room-Temperature C-C Bond Activation of Benzene by an Isolable Metal Complex. *J Am Chem Soc* **2019,** *141* (28), 11000-11003.

56. Kurumada, S.; Takamori, S.; Yamashita, M., An alkyl-substituted aluminium anion with strong basicity and nucleophilicity. *Nat Chem* **2020,** *12* (1), 36-39.
57. Sugita, K.; Nakano, R.; Yamashita, M., Cycloaddition of Dialkylalumanyl Anion toward Unsaturated Hydrocarbons in (1+2) and (1+4) Modes. *Chem-Eur J* **2020,** *26* (10), 2174-2177.
58. Fedushkin, I. L.; Moskalev, M. V.; Lukoyanov, A. N.; Tishkina, A. N.; Baranov, E. V.; Abakumov, G. A., Dialane with a Redox-Active Bis-amido Ligand: Unique Reactivity towards Alkynes. *Chem-Eur J* **2012,** *18* (36), 11264-11276.
59. Zhao, Y. X.; Lei, Y. B.; Dong, Q. S.; Wu, B.; Yang, X. J., Reactivity of Dialumane and "Dialumene" Compounds toward Alkenes. *Chem-Eur J* **2013,** *19* (36), 12059-12066.
60. Zhao, Y. X.; Liu, Y. Y.; Lei, Y. B.; Wu, B. A.; Yang, X. J., Activation of alkynes by an alpha-diimine-stabilized Al-Al-bonded compound: insertion into the Al-Al bond or cycloaddition to AlN2C2 rings. *Chem Commun* **2013,** *49* (40), 4546-4548.
61. Wright, R. J.; Phillips, A. D.; Power, P. P., The 2+4 Diels-Alder cycloadditon product of a probable dialuminene, Ar ' AlAlAr ' (Ar ' = C6H3-2,6-Dipp(2); Dipp = C6H3-2,6-Pr-2(i)), with toluene. *J Am Chem Soc* **2003,** *125* (36), 10784-10785.
62. Agou, T.; Nagata, K.; Tokitoh, N., Synthesis of a Dialumene-Benzene Adduct and Its Reactivity as a Synthetic Equivalent of a Dialumene. *Angewandte Chemie-International Edition* **2013,** *52* (41), 10818-10821.
63. Bag, P.; Porzelt, A.; Altmann, P. J.; Inoue, S., A Stable Neutral Compound with an Aluminum-Aluminum Double Bond. *J Am Chem Soc* **2017,** *139* (41), 14384-14387.
64. Weetman, C.; Porzelt, A.; Bag, P.; Hanusch, F.; Inoue, S., Dialumenes - aryl vs. silyl stabilisation for small molecule activation and catalysis. *Chem Sci* **2020,** *11* (18), 4817-4827.
65. Hardman, N. J.; Wright, R. J.; Phillips, A. D.; Power, P. P., Structures, bonding, and reaction chemistry of the neutral organogallium(I) compounds (GaAr)(n) (n=1 or 2) (Ar = terphenyl or related ligand): An experimental investigation of Ga-Ga multiple bonding. *J Am Chem Soc* **2003,** *125* (9), 2667-2679.
66. Cordero, B.; Gomez, V.; Platero-Prats, A. E.; Reves, M.; Echeverria, J.; Cremades, E.; Barragan, F.; Alvarez, S., Covalent radii revisited. *Dalton T* **2008,** (21), 2832-2838.
67. Zhu, Z. L.; Wang, X. P.; Olmstead, M. M.; Power, P. P., Synthesis and Characterization of [Ar ' GaC(Ph)CH](2) and K-2[Ar ' GaC(Ph)CH](2)center dot OEt2: From Digallene to Digallacyclohexadiene to Digallatabenzene. *Angewandte Chemie-International Edition* **2009,** *48* (11), 2027-2030.
68. Caputo, C. A.; Zhu, Z. L.; Brown, Z. D.; Fettinger, J. C.; Power, P. P., Activation of olefins with low-valent gallium compounds under ambient conditions. *Chem Commun* **2011,** *47* (26), 7506-7508.
69. Caputo, C. A.; Koivistoinen, J.; Moilanen, J.; Boynton, J. N.; Tuononen, H. M.; Power, P. P., Counterintuitive Mechanisms of the Addition of Hydrogen and Simple Olefins to Heavy Group 13 Alkene Analogues. *J Am Chem Soc* **2013,** *135* (5), 1952-1960.
70. Fedushkin, I. L.; Lukoyanov, A. N.; Ketkov, S. Y.; Hummert, M.; Schumann, H., [(dpp-bian)Ga-Ga(dpp-bian)] and [(dpp-bian)Zn-Ga(dpp-bian)]: Synthesis, molecular structures, and DFT studies of these novel bimetallic molecular compounds. *Chem-Eur J* **2007,** *13* (25), 7050-7056.
71. Fedushkin, I. L.; Nikipelov, A. S.; Lyssenko, K. A., Reversible Addition of Alkynes to Gallium Complex of Chelating Diamide Ligand. *J Am Chem Soc* **2010,** *132* (23), 7874-+.
72. Fedushkin, I. L.; Nikipelov, A. S.; Morozov, A. G.; Skatova, A. A.; Cherkasov, A. V.; Abakumov, G. A., Addition of Alkynes to a Gallium Bis-Amido Complex: Imitation of Transition-Metal-Based Catalytic Systems. *Chem-Eur J* **2012,** *18* (1), 255-266.
73. Ebner, C.; Carreira, E. M., Cyclopropanation Strategies in Recent Total Syntheses. *Chemical Reviews* **2017,** *117* (18), 11651-11679.

74. Moerdyk, J. P.; Schilter, D.; Bielawski, C. W., N,N'-Diamidocarbenes: Isolable Divalent Carbons with Bona Fide Carbene Reactivity. *Accounts Chem Res* **2016,** *49* (8), 1458-1468.
75. Ya, V. a. S., A., Heavy Analogs of Carbenes: Silylenes, Germylenes, Stannylenes and Plumbylenes. In *Organometallic Compounds of Low - Coordinate Si, Ge , Sn and Pb: From Phantom Species to Stable Compounds*, John Wiley & Sons, L., Ed. 2010.
76. Kira, M.; Ishida, S.; Iwamoto, T.; Kabuto, C., The first isolable dialkylsilylene. *J Am Chem Soc* **1999,** *121* (41), 9722-9723.
77. Ishida, S.; Iwamoto, T.; Kira, M., Addition of a Stable Dialkylsilylene to Carbon-Carbon Unsaturated Bonds. *Heteroatom Chem* **2011,** *22* (3-4), 432-437.
78. Gau, D.; Kato, T.; Saffon-Merceron, N.; Cossio, F. P.; Baceiredo, A., Stable Phosphonium Sila-ylide with Reactivity as a Sila-Wittig Reagent. *J Am Chem Soc* **2009,** *131* (25), 8762-+.
79. Rodriguez, R.; Gau, D.; Kato, T.; Saffon-Merceron, N.; De Cozar, A.; Cossio, F. P.; Baceiredo, A., Reversible Binding of Ethylene to Silylene-Phosphine Complexes at Room Temperature. *Angewandte Chemie-International Edition* **2011,** *50* (44), 10414-10416.
80. Lips, F.; Fettinger, J. C.; Mansikkamaki, A.; Tuononen, H. M.; Power, P. P., Reversible Complexation of Ethylene by a Silylene under Ambient Conditions. *J Am Chem Soc* **2014,** *136* (2), 634-637.
81. Wendel, D.; Eisenreich, W.; Jandl, C.; Pothig, A.; Rieger, B., Reactivity of an Acyclic Silylsilylene toward Ethylene: Migratory Insertion into the Si-Si Bond. *Organometallics* **2016,** *35* (1), 1-4.
82. Sen, S. S.; Roesky, H. W.; Stern, D.; Henn, J.; Stalke, D., High Yield Access to Silylene RSiCl (R = PhC(NtBu)(2)) and Its Reactivity toward Alkyne: Synthesis of Stable Disilacyclobutene. *J Am Chem Soc* **2010,** *132* (3), 1123-1126.
83. Driess, M.; Yao, S. L.; Brym, M.; van Wuellen, C.; Lentz, D., A new type of N-heterocyclic silylene with ambivalent reactivity. *J Am Chem Soc* **2006,** *128* (30), 9628-9629.
84. Yao, S. L.; van Wullen, C.; Sun, X. Y.; Driess, M., Dichotomic reactivity of a stable silylene toward terminal alkynes: Facile c-h bond insertion versus autocatalytic formation of silacycloprop-3-ene. *Angewandte Chemie-International Edition* **2008,** *47* (17), 3250-3253.
85. Xiong, Y.; Yao, S. L.; Driess, M., Unusual [3+1] Cycloaddition of a Stable Silylene with a 2,3-Diazabuta-1,3-diene versus [4+1] Cycloaddition toward a Buta-1,3-diene. *Organometallics* **2010,** *29* (4), 987-990.
86. Sekiguchi, A.; Kinjo, R.; Ichinohe, M., A stable compound containing a silicon-silicon triple bond. *Science* **2004,** *305* (5691), 1755-1757.
87. Kinjo, R.; Ichinohe, M.; Sekiguchi, A.; Takagi, N.; Sumimoto, M.; Nagase, S., Reactivity of a disilyne RSi SiR (R = (SiPr)-Pr-i[CH(SiMe3)(2)](2)) toward pi-bonds: Stereospecific addition and a new route to an isolable 1,2-disilabenzene. *J Am Chem Soc* **2007,** *129* (25), 7766-+.
88. Han, J. S.; Sasamori, T.; Mizuhata, Y.; Tokitoh, N., Reactivity of an Aryl-Substituted Silicon-Silicon Triple Bond: Reactions of a 1,2-Diaryldisilyne with Alkenes. *J Am Chem Soc* **2010,** *132* (8), 2546-+.
89. Ohgaki, H.; Kabe, Y.; Ando, W., Reaction of a Germylene with Ethylene - a Stable Digermacyclobutane Via a Germirane Intermediate. *Organometallics* **1995,** *14* (5), 2139-2141.
90. Sasamori, T.; Sugahara, T.; Agou, T.; Sugamata, K.; Guo, J. D.; Nagase, S.; Tokitoh, N., Reaction of a diaryldigermyne with ethylene. *Chem Sci* **2015,** *6* (10), 5526-5530.
91. Sugahara, T.; Guo, J. D.; Sasamori, T.; Nagase, S.; Tokitoh, N., Reversible addition of terminal alkenes to digermynes. *Chem Commun* **2018,** *54* (5), 519-522.
92. Gullett, K. L.; Lai, T. Y.; Chen, C. Y.; Fettinger, J. C.; Power, P. P., Reversible Binding of Ethylene and Propylene by Germylenes. *Organometallics* **2019,** *38* (7), 1425-1428.

93. Tao, L. Z.; Lai, T. Y.; Power, P. P.; Britt, R. D., Germanium Hydride Radical Trapped during the Photolysis/ Thermolysis of Diarylgermylene. *Inorg Chem* **2019,** *58* (22), 15034-15038.
94. Lai, T. Y.; Gullett, K. L.; Chen, C. Y.; Fettinger, J. C.; Power, P. P., Reversible Complexation of Alkynes by a Germylene. *Organometallics* **2019,** *38* (7), 1421-1424.
95. Peng, Y., Reversible reactions of ethylene with distannynes under ambient conditions (September, pg 1668, 2009). *Science* **2010,** *327* (5967), 781-781.
96. Lai, T. Y.; Guo, J. D.; Fettinger, J. C.; Nagase, S.; Power, P. P., Facile insertion of ethylene into a group 14 element-carbon bond: effects of the HOMO-LUMO energy gap on reactivity. *Chem Commun* **2019,** *55* (3), 405-407.
97. Sita, L. R. a. B., R. D., Synthesis and Crystal Structure of the First Stannacyclopropene Derivative. *J Am Chem Soc* **1988,** *110*, 5208-5209.
98. Li, X. H.; Weissman, S. I.; Lin, T. S.; Gaspar, P. P.; Cowley, A. H.; Smirnov, A. I., Observation of a Triplet Phosphinidene by Esr Spectroscopy. *J Am Chem Soc* **1994,** *116* (17), 7899-7900.
99. Benko, Z.; Streubel, R.; Nyulaszi, L., Stability of phosphinidenes - Are they synthetically accessible? *Dalton T* **2006,** (36), 4321-4327.
100. Lammertsma, K., Phosphinidenes. *Top Curr Chem* **2003,** *229*, 95-119.
101. Mathey, F., The Development of a Carbene-Like Chemistry with Terminal Phosphinidene Complexes. *Angew Chem Int Edit* **1987,** *26* (4), 275-286.
102. Ehlers, A. W.; Baerends, E. J.; Lammertsma, K., Nucleophilic or electrophilic phosphinidene complexes MLn=PH; what makes the difference? *J Am Chem Soc* **2002,** *124* (11), 2831-2838.
103. Aktas, H.; Slootweg, J. C.; Lammertsma, K., Nucleophilic Phosphinidene Complexes: Access and Applicability. *Angewandte Chemie-International Edition* **2010,** *49* (12), 2102-2113.
104. Nguyen, M. T.; VanKeer, A.; Vanquickenborne, L. G., In search of singlet phosphinidenes. *J Org Chem* **1996,** *61* (20), 7077-7084.
105. Marinetti, A.; Mathey, F., A NOVEL ENTRY TO THE PC-DOUBLE BOND - THE PHOSPHA-WITTIG REACTION. *Angew Chem Int Edit* **1988,** *27* (10), 1382-1384.
106. Shah, S.; Protasiewicz, J. D., 'Phospha-Wittig' reactions using isolable phosphoranylidenephosphines ArP=PR3 (Ar = 2,6-Mes(2)C(6)H(3) or 2,4,6-Bu(t)3C(6)H(2)). *Chem Commun* **1998,** (15), 1585-1586.
107. Fritz, G.; Vaahs, T.; Fleischer, H.; Matern, E., Tbu2p-P=Pbrtbu2.Libr and the Formation of Tbu2p-P. *Angew Chem Int Edit* **1989,** *28* (3), 315-316.
108. Hyvl, J.; Yoshida, W. Y.; Rheingold, A. L.; Hughes, R. P.; Cain, M. F., A Masked Phosphinidene Trapped in a Fluxional NCN Pincer. *Chem-Eur J* **2016,** *22* (49), 17562-17565.
109. Nguyen, M. T.; Gabidullin, B.; Nikonov, G. I., Imino-stabilised phosphinidene (or azaphosphole?) and some of its derivatives. *Dalton T* **2018,** *47* (47), 17011-17019.
110. Liu, L.; Ruiz, D. A.; Munz, D.; Bertrand, G., A Singlet Phosphinidene Stable at Room Temperature. *Chem-Us* **2016,** *1* (1), 147-153.
111. Hansmann, M. M.; Jazzar, R.; Bertrand, G., Singlet (Phosphino)phosphinidenes are Electrophilic. *J Am Chem Soc* **2016,** *138* (27), 8356-8359.
112. Weber, L.; Lassahn, U.; Stammler, H. G.; Neumann, B., Inversely polarized phosphaalkenes as phosphinidene- and carbene-transfer reagents. *Eur J Inorg Chem* **2005,** (22), 4590-4597.
113. Hansen, K.; Szilvasi, T.; Blom, B.; Inoue, S.; Epping, J.; Driess, M., A Fragile Zwitterionic Phosphasilene as a Transfer Agent of the Elusive Parent Phosphinidene (:PH). *J Am Chem Soc* **2013,** *135* (32), 11795-11798.
114. Transue, W. J.; Velian, A.; Nava, M.; Garcia-Iriepa, C.; Temprado, M.; Cummins, C. C., Mechanism and Scope of Phosphinidene Transfer from Dibenzo-7-phosphanorbornadiene Compounds. *J Am Chem Soc* **2017,** *139* (31), 10822-10831.

115. Krachko, T.; Bispinghoff, M.; Tondreau, A. M.; Stein, D.; Baker, M.; Ehlers, A. W.; Slootweg, J. C.; Grutzmacher, H., Facile Phenylphosphinidene Transfer Reactions from Carbene-Phosphinidene Zinc Complexes. *Angewandte Chemie-International Edition* **2017,** *56* (27), 7948-7951.
116. Jutzi, P.; Mohrke, A., Surprising Reactions of Decamethylsilicocene with Pi-Systems of the Type X = C = Y. *Angew Chem Int Edit* **1989,** *28* (6), 762-763.
117. Jutzi, P.; Eikenberg, D.; Mohrke, A.; Neumann, B.; Stammler, H. G., Decamethylsilicocene chemistry: Unprecedented multistep reactions of a silicon(II) compound with the heterocumulenes CO2, COS, CS2, and RNCS (R=methyl, phenyl). *Organometallics* **1996,** *15* (2), 753-759.
118. Dmitrienko, A.; Britten, J. F.; Spasyuk, D.; Nikonov, G. I., Adduct of NacNacAl with Benzophenone and its Coupling Chemistry. *Chem-Eur J* **2020,** *26* (1), 206-211.
119. Dmitrienko, A.; Pilkington, M.; Nikonov, G. I., Selective Cross-Coupling of Unsaturated Substrates on Al-I. *Chem-Eur J* **2021,** *27* (18), 5730-5736.
120. Chu, T.; Vyboishchikov, S. F.; Gabidullin, B. M.; Nikonov, G. I., Unusual Reactions of NacNacAl with Urea and Phosphine Oxides. *Inorg Chem* **2017,** *56* (10), 5993-5997.
121. Chu, T.; Vyboishchikov, S. F.; Gabidullin, B. M.; Nikonov, G. I., Oxidative Cleavage of the C=N Bond on AI(I). *J Am Chem Soc* **2017,** *139* (26), 8804-8807.
122. Chu, T.; Vyboishchikov, S. F.; Gabidullin, B.; Nikonov, G. I., Oxidative Cleavage of C=S and P=S Bonds at an Al-I Center: Preparation of Terminally Bound Aluminum Sulfides. *Angewandte Chemie-International Edition* **2016,** *55* (42), 13306-13311.
123. Hicks, J.; Heilmann, A.; Vasko, P.; Goicoechea, J. M.; Aldridge, S., Trapping and Reactivity of a Molecular Aluminium Oxide Ion. *Angewandte Chemie-International Edition* **2019,** *58* (48), 17265-17268.
124. Anker, M. D.; Coles, M. P., Aluminium-Mediated Carbon Dioxide Reduction by an Isolated Monoalumoxane Anion. *Angewandte Chemie-International Edition* **2019,** *58* (50), 18261-18265.
125. Koptseva, T. S.; Sokolov, V. G.; Ketkov, S. Y.; Rychagova, E. A.; Cherkasov, A. V.; Skatova, A. A.; Fedushkin, I. L., Reversible Addition of Carbon Dioxide to Main Group Metal Complexes at Temperatures about 0 degrees C. *Chem-Eur J* **2021,** *27* (18), 5745-5753.
126. Weetman, C.; Bag, P.; Szilvasi, T.; Jandl, C.; Inoue, S., CO2 Fixation and Catalytic Reduction by a Neutral Aluminum Double Bond. *Angewandte Chemie-International Edition* **2019,** *58* (32), 10961-10965.
127. Zhao, Y. X.; Liu, Y. Y.; Wang, Z.; Xu, W. H.; Liu, B.; Su, J. H.; Wu, B.; Yang, X. J., Gallium complexes with alpha-diimine and phenazine in various reduced states. *Chem Commun* **2015,** *51* (7), 1237-1239.
128. Zhang, W.; Dodonov, V. A.; Chen, W. X.; Zhao, Y. X.; Skatova, A. A.; Fedushkin, I. L.; Roesky, P. W.; Wu, B.; Yang, X. J., Cycloaddition versus Cleavage of the C=S Bond of Isothiocyanates Promoted by Digallane Compounds with Noninnocent alpha-Diimine Ligands. *Chem-Eur J* **2018,** *24* (56), 14994-15002.
129. Dodonov, V. A.; Xiao, L.; Kushnerova, O. A.; Baranov, E. V.; Zhao, Y. X.; Yang, X. J.; Fedushkin, I. L., Transformation of carbodiimides to guanidine derivatives facilitated by gallylenes. *Chem Commun* **2020,** *56* (54), 7475-7478.
130. Dodonov, V. A.; Kushnerova, O. A.; Baranov, E. V.; Novikov, A. S.; Fedushkin, I. L., Activation and modification of carbon dioxide by redox-active low-valent gallium species. *Dalton T* **2021,** *50* (25), 8899-8906.
131. Jutzi, P.; Kanne, D.; Kruger, C., Decamethylsilicocene - Synthesis and Structure. *Angew Chem Int Edit* **1986,** *25* (2), 164-164.

132. Suzuki, H.; Tokitoh, N.; Okazaki, R.; Harada, J.; Ogawa, K.; Tomoda, S.; Goto, M., Synthesis and Structures of Extremely Hindered and Stable Disilenes. *Organometallics* **1995,** *14* (2), 1016-1022.
133. Tokitoh, N.; Suzuki, H.; Okazaki, R., The first 1,2,4-thiadisiletane ring compound: Synthesis from an overcrowded silylene and carbon disulfide. *Chem Commun* **1996,** (2), 125-126.
134. Sen, S. S.; Jana, A.; Roesky, H. W.; Schulzke, C., A Remarkable Base-Stabilized Bis(silylene) with a Silicon(I)-Silicon(I) Bond. *Angewandte Chemie-International Edition* **2009,** *48* (45), 8536-8538.
135. Sen, S. S.; Tavcar, G.; Roesky, H. W.; Kratzert, D.; Hey, J.; Stalke, D., Synthesis of a Stable Four-Membered Si2O2 Ring and a Dimer with Two Four-Membered Si2O2 Rings Bridged by Two Oxygen Atoms, with Five-Coordinate Silicon Atoms in Both Ring Systems. *Organometallics* **2010,** *29* (10), 2343-2347.
136. Gau, D.; Rodriguez, R.; Kato, T.; Saffon-Merceron, N.; de Cozar, A.; Cossio, F. P.; Baceiredo, A., Synthesis of a Stable Disilyne Bisphosphine Adduct and Its Non-Metal-Mediated CO2 Reduction to CO. *Angewandte Chemie-International Edition* **2011,** *50* (5), 1092-1096.
137. Liu, X. P.; Xiao, X. Q.; Xu, Z.; Yang, X. M.; Li, Z. F.; Dong, Z. W.; Yan, C. T.; Lai, G. Q.; Kira, M., Reactions of an Isolable Dialkylsilylene with Carbon Dioxide and Related Heterocumulenes. *Organometallics* **2014,** *33* (19), 5434-5439.
138. Xiong, Y.; Yao, S. L.; Driess, M., Versatile Reactivity of a Zwitterionic Isolable Silylene toward Ketones: Silicon-Mediated, Regio- and Stereoselective C-H Activation. *Chem-Eur J* **2009,** *15* (22), 5545-5551.
139. Protchenko, A. V.; Birjkumar, K. H.; Dange, D.; Schwarz, A. D.; Vidovic, D.; Jones, C.; Kaltsoyannis, N.; Mountford, P.; Aldridge, S., A Stable Two-Coordinate Acyclic Silylene. *J Am Chem Soc* **2012,** *134* (15), 6500-6503.
140. Protchenko, A. V.; Vasko, P.; Do, D. C. H.; Hicks, J.; Fuentes, M. A.; Jones, C.; Aldridge, S., Reduction of Carbon Oxides by an Acyclic Silylene: Reductive Coupling of CO. *Angewandte Chemie-International Edition* **2019,** *58* (6), 1808-1812.
141. Li, J. Y.; Hermann, M.; Frenking, G.; Jones, C., The Facile Reduction of Carbon Dioxide to Carbon Monoxide with an Amido-Digermyne. *Angewandte Chemie-International Edition* **2012,** *51* (34), 8611-8614.
142. Yan, C. T.; Xu, Z.; Xiao, X. Q.; Li, Z. F.; Lu, Q.; Lai, G. Q.; Kira, M., Reactions of an Isolable Dialkylstannylene with Carbon Disulfide and Related Heterocumulenes. *Organometallics* **2016,** *35* (9), 1323-1328.
143. Wang, Y. C.; Lai, X. J.; Huang, K. K.; Yadav, S.; Qiu, G. Y. S.; Zhang, L. P.; Zhou, H. W., Unravelling nitrene chemistry from acyclic precursors: recent advances and challenges. *Org Chem Front* **2021,** *8* (7), 1677-1693.
144. Schultz, P. G.; Dervan, P. B., Synthesis and Direct Spectroscopic Observation of N-(2,2,5,5-Tetramethylpyrrolidyl)Nitrene - Comparison of 5-Membered and 6-Membered Cyclic 1,1-Dialkyldiazenes. *J Am Chem Soc* **1980,** *102* (2), 878-880.
145. Schultz, P. G.; Dervan, P. B., Photochemistry of 1,1-Diazenes - Direct and Sensitized Photolyses of N-(2,2,5,5-Tetramethylpyrrolidyl)Nitrene, Dl-N-(2,5-Diethyl-2,5-Dimethylpyrrolidyl)Nitrene, and N-(2,2,6,6-Tetramethylpiperidyl)Nitrene. *J Am Chem Soc* **1982,** *104* (24), 6660-6668.
146. Dielmann, F.; Back, O.; Henry-Ellinger, M.; Jerabek, P.; Frenking, G.; Bertrand, G., A Crystalline Singlet Phosphinonitrene: A Nitrogen Atom-Transfer Agent. *Science* **2012,** *337* (6101), 1526-1528.
147. Dielmann, F.; Bertrand, G., Reactivity of a Stable Phosphinonitrene towards Small Molecules. *Chem-Eur J* **2015,** *21* (1), 191-198.
148. Arduengo, A. J.; Dias, H. V. R.; Calabrese, J. C., A carbene center dot phosphinidene adduct: "Phosphaalkene". *Chem Lett* **1997,** (2), 143-144.

149. Arduengo, A. J.; Carmalt, C. J.; Clyburne, J. A. C.; Cowley, A. H.; Pyati, R., Nature of the bonding in a carbene-phosphinidene: A main group analogue of a Fischer carbene complex? Isolation and characterisation of a bis(borane) adduct. *Chem Commun* **1997,** (10), 981-982.
150. Jutzi, P., New Element Carbon (P-P)Pi Bonds. *Angew Chem Int Edit* **1975,** *14* (4), 232-245.
151. West, R.; Fink, M. J.; Michl, J., Tetramesityldisilene, a Stable Compound Containing a Silicon-Silicon Double-Bond. *Science* **1981,** *214* (4527), 1343-1344.
152. Brook, A. G.; Abdesaken, F.; Gutekunst, B.; Gutekunst, G.; Kallury, R. K., A Solid Silaethene - Isolation and Characterization. *J Chem Soc Chem Comm* **1981,** (4), 191-192.
153. Yoshifuji, M.; Shima, I.; Inamoto, N.; Hirotsu, K.; Higuchi, T., Synthesis and Structure of Bis(2,4,6-Tri-Tert-Butylphenyl)Diphosphene - Isolation of a True Phosphobenzene. *J Am Chem Soc* **1981,** *103* (15), 4587-4589.
154. Weetman, C., Main Group Multiple Bonds for Bond Activations and Catalysis. *Chem-Eur J* **2020**.
155. Power, P. P., Interaction of Multiple Bonded and Unsaturated Heavier Main Group Compounds with Hydrogen, Ammonia, Olefins, and Related Molecules. *Accounts Chem Res* **2011,** *44* (8), 627-637.
156. Schulz, S.; Haming, L.; Herbstirmer, R.; Roesky, H. W.; Sheldrick, G. M., Synthesis and Structure of the First Dimeric Iminoalane Containing an Al2n2 Heterocycle. *Angew Chem Int Edit* **1994,** *33* (9), 969-970.
157. Fisher, J. D.; Shapiro, P. J.; Yap, G. P. A.; Rheingold, A. L., [CpAlN(2,6-i-Pr2C6H3)](2): A dimeric iminoalane obtained by alkane elimination. *Inorg Chem* **1996,** *35* (2), 271-&.
158. Waggoner, K. M.; Power, P. P., Reactions of Trimethylaluminum or Trimethylgallium with Bulky Primary Amines - Structural Characterization of the Thermolysis Products. *J Am Chem Soc* **1991,** *113* (9), 3385-3393.
159. Zhu, H. P.; Chai, J. F.; Chandrasekhar, V.; Roesky, H. W.; Magull, J.; Vidovic, D.; Schmidt, H. G.; Noltemeyer, M.; Power, P. P.; Merrill, W. A., Two types of intramolecular addition of an Al-N multiple-bonded monomer LAlNAr ' arising from the reaction of LAl with N3Ar ' (L = HC[(CMe)(NAr)](2), Ar ' = 2,6-Ar2C6H3, Ar = 2,6-iPr(2)C(6)H(3)). *J Am Chem Soc* **2004,** *126* (31), 9472-9473.
160. Zhu, H. P.; Yang, Z.; Magull, J.; Roesky, H. W.; Schmidt, H. G.; Noltemeyer, M., Syntheses and structural characterization of a LAl(N-3)N[mu-Si(N-3)(tBu)](2)NAl(N-3)L and a monomeric aluminum hydride amide LAlH(NHAr) (L=HC[(CMe)(NAr)](2), Ar=2,6-iPr(2)C(6)H(3)). *Organometallics* **2005,** *24* (26), 6420-6425.
161. Cui, C. M.; Roesky, H. W.; Schmidt, H. G.; Noltemeyer, M., [HC{(CMe)(NAr)}(2)]Al[(NSiMe3)(2)N-2] (Ar=2,6-iPr(2)C(6)H(3)): The first five-membered AlN4 ring system. *Angewandte Chemie-International Edition* **2000,** *39* (24), 4531-+.
162. Hardman, N. J.; Power, P. P., Unique structural isomerism involving tetrazole and amide/azide derivatives of gallium. *Chem Commun* **2001,** (13), 1184-1185.
163. Timoshkin, A. Y., Group 13 imido metallanes and their heavier analogs [RMYR '](n) (M = Al, Ga, In; Y=N, P, As, Sb). *Coordin Chem Rev* **2005,** *249* (19-20), 2094-2131.
164. Hardman, N. J.; Cui, C. M.; Roesky, H. W.; Fink, W. H.; Power, P. P., Stable, monomeric imides of aluminum and gallium: Synthesis and characterization of [{HC(MeCDippN)(2)}MN-2,6-Trip(2)C(6)H(3)] (M = Al or Ga; Dipp=2,6-iPr(2)C(6)H(3); Trip=2,4,6-iPr(3)C(6)H(2)). *Angewandte Chemie-International Edition* **2001,** *40* (11), 2172-2174.
165. Fischer, R. C.; Power, P. P., pi-Bonding and the Lone Pair Effect in Multiple Bonds Involving Heavier Main Group Elements: Developments in the New Millennium. *Chemical Reviews* **2010,** *110* (7), 3877-3923.
166. Hardman, N. J.; Phillips, A. D.; Power, P. P., Bonding and reactivity of a beta-diketiminate, gallium(I), carbene analogue. *Acs Sym Ser* **2002,** *822*, 2-15.

167. Wright, R. J.; Phillips, A. D.; Allen, T. L.; Fink, W. H.; Power, P. P., Synthesis and characterization of the monomeric imides Ar ' MNAr " (M = Ga or In; Ar ' or Ar " = terphenyl ligands) with two-coordinate gallium and indium. *J Am Chem Soc* **2003,** *125* (7), 1694-1695.
168. Wright, R. J.; Brynda, M.; Fettinger, J. C.; Betzer, A. R.; Power, P. P., Quasi-isomeric gallium amides and imides GaNR2 and RGaNR (R = organic group): Reactions of the digallene, Ar ' GaGaAr ' (Ar ' = C6H3-2,6-(C6H3-2,6-Pr-2(i))(2)) with unsaturated nitrogen compounds. *J Am Chem Soc* **2006,** *128* (38), 12498-12509.
169. Dange, D.; Li, J. Y.; Schenk, C.; Schnockel, H.; Jones, C., Monomeric Group 13 Metal(I) Amides: Enforcing One-Coordination Through Extreme Ligand Steric Bulk. *Inorg Chem* **2012,** *51* (23), 13050-13059.
170. Li, J. F.; Li, X. F.; Huang, W.; Hu, H. F.; Zhang, J. Y.; Cui, C. M., Synthesis, Structure, and Reactivity of a Monomeric Iminoalane. *Chem-Eur J* **2012,** *18* (48), 15263-15266.
171. Li, X. F.; Cheng, X. Y.; Song, H. B.; Cui, C. M., Synthesis of HC[(CBut)(NAr)](2)Al (Ar=2,6-(Pr2C6H3)-C-i) and its reaction with isocyanides, a bulky azide, and H2O. *Organometallics* **2007,** *26* (4), 1039-1043.
172. Schwamm, R. J.; Anker, M. D.; Lein, M.; Coles, M. P.; Fitchett, C. M., Indyllithium and the Indyl Anion [InL](-) : Heavy Analogues of N-Heterocyclic Carbenes. *Angewandte Chemie-International Edition* **2018,** *57* (20), 5885-5887.
173. Anker, M. D.; Lein, M.; Coles, M. P., Reduction of organic azides by indyl-anions. Isolation and reactivity studies of indium-nitrogen multiple bonds. *Chem Sci* **2019,** *10* (4), 1212-1218.
174. Anker, M. D.; Schwamm, R. J.; Coles, M. P., Synthesis and reactivity of a terminal aluminium-imide bond. *Chem Commun* **2020,** *56* (15), 2288-2291.
175. Heilmann, A.; Hicks, J.; Vasko, P.; Goicoechea, J. M.; Aldridge, S., Carbon Monoxide Activation by a Molecular Aluminium Imide: C-O Bond Cleavage and C-C Bond Formation. *Angewandte Chemie-International Edition* **2020,** *59* (12), 4897-4901.
176. Queen, J. D.; Lehmann, A.; Fettinger, J. C.; Tuononen, H. M.; Power, P. P., The Monomeric Alanediyl :AlAriPr8 (Ar-iPr8 = C6H-2,6-(C6H2-2,4,6-Pr-3(i))(2)-3,5-Pr-2(i)): An Organoaluminum(I) Compound with a One-Coordinate Aluminum Atom. *J Am Chem Soc* **2020,** *142* (49), 20554-20559.
177. Queen, J. D.; Irvankoski, S.; Fettinger, J. C.; Tuononen, H. M.; Power, P. P., A Monomeric Aluminum Imide (Iminoalane) with Al-N Triple-Bonding: Bonding Analysis and Dispersion Energy Stabilization. *J Am Chem Soc* **2021,** *143* (17), 6351-6356.
178. Franz, D.; Inoue, S., Advances in the development of complexes that contain a group 13 element chalcogen multiple bond. *Dalton T* **2016,** *45* (23), 9385-9397.
179. Vidovic, D.; Moore, J. A.; Jones, J. N.; Cowley, A. H., Synthesis and characterization of a coordinated oxoborane: Lewis acid stabilization of a boron-oxygen double bond. *J Am Chem Soc* **2005,** *127* (13), 4566-4567.
180. Wang, Y.; Hu, H. F.; Zhang, J. Y.; Cui, C. M., Comparison of Anionic and Lewis Acid Stabilized N-Heterocyclic Oxoboranes: Their Facile Synthesis from a Borinic Acid. *Angewandte Chemie-International Edition* **2011,** *50* (12), 2816-2819.
181. Neculai, D.; Roesky, H. W.; Neculai, A. M.; Magull, J.; Walfort, B.; Stalke, D., Formation and characterization of the first monoalumoxane, LAlO center dot B(C6F5)(3). *Angewandte Chemie-International Edition* **2002,** *41* (22), 4294-4296.
182. Chu, T.; Korobkov, I.; Nikonov, G. I., Oxidative Addition of sigma Bonds to an Al(I) Center. *J Am Chem Soc* **2014,** *136* (25), 9195-9202.
183. Green, M. L. H.; Mountford, P.; Smout, G. J.; Speel, S. R., New Synthetic Pathways into the Organometallic Chemistry of Gallium. *Polyhedron* **1990,** *9* (22), 2763-2765.
184. Hardman, N. J.; Power, P. P., Dimeric gallium oxide and sulfide species stabilized by a sterically encumbered beta-diketiminate ligand. *Inorg Chem* **2001,** *40* (11), 2474-+.

185. Bissinger, P.; Braunschweig, H.; Damme, A.; Dewhurst, R. D.; Kupfer, T.; Radacki, K.; Wagner, K., Generation of a Carbene-Stabilized Bora-borylene and its Insertion into a C-H Bond. *J Am Chem Soc* **2011,** *133* (47), 19044-19047.
186. Agou, T.; Sugiyama, Y.; Sasamori, T.; Sakai, H.; Furukawa, Y.; Takagi, N.; Guo, J. D.; Nagase, S.; Hashizume, D.; Tokitoh, N., Synthesis of Kinetically Stabilized 1,2-Dihydrodisilenes. *J Am Chem Soc* **2012,** *134* (9), 4120-4123.
187. Kaese, T.; Trageser, T.; Budy, H.; Bolte, M.; Lerner, H. W.; Wagner, M., A redox-active diborane platform performs C(sp(3))-H activation and nucleophilic substitution reactions. *Chem Sci* **2018,** *9* (15), 3881-3891.
188. Brand, S.; Elsen, H.; Langer, J.; Grams, S.; Harder, S., Calcium-Catalyzed Arene C-H Bond Activation by Low-Valent Al-I. *Angewandte Chemie-International Edition* **2019,** *58* (43), 15496-15503.
189. Bohnke, J.; Bruckner, T.; Hermann, A.; Gonzalez-Belman, O. F.; Arrowsmith, M.; Jimenez-Halla, J. O. C.; Braunschweig, H., Single and double activation of acetone by isolobal B N and B B triple bonds. *Chem Sci* **2018,** *9* (24), 5354-5359.
190. Hansen, K.; Szilvasi, T.; Blom, B.; Driess, M., An Amplified Ylidic "Half-Parent" Iminosilane LSi=NH. *J Am Chem Soc* **2014,** *136* (40), 14207-14214.
191. Kristinsdottir, L.; Oldroyd, N. L.; Grabiner, R.; Knights, A. W.; Heilmann, A.; Protchenko, A. V.; Niu, H. Y.; Kolychev, E. L.; Campos, J.; Hicks, J.; Christensen, K. E.; Aldridge, S., Synthetic, structural and reaction chemistry of N-heterocyclic germylene and stannylene compounds featuring N-boryl substituents. *Dalton T* **2019,** *48* (31), 11951-11960.
192. Roesky, H. W.; Singh, S.; Jancik, V.; Chandrasekhar, V., A paradigm change in assembling OH functionalities on metal centers. *Accounts Chem Res* **2004,** *37* (12), 969-981.
193. Singh, S.; Jancik, V.; Roesky, H. W.; Herbst-Irmer, R., Synthesis, characterization, and X-ray crystal structure of a gallium monohydroxide and a hetero-bimetallic gallium zirconium oxide. *Inorg Chem* **2006,** *45* (3), 949-951.
194. Hennersdorf, F.; Frotschel, J.; Weigand, J. J., Selective Derivatization of a Hexaphosphane from Functionalization of White Phosphorus. *J Am Chem Soc* **2017,** *139* (41), 14592-14604.
195. Bernabe-Pablo, E.; Jancik, V.; Moya-Cabrera, M., A Synthetic Route to a Molecular Galloxane Dihydroxide and Its Group 4 Heterobimetallic Compounds. *Inorg Chem* **2013,** *52* (12), 6944-6950.
196. Solis-Ibarra, D.; Velasquez-Hernandez, M. D.; Huerta-Lavorie, R.; Jancik, V., Molecular Gallosilicates and Their Group 4 Multimetallic Derivatives. *Inorg Chem* **2011,** *50* (18), 8907-8917.
197. Jancik, V.; Pineda, L. W.; Stuckl, A. C.; Roesky, H. W.; Herbst-Irmer, R., Preparation of monomeric LGa(NH2)(2) and of LGa(OH)(2) in the presence of a N-heterocyclic carbene as HCl acceptor. *Organometallics* **2005,** *24* (7), 1511-1515.
198. Emsley, J., *The Elements*. Clarendon Press: Oxford, 1998.
199. Marenich, A. V.; Cramer, C. J.; Truhlar, D. G., Universal Solvation Model Based on Solute Electron Density and on a Continuum Model of the Solvent Defined by the Bulk Dielectric Constant and Atomic Surface Tensions. *J Phys Chem B* **2009,** *113* (18), 6378-6396.
200. Grubbs, R. H., *Handbook of Metathesis*. Wiley-VCH: Weinheim, Germany, 2003.
201. Zhu, H. P.; Chai, J. F.; Stasch, A.; Roesky, H. W.; Blunck, T.; Vidovic, D.; Magull, J.; Schmidt, H. G.; Noltemeyer, M., Reactions of the aluminum(I) monomer LAl [L = HC{(CMe)(NAr)}(2); Ar=2,6-iPr(2)C(6)H(3)]with imidazol-2-ylidene and diphenyldiazomethane. A hydrogen transfer from the L ligand to the central aluminum atom and formation of the diiminylaluminum compound LAl(N=CPh2)(2). *Eur J Inorg Chem* **2004,** (20), 4046-4051.
202. Xiong, Y.; Yao, S. L.; Driess, M., Striking Reactivity of a Stable, Zwitterionic Silylene Towards Substituted Diazomethanes, Azides, and Isocyanides. *Chem-Eur J* **2009,** *15* (34), 8542-8547.

203. Jana, A.; Sen, S. S.; Roesky, H. W.; Schulzke, C.; Dutta, S.; Pati, S. K., End-On Nitrogen Insertion of a Diazo Compound into a Germanium(II) Hydrogen Bond and a Comparable Reaction with Diethyl Azodicarboxylate. *Angewandte Chemie-International Edition* **2009,** *48* (23), 4246-4248.
204. Jana, A.; Objartel, I.; Roesky, H. W.; Stalke, D., Dehydrogenation of LGeH by a Lewis N-Heterocyclic Carbene Borane Pair under the Formation of L ' Ge and its Reactions with B(C6F5)(3) and Trimethylsilyl Diazomethane: An Unprecedented Rearrangement of a Diazocompound to an Isonitrile. *Inorg Chem* **2009,** *48* (16), 7645-7649.
205. Huisgen, R.; Seidel, M.; Sauer, J.; Mcfarland, J. W.; Wallbillich, G., The Formation of Nitrile Imines in the Thermal Breakdown of 2,5-Disubstituted Tetrazoles. *J Org Chem* **1959,** *24* (6), 892-893.
206. Boche, G.; Harms, K.; Marsch, M.; Schubert, F., (LITHIO(TRIMETHYLSILYL)DIAZOMETHANE.2 LITIO 4,5-BIS(TRIMETHYLSILYL)TRIAZENE .7 DIETHYL-ETHER) - THE 1ST X-RAY STRUCTURE-ANALYSIS OF A LITHIATED DIAZOALKANE. *Chem Ber* **1994,** *127* (11), 2193-2195.
207. Boche, G.; Lohrenz, J. C. W.; Schubert, F., Lithio-Diazomethane and Lithio-(Trimethylsilyl)Diazomethane - Theoretical and Experimental Studies of Their Structures, Reactions and Reaction-Products. *Tetrahedron* **1994,** *50* (20), 5889-5902.
208. Leue, C.; Reau, R.; Neumann, B.; Stammler, H. G.; Jutzi, P.; Bertrand, G., Preparation of Mono(Germyl)Nitrilimines and Bis(Germyl)Nitrilimines from Germylenes and Stannyl Diazo Derivatives. *Organometallics* **1994,** *13* (2), 436-438.
209. Emig, N.; Gabbai, F. P.; Krautscheid, H.; Reau, R.; Bertrand, G., The azide-nitrilimine analogy in aluminum chemistry. *Angewandte Chemie-International Edition* **1998,** *37* (7), 989-992.
210. Chu, J. X.; Kefalidis, C. E.; Maron, L.; Leng, X. B.; Chen, Y. F., Chameleon Behavior of a Newly Synthesized Scandium Nitrilimine Derivative. *J Am Chem Soc* **2013,** *135* (22), 8165-8168.
211. Aghazada, S.; Miehlich, M.; Messelberger, J.; Heinemann, F. W.; Munz, D.; Meyer, K., ATerminal Iron Nitrilimine Complex: Accessing the Terminal Nitride through Diazo N-N Bond Cleavage. *Angewandte Chemie-International Edition* **2019,** *58* (51), 18547-18551.